Casimir–Polder forces on atoms in the presence of magnetoelectric bodies

(Casimir–Polder-Kräfte auf Atome bei Anwesenheit magnetoelektrischer Körper)

Dissertation

zur Erlangung des akademischen Grades

doctor rerum naturalium (Dr. rer. nat.)

vorgelegt dem Rat der Physikalisch–Astronomischen Fakultät

der Friedrich-Schiller-Universität Jena

von BSc(Hons) Stefan Yoshi Buhmann

geboren am 25.6.1977 in Münster

Gutachter

1. Prof. Dr. Dirk-Gunnar Welsch

2. Prof. Dr. Carlos Víllarreal

3. Prof. Dr. Michael Fleischhauer

Tag der letzten Rigorosumsprüfung: 21.05.2007

Tag der öffentlichen Verteidigung: 05.07.2007

Contents

Chapter 1

Introduction

Dispersion forces are effective electromagnetic forces between neutral, unpolarised objects. In particular, the dispersion force acting between a single atom and macroscopic bodies is known as the Casimir–Polder (CP) force. Recent progress in experimental techniques has led to accurate measurements of CP forces and revealed their relevance to applications in nanotechnology. The experimental results have confirmed some of the theoretical predictions while posing new questions at the same time.

1.1 Dispersion forces

The prediction of dispersion forces is one of the most prominent achievements of quantum electrodynamics (QED), where they can be regarded as a consequence of quantum ground-state fluctuations. To obtain an intuitive insight to dispersion forces, consider first the corresponding classical situation: According to classical electrodynamics, two neutral, unpolarised objects will not interact with each other in general, even if they are polarisable. An interaction can only occur if (i) at least one of the objects is polarised or (ii) an electromagnetic field is applied to at least one of the objects: In the former case the object's polarisation will give rise to an electromagnetic field, which can induce a polarisation of the other polarisable object; in the latter case the applied field induces a polarisation of the first object, which in turn gives rise to an electromagnetic field acting on the other object. Both cases lead to an arrangement of polarised objects interacting via an electromagnetic field, the resulting force being a consequence of the departure from the classical ground state (unpolarised objects and vanishing electromagnetic field).

In QED, the ground state is given by the objects being in their quantum ground states and the electromagnetic field being in its vacuum state, where both polarisation and electromagnetic field vanish on the quantum average. At first glance, one could hence expect the absence of any interaction between the objects. However, the Heisenberg uncertainty principle implying the existence of ground-state fluctuations, both (i) a fluctuating polarisation and (ii) a fluctuating electromagnetic field will always be present. They give rise to an interaction and consequently a non-vanishing dispersion force between the objects – manifesting itself as a pure quantum effect.

Thus, dispersion forces are ever-present effective electromagnetic forces between atoms

1

and/or macroscopic bodies. In particular, we will in the following refer to the atom–atom [1, 2], atom–body [2, 3] and body–body dispersion forces [4, 5] as van der Waals (vdW), CP and Casimir forces, respectively.[1] Naturally, dispersion forces have many important consequences. On a microscopic level, they influence the properties of weakly bound molecules [6, 7]. A prominent macroscopic signature of dispersion forces is the well-known correction to the equation of state of an ideal gas, leading to the more general vdW equation of state [8]. But the signature of dispersion forces is also manifest in the macroscopic properties of liquids and solids, where inter alia they are crucial for an understanding of the adhesion and fracture of solids [9]; the phase behaviour of dipolar fluids [10]; the melting of weakly bound crystals [11]; the anomalies of water [12]; and the magnetic, thermal and optical properties of solid oxygen [13].

The influence of dispersion forces becomes even more pronounced in the presence of interfaces between different phases and/or media. Dispersion interactions drive the adsorption of inert gas atoms to solid surfaces [14, 15], influence the wetting properties of liquids on such surfaces [15, 16] and lead to the phenomenon of capillarity [17]. The mutual dispersion attractions of colloidal particles suspended in a liquid [18] influence the stability of such suspensions [19]; unless sufficiently balanced by repulsive forces, they lead to a clustering of the particles, commonly known as flocculation [20].

The abovementioned relevance of dispersion forces to material sciences and physical chemistry being rather obvious, it is perhaps more surprising to note that they also play a role in astrophysics and biology. Thus, dispersion forces initiate the preplanetary dust aggregation leading to the formation of planets around a star [21]. Furthermore, they are crucial for an understanding of the properties of proteins [22], the interaction of molecules with cell membranes [8, 23, 24], and the cell adhesion driven by mutual cell-membrane interactions [8, 23, 25]. Recently, dispersion forces have been found to be responsible for the remarkable abilities of some gecko [26] and spider species [27] to climb smooth, dry surfaces.

1.2 The Casimir–Polder force

In this work, the CP force between a single neutral atom or molecule[2] and neutral magnetoelectric[3] bodies is studied. The focus will be on the pure vacuum CP force, i.e., the

---

[1]Note that alternative naming conventions are common in the literature. So, the notions vdW/CP force are often used to distinguish between different separations (small/large) instead of nature (atom/body) of the interacting objects. Furthermore, the term vdW force is often thought to even include body–body forces.

[2]For brevity, we will only speak of atoms in the following.

[3]The term electric is used where no explicit distinction is made between metals (conductors) and dielectrics (insulators). Likewise, the notion magnetoelectric is used to refer to metals or dielectrics possessing

electromagnetic field will in general be understood to be in its ground state. Furthermore, we assume that the atom–body separation is sufficiently large to ensure that the atom is adequately characterised as an electric dipole, while the body can be described by its macroscopic magnetoelectric properties; and that repulsive exchange forces [28] due to the overlap between the electronic wave functions of the atom and the bodies can be neglected. Interactions due to non-vanishing net charges, permanent electric dipole moments, magnetisability, quadrupole (or higher multipole) polarisabilities of the atom and those resulting from non-local or anisotropic magnetoelectric properties of the bodies will be ignored. A generalisation of the theory to include such effects is in most cases possible by supplementing the results with additive corrections.

1.2.1 Experiments

The simplest way to measure a force between a microscopic object and a macroscopic body is by performing a scattering experiment. Consequently, first evidence for CP forces was found in a series of experiments where the deflexion of a beam of ground-state atoms passing near metal and dielectric cylinders was observed, showing the existence of an attractive CP force proportional to $1/z^4$ for sufficiently small atom–body separations z [29]. Following a similar idea, the deflexion of atoms passing between two metal plates was monitored by measuring atom flux losses due to the sticking of atoms to the plates, where a strong enhancement of the CP interaction for excited atoms[4] was observed [30], and it was shown that the ground-state force becomes proportional to $1/z^5$ for large z [31, 32].[5]

More detailed studies of the CP force are possible by introducing a controllable compensating force, e.g., by using an evanescent-wave mirror [35]. Here, total reflexion of a laser beam inside a dielectric leads to an exponentially decaying electric field at its exterior. An atom placed in the vicinity of the body will interact with the evanescent field, leading to the required compensating force, sign and magnitude of which can be controlled by varying laser frequency and intensity. Following this idea, CP forces have been measured by monitoring the reflexion of ground-state atoms incident on evanescent-wave mirrors [36, 37]. Alternatively, compensating forces for CP force measurements can be provided by the magnetic fields created by magnetic films, with the strength being controlled by varying the film thickness [37]. An even more controlled access to CP forces can be obtained by studying the motion of atoms trapped in a known trapping potential which is then deformed by the atoms' CP interaction with a nearby body. Observation of the resulting change in the atomic

---

non-trivial magnetic properties.

[4]Unless otherwise stated, the term refers to atoms in excited energy eigenstates.

[5]For further reading, cf. the reviews [33, 34].

motion leads to very accurate measurements which was demonstrated using an excited ion trapped in a standing electromagnetic wave [38]; and gases of ground-state atoms confined in a magnetic trap [39] or an optical lattice [40]. In the latter experiment, a temperature dependence of the force has been observed.

Effects due to the wave nature of atomic motion become relevant for small centre-of-mass momentum, such that the atomic de Broglie wave length is sufficiently large. In this case, quantum reflexion of atoms from an attractive CP potential[6] may occur [41]. Quantum reflexion of atoms which are incident on the surface of dielectric bodies, was observed in various experiments [42] and by recording the reflectivities at different (normal) momenta, a detailed measurement of the CP potential was achieved for ground-state [43] as well as excited atoms [44]. Another prominent wave phenomenon that can be exploited for the measurement of the CP potential is the diffraction of an atomic wave which is incident on a periodic array of parallel slits (commonly referred to as a transmission grating). When passing through the slits, the atomic wave acquires phase shifts due to the CP interaction, which influence the interference pattern forming behind the slits. By comparing the experimental observations with theoretical simulations, the CP potential of ground-state [45, 46] as well as excited atoms [47] with dielectrics, has been measured.

Spectroscopic measurements provide a powerful indirect method for studying the CP interaction [34]. Here, the fact is exploited that the CP potential of an atom prepared in a certain energy eigenstate can be identified with the position-dependent shift of the respective atomic energy level [2]. Spectroscopic measurements of atomic transition frequencies thus provide information on the difference between the CP potentials of an atom, for instance, in excited and ground states. The transition-frequency shifts being usually dominated by the excited-state contribution, spectroscopy thus yields good estimates of the CP potentials of excited atoms. This has been demonstrated in experiments measuring the CP potentials of excited atoms inside planar [32, 48, 49] and spherical metallic cavities [50] or near a dielectric half space [51] and of an excited ion near a metal plate [52]. In this context, selective reflexion spectroscopy of atomic gases has proven to be a particularly powerful method [53]. It is based on the fact that the reflexion of a laser beam incident on a gas cell is modified due to the laser-induced polarisation of the gas atoms, which in turn is strongly influenced by the CP interaction of the atoms with the walls of the cell. By comparing measured reflectivity spectra with theoretically computed ones, very accurate information on the CP interaction of atoms with dielectric plates has been obtained [54],[7] including

---

[6]Note that the CP force is commonly regarded as a conservative force, with the resective potential being referred to as the CP potential.

[7]Note that the CP interaction with metallic plates is much more difficult to observe via selective reflexion spectroscopy [55].

the potentials of atoms in very short-lived excited states, which are difficult to study by scattering methods. As a major achievement, the method has shown that CP forces on excited atoms can be repulsive [56]. Recently, spectroscopic methods have been used to observe the motion of an atom placed within a cavity under the influence of the force due to strong, resonant coupling with a single cavity mode [49, 57]. It has been shown that for a suitably prepared state of the atom–field system, the atom is attracted to the antinodes of the mode.

1.2.2 Applications

Based on the methods described in the previous section, CP forces can nowadays be studied with an unprecedented accuracy – high precision measurements even place limits on non-standard gravitational forces on small length scales [39]. As a consequence, the focus of research has slightly shifted from the mere detection of CP forces towards controlling or even using them. Casimir–Polder forces often have a disturbing effect when atom traps are operated near surfaces. In particular, they can diminish the depth of magneto-optical traps, thereby imposing limits upon the near-surface operation of such traps [58]. Traps that are based on evanescent waves [59] or miniaturised charge and current-carrying wires [60] necessarily operate in the near-surface regime, so that CP forces cannot be avoided. On the other hand, it has been demonstrated that the CP forces arising for strong atom–field coupling can be used to construct single-photon based atom traps [57]. The disturbing influence of CP forces needs to be taken into account when constructing wire [60, 61] and/or evanescent-wave based elements for atom guiding [62], where the latter have been shown to provide a tool for controlled atom deposition on surfaces [63].

CP forces are indispensable in atom optics [64] where mirrors and beam splitters for atomic matter waves are realised, based on the CP potentials of flat surfaces and transmission gratings, respectively. Using several transmission gratings, a Mach–Zehnder interferometer for atoms has been realised [46]. Flat quantum reflective mirrors have been demonstrated to provide a one-dimensional focussing mechanism when the CP potential is combined with gravitational forces in an appropriate way [65]. In addition, by locally enhancing the reflectivity of such mirrors via a Fresnel reflexion structure [66], a reflective double-slit type interferometer [67] as well as more complex reflexion holograms for atomic matter waves have been realised [68]. By using evanescent waves, one can enhance and control the reflectivity of atomic mirrors [69]. As recently predicted, the quantum reflexion of ultracold gases at dielectric surfaces can (by means of the interference of incident and reflected matter waves) give rise to interesting phenomena, such as the excitation of solitons

and vortex structures [70].[8]

Further impact on the application of CP forces has been made by the recent proposal [72] and subsequent fabrication [73] of materials with tailored magnetodielectric properties, also known as metamaterials. Metamaterials displaying simultaneous negative permittivity and permeability in some frequency range, allow for the existence of travelling electromagnetic waves whose electric-field, magnetic-field and wave vector, form a left-handed triad,[9] leading to a number of unusual effects [75, SB3, SB4]. It is yet an open question whether left-handed properties can lead to new phenomena in the context of CP forces and to what extent metamaterials can be exploited to tailor the shape and sign of these forces. An interesting behaviour of dispersion forces may also occur in conjunction with soft-magnetic alloys, such as permalloy or Mumetal [76] which are in a state of extremely high permeability [77].

1.2.3 Theory

As already mentioned, CP forces arise from quantum zero-point fluctuations, namely the fluctuating charge and current distributions of the interacting objects and the vacuum fluctuations of the (transverse) electromagnetic field. If the atom–body separation is smaller than the wave lengths of the relevant field fluctuations, then the latter can be disregarded, allowing for a simplified treatment of dispersion forces. In this non-retarded regime, dispersion forces are dominated by the Coulomb interaction of fluctuating charge densities. Within a leading-order multipole expansion, this interaction may further be approximated by a dipole–dipole interaction. Such an approach was first employed by Lennard-Jones [3] who studied the CP interaction of a ground-state atom with a perfectly conducting plate. For this idealised problem, the Coulomb potential can be described by the atomic electric dipole moment interacting with its image in the plate. Taking the ground-state expectation value of the dipole–image interaction, Lennard-Jones obtained an attractive $1/z^4$ CP force. In subsequent works it was shown that the CP potential found for a perfect conductor has to be regarded as an upper bound to the result found for real metals [78] which is approached in the limits of rapid response and high density of the free metal electrons [79]. The image dipole method has been extended to include quadrupole [80] as well as higher multipole moments [81, 82] of the atom, leading to additional attractive force components which fall off more strongly with increasing atom–body separation. Furthermore, it has been applied to the interaction of ground-state atoms with semi-infinite metal half spaces

---

[8]For a theoretical analysis of interference phenomena within the context of ultracold gases, cf. also Refs. [71].

[9]For this reason materials with such properties are commonly referred to as left-handed materials. As proposed very recently, left-handed media might alternatively be realised by using a gas of atoms exhibiting suitable electric and magnetic dipole transitions [74].

[83] and non-dispersive dielectric multilayer plates [84] and can even be generalised to study the CP potential of a ground-state [85] or excited atom [86] near a dispersive and absorbing dielectric half space. In the latter case, resonant force components arise that exhibit the same $1/z^4$ distance dependence as the ground-state potential, but whose sign and magnitude delicately depend on the relative positions of the atomic and medium resonances.

In spite of its success and appealing simplicity, the image dipole method suffers from three main problems: Firstly, it predicts an infinitely strong potential in the limit $z \to 0$ (in contradiction with the finite binding energies of atoms on surfaces); secondly, the properties of the body are either strongly idealised (as in the case of the perfect conductor) or described in terms of quantities that are difficult to obtain by both theoretical and experimental means (as in early attempts to treat real metals in a more realistic way [78, 79]); and thirdly, it only applies to a very limited class of simple body shapes. It was found that these problems could be overcome by describing the atom and the body on an equal footing in terms of their charge densities and expressing the resulting interaction potential in terms of electrostatic linear response functions of the two systems.[10] This was first demonstrated for a ground-state atom interacting with a realistic electric half space exhibiting a non-local response [87] (cf. also Ref. [88]). The approach was shown to lead to a finite value of the interaction potential in the limit $z \to 0$ [81, 89, 90] (cf. also Ref. [91]). For sufficiently large values of z, the force on an atom in front of a half space can be given by an asymptotic power series in $1/z$ [81, 87, 90, 92] with the leading-order $1/z^4$ term being given in terms of the atomic dipole polarisability and the local electric permittivity of the half space. Next-order corrections are due to the atomic quadrupole polarisability on the one hand and the leading-order non-local response of the half space on the other hand. The response-function approach has been used to determine the (ground-state) force on an ion [93] and a permanently polarised atom [94] in front of a metal half space as well as that on an anisotropic molecule in front of an electric half space [95]. Extensions include the interaction of an excited atom with an electric [96] and birefringent dielectric half space [97], effects due to a constant external magnetic field [98], and friction forces exerted on moving atoms [99]. One major strength of the linear-response formalism is the fact that it can easily be applied to various geometries where the interaction of ground-state atoms with perfectly conducting [100], electric [100] and non-local metal spheres [101]; electric [102] and non-local metal cylinders [103]; and perfectly conducting planar [104] and non-local metallic spherical cavities [105], has been studied.

Even though electrostatic methods have been developed into a sophisticated theory cov-

---

[10]In contrast to the quantities appearing in the abovementioned early attempts, the two response functions are directly accessible to measurements.

ering various aspects of CP forces, they can only render approximate results valid in the non-retarded regime. For atom–body separations that are comparable to, or even larger than the relevant atomic and medium wave lengths, the interaction is no longer governed by the Coulomb potential alone and the transverse degrees of freedom of the electromagnetic field need to be included. Such a nonrelativistic QED description was first given by Casimir and Polder [2], who reconsidered the interaction of a ground-state atom with a perfectly conducting plate. Central ingredient to their approach is the quantisation of the electromagnetic field in terms of normal modes, which are the solutions to the free-space wave equation for the electromagnetic field obeying the idealised boundary conditions imposed by the perfect conductor. As demonstrated by Casimir and Polder the interaction of the atom with the quantised electromagnetic field, leads to a position-dependent shift of the atom's ground-state energy which is identified as the CP potential. Calculating this energy shift within leading-order perturbation theory, they were able to show that in the non-retarded regime their result reduces to the $1/z^4$ force found by Lennard-Jones, while in the opposite retarded regime (the atom–plate separation being much larger than the wave lengths of the relevant field fluctuations so that retardation effects due to the finite speed of electromagnetic waves play a major role), the force is proportional to $1/z^5$. The results of Casimir and Polder have been rederived [106, 107] and extended[11] where atoms carrying permanent electric dipole moments [108] or being magnetisable [109, 110] have been considered, the influence of relativistic effects [111] and current fluctuations [112] has been studied, and fluctuations of the force have been calculated [113]. It was found that the retarded ground-state force at finite temperature decreases more slowly ($\propto 1/z^4$) than in the zero-temperature limit as soon as the atom–plate separation exceeds the thermal wave length [114, 115] and that the force on an excited atom exhibits an oscillatory behaviour in the retarded regime [116, 117, 118, 119] – making the influence of transverse electromagnetic waves on the interaction even more explicit than in the case of a ground-state atom. Furthermore, the theory has been extended beyond the case of a single plate: Forces on ground-state atoms inside perfectly conducting parabolic cavities [120] and on ground-state [121] and excited atoms [108, 122] placed within perfectly conducting planar cavities, have been determined by using perturbation theory in conjunction with the normal modes associated with these geometries.

In this context, it should be noted that perturbative techniques may fail when an excited atom near-resonantly interacts with a single mode of a cavity. Instead, the arising strong atom–field coupling may be treated within the Jaynes–Cummings model [123] where the

---

[11]For a review, cf. Refs. [33, 34].

attention is restricted to the interaction of a two-level atom with the cavity mode. Within this model, the eigenstates of the system – commonly known as dressed states – can be found in a non-perturbative way, with the associated eigenenergies being interpreted as the CP potential in straightforward generalisation of the perturbative case [119, 124]. It turns out that, depending on the dressed state the system is prepared in, the atom may be attracted to or repelled from the nodes of the cavity mode.

Returning to the discussion of the perturbative force, it can be noted that a major development of the normal-mode approach consisted in the extension to bodies with more realistic material properties. To this end, the normal-mode concept had to be generalised by allowing for the more general boundary conditions imposed by these bodies. The interaction of a ground-state atom with a metal half space was addressed by considering the boundary conditions given by the behaviour of the free metal electrons [125], revealing that the result of Casimir and Polder has to be regarded as an upper limit to the CP potentials created by real metals. For (magneto)electric bodies, the appropriate boundary conditions for the normal modes follow from the well-known conditions of continuity of the macroscopic electromagnetic field. The resulting normal-mode expansions for the QED field have been used to derive the ground-state CP potentials of atoms near electric [126], magnetoelectric half spaces [127]; inside planar electric cavities [128, 129]; as well as the CP potentials of excited atoms near an electric half space [130] or multilayer system [131]; and inside a spherical electric cavity [132].

Normal-mode QED has thus shown to render an exact approach to the problem of the CP interaction that extends the electrostatic results beyond the non-retarded limit. The method, however, suffers from two major limitations: It is not applicable in the presence of absorbing bodies, and the extension to bodies of various shapes is extremely cumbersome even for relatively simple geometries. Particularly in view of the second limitation, linear-response theory[12] was used to develop an approach that does not rely on an explicit field quantisation and can hence render geometry-independent results: Making use of the fluctuation–dissipation theorem, the perturbative interaction energy of the atom and the QED field could be reformulated in terms of the linear response functions of the two systems – the atomic polarisability on the one hand and the Green tensor for the electromagnetic field on the other [133, 134, 135, 136, 137, 138][13]. The obtained result can hence be applied to bodies of various shapes and materials in a straightforward way by using the appropriate Green tensor. This was demonstrated by calculating the CP interaction of a ground-state

---

[12]Note that the method is a natural extension of the linear-response techniques employed within the context of electrostatic theory.

[13]For an alternative, semiclassical approach based on finding the eigenenergies of the classical electromagnetic field interacting with a harmonic-oscillator atom, see Ref. [139].

atom with a multitude of bodies such as: Perfectly conducting plates [133, 135, 138]; electric [32, 134, 135, 138, 140] and magnetoelectric half spaces [141]; metal half spaces exhibiting non-local properties [137, 142] and/or surface roughness [137] or being covered by a thin overlayer [143]; perfectly conducting [144] and dielectric spheres [140, 145, 146]; dielectric cylinders [140, 147, 148]; perfectly conducting and electric planar cavities [149]; dielectric spherical [150], cylindrical [148] and perfectly conducting wedge-shaped cavities [146]. The linear-response result for the CP potential being based on the fluctuation–dissipation theorem (which is only valid in equilibrium situations), cannot be directly applied to excited atoms. An extension to excited atoms was developed by starting again from the perturbative expression for the atom–field coupling energy, but only expressing the field contribution in terms of the respective response function. In this way, CP forces on excited atoms in front of perfectly conducting plates and dielectric half spaces [151, 152] with the latter exhibiting birefringence [153] or surface roughness [154], has been derived. In further extensions of the QED-based linear-response approach the influence of finite temperature [155, 156, 157], anisotropic atomic polarisabilities [158], and non-vanishing atomic velocities [156] on the force, was investigated.

The approaches to the CP interaction of an atom with a body presented so far have been based on an essentially macroscopic description of the body. In contrast, a number of microscopic models have also been developed, where the body is being thought of as composed of a collection of atoms. Such an approach was first used for studying the interaction of a ground-state atom with a dielectric half space [159]. Modelling both single and body atoms by harmonic oscillators interacting via the free-space QED field, an exact expression for the total CP force on the single atom due to its vdW interactions with the half-space atoms could be derived, which was shown to be equivalent to the respective result obtained from macroscopic theories. These considerations, which may be regarded as a substantiation of the macroscopic approaches, were later extended to dielectric bodies of arbitrary shape [160] and beyond the harmonic oscillator model [107, 161]. Further extensions include excited atoms [162] or even excited bodies [163].

While in microscopic approaches the CP force between an atom and a body is derived from interatomic vdW forces, one can also go to the other (macroscopic) extreme and infer the atom–body force from the Casimir force between two bodies. This was first demonstrated for a planar geometry by starting from the Casimir force between two dielectric half spaces and assuming one of the half spaces to be filled with a dilute gas of atoms [5, 164]. In this case, the force on the respective half space can be written as a volume integral over the CP forces exerted on the gas atoms by the second half space, so the latter can be

deduced from the former in a straightforward way. The method was also applied to the finite-temperature case [165], and by taking advantage of the fact that solutions for the Casimir force are readily available for a wide class of geometries, the CP interaction of ground-state atoms with various bodies, such as rough [166] or anisotropic electric [167], (isotropic) magnetoelectric half spaces [168]; electric spheres [169]; spherical cavities [169] and cylinders [167, 169]; and cylindrical cavities [169] was obtained.

1.3 Motivation and outline

Owing to the recent progress in high-precision measurements of CP forces and in view of modern applications in nano physics, the current work aims at formulating a unified theory of CP forces. Since concepts of macroscopic electrodynamics remain valid even on micro and nano scales, involved microscopic treatments can be avoided in virtually all cases of interest. As outlined above, a number of macroscopic approaches to the CP force have been developed (rendering results that are valid provided that all atom–body separations are large with respect to the typical length scales associated with the internal, microscopic structure of the bodies), with each method having its intrinsic advantages and limitations.

Time-independent, perturbative calculations based on normal-mode QED give an exact Hamiltonian approach to the CP force; however, applications to various problems have shown that the method is not very flexible, because the geometry of the present bodies must be taken into account at a very early stage of the calculation. Normal-mode techniques fail in the presence of absorbing bodies and have not yet been fully developed for bodies possessing magnetic properties. Furthermore, leading-order perturbation theory cannot account for the influence of the finite shifts and widths of atomic transitions on the force; and a static description completely disregards the dynamics of the CP force to be expected for excited atoms, in particular the phenomena expected to occur for strong atom–field coupling.

Methods based on linear-response theory overcome some of these problems by rendering general results that have been demonstrated to be easily applicable to various geometries. The price paid for the increased practicability is the fact that the theory is not based on an explicit quantisation scheme and is thus less rigorous. Unless founded on the corresponding normal-mode results, it has to be regarded as a semi-phenomenological theory, which is based on the fluctuation–dissipation theorem as a central assumption. This holds particularly for its applicability in the presence of absorbing or magnetic bodies, where no normal-mode QED foundation is available. Since the theory effectively remains in the perturbative realm,

the abovementioned questions regarding the role of finite line shifts and widths remain unanswered; and the static, equilibrium approach is not able to address dynamical aspects like the phenomenon of strong coupling.

These deficiencies shall be overcome in the current work by developing a unified (macroscopic) theory of the CP force that incorporates the benefits of both normal-mode QED and linear-response theory approaches. Prominent results that have been obtained by various means will thus be founded and extended within a common framework that is sufficiently general to allow for a discussion of entirely new aspects of the CP force. In particular, the theory is required to

- apply to bodies with both electric and magnetic properties,
- account for both dispersion and material absorption,
- render general results that can easily applied to various geometries,
- allow for including local-field effects,
- be able to address the relation between the CP force and microscopic vdW forces,
- explicitly reveal the influence of atomic line shifts and widths,
- allow for a dynamical description,
- be applicable for both weak and strong atom–field coupling.

As a starting point for achieving these goals, a Hamiltonian-based, geometry-independent quantisation for the electromagnetic field in the presence of dispersing and absorbing magnetodielectric bodies will be presented in chapter 2. Within the context of this work, the existing macroscopic QED in linear, causal dielectrics [170] has been extended to magnetoelectric bodies [SB1, SB3, SB4] in order to provide for a sufficiently general basis. As shown, the interaction of the body-assisted electromagnetic field with atoms can be introduced in straightforward generalisation of procedures commonly used in the context of normal-mode QED, where both minimal and multipolar coupling schemes are elaborated [SB6].

In chapter 3, macroscopic QED is used to investigate the static aspects of the CP force on an atom prepared in an arbitrary energy eigenstate. It is shown that Casimir and Polder's pioneering concept of deriving the CP from the atom–field coupling energy [2] can be used within the context of macroscopic QED, leading to very general expressions for the CP potential of an atom in the presence of an arbitrary arrangement of magnetoelectric bodies [SB1, SB5, SB6, SB7, SB8]. Formulae of this kind, which for electric bodies have been obtained previously on the basis of linear response theory, are thus derived for the first time by means of an exact quantisation scheme that explicitly allows for dispersing and absorbing magnetoelectric bodies. It is shown that minimal and multipolar coupling schemes lead to formally equivalent expressions [SB6]. Macroscopic theories of the CP potential typically

being only valid for atoms situated in free-space regions, we extend our results to atoms embedded in a body [SB15] by including local-field effects via the real-cavity model [SB11]. A useful approximation scheme for calculating the CP potentials of atoms placed near weakly magnetodielectric bodies is developed by means of the Born expansion [SB1, SB10]. In particular, the Born expansion is used together with the Clausius–Mosotti law to illustrate the microscopic origin of the CP potential [SB10, SB13]. As a side result, the derivation renders general formulae for the vdW interaction of two or more atoms in the presence of magnetoelectric bodies [SB1, SB10, SB12, SB13, SB14], which are consistent with the prominent results for atoms situated in free space. Next, we illustrate the application of the general formulae for the CP force to specific arrangements of bodies. In particular, we consider ground-state atoms placed within planar multilayer systems [SB1, SB7, SB8, SB9], generalising known results for atoms interacting with a perfectly conducting plate, semi-infinite half space, plate of finite thickness, and planar cavity to the magnetoelectric case. Finally, the results obtained for the various scenarios are summarised and supplemented with further examples [SB5, SB10, SB13] to give a comparison of dispersion forces between various polarisable and magnetisable ground-state objects.

Chapter 4 is devoted to the dynamical aspects of the CP force which have never been addressed so far. The starting point is the time-dependent operator Lorentz force which is deduced from the Heisenberg equation for the centre-of-mass motion of the atom. The calculation renders general formulae for the force expressed in terms of the atomic and field variables [SB1, SB6, SB7, SB8]. After explicitly verifying that minimal and multipolar coupling lead to identical results [SB6], the attention is restricted to the multipolar coupling scheme for simplicity. While our approach can be used to study radiation forces on atoms under quite general conditions, the CP force is given by the particular case of the body-assisted field initially being prepared in its ground state; explicit expressions can be obtained by solving the atom–field dynamics. For weak atom–field coupling, this may be done by means of the Markov approximation, and it is found that the CP force may be written as a linear superposition of force components which are weigthed by the respective internal atomic density matrix elements [SB1, SB6, SB7, SB8]. The force components are influenced by the body-induced shifting and broadening of atomic transitions; this is studied in more detail by considering the example of an atom placed near a half space. The strong atom–field coupling that may occur when an excited atom interacts with a narrow quasi-mode of the body-assisted field, is more adequately addressed by solving the strongly coupled dynamics of a single atomic transition and the quasi-mode in an exact way. It is found that the resonant part of the CP force undergoes Rabi oscillations, the amplitude and mean value

of which delicately depends on the initial state of the atom–field system [SB1, SB16]. As demonstrated, the results for the system being initially prepared in a quasi-stationary state, agree in some approximation with the findings of the well-known dressed-state approach [SB16].

The main results of this work are summarised in chapter 5, where remaining open questions and possible extensions are also addressed – some of them being subject to ongoing research.

Chapter 2

QED in linear magnetoelectrics

In this chapter, as a general basis, a quantisation scheme for the macroscopic electromagnetic field in the presence of magnetoelectric bodies is given, with special emphasis on the interaction of the field with single atoms. The macroscopic QED outlined in the following has been developed by extending existing quantisation schemes for purely electric bodies [170] to the magnetoelectric case [SB1, SB3, SB4]. It may be regarded as the generalisation of the well-known normal-mode QED to the case of dispersing and absorbing bodies.

2.1   Medium-assisted electromagnetic field

A good starting point for the quantisation of the (macroscopic) electromagnetic field in the presence of magnetoelectric media is given by the Maxwell equations. For the field components in the frequency domain,

$$\hat{O}(\boldsymbol{r}) = \int_0^\infty \mathrm{d}\omega\, \underline{\hat{O}}(\boldsymbol{r}, \omega) + \mathrm{H.c.}, \tag{2.1}$$

these equations, in the absence of free charges and currents, are given by [SB1, SB3, SB4]

$$\boldsymbol{\nabla}\cdot\underline{\hat{\boldsymbol{B}}}(\boldsymbol{r},\omega) = 0, \tag{2.2}$$

$$\boldsymbol{\nabla}\cdot\underline{\hat{\boldsymbol{D}}}(\boldsymbol{r},\omega) = 0, \tag{2.3}$$

$$\boldsymbol{\nabla}\times\underline{\hat{\boldsymbol{E}}}(\boldsymbol{r},\omega) - \mathrm{i}\omega\underline{\hat{\boldsymbol{B}}}(\boldsymbol{r},\omega) = \boldsymbol{0}, \tag{2.4}$$

$$\boldsymbol{\nabla}\times\underline{\hat{\boldsymbol{H}}}(\boldsymbol{r},\omega) + \mathrm{i}\omega\underline{\hat{\boldsymbol{D}}}(\boldsymbol{r},\omega) = \boldsymbol{0} \tag{2.5}$$

together with

$$\underline{\hat{\boldsymbol{D}}}(\boldsymbol{r},\omega) = \varepsilon_0\underline{\hat{\boldsymbol{E}}}(\boldsymbol{r},\omega) + \underline{\hat{\boldsymbol{P}}}(\boldsymbol{r},\omega), \tag{2.6}$$

$$\underline{\hat{\boldsymbol{H}}}(\boldsymbol{r},\omega) = \kappa_0\underline{\hat{\boldsymbol{B}}}(\boldsymbol{r},\omega) - \underline{\hat{\boldsymbol{M}}}(\boldsymbol{r},\omega) \tag{2.7}$$

($\kappa_0 = \mu_0^{-1}$). Here, $\hat{\boldsymbol{E}}$ and $\hat{\boldsymbol{B}}$ denote electric field and (magnetic) induction field, $\hat{\boldsymbol{D}}$ and $\hat{\boldsymbol{H}}$ refer to (electric) displacement field and magnetic field, and $\hat{\boldsymbol{P}}$ and $\hat{\boldsymbol{M}}$ are the medium polarisation and magnetisation, respectively. In particular, it is assumed that the response of the media is linear, isotropic and local, in which case the constitutive relations read

$$\underline{\hat{\boldsymbol{P}}}(\boldsymbol{r},\omega) = \varepsilon_0[\varepsilon(\boldsymbol{r},\omega) - 1]\underline{\hat{\boldsymbol{E}}}(\boldsymbol{r},\omega) + \underline{\hat{\boldsymbol{P}}}_{\mathrm{N}}(\boldsymbol{r},\omega), \tag{2.8}$$

$$\underline{\hat{\boldsymbol{M}}}(\boldsymbol{r},\omega) = \kappa_0[1 - \kappa(\boldsymbol{r},\omega)]\underline{\hat{\boldsymbol{B}}}(\boldsymbol{r},\omega) + \underline{\hat{\boldsymbol{M}}}_{\mathrm{N}}(\boldsymbol{r},\omega) \tag{2.9}$$

$[\kappa(\boldsymbol{r},\omega) = \mu^{-1}(\boldsymbol{r},\omega)]$, with $\varepsilon(\boldsymbol{r},\omega)$ and $\mu(\boldsymbol{r},\omega)$ denoting the (relative) electric permittivity[1] and magnetic permeability of the media, respectively. Both quantities are complex-valued functions that vary with space and frequency, with the Kramers–Kronig relations being satisfied in accordance with causality [171]. Since the media are absorbing $[\mathrm{Im}\,\varepsilon(\boldsymbol{r},\omega) > 0$ and $\mathrm{Im}\,\mu(\boldsymbol{r},\omega) > 0]$, noise polarisation $\hat{\boldsymbol{P}}_{\mathrm{N}}$ and noise magnetisation $\hat{\boldsymbol{M}}_{\mathrm{N}}$ have been included, which are unavoidably associated with electric and magnetic losses.

Note that the theory presented so far is completely analogous to classical electrodynamics in the presence of dispersing and absorbing media. An explicit quantisation is accomplished by solving the set of equations (2.2)–(2.9) in terms of the fundamental degrees of freedom and imposing suitable commutation relations. Substituting Eqs. (2.6)–(2.9) into Eq. (2.5) and making use of Eq. (2.4), one may verify that the electric field obeys a Helmholtz equation

$$\left[\boldsymbol{\nabla}\times\kappa(\boldsymbol{r},\omega)\boldsymbol{\nabla}\times\; -\frac{\omega^2}{c^2}\,\varepsilon(\boldsymbol{r},\omega)\right]\underline{\hat{\boldsymbol{E}}}(\boldsymbol{r},\omega) = \mathrm{i}\omega\mu_0\underline{\hat{\boldsymbol{j}}}_{\mathrm{N}}(\boldsymbol{r},\omega), \qquad (2.10)$$

the source term of which is given by the noise current density

$$\underline{\hat{\boldsymbol{j}}}_{\mathrm{N}}(\boldsymbol{r},\omega) = -\mathrm{i}\omega\underline{\hat{\boldsymbol{P}}}_{\mathrm{N}}(\boldsymbol{r},\omega) + \boldsymbol{\nabla}\times\underline{\hat{\boldsymbol{M}}}_{\mathrm{N}}(\boldsymbol{r},\omega). \qquad (2.11)$$

Note that noise current density and noise charge density

$$\hat{\underline{\rho}}_{\mathrm{N}}(\boldsymbol{r},\omega) = -\boldsymbol{\nabla}\cdot\hat{\underline{\boldsymbol{P}}}_{\mathrm{N}}(\boldsymbol{r},\omega) \qquad (2.12)$$

fulfil the continuity equation

$$-\mathrm{i}\omega\hat{\underline{\rho}}_{\mathrm{N}}(\boldsymbol{r},\omega) + \boldsymbol{\nabla}\cdot\hat{\underline{\boldsymbol{j}}}_{\mathrm{N}}(\boldsymbol{r},\omega) = 0. \qquad (2.13)$$

Upon introducing the (classical) Green tensor which is defined by the equation

$$\left[\boldsymbol{\nabla}\times\kappa(\boldsymbol{r},\omega)\boldsymbol{\nabla}\times\; -\frac{\omega^2}{c^2}\,\varepsilon(\boldsymbol{r},\omega)\right]\boldsymbol{G}(\boldsymbol{r},\boldsymbol{r}',\omega) = \delta(\boldsymbol{r}-\boldsymbol{r}')\boldsymbol{I} \qquad (2.14)$$

($\boldsymbol{I}$, unit tensor) together with the boundary condition $\boldsymbol{G}(\boldsymbol{r},\boldsymbol{r}',\omega)\to\boldsymbol{0}$ for $|\boldsymbol{r}-\boldsymbol{r}'|\to\infty$, the solution to Eq. (2.10) can be given in the form

$$\underline{\hat{\boldsymbol{E}}}(\boldsymbol{r},\omega) = \mathrm{i}\omega\mu_0\int\mathrm{d}^3r'\,\boldsymbol{G}(\boldsymbol{r},\boldsymbol{r}',\omega)\cdot\underline{\hat{\boldsymbol{j}}}_{\mathrm{N}}(\boldsymbol{r}',\omega). \qquad (2.15)$$

It should be pointed out that the Green tensor is uniquely defined by Eq. (2.14) provided that the strict inequalities $\mathrm{Im}\,\varepsilon(\boldsymbol{r},\omega) > 0$ and $\mathrm{Im}\,\mu(\boldsymbol{r},\omega) > 0$ hold. Note that it is an analytic

---

[1]Note that both metals and dielectrics can be described in terms of their permittivity, where it is commonly assumed that the permittivity of a dielectric is analytic in the whole upper half of the complex frequency plane, whereas that of a metal exhibits a single pole at $\omega = 0$ [171].

function of ω in the upper complex half plane and has the following useful properties [170, SB3]:

$$\boldsymbol{G}^*(\boldsymbol{r}, \boldsymbol{r}', \omega) = \boldsymbol{G}(\boldsymbol{r}, \boldsymbol{r}', -\omega^*), \tag{2.16}$$

$$\boldsymbol{G}(\boldsymbol{r}, \boldsymbol{r}', \omega) = \boldsymbol{G}^{\mathrm{T}}(\boldsymbol{r}', \boldsymbol{r}, \omega), \tag{2.17}$$

$$\int \mathrm{d}^3 s \left\{ \mathrm{Im}\, \kappa(\boldsymbol{s}, \omega) \left[\boldsymbol{G}(\boldsymbol{r}, \boldsymbol{s}, \omega) \times \overleftarrow{\boldsymbol{\nabla}}_{\boldsymbol{s}} \right] \cdot \left[\boldsymbol{\nabla}_{\boldsymbol{s}} \times \boldsymbol{G}^*(\boldsymbol{s}, \boldsymbol{r}', \omega) \right] \right.$$

$$\left. + \frac{\omega^2}{c^2} \mathrm{Im}\, \varepsilon(\boldsymbol{s}, \omega)\, \boldsymbol{G}(\boldsymbol{r}, \boldsymbol{s}, \omega) \cdot \boldsymbol{G}^*(\boldsymbol{s}, \boldsymbol{r}', \omega) \right\} = \mathrm{Im}\, \boldsymbol{G}(\boldsymbol{r}, \boldsymbol{r}', \omega) \tag{2.18}$$

($A_{ij}^{\mathrm{T}} = A_{ji}$; $\overleftarrow{\boldsymbol{\nabla}}$ introduces differentiation to the left).

Having thus expressed the electric field in terms of noise polarisation and noise magnetisation, (explicit) quantisation can be performed by relating these quantities to the dynamical variables $\hat{\boldsymbol{f}}_e(\boldsymbol{r}, \omega)$ and $\hat{\boldsymbol{f}}_m(\boldsymbol{r}, \omega)$ ($\lambda, \lambda' \in \{e, m\}$) of the system (which consists of the electromagnetic field and the magnetoelectric matter, including the dissipative system responsible for absorption), as follows [SB1, SB3, SB4]:

$$\underline{\hat{\boldsymbol{P}}}_{\mathrm{N}}(\boldsymbol{r}, \omega) = \mathrm{i}\, \sqrt{\frac{\hbar \varepsilon_0}{\pi} \mathrm{Im}\, \varepsilon(\boldsymbol{r}, \omega)}\, \hat{\boldsymbol{f}}_e(\boldsymbol{r}, \omega), \tag{2.19}$$

$$\underline{\hat{\boldsymbol{M}}}_{\mathrm{N}}(\boldsymbol{r}, \omega) = \sqrt{-\frac{\hbar \kappa_0}{\pi} \mathrm{Im}\, \kappa(\boldsymbol{r}, \omega)}\, \hat{\boldsymbol{f}}_m(\boldsymbol{r}, \omega) = \sqrt{\frac{\hbar}{\pi \mu_0} \frac{\mathrm{Im}\, \mu(\boldsymbol{r}, \omega)}{|\mu(\boldsymbol{r}, \omega)|^2}}\, \hat{\boldsymbol{f}}_m(\boldsymbol{r}, \omega), \tag{2.20}$$

with $\hat{\boldsymbol{f}}_\lambda(\boldsymbol{r}, \omega)$ and $\hat{\boldsymbol{f}}_\lambda^\dagger(\boldsymbol{r}, \omega)$ being attributed to the collective Bosonic excitations of the system,

$$\left[\hat{f}_{\lambda i}(\boldsymbol{r}, \omega), \hat{f}_{\lambda' j}(\boldsymbol{r}', \omega') \right] = 0 = \left[\hat{f}_{\lambda i}^\dagger(\boldsymbol{r}, \omega), \hat{f}_{\lambda' j}^\dagger(\boldsymbol{r}', \omega') \right], \tag{2.21}$$

$$\left[\hat{f}_{\lambda i}(\boldsymbol{r}, \omega), \hat{f}_{\lambda' j}^\dagger(\boldsymbol{r}', \omega') \right] = \delta_{\lambda \lambda'} \delta_{ij} \delta(\boldsymbol{r} - \boldsymbol{r}') \delta(\omega - \omega'). \tag{2.22}$$

By substituting Eqs. (2.19) and (2.20) into Eq. (2.15) together with Eq. (2.11) and recalling Eq. (2.1), the medium-assisted electric field may be expressed in terms of the dynamical variables,

$$\hat{\boldsymbol{E}}(\boldsymbol{r}) = \int_0^\infty \mathrm{d}\omega\, \underline{\hat{\boldsymbol{E}}}(\boldsymbol{r}, \omega) + \mathrm{H.c.}$$

$$= \sum_{\lambda = e, m} \int \mathrm{d}^3 r' \int_0^\infty \mathrm{d}\omega\, \boldsymbol{G}_\lambda(\boldsymbol{r}, \boldsymbol{r}', \omega) \cdot \hat{\boldsymbol{f}}_\lambda(\boldsymbol{r}', \omega) + \mathrm{H.c.} \tag{2.23}$$

with

$$\boldsymbol{G}_e(\boldsymbol{r}, \boldsymbol{r}', \omega) = \mathrm{i}\, \frac{\omega^2}{c^2} \sqrt{\frac{\hbar}{\pi \varepsilon_0} \mathrm{Im}\, \varepsilon(\boldsymbol{r}', \omega)}\, \boldsymbol{G}(\boldsymbol{r}, \boldsymbol{r}', \omega), \tag{2.24}$$

$$\boldsymbol{G}_m(\boldsymbol{r}, \boldsymbol{r}', \omega) = \mathrm{i}\, \frac{\omega}{c} \sqrt{-\frac{\hbar}{\pi \varepsilon_0} \mathrm{Im}\, \kappa(\boldsymbol{r}', \omega)}\, \left[\boldsymbol{\nabla}' \times \boldsymbol{G}(\boldsymbol{r}', \boldsymbol{r}, \omega) \right]^{\mathrm{T}}. \tag{2.25}$$

Note that the integral relation (2.18) implies

$$\sum_{\lambda=e,m} \int \mathrm{d}^3 s \, \boldsymbol{G}_\lambda(\boldsymbol{r}, \boldsymbol{s}, \omega) \cdot \boldsymbol{G}_\lambda^{*\mathrm{T}}(\boldsymbol{r}', \boldsymbol{s}, \omega) = \frac{\hbar\mu_0}{\pi} \, \omega^2 \mathrm{Im} \, \boldsymbol{G}(\boldsymbol{r}, \boldsymbol{r}', \omega). \qquad (2.26)$$

Expressions of all other relevant fields in terms of the dynamical variables follow from this result by virtue of the Maxwell equations in frequency space together with the constitutive relations. Thus, Eq. (2.4) leads to

$$\hat{\boldsymbol{B}}(\boldsymbol{r}) = \sum_{\lambda=e,m} \int \mathrm{d}^3 r' \int_0^\infty \frac{\mathrm{d}\omega}{\mathrm{i}\omega} \, \boldsymbol{\nabla} \times \boldsymbol{G}_\lambda(\boldsymbol{r}, \boldsymbol{r}', \omega) \cdot \hat{\boldsymbol{f}}_\lambda(\boldsymbol{r}', \omega) + \mathrm{H.c.} \qquad (2.27)$$

while $\hat{\boldsymbol{D}}$, $\hat{\boldsymbol{H}}$, $\hat{\boldsymbol{P}}$ and $\hat{\boldsymbol{M}}$ can be found from Eqs. (2.6)–(2.9), (2.19) and (2.20). Commutation relations for the fields can be deduced from the commutation relations of the dynamical variables $\hat{\boldsymbol{f}}_\lambda(\boldsymbol{r}, \omega)$ and $\hat{\boldsymbol{f}}_\lambda^\dagger(\boldsymbol{r}, \omega)$ in a straightforward way [SB3]. In particular, it may be shown that electric field and induction field obey the well-known equal-time commutation relations (App. A.1)

$$\left[\hat{E}_i(\boldsymbol{r}), \hat{E}_j(\boldsymbol{r}')\right] = 0 = \left[\hat{B}_i(\boldsymbol{r}), \hat{B}_j(\boldsymbol{r}')\right], \qquad (2.28)$$

$$\left[\hat{E}_i(\boldsymbol{r}), \hat{B}_j(\boldsymbol{r}')\right] = -\mathrm{i}\hbar\varepsilon_0^{-1}\epsilon_{ijk}\partial_k\delta(\boldsymbol{r} - \boldsymbol{r}'). \qquad (2.29)$$

The ground state $|\{0\}\rangle$ of the medium-assisted electromagnetic field is defined by

$$\hat{\boldsymbol{f}}_\lambda(\boldsymbol{r}, \omega)|\{0\}\rangle = \boldsymbol{0} \quad \forall \, \lambda, \boldsymbol{r}, \omega \qquad (2.30)$$

and the Hilbert space can be spanned by Fock states obtained in the usual way by repeated application of the creation operators $\hat{\boldsymbol{f}}_\lambda^\dagger(\boldsymbol{r}, \omega)$ to this ground state. Obviously, the electric field (2.23) is vanishing on its vacuum average,

$$\langle \hat{\boldsymbol{E}}(\boldsymbol{r}) \rangle = \langle\{0\}|\hat{\boldsymbol{E}}(\boldsymbol{r})|\{0\}\rangle = \boldsymbol{0}, \qquad (2.31)$$

while it exhibits non-zero fluctuations (App. A.1)

$$\langle [\Delta\hat{\boldsymbol{E}}(\boldsymbol{r})]^2 \rangle = \langle\{0\}|\hat{\boldsymbol{E}}^2(\boldsymbol{r})|\{0\}\rangle - \langle\{0\}|\hat{\boldsymbol{E}}(\boldsymbol{r})|\{0\}\rangle^2 = \frac{\hbar\mu_0}{\pi} \int_0^\infty \mathrm{d}\omega \, \omega^2 \, \mathrm{tr}\left[\mathrm{Im} \, \boldsymbol{G}(\boldsymbol{r}, \boldsymbol{r}, \omega)\right] \qquad (2.32)$$

which are determined by the imaginary part of the Green tensor – in consistence with the fluctuation–dissipation theorem [172].

It is an almost trivial consequence of the presented quantisation procedure that upon choosing the Hamiltonian of the medium-assisted field to be

$$\hat{H}_\mathrm{F} = \sum_{\lambda=e,m} \int \mathrm{d}^3 r \int_0^\infty \mathrm{d}\omega \, \hbar\omega \, \hat{\boldsymbol{f}}_\lambda^\dagger(\boldsymbol{r}, \omega) \cdot \hat{\boldsymbol{f}}_\lambda(\boldsymbol{r}, \omega), \qquad (2.33)$$

the Heisenberg equation of motion

$$\dot{\hat{O}} = i\hbar^{-1}\left[\hat{H}, \hat{O}\right] \tag{2.34}$$

generates the correct time-dependence for the fields, such that the Maxwell equations

$$\boldsymbol{\nabla}\cdot\hat{\boldsymbol{B}}(\boldsymbol{r}) = 0, \tag{2.35}$$

$$\boldsymbol{\nabla}\cdot\hat{\boldsymbol{D}}(\boldsymbol{r}) = 0, \tag{2.36}$$

$$\boldsymbol{\nabla}\times\hat{\boldsymbol{E}}(\boldsymbol{r}) + \dot{\hat{\boldsymbol{B}}}(\boldsymbol{r}) = \boldsymbol{0}, \tag{2.37}$$

$$\boldsymbol{\nabla}\times\hat{\boldsymbol{H}}(\boldsymbol{r}) - \dot{\hat{\boldsymbol{D}}}(\boldsymbol{r}) = \boldsymbol{0} \tag{2.38}$$

are fulfilled (App. A.2).

In view of the treatment of atom–field interactions, it is useful to introduce scalar and vector potentials for the electric and induction fields,

$$\hat{\boldsymbol{E}}(\boldsymbol{r}) = -\boldsymbol{\nabla}\hat{\varphi}(\boldsymbol{r}) - \dot{\hat{\boldsymbol{A}}}(\boldsymbol{r}), \tag{2.39}$$

$$\hat{\boldsymbol{B}}(\boldsymbol{r}) = \boldsymbol{\nabla}\times\hat{\boldsymbol{A}}(\boldsymbol{r}). \tag{2.40}$$

In Coulomb gauge, $\boldsymbol{\nabla}\cdot\hat{\boldsymbol{A}}(\boldsymbol{r}){=}0$, the first and second terms on the right hand side of Eq. (2.39) are equal to the longitudinal ($\parallel$) and transverse ($\perp$) parts of the electric field where

$$\boldsymbol{a}^{\parallel(\perp)}(\boldsymbol{r}) = \int \mathrm{d}^3r'\,\boldsymbol{\delta}^{\parallel(\perp)}(\boldsymbol{r} - \boldsymbol{r}')\cdot\boldsymbol{a}(\boldsymbol{r}') \tag{2.41}$$

with

$$\boldsymbol{\delta}^{\parallel}(\boldsymbol{r}) = -\boldsymbol{\nabla}\boldsymbol{\nabla}\left(\frac{1}{4\pi r}\right), \qquad \boldsymbol{\delta}^{\perp}(\boldsymbol{r}) = \delta(\boldsymbol{r})\boldsymbol{I} - \boldsymbol{\delta}^{\parallel}(\boldsymbol{r}) \tag{2.42}$$

for an arbitrary vector field $\boldsymbol{a}(\boldsymbol{r})$; hence Eqs. (2.23), (2.33) and (2.34) imply that

$$\boldsymbol{\nabla}\hat{\varphi}(\boldsymbol{r}) = -\sum_{\lambda=e,m}\int \mathrm{d}^3r'\int_0^\infty \mathrm{d}\omega\,{}^{\parallel}\boldsymbol{G}_\lambda(\boldsymbol{r}, \boldsymbol{r}', \omega)\cdot\hat{\boldsymbol{f}}_\lambda(\boldsymbol{r}', \omega) + \mathrm{H.c.}, \tag{2.43}$$

$$\hat{\boldsymbol{A}}(\boldsymbol{r}) = \sum_{\lambda=e,m}\int \mathrm{d}^3r'\int_0^\infty \frac{\mathrm{d}\omega}{i\omega}\,{}^{\perp}\boldsymbol{G}_\lambda(\boldsymbol{r}, \boldsymbol{r}', \omega)\cdot\hat{\boldsymbol{f}}_\lambda(\boldsymbol{r}', \omega) + \mathrm{H.c.} \tag{2.44}$$

where

$${}^{\parallel(\perp)}\boldsymbol{T}^{\parallel(\perp)}(\boldsymbol{r}, \boldsymbol{r}') = \int \mathrm{d}^3s\int \mathrm{d}^3s'\,\boldsymbol{\delta}^{\parallel(\perp)}(\boldsymbol{r} - \boldsymbol{s})\cdot\boldsymbol{T}(\boldsymbol{s}, \boldsymbol{s}')\cdot\boldsymbol{\delta}^{\parallel(\perp)}(\boldsymbol{s}' - \boldsymbol{r}') \tag{2.45}$$

for an arbitrary tensor field $\boldsymbol{T}(\boldsymbol{r}, \boldsymbol{r}')$. Introducing the canonically conjugated momentum associated with the vector potential according to

$$\hat{\boldsymbol{\Pi}}(\boldsymbol{r}) = -\varepsilon_0\hat{\boldsymbol{E}}^{\perp}(\boldsymbol{r}), \tag{2.46}$$

one can easily verify the canonical equal-time commutation relations (App. A.1)

$$\left[\hat{A}_i(\boldsymbol{r}), \hat{A}_j(\boldsymbol{r}')\right] = 0 = \left[\hat{\Pi}_i(\boldsymbol{r}), \hat{\Pi}_j(\boldsymbol{r}')\right], \tag{2.47}$$

$$\left[\hat{A}_i(\boldsymbol{r}), \hat{\Pi}_j(\boldsymbol{r}')\right] = i\hbar\delta_{ij}^{\perp}(\boldsymbol{r} - \boldsymbol{r}'). \tag{2.48}$$

We conclude the section with some remarks concerning the validity of the quantisation scheme outlined above. It should be stressed that $\mathrm{Im}\,\varepsilon(\boldsymbol{r},\omega) > 0$ and $\mathrm{Im}\,\mu(\boldsymbol{r},\omega) > 0$ are assumed to hold everywhere. Even in almost empty regions or regions where absorption is very small and can be neglected in practice, the imaginary parts of the permittivity and permeability must not be set equal to zero in the integrands of expressions of the type (2.23). To allow for empty-space regions, the limits $\mathrm{Im}\,\varepsilon(\boldsymbol{r},\omega) \to 0$ and $\mathrm{Im}\,\mu(\boldsymbol{r},\omega) \to 0$ may be performed *a posteriori*, i.e., after taking the desired expectation values and having carried out all spatial integrals. In this sense the theory provides the quantised electromagnetic field in the presence of an arbitrary arrangement of linear, causal magnetoelectric bodies characterised by their permittivities and permeabilities, where $\mathrm{Im}\,\varepsilon(\boldsymbol{r},\omega) \geq 0$ and $\mathrm{Im}\,\mu(\boldsymbol{r},\omega) \geq 0$. The quantisation scheme (cf. also similar treatments treatments [173]) is in full agreement with the results of (quasi-)microscopic models of dielectric matter, where the polarisation is modelled by harmonic-oscillator fields and damping is accounted for by introducing a bath of additional harmonic oscillators [174].

2.2   Atom–field interactions

A neutral atom or a molecule A (briefly referred to as atom in the following) may be characterised as a system of particles $\alpha \in A$ with charges q_α ($\sum_{\alpha \in A} q_\alpha = 0$), masses m_α, positions $\hat{\boldsymbol{r}}_\alpha$ and canonically conjugated momenta $\hat{\boldsymbol{p}}_\alpha$, where the standard commutation relations [176]

$$\left[\hat{r}_{\alpha i}, \hat{r}_{\beta j}\right] = \left[\hat{p}_{\alpha i}, \hat{p}_{\beta j}\right] = 0, \qquad \left[\hat{r}_{\alpha i}, \hat{p}_{\beta j}\right] = \mathrm{i}\hbar\delta_{\alpha\beta}\delta_{ij} \tag{2.49}$$

hold. The nonrelativistic Hamiltonian governing the dynamics of the atom reads [176]

$$\hat{H}_A = \sum_{\alpha \in A} \frac{\hat{\boldsymbol{p}}_\alpha^2}{2m_\alpha} + \frac{1}{2}\int \mathrm{d}^3 r\,\hat{\rho}_A(\boldsymbol{r})\hat{\varphi}_A(\boldsymbol{r}) \tag{2.50}$$

with

$$\hat{\rho}_A(\boldsymbol{r}) = \sum_{\alpha \in A} q_\alpha \delta(\boldsymbol{r} - \hat{\boldsymbol{r}}_\alpha), \tag{2.51}$$

$$\hat{\varphi}_A(\boldsymbol{r}) = \int \mathrm{d}^3 r' \frac{\hat{\rho}_A(\boldsymbol{r}')}{4\pi\varepsilon_0 |\boldsymbol{r} - \boldsymbol{r}'|} = \sum_{\alpha \in A} \frac{q_\alpha}{4\pi\varepsilon_0 |\boldsymbol{r} - \hat{\boldsymbol{r}}_\alpha|} \tag{2.52}$$

denoting the charge density and scalar potential associated with the atom, respectively. Obviously, they obey the Poisson equation

$$\Delta\hat{\varphi}_A(\boldsymbol{r}) = -\varepsilon_0^{-1}\hat{\rho}_A(\boldsymbol{r}); \tag{2.53}$$

and the continuity equation

$$\dot{\hat{\rho}}_A(\boldsymbol{r}) + \boldsymbol{\nabla}\cdot\hat{\boldsymbol{j}}_A(\boldsymbol{r}) = 0 \tag{2.54}$$

holds, with the atomic current density being given by

$$\hat{\boldsymbol{j}}_A(\boldsymbol{r}) = \sum_{\alpha \in A} \frac{q_\alpha}{2} \Big[\dot{\hat{\boldsymbol{r}}}_\alpha \delta(\boldsymbol{r} - \hat{\boldsymbol{r}}_\alpha) + \delta(\boldsymbol{r} - \hat{\boldsymbol{r}}_\alpha) \dot{\hat{\boldsymbol{r}}}_\alpha \Big]. \tag{2.55}$$

It may be useful to introduce centre-of-mass and relative coordinates

$$\hat{\boldsymbol{r}}_A = \sum_{\alpha \in A} \frac{m_\alpha}{m_A} \hat{\boldsymbol{r}}_\alpha, \qquad \hat{\bar{\boldsymbol{r}}}_\alpha = \hat{\boldsymbol{r}}_\alpha - \hat{\boldsymbol{r}}_A \tag{2.56}$$

$(m_A = \sum_{\alpha \in A} m_\alpha)$ with the appropriate associated momenta being [175]

$$\hat{\boldsymbol{p}}_A = \sum_{\alpha \in A} \hat{\boldsymbol{p}}_\alpha, \qquad \hat{\bar{\boldsymbol{p}}}_\alpha = \hat{\boldsymbol{p}}_\alpha - \frac{m_\alpha}{m_A} \hat{\boldsymbol{p}}_A \tag{2.57}$$

such that the commutation relations

$$\big[\hat{r}_{Ai}, \hat{r}_{Aj} \big] = \big[\hat{p}_{Ai}, \hat{p}_{Aj} \big] = 0, \qquad \big[\hat{r}_{Ai}, \hat{p}_{Aj} \big] = \mathrm{i}\hbar\delta_{ij}, \tag{2.58}$$

$$\big[\hat{\bar{r}}_{\alpha i}, \hat{\bar{r}}_{\beta j} \big] = \big[\hat{\bar{p}}_{\alpha i}, \hat{\bar{p}}_{\beta j} \big] = 0, \qquad \big[\hat{\bar{r}}_{\alpha i}, \hat{\bar{p}}_{\beta j} \big] = \mathrm{i}\hbar \Big(\delta_{\alpha\beta} - \frac{m_\beta}{m_A} \Big) \delta_{ij} \simeq \mathrm{i}\hbar\delta_{\alpha\beta}\delta_{ij}, \tag{2.59}$$

$$\big[\hat{\bar{r}}_{\alpha i}, \hat{r}_{Aj} \big] = \big[\hat{\bar{p}}_{\alpha i}, \hat{p}_{Aj} \big] = \big[\hat{\bar{r}}_{\alpha i}, \hat{p}_{Aj} \big] = \big[\hat{r}_{Ai}, \hat{\bar{p}}_{\alpha j} \big] = 0, \tag{2.60}$$

follow from Eqs. (2.49), where the approximation in Eq. (2.59) is valid for electrons. Combining Eqs. (2.50) and (2.57), the atomic Hamiltonian may be written in the form

$$\hat{H}_A = \frac{\hat{\boldsymbol{p}}_A^2}{2m_A} + \sum_{\alpha \in A} \frac{\hat{\bar{\boldsymbol{p}}}_\alpha^2}{2m_\alpha} + \frac{1}{2} \int \mathrm{d}^3 r \, \hat{\rho}_A(\boldsymbol{r}) \hat{\varphi}_A(\boldsymbol{r}) = \frac{\hat{\boldsymbol{p}}_A^2}{2m_A} + \sum_n E_n |n\rangle\langle n| \tag{2.61}$$

with E_n and $|n\rangle$ denoting the eigenenergies and eigenstates of the internal Hamiltonian.

Further atomic quantities of interest are the atomic polarisation and magnetisation

$$\hat{\boldsymbol{P}}_A(\boldsymbol{r}) = \sum_{\alpha \in A} q_\alpha \hat{\bar{\boldsymbol{r}}}_\alpha \int_0^1 \mathrm{d}\sigma \, \delta\big(\boldsymbol{r} - \hat{\boldsymbol{r}}_A - \sigma\hat{\bar{\boldsymbol{r}}}_\alpha \big), \tag{2.62}$$

$$\hat{\boldsymbol{M}}_A(\boldsymbol{r}) = \sum_{\alpha \in A} \frac{q_\alpha}{2} \int_0^1 \mathrm{d}\sigma \, \sigma \big[\delta\big(\boldsymbol{r} - \hat{\boldsymbol{r}}_A - \sigma\hat{\bar{\boldsymbol{r}}}_\alpha \big) \hat{\bar{\boldsymbol{r}}}_\alpha \times \dot{\hat{\bar{\boldsymbol{r}}}}_\alpha - \dot{\hat{\bar{\boldsymbol{r}}}}_\alpha \times \hat{\bar{\boldsymbol{r}}}_\alpha \delta\big(\boldsymbol{r} - \hat{\boldsymbol{r}}_A - \sigma\hat{\bar{\boldsymbol{r}}}_\alpha \big) \big] \tag{2.63}$$

and the electric and magnetic dipole moments of the atom,

$$\hat{\boldsymbol{d}} = \sum_{\alpha \in A} q_\alpha \hat{\bar{\boldsymbol{r}}}_\alpha = \sum_{\alpha \in A} q_\alpha \hat{\boldsymbol{r}}_\alpha, \tag{2.64}$$

$$\hat{\boldsymbol{m}} = \sum_{\alpha \in A} \frac{q_\alpha}{2} \hat{\bar{\boldsymbol{r}}}_\alpha \times \dot{\hat{\bar{\boldsymbol{r}}}}_\alpha, \tag{2.65}$$

where the second equality in Eq. (2.64) holds for a neutral atom. As a direct consequence of the definitions, the atomic charge and current densities for a neutral atom can be expressed in terms of the atomic polarisation and magnetisation:

$$\hat{\rho}_A(\boldsymbol{r}) = -\boldsymbol{\nabla}\cdot\hat{\boldsymbol{P}}_A(\boldsymbol{r}), \tag{2.66}$$

$$\hat{\boldsymbol{j}}_A(\boldsymbol{r}) = \dot{\hat{\boldsymbol{P}}}_A(\boldsymbol{r}) + \boldsymbol{\nabla}\times\hat{\boldsymbol{M}}_A(\boldsymbol{r}) + \hat{\boldsymbol{j}}_{\mathrm{Ro}}(\boldsymbol{r}), \tag{2.67}$$

$$\hat{\boldsymbol{j}}_{\mathrm{Ro}}(\boldsymbol{r}) = \tfrac{1}{2}\,\boldsymbol{\nabla}\times\Big[\hat{\boldsymbol{P}}_A(\boldsymbol{r})\times\dot{\hat{\boldsymbol{r}}}_A - \dot{\hat{\boldsymbol{r}}}_A\times\hat{\boldsymbol{P}}_A(\boldsymbol{r}) \Big], \tag{2.68}$$

where $\hat{\boldsymbol{j}}_{\mathrm{Ro}}(\boldsymbol{r})$ is the Röntgen current [175, 176] which is due to the centre-of-mass motion of the atom. Equations (2.53) and (2.66) imply that

$$\boldsymbol{\nabla}\hat{\varphi}_A(\boldsymbol{r}) = \varepsilon_0^{-1}\hat{\boldsymbol{P}}_A^{\parallel}(\boldsymbol{r}). \tag{2.69}$$

Finally, note that using the atomic Hamiltonian (2.61) together with the commutation relations (2.59) and the definition (2.57), one can easily verify the useful relation

$$\sum_{\alpha \in A}\frac{q_\alpha}{m_\alpha}\,\langle m|\hat{\bar{\boldsymbol{p}}}_\alpha|n\rangle = \mathrm{i}\omega_{mn}\boldsymbol{d}_{mn} \tag{2.70}$$

with $\omega_{mn} = (E_m - E_n)/\hbar$ and $\boldsymbol{d}_{mn} = \langle m|\hat{\boldsymbol{d}}|n\rangle$ which in turn implies the well-known sum rule

$$\frac{1}{2\hbar}\sum_k \omega_{kn}(\boldsymbol{d}_{nk}\boldsymbol{d}_{kn} + \boldsymbol{d}_{kn}\boldsymbol{d}_{nk}) = \sum_{\alpha \in A}\frac{q_\alpha^2}{2m_\alpha}\,\boldsymbol{I}. \tag{2.71}$$

2.2.1 Minimal coupling

Having established the separate Hamiltonians of the body-assisted field and the atom, we next consider the atom–field interaction. According to the minimal coupling scheme (cf., e.g., Ref. [176]), this may be done by making the replacement $\hat{\boldsymbol{p}}_\alpha \mapsto \hat{\boldsymbol{p}}_\alpha - q_\alpha\hat{\boldsymbol{A}}(\hat{\boldsymbol{r}}_\alpha)$ in the atomic Hamiltonian, summing $\hat{H}_{\mathrm{F}}$ and $\hat{H}_A$ and adding the Coulomb interaction of the atom with the body-assisted field, leading to [SB1, SB3, SB4, SB6]

$$\hat{H} = \sum_{\lambda=e,m}\int \mathrm{d}^3r \int_0^\infty \mathrm{d}\omega\,\hbar\omega\,\hat{\boldsymbol{f}}_\lambda^\dagger(\boldsymbol{r},\omega)\cdot\hat{\boldsymbol{f}}_\lambda(\boldsymbol{r},\omega) + \sum_{\alpha \in A}\frac{1}{2m_\alpha}\Big[\hat{\boldsymbol{p}}_\alpha - q_\alpha\hat{\boldsymbol{A}}(\hat{\boldsymbol{r}}_\alpha)\Big]^2$$

$$+ \frac{1}{2}\int \mathrm{d}^3r\,\hat{\rho}_A(\boldsymbol{r})\hat{\varphi}_A(\boldsymbol{r}) + \int \mathrm{d}^3r\,\hat{\rho}_A(\boldsymbol{r})\hat{\varphi}(\boldsymbol{r}) = \hat{H}_{\mathrm{F}} + \hat{H}_A + \hat{H}_{AF} \tag{2.72}$$

where $\hat{H}_{\mathrm{F}}$ and $\hat{H}_A$ are given by Eqs. (2.33) and (2.50), respectively, and the atom–field interaction reads

$$\hat{H}_{AF} = \sum_{\alpha \in A}q_\alpha\hat{\varphi}(\hat{\boldsymbol{r}}_\alpha) - \sum_{\alpha \in A}\frac{q_\alpha}{m_\alpha}\,\hat{\boldsymbol{p}}_\alpha\cdot\hat{\boldsymbol{A}}(\hat{\boldsymbol{r}}_\alpha) + \sum_{\alpha \in A}\frac{q_\alpha^2}{2m_\alpha}\,\hat{\boldsymbol{A}}^2(\hat{\boldsymbol{r}}_\alpha) \tag{2.73}$$

[note that the scalar product of $\hat{\boldsymbol{p}}_\alpha$ and $\hat{\boldsymbol{A}}(\hat{\boldsymbol{r}}_\alpha)$ commutes in Coulomb gauge].

It is a straightforward exercise to verify that this Hamiltonian generates the correct equations of motion. Thus the total fields in the presence of the atom,

$$\hat{\boldsymbol{\mathcal{E}}}(\boldsymbol{r}) = \hat{\boldsymbol{E}}(\boldsymbol{r}) - \boldsymbol{\nabla}\hat{\varphi}_A(\boldsymbol{r}), \qquad \hat{\boldsymbol{\mathcal{B}}}(\boldsymbol{r}) = \hat{\boldsymbol{B}}(\boldsymbol{r}), \tag{2.74}$$

$$\hat{\boldsymbol{\mathcal{D}}}(r) = \hat{\boldsymbol{D}}(r) - \varepsilon_0\boldsymbol{\nabla}\hat{\varphi}_A(\boldsymbol{r}), \qquad \hat{\boldsymbol{\mathcal{H}}}(r) = \hat{\boldsymbol{H}}(\boldsymbol{r}), \tag{2.75}$$

obey the Maxwell equations (App. A.2)

$$\boldsymbol{\nabla}\cdot\hat{\boldsymbol{\mathcal{B}}}(\boldsymbol{r}) = 0, \tag{2.76}$$

$$\boldsymbol{\nabla}\cdot\hat{\boldsymbol{\mathcal{D}}}(\boldsymbol{r}) = \hat{\rho}_A(\boldsymbol{r}), \tag{2.77}$$

$$\boldsymbol{\nabla}\times\hat{\boldsymbol{\mathcal{E}}}(\boldsymbol{r}) + \dot{\hat{\boldsymbol{\mathcal{B}}}}(\boldsymbol{r}) = \boldsymbol{0}, \tag{2.78}$$

$$\boldsymbol{\nabla}\times\hat{\boldsymbol{\mathcal{H}}}(\boldsymbol{r}) - \dot{\hat{\boldsymbol{\mathcal{D}}}}(\boldsymbol{r}) = \hat{\boldsymbol{j}}_A(\boldsymbol{r}), \tag{2.79}$$

while the motion of the charged particles is governed by the Newton equations (App. A.2)

$$m_\alpha\ddot{\hat{\boldsymbol{r}}}_\alpha = q_\alpha\hat{\boldsymbol{\mathcal{E}}}(\boldsymbol{r}_\alpha) + \tfrac{1}{2}\,q_\alpha\Big[\dot{\hat{\boldsymbol{r}}}_\alpha\times\hat{\boldsymbol{\mathcal{B}}}(\boldsymbol{r}_\alpha) - \hat{\boldsymbol{\mathcal{B}}}(\boldsymbol{r}_\alpha)\times\dot{\hat{\boldsymbol{r}}}_\alpha\Big] \tag{2.80}$$

with

$$\dot{\hat{\boldsymbol{r}}}_\alpha = m_\alpha^{-1}\Big[\hat{\boldsymbol{p}}_\alpha - q_\alpha\hat{\boldsymbol{A}}(\hat{\boldsymbol{r}}_\alpha)\Big]. \tag{2.81}$$

In most cases of practical interest one may assume that the atom is small compared to the wave length of the relevant electromagnetic field. It is then useful to employ centre-of-mass and relative coordinates (2.56), and apply the long wave-length approximation by performing a leading-order expansion of the interaction Hamiltonian (2.73) in terms of the relative particle coordinates, which for a neutral atom results in

$$\hat{H}_{AF} = -\hat{\boldsymbol{d}}\cdot\hat{\boldsymbol{E}}^{\parallel}(\hat{\boldsymbol{r}}_A) - \sum_{\alpha\in A}\frac{q_\alpha}{m_\alpha}\hat{\bar{\boldsymbol{p}}}_\alpha\cdot\hat{\boldsymbol{A}}(\hat{\boldsymbol{r}}_A) + \sum_{\alpha\in A}\frac{q_\alpha^2}{2m_\alpha}\,\hat{\boldsymbol{A}}^2(\hat{\boldsymbol{r}}_A). \tag{2.82}$$

Note that the last term of the interaction Hamiltonian has become independent of the relative particle coordinates, hence it does not affect the internal state of the atom. When considering processes caused by resonant transitions between different internal states of the atom, it may therefore be neglected.

2.2.2   Multipolar coupling

An equivalent description of the atom–field dynamics that is widely used, is the multipolar coupling scheme. The multipolar-coupling Hamiltonian can be obtained from the minimal coupling form by means of a Power–Zienau–Woolley transformation [177]

$$\hat{O}' = \hat{U}\hat{O}\hat{U}^\dagger \quad\text{with } \hat{U} = \exp\left[\frac{\mathrm{i}}{\hbar}\int \mathrm{d}^3r\,\hat{\boldsymbol{P}}_A(\boldsymbol{r})\cdot\hat{\boldsymbol{A}}(\boldsymbol{r})\right]. \tag{2.83}$$

The transformed variables can be calculated with the aid of the operator identity

$$\mathrm{e}^{\hat{S}}\hat{O}\mathrm{e}^{-\hat{S}} = \hat{O} + \Big[\hat{S},\hat{O}\Big] + \tfrac{1}{2!}\Big[\hat{S},\Big[\hat{S},\hat{O}\Big]\Big] + \dots \tag{2.84}$$

In particular, from Eqs. (2.21), (2.22) and (2.44) it follows that

$$\hat{\boldsymbol{f}}'_\lambda(\boldsymbol{r},\omega) = \hat{\boldsymbol{f}}_\lambda(\boldsymbol{r},\omega) + \frac{1}{\hbar\omega}\int \mathrm{d}^3r'\,\hat{\boldsymbol{P}}_A^\perp(\boldsymbol{r}')\cdot\boldsymbol{G}_\lambda^*(\boldsymbol{r}',\boldsymbol{r},\omega), \tag{2.85}$$

where the expansions of the fields in terms of the fundamental variables remain valid after the transformation, i.e., Eqs. (2.23), (2.27), (2.43) and (2.44) hold with primed operators instead of unprimed ones. Similarly, the definitions of derived atomic quantities, Eqs. (2.51), (2.52), (2.55)–(2.57) and (2.62)–(2.65), remain valid with primed operators. Explicit expressions of the transformed variables in terms of the untransformed ones are given in App. B, they may be summarised by noting that the Power–Zienau–Woolley transformation affects the canonically conjugated momenta $\hat{\boldsymbol{\Pi}}(\boldsymbol{r})$ and $\hat{\boldsymbol{p}}_\alpha$ while leaving $\hat{\boldsymbol{A}}(\boldsymbol{r})$ and $\hat{\boldsymbol{r}}_\alpha$ unchanged. From the unitarity of the transformation (together with the fact that all equal-time commutators are c-numbers) it follows that the transformed variables obey the same equal-time commutation relations as the unprimed ones.

Expressing the Hamiltonian (2.72) in terms of the transformed variables, we obtain the multipolar Hamiltonian, which for a neutral atom reads (App. B) [SB1, SB6]

$$\hat{H} = \sum_{\lambda=e,m} \int \mathrm{d}^3r \int_0^\infty \mathrm{d}\omega\, \hbar\omega \hat{\boldsymbol{f}}_\lambda'^\dagger(\boldsymbol{r},\omega)\cdot\hat{\boldsymbol{f}}_\lambda'(\boldsymbol{r},\omega) + \sum_{\alpha\in A} \frac{1}{2m_\alpha}\left[\hat{\boldsymbol{p}}_\alpha' + \int \mathrm{d}^3r\, \hat{\boldsymbol{\Xi}}_\alpha'(\boldsymbol{r})\times\hat{\boldsymbol{B}}'(\boldsymbol{r})\right]^2$$

$$+ \frac{1}{2\varepsilon_0}\int \mathrm{d}^3r\, \hat{\boldsymbol{P}}_A'^2(\boldsymbol{r}) - \int \mathrm{d}^3r\, \hat{\boldsymbol{P}}_A'(\boldsymbol{r})\cdot\hat{\boldsymbol{E}}'(\boldsymbol{r}) = \hat{H}_F' + \hat{H}_A' + \hat{H}_{AF}' \quad (2.86)$$

where

$$\hat{H}_F' = \sum_{\lambda=e,m} \int \mathrm{d}^3r \int_0^\infty \mathrm{d}\omega\, \hbar\omega \hat{\boldsymbol{f}}_\lambda'^\dagger(\boldsymbol{r},\omega)\cdot\hat{\boldsymbol{f}}_\lambda'(\boldsymbol{r},\omega), \quad (2.87)$$

$$\hat{H}_A' = \sum_{\alpha\in A} \frac{\hat{\boldsymbol{p}}_\alpha'^2}{2m_\alpha} + \frac{1}{2\varepsilon_0}\int \mathrm{d}^3r\, \hat{\boldsymbol{P}}_A'^2(\boldsymbol{r}) = \frac{\hat{\boldsymbol{p}}_A'^2}{2m_A} + \sum_{\alpha\in A} \frac{\hat{\bar{\boldsymbol{p}}}_\alpha'^2}{2m_\alpha} + \frac{1}{2\varepsilon_0}\int \mathrm{d}^3r\, \hat{\boldsymbol{P}}_A'^2(\boldsymbol{r})$$

$$= \frac{\hat{\boldsymbol{p}}_A'^2}{2m_A} + \sum_n E_n'|n'\rangle\langle n'|, \quad (2.88)$$

$$\hat{H}_{AF}' = -\int \mathrm{d}^3r\, \hat{\boldsymbol{P}}_A'(\boldsymbol{r})\cdot\hat{\boldsymbol{E}}'(\boldsymbol{r}) - \int \mathrm{d}^3r\, \hat{\widetilde{\boldsymbol{M}}}_A'(\boldsymbol{r})\cdot\hat{\boldsymbol{B}}'(\boldsymbol{r}) + \sum_{\alpha\in A}\frac{1}{2m_\alpha}\left[\int \mathrm{d}^3r\, \hat{\boldsymbol{\Xi}}_\alpha'(\boldsymbol{r})\times\hat{\boldsymbol{B}}'(\boldsymbol{r})\right]^2$$

$$+ \frac{1}{m_A}\int \mathrm{d}^3r\, \hat{\boldsymbol{p}}_A'\cdot\hat{\boldsymbol{P}}_A'(\boldsymbol{r})\times\hat{\boldsymbol{B}}'(\boldsymbol{r}) \quad (2.89)$$

and the definitions

$$\hat{\widetilde{\boldsymbol{M}}}_A'(\boldsymbol{r}) = \sum_{\alpha\in A}\frac{q_\alpha}{2m_\alpha}\int_0^1 \mathrm{d}\sigma\, \sigma\left[\delta\big(\boldsymbol{r}-\hat{\boldsymbol{r}}_A'-\sigma\hat{\bar{\boldsymbol{r}}}_\alpha'\big)\hat{\bar{\boldsymbol{r}}}_\alpha'\times\hat{\bar{\boldsymbol{p}}}_\alpha' - \hat{\bar{\boldsymbol{p}}}_\alpha'\times\hat{\bar{\boldsymbol{r}}}_\alpha'\delta\big(\boldsymbol{r}-\hat{\boldsymbol{r}}_A'-\sigma\hat{\bar{\boldsymbol{r}}}_\alpha'\big)\right], \quad (2.90)$$

$$\hat{\boldsymbol{\Xi}}_\alpha'(\boldsymbol{r}) = q_\alpha\hat{\bar{\boldsymbol{r}}}_\alpha'\int_0^1 \mathrm{d}\sigma\, \sigma\delta\big(\boldsymbol{r}-\hat{\boldsymbol{r}}_A'-\sigma\hat{\bar{\boldsymbol{r}}}_\alpha'\big) - \frac{m_\alpha}{m_A}\sum_{\beta\in A}q_\beta\hat{\bar{\boldsymbol{r}}}_\beta'\int_0^1 \mathrm{d}\sigma\, \sigma\delta\big(\boldsymbol{r}-\hat{\boldsymbol{r}}_A'-\sigma\hat{\bar{\boldsymbol{r}}}_\beta'\big)$$

$$+ m_\alpha m_A^{-1}\hat{\boldsymbol{P}}_A'(\boldsymbol{r}) \quad (2.91)$$

have been introduced. Note that in contrast to the physical magnetisation $\hat{\boldsymbol{M}}_A$, as given by Eq. (2.63), $\widetilde{\boldsymbol{M}}_A$ is defined in terms of the canonically conjugated momenta rather than the velocities, as is required in a Hamiltonian formalism. The Hamiltonian (2.86) is the

generalisation of the multipolar Hamiltonian obtained earlier for moving atoms in free space [175, 178, 179] to the case where dispersing and absorbing magnetoelectric bodies are present. Note that the derivation of the multipolar coupling scheme presented in this section can easily be extended to the case of two or more atoms [SB12].

One major advantage of the multipolar coupling scheme is the fact that it allows for a systematic expansion in terms of the electric and magnetic multipole moments of the atom. Thus in the long wave-length approximation, by retaining only the leading-order terms in the relative coordinates, the multipolar-coupling Hamiltonian simplifies to

$$\hat{H}'_{AF} = -\hat{\boldsymbol{d}}' \cdot \hat{\boldsymbol{E}}'(\hat{\boldsymbol{r}}'_A) - \widehat{\widetilde{\boldsymbol{m}}}' \cdot \hat{\boldsymbol{B}}'(\hat{\boldsymbol{r}}'_A) + \sum_{\alpha \in A} \frac{q_\alpha^2}{8m_\alpha} \left[\hat{\bar{\boldsymbol{r}}}'_\alpha \times \hat{\boldsymbol{B}}'(\hat{\boldsymbol{r}}'_A) \right]^2 + \frac{3}{8m_A} \left[\hat{\boldsymbol{d}}' \times \hat{\boldsymbol{B}}'(\hat{\boldsymbol{r}}'_A) \right]^2$$
$$+ m_A^{-1} \hat{\boldsymbol{p}}'_A \cdot \hat{\boldsymbol{d}}' \times \hat{\boldsymbol{B}}'(\hat{\boldsymbol{r}}'_A) \quad (2.92)$$

where

$$\widehat{\widetilde{\boldsymbol{m}}}' = \sum_{\alpha \in A} \frac{q_\alpha}{2m_\alpha} \hat{\bar{\boldsymbol{r}}}'_\alpha \times \hat{\bar{\boldsymbol{p}}}'_\alpha \quad (2.93)$$

is again different from $\hat{\boldsymbol{m}}$, recall Eq. (2.65). The first two terms on the right hand side of Eq. (2.92) represent electric and magnetic dipole interactions, respectively; the next two terms describe the (generalised) diamagnetic interaction; and the term on the second line is the Röntgen interaction due to the centre-of-mass motion. For nonmagnetic atoms, Eq. (2.92) reduces to the electric-dipole form

$$\hat{H}'_{AF} = -\hat{\boldsymbol{d}}' \cdot \hat{\boldsymbol{E}}'(\hat{\boldsymbol{r}}'_A) + m_A^{-1} \hat{\boldsymbol{p}}'_A \cdot \hat{\boldsymbol{d}}' \times \hat{\boldsymbol{B}}'(\hat{\boldsymbol{r}}'_A). \quad (2.94)$$

At the end of this section, let us compare the minimal and multipolar coupling schemes. As the total Hamiltonian is the same in both formalisms, the eigenenergies of the total system and the equations of motion for the physical variables are the same in both schemes. However, the separation of the total Hamiltonian into a (body-assisted) field part, an atomic part and an interaction part is different in the two schemes, as can be seen by comparing Eqs. (2.72) and Eq. (2.86). Hence, the ground state $|\{0'\}\rangle$ of $\hat{H}'_F$,

$$\hat{\boldsymbol{f}}'_\lambda(\boldsymbol{r}, \omega) |\{0'\}\rangle = \boldsymbol{0} \quad \forall \lambda, \boldsymbol{r}, \omega, \quad (2.95)$$

is different from that of $\hat{H}_F$, Eq. (2.30); and similarly the eigenstates $|n'\rangle$ of $\hat{H}'_A$ are different from the eigenstates $|n\rangle$ of $\hat{H}_A$ [note that the uncoupled eigenstates are not simply related to each other via the Power–Zienau–Woolley transformation]. When accounting for the atom–field interaction only in a perturbative way, two different approximations to the same exact eigenenergy of the coupled system may thus occur in general, none of them being physically more relevant than the other. The second main difference between the two formalisms is

the different relation of the canonically conjugated momenta to the physical variables. In the minimal coupling scheme, physical and canonical particle momenta differ by the term $q_\alpha \hat{\boldsymbol{A}}(\hat{\boldsymbol{r}}_\alpha)$ [recall Eq. (2.81)], whereas in the multipolar formalism we have (App. B)

$$m_\alpha \dot{\hat{\boldsymbol{r}}}_\alpha = m_\alpha \dot{\hat{\boldsymbol{r}}}'_\alpha = \hat{\boldsymbol{p}}'_\alpha + \int \mathrm{d}^3 r \, \hat{\boldsymbol{\Xi}}_\alpha(\boldsymbol{r}) \times \hat{\boldsymbol{B}}(\boldsymbol{r}). \tag{2.96}$$

While the field $\hat{\boldsymbol{E}}$ in the minimal coupling scheme is the physical body-assisted electric field appearing in the Maxwell equations [recall Eqs. (2.74)–(2.79)], the field $\hat{\boldsymbol{E}}'$ in the multipolar coupling scheme has the physical meaning of a displacement field with respect to the atomic polarisation (App. B),

$$\hat{\boldsymbol{E}}'(\boldsymbol{r}) = \hat{\boldsymbol{E}}(\boldsymbol{r}) + \varepsilon_0^{-1} \hat{\boldsymbol{P}}_A^\perp(\boldsymbol{r}). \tag{2.97}$$

Chapter 3
Static Casimir–Polder potential

In this chapter, a static, perturbative theory of the CP force is developed by combining the formalism of macroscopic QED with Casimir and Polder's famous concept [2] according to which the force on an atom in an energy eigenstate may be derived from the position-dependent part of the atom–field coupling energy – the CP potential. Perturbative calculations performed within both minimal and multipolar coupling schemes are shown to lead to general expressions for the potential of an atom in the presence of an arbitrary environment of bodies [SB1, SB5, SB6, SB7, SB8], thus confirming and extending similar linear-response results within the framework of an exact quantization scheme. Endowed with this general basis, we discuss some aspects of the CP force for the first time (such as local-field effects [SB15] and approximative Born-expansion methods [SB1, SB10]) and elaborate others beyond previously discussed special cases (such as the microscopic origin of the force [SB10, SB13]). Finally, applications to ground-state atoms interacting with specific arrangements of bodies are given, where the potentials of atoms interacting with various multilayer systems are worked out in detail [SB1, SB7, SB8, SB9] and further examples are briefly stated [SB5, SB10, SB13].

Let us start from the Hamiltonian of the atom–field system which according to the minimal coupling scheme and in electric dipole approximation, can be written in the form

$$\hat{H} = \frac{\hat{\boldsymbol{p}}_A^2}{2m_A} + \sum_k E_k |k\rangle\langle k| + \hat{H}_{\mathrm{F}} + \hat{H}_{\mathrm{AF}}, \tag{3.1}$$

recall Eq. (2.72) together with Eq. (2.61). It is assumed that the atom is initially prepared in its internal-energy eigenstate $|n\rangle$ while the body-assisted field is in its ground state $|\{0\}\rangle$. We apply the Born–Oppenheimer approximation by assuming that the fast internal (electronic) motion effectively decouples from the slow centre-of-mass motion. The internal motion can thus be integrated out by calculating the internal eigenenergies for given values of $\hat{\boldsymbol{r}}_A$ and $\hat{\boldsymbol{p}}_A$, leading to an effective Hamiltonian for the centre-of-mass motion,

$$\hat{H}_{\mathrm{eff}} = \frac{\hat{\boldsymbol{p}}_A^2}{2m_A} + E_n + \Delta E_n, \tag{3.2}$$

where ΔE_n is the energy shift due to the atom–field coupling $\hat{H}_{\mathrm{AF}}$, which for sufficiently weak atom–field coupling may be calculated by leading-order perturbation theory. Equation (2.82) shows that ΔE_n is independent of $\hat{\boldsymbol{p}}_A$, so that we may write

$$\Delta E_n = \Delta^{(0)} E_n + \Delta^{(1)} E_n(\hat{\boldsymbol{r}}_A), \tag{3.3}$$

where the coupling energy has been separated into a constant part and a $\hat{\boldsymbol{r}}_A$-dependent part. Note that the constant part $\Delta^{(0)} E_n$ is the well-known (free-space) Lamb shift (cf., e.g., Ref. [107]).

By means of the commutation relations (2.58), the effective Hamiltonian generates the following equations of motion for the centre-of-mass coordinate:

$$m_A \dot{\hat{\boldsymbol{r}}}_A = \mathrm{i}\hbar^{-1} \left[\hat{H}_{\text{eff}}, m_A \hat{\boldsymbol{r}}_A \right] = \hat{\boldsymbol{p}}_A, \tag{3.4}$$

$$\boldsymbol{F}_n(\hat{\boldsymbol{r}}_A) = m_A \ddot{\hat{\boldsymbol{r}}}_A = \mathrm{i}\hbar^{-1} \left[\hat{H}_{\text{eff}}, m_A \dot{\hat{\boldsymbol{r}}}_A \right] = -\boldsymbol{\nabla}_A U_n(\hat{\boldsymbol{r}}_A) \tag{3.5}$$

where

$$U_n(\hat{\boldsymbol{r}}_A) = \Delta^{(1)} E_n(\hat{\boldsymbol{r}}_A) \tag{3.6}$$

is the CP potential. Note that a completely analogous derivation holds when working within the multipolar coupling scheme, where in addition one has to note that the $\hat{\boldsymbol{p}}'_A$-dependent part of $\hat{H}'_{AF}$, Eq. (2.94), gives rise to contributions of the order of v/c (v: centre-of-mass speed), which can be neglected for nonrelativistic centre-of-mass motion.

The potential and force expressions in Eq. (3.5) can be used in two ways. First, they are the starting point for a full quantum treatment of the centre-of-mass motion (cf., e.g., the analysis of quantum reflexion presented in Ref. [41]). Second, they also appear in the c-number equations of motion that follow for effectively classical centre-of-mass motion. Since there is no need to distinguish between the operator and c-number results, the operator hat can be dropped. In the following, we calculate the CP potential (3.6) on the basis of leading-order perturbation theory.

3.1 Minimal coupling

In the minimal coupling scheme, the interaction Hamiltonian (2.82) consists of three terms, the first two being linear in the field variables (so that they have no diagonal matrix elements and contribute only within second-order perturbation theory) and the last one being quadratic in the field variables (contributing already within first order perturbation theory). The leading-order perturbative energy shift is hence given by

$$\Delta E_n = \Delta_1 E_n + \Delta_2 E_n \tag{3.7}$$

where

$$\Delta_1 E_n = \langle n | \langle \{0\} | \sum_{\alpha \in A} \frac{q_\alpha^2}{2m_\alpha} \, \hat{\boldsymbol{A}}^2(\boldsymbol{r}_A) | \{0\} \rangle | n \rangle \tag{3.8}$$

and

$$\Delta_2 E_n = -\frac{1}{\hbar} \sum_k \sum_{\lambda=e,m} \int \mathrm{d}^3 r \, \mathcal{P} \int_0^\infty \frac{\mathrm{d}\omega}{\omega_{kn}+\omega}$$

$$\times \left| \langle n | \langle \{0\} | -\hat{\boldsymbol{d}}\cdot\hat{\boldsymbol{E}}^\parallel(\boldsymbol{r}_A) - \sum_{\alpha\in A} \frac{q_\alpha}{m_\alpha} \hat{\bar{\boldsymbol{p}}}_\alpha\cdot\hat{\boldsymbol{A}}(\boldsymbol{r}_A) | \boldsymbol{1}_\lambda(\boldsymbol{r},\omega)\rangle | k \rangle \right|^2 \quad (3.9)$$

($\mathcal{P}$, principal part; $|\boldsymbol{1}_\lambda(\boldsymbol{r},\omega)\rangle = \hat{\boldsymbol{f}}_\lambda^\dagger(\boldsymbol{r},\omega)|\{0\}\rangle$). Recalling definition (2.44), making use of the commutation relations (2.21) and (2.22) and applying the integral relation (2.26), the first-order contribution is found to be

$$\Delta_1 E_n = \frac{\hbar\mu_0}{\pi} \sum_{\alpha\in A} \frac{q_\alpha^2}{2m_\alpha} \int_0^\infty \mathrm{d}\omega \, \mathrm{tr}\big[\mathrm{Im}\,^\perp\boldsymbol{G}^\perp(\boldsymbol{r}_A,\boldsymbol{r}_A,\omega) \big]. \quad (3.10)$$

With aid of the sum rule (2.71), this result can be rewritten as

$$\Delta_1 E_n = \frac{\mu_0}{\pi} \sum_k \omega_{kn} \int_0^\infty \mathrm{d}\omega \, \boldsymbol{d}_{nk}\cdot\mathrm{Im}\,^\perp\boldsymbol{G}^\perp(\boldsymbol{r}_A,\boldsymbol{r}_A,\omega)\cdot\boldsymbol{d}_{kn} \quad (3.11)$$

where we have exploited the symmetry of the Green tensor (2.17). Similarly, by invoking definitions (2.23) and (2.44) and making use of the commutation relations (2.21) and (2.22) as well as the identity (2.70), the matrix elements in Eq. (3.9) are found to be

$$\langle n | \langle \{0\} | -\hat{\boldsymbol{d}}\cdot\hat{\boldsymbol{E}}^\parallel(\boldsymbol{r}_A) | \boldsymbol{1}_\lambda(\boldsymbol{r},\omega)\rangle | k \rangle = -\boldsymbol{d}_{nk}\cdot{}^\parallel\boldsymbol{G}_\lambda(\boldsymbol{r}_A,\boldsymbol{r},\omega), \quad (3.12)$$

$$\langle n | \langle \{0\} | -\sum_{\alpha\in A} \frac{q_\alpha}{m_\alpha} \hat{\bar{\boldsymbol{p}}}_\alpha\cdot\hat{\boldsymbol{A}}(\boldsymbol{r}_A) | \boldsymbol{1}_\lambda(\boldsymbol{r},\omega)\rangle | k \rangle = \frac{\omega_{kn}}{\omega} \boldsymbol{d}_{nk}\cdot{}^\perp\boldsymbol{G}_\lambda(\boldsymbol{r}_A,\boldsymbol{r},\omega), \quad (3.13)$$

so the second-order contribution reads

$$\Delta_2 E_n = \frac{\mu_0}{\pi} \sum_k \mathcal{P} \int_0^\infty \frac{\mathrm{d}\omega}{\omega_{kn}+\omega} \boldsymbol{d}_{nk}\cdot\mathrm{Im}\left\{ -\omega^{2\parallel}\boldsymbol{G}^\parallel(\boldsymbol{r}_A,\boldsymbol{r}_A,\omega) + \omega_{kn}\omega\big[{}^\parallel\boldsymbol{G}^\perp(\boldsymbol{r}_A,\boldsymbol{r}_A,\omega) \right.$$

$$\left. + {}^\perp\boldsymbol{G}^\parallel(\boldsymbol{r}_A,\boldsymbol{r}_A,\omega)\big] - \omega_{kn}^{2\,\perp}\boldsymbol{G}^\perp(\boldsymbol{r}_A,\boldsymbol{r}_A,\omega) \right\}\cdot\boldsymbol{d}_{kn} \quad (3.14)$$

where we have again used the integral relation (2.26). Adding Eqs. (3.11) and (3.14) and using the identity $\boldsymbol{G} = {}^\perp\boldsymbol{G}^\perp + {}^\perp\boldsymbol{G}^\parallel + {}^\parallel\boldsymbol{G}^\perp + {}^\parallel\boldsymbol{G}^\parallel$, one obtains

$$\Delta E_n = \frac{\mu_0}{\pi} \sum_k \mathcal{P} \int_0^\infty \frac{\mathrm{d}\omega}{\omega_{kn}+\omega} \boldsymbol{d}_{nk}\cdot\mathrm{Im}\left\{ \omega_{kn}\omega\big[\boldsymbol{G}(\boldsymbol{r}_A,\boldsymbol{r}_A,\omega) - {}^\parallel\boldsymbol{G}^\parallel(\boldsymbol{r}_A,\boldsymbol{r}_A,\omega)\big] \right.$$

$$\left. - \omega^{2\parallel}\boldsymbol{G}^\parallel(\boldsymbol{r}_A,\boldsymbol{r}_A,\omega) \right\}\cdot\boldsymbol{d}_{kn}. \quad (3.15)$$

According to Eq. (3.6), the CP potential is the position-dependent part of the energy shift. This part can be extracted from Eq. (3.15) by decomposing the Green tensor into the bulk Green tensor $\boldsymbol{G}^{(0)}$ and the scattering Green tensor $\boldsymbol{G}^{(1)}$ that accounts for the spatial variation of the permittivity and permeability,

$$\boldsymbol{G}(\boldsymbol{r},\boldsymbol{r}',\omega) = \boldsymbol{G}^{(0)}(\boldsymbol{r},\boldsymbol{r}',\omega) + \boldsymbol{G}^{(1)}(\boldsymbol{r},\boldsymbol{r}',\omega), \quad (3.16)$$

where it is assumed that the atom is situated in a free-space region so that macroscopic QED applies. The translationally invariant bulk Green tensor leads to the position-independent, free-space Lamb shift $\Delta^{(0)} E_n$ which is not of interest here. The scattering Green tensor gives rise to the CP potential $U_n(\boldsymbol{r}_A)$. Upon making the replacement $\boldsymbol{G} \mapsto \boldsymbol{G}^{(1)}$, writing $\operatorname{Im} z = (z - z^*)/(2\mathrm{i})$ and recalling Eq. (2.16), Eq. (3.15) hence implies

$$
\begin{aligned}
U_n(\boldsymbol{r}_A) = \frac{\mu_0}{2\mathrm{i}\pi} \sum_k \boldsymbol{d}_{nk} \cdot \Bigg[& \mathcal{P} \int_0^\infty \frac{\mathrm{d}\omega}{\omega_{kn} + \omega} \Big\{ \omega_{kn}\omega \big[\boldsymbol{G}^{(1)}(\boldsymbol{r}_A, \boldsymbol{r}_A, \omega) - {}^\| \boldsymbol{G}^{(1)\|}(\boldsymbol{r}_A, \boldsymbol{r}_A, \omega) \big] \\
& - \omega^2{}^\| \boldsymbol{G}^{(1)\|}(\boldsymbol{r}_A, \boldsymbol{r}_A, \omega) \Big\} - \mathcal{P} \int_0^{-\infty} \frac{\mathrm{d}\omega}{\omega_{kn} - \omega} \Big\{ \omega_{kn}\omega \big[\boldsymbol{G}^{(1)}(\boldsymbol{r}_A, \boldsymbol{r}_A, \omega) \\
& - {}^\| \boldsymbol{G}^{(1)\|}(\boldsymbol{r}_A, \boldsymbol{r}_A, \omega) \big] + \omega^2{}^\| \boldsymbol{G}^{(1)\|}(\boldsymbol{r}_A, \boldsymbol{r}_A, \omega) \Big\} \Bigg] \cdot \boldsymbol{d}_{kn}. \quad (3.17)
\end{aligned}
$$

This equation can be greatly simplified by using contour-integral techniques. $\boldsymbol{G}^{(1)}(\boldsymbol{r}_A, \boldsymbol{r}_A, \omega)$ is an analytic function in the upper half of the complex frequency plane including the real axis (apart from a possible pole at $\omega = 0$). We may therefore apply Cauchy's theorem and replace the principal-value integral over the positive (negative) real half axis by a contour integral along the positive imaginary half axis (introducing the purely imaginary coordinate $\omega = \mathrm{i}\xi$); and along an infinitely small and an infinitely large quarter circle in the first (second) quadrant of the complex frequency plane; plus, in the case that $\omega_{nk} > 0$, a contour integral along an infinitesimally small half circle around $\omega = \omega_{nk}$ ($\omega = -\omega_{nk}$) in the first (second) quadrant of the complex frequency plane. The asymptotic behaviour of the Green tensor in the limit of small and large $|\omega|$ (cf. Ref. [SB3]) is such that the integrals along the quarter circles vanish, so we finally arrive at [SB1, SB5, SB6]

$$
U_n(\boldsymbol{r}_A) = U_n^{\mathrm{or}}(\boldsymbol{r}_A) + U_n^{\mathrm{r}}(\boldsymbol{r}_A), \tag{3.18}
$$

where

$$
U_n^{\mathrm{or}}(\boldsymbol{r}_A) = \frac{\mu_0}{\pi} \sum_k \int_0^\infty \mathrm{d}\xi\, \frac{\omega_{kn}\xi^2}{\omega_{kn}^2 + \xi^2}\, \boldsymbol{d}_{nk} \cdot \boldsymbol{G}^{(1)}(\boldsymbol{r}_A, \boldsymbol{r}_A, \mathrm{i}\xi) \cdot \boldsymbol{d}_{kn} \tag{3.19}
$$

is the off-resonant part of the CP potential and

$$
U_n^{\mathrm{r}}(\boldsymbol{r}_A) = -\mu_0 \sum_k \Theta(\omega_{nk}) \omega_{nk}^2 \boldsymbol{d}_{nk} \cdot \operatorname{Re} \boldsymbol{G}^{(1)}(\boldsymbol{r}_A, \boldsymbol{r}_A, \omega_{nk}) \cdot \boldsymbol{d}_{kn} \tag{3.20}
$$

[$\Theta(z)$: unit step function] is the resonant part arising from the residua at the poles. By introducing the polarisability tensor of the atom in lowest-order perturbation theory [180],

$$
\boldsymbol{\alpha}_n(\omega) = \lim_{\epsilon \to 0} \frac{1}{\hbar} \sum_k \left[\frac{\boldsymbol{d}_{nk}\boldsymbol{d}_{kn}}{\omega_{kn} - \omega - \mathrm{i}\epsilon} + \frac{\boldsymbol{d}_{kn}\boldsymbol{d}_{nk}}{\omega_{kn} + \omega + \mathrm{i}\epsilon} \right], \tag{3.21}
$$

the off-resonant part may be written in the more compact form

$$
U_n^{\mathrm{or}}(\boldsymbol{r}_A) = \frac{\hbar\mu_0}{2\pi} \int_0^\infty \mathrm{d}\xi\, \xi^2 \operatorname{tr}\big[\boldsymbol{\alpha}_n(\mathrm{i}\xi) \cdot \boldsymbol{G}^{(1)}(\boldsymbol{r}_A, \boldsymbol{r}_A, \mathrm{i}\xi) \big]. \tag{3.22}
$$

In particular for an atom in a spherically symmetric state, we have

$$\boldsymbol{\alpha}_n(\omega) = \alpha_n(\omega)\boldsymbol{I} = \lim_{\epsilon \to 0} \frac{2}{3\hbar} \sum_k \frac{|\boldsymbol{d}_{nk}|^2 \omega_{kn}}{\omega_{kn}^2 - \omega^2 - \mathrm{i}\omega\epsilon} \boldsymbol{I} \tag{3.23}$$

and the two parts of the potential simplify to

$$U_n^{\mathrm{or}}(\boldsymbol{r}_A) = \frac{\hbar\mu_0}{2\pi} \int_0^\infty \mathrm{d}\xi\, \xi^2 \alpha_n(\mathrm{i}\xi)\, \mathrm{tr}\, \boldsymbol{G}^{(1)}(\boldsymbol{r}_A, \boldsymbol{r}_A, \mathrm{i}\xi), \tag{3.24}$$

$$U_n^{\mathrm{r}}(\boldsymbol{r}_A) = -\frac{\mu_0}{3} \sum_k \Theta(\omega_{nk})\omega_{nk}^2 |\boldsymbol{d}_{nk}|^2 \, \mathrm{tr}\big[\mathrm{Re}\, \boldsymbol{G}^{(1)}(\boldsymbol{r}_A, \boldsymbol{r}_A, \omega_{nk})\big]. \tag{3.25}$$

Equation (3.18) [together with Eqs. (3.20) and (3.22)] gives the CP potential of a single atom prepared in an arbitrary energy eigenstate $|n\rangle$ in the presence of an arbitrary arrangement of linear bodies. These equations are the natural extension of the (geometry-dependent) QED results derived on the basis of the familiar normal-mode formalism which ignores material absorption; they may be regarded as the foundation of similar results obtained on the basis of linear-response theory [152].[1] Moreover, they do not only apply to arbitrary electric bodies, but they present the first general expression for the CP potential that explicitly allows for the presence of magnetoelectric matter such as left-handed material, for which standard quantisation concepts run into difficulties. Note that all information about the electric and magnetic properties of the matter is contained in the scattering Green tensor, while the atomic properties enter via the atomic polarisability (for the off-resonant contribution to the CP potential) and the transition frequencies and dipole matrix elements (for the resonant part), respectively.

Let us discuss our result, starting with the resonant part of the CP potential, which is only present for excited atoms where it dominates over the off-resonant part, in general. The resonant part may be attributed to real energy-conserving processes of the atom making a transition to a lower level while emitting one photon ($E_n = E_k + \hbar\omega$), can partly be understood in classical terms. To see this, consider a classical oscillating dipole

$$\boldsymbol{d}(t) = 2^{-1/2}\boldsymbol{d}_{\mathrm{cl}}\mathrm{e}^{\mathrm{i}\omega_{\mathrm{cl}}t} + \mathrm{C.c.} \tag{3.26}$$

placed at $\boldsymbol{r}_A$ within an arbitrary arrangement of magnetoelectric bodies (where the normalisation has been chosen such that the long-time average of the dipole moment is $\overline{\boldsymbol{d}^2(t)}$ $= |\boldsymbol{d}_{\mathrm{cl}}|^2$). The dipole gives rise to an electric field which is reflected at the surface of the bodies. Writing the current density associated with the dipole in the form

$$\boldsymbol{j}(\boldsymbol{r}, t) = \dot{\boldsymbol{d}}(t)\delta(\boldsymbol{r} - \boldsymbol{r}_A) = 2^{-1/2}\mathrm{i}\omega_{\mathrm{cl}}\boldsymbol{d}_{\mathrm{cl}}\mathrm{e}^{\mathrm{i}\omega_{\mathrm{cl}}t}\delta(\boldsymbol{r} - \boldsymbol{r}_A) + \mathrm{C.c.}, \tag{3.27}$$

---

[1]Note that results of the form (3.22) for ground-state atoms have been derived by means of various methods, including linear-response theory [133, 135, 138, 141], a QED path-integral approach [136], semiclassical considerations [139] and a perturbative calculation based on macroscopic QED very similar to that presented here [181].

Eqs. (2.15) and (3.16) imply that this reflected field is given by

$$\boldsymbol{E}^{(1)}(\boldsymbol{r},t) = 2^{-1/2}\mu_0\omega_{\rm cl}^2{\rm e}^{{\rm i}\omega_{\rm cl}t}\boldsymbol{G}^{(1)*}(\boldsymbol{r},\boldsymbol{r}_A,\omega_{\rm cl})\cdot\boldsymbol{d}_{\rm cl} + {\rm C.c.} \tag{3.28}$$

The interaction energy of the classical dipole in its own (reflected) field is hence on the long-time average given by

$$\overline{W(\boldsymbol{r}_A,t)} = -\tfrac{1}{2}\overline{\boldsymbol{d}(t)\cdot\boldsymbol{E}^{(1)}(\boldsymbol{r}_A,t)} = -\tfrac{1}{2}\mu_0\omega_{\rm cl}^2\boldsymbol{d}_{\rm cl}\cdot{\rm Re}\,\boldsymbol{G}^{(1)}(\boldsymbol{r}_A,\boldsymbol{r}_A,\omega_{\rm cl})\cdot\boldsymbol{d}_{\rm cl}^*, \tag{3.29}$$

which is one half the corresponding (quantum) terms contributing to the resonant part of the CP potential, Eq. (3.20). This can be understood from the fact that the other half of the resonant CP interaction is due to fluctuations of the electromagnetic field, which are of course absent in the classical theory [118].

The off-resonant part of the CP potential (3.19) is a pure quantum effect that has no classical analogue. By applying contour-integral techniques in a similar way as presented below Eq. (3.17), it can be written in the form

$$U_n^{\rm or}(\boldsymbol{r}_A) = -\frac{\hbar\mu_0}{2\pi}\int_0^\infty {\rm d}\omega\,\omega^2{\rm tr}\Big\{{\rm Im}\big[\boldsymbol{\alpha}_n(\omega)\cdot\boldsymbol{G}^{(1)}(\boldsymbol{r}_A,\boldsymbol{r}_A,\omega)\big]\Big\}. \tag{3.30}$$

As shown in Ref. [157], this expression allows for a simple physical interpretation of the off-resonant CP force as being due to correlations of the fluctuating electromagnetic field with the corresponding induced electric dipole of the atomic system plus the correlations of the fluctuating electric dipole with its induced electric field.

In order to discuss the relative influence of the three terms in the interaction Hamiltonian (2.82), it is useful to consider the asymptotic behaviour of the CP potential for large and small atom–body separations. In the retarded limit, where all atom–body separations are large with respect to the characteristic wave lengths associated with the atom and the magnetoelectric medium constituting the bodies, the off-resonant part of the CP potential reduces to (App. D.1)

$$U_n^{\rm or}(\boldsymbol{r}_A) = \frac{\hbar\mu_0}{2\pi}{\rm tr}\bigg[\boldsymbol{\alpha}_n(0)\cdot\int_0^\infty {\rm d}\xi\,\xi^2\,\boldsymbol{G}_{\rm zero}^{(1)}(\boldsymbol{r}_A,\boldsymbol{r}_A,{\rm i}\xi)\bigg] \tag{3.31}$$

where $\boldsymbol{G}_{\rm zero}$ is defined by

$$\bigg[\boldsymbol{\nabla}\times\kappa(\boldsymbol{r},0)\boldsymbol{\nabla}\times\,-\,\frac{\omega^2}{c^2}\,\varepsilon(\boldsymbol{r},0)\bigg]\boldsymbol{G}_{\rm zero}(\boldsymbol{r},\boldsymbol{r}',\omega) = \delta(\boldsymbol{r}-\boldsymbol{r}')\boldsymbol{I}, \tag{3.32}$$

and the resonant part approximates to

$$U_n^{\rm r}(\boldsymbol{r}_A) = -\mu_0\sum_k\Theta(\omega_{nk})\omega_{nk}^2\boldsymbol{d}_{nk}\cdot{\rm Re}\,^\perp\boldsymbol{G}^{(1)\perp}(\boldsymbol{r}_A,\boldsymbol{r}_A,\omega_{nk})\cdot\boldsymbol{d}_{kn}. \tag{3.33}$$

In the opposite, non-retarded limit where all atom–body separations are small with respect to the characteristic atomic and medium wave lengths, the two parts of the CP potential can be given as (App. D.1)

$$U_n^{\text{or}}(\boldsymbol{r}_A) = \frac{\hbar \mu_0}{2\pi} \int_0^\infty \mathrm{d}\xi \, \xi^2 \mathrm{tr}\Big[\boldsymbol{\alpha}_n(\mathrm{i}\xi)\cdot{}^{\|}\boldsymbol{G}^{(1)\|}(\boldsymbol{r}_A, \boldsymbol{r}_A, \mathrm{i}\xi)\Big] \tag{3.34}$$

and

$$U_n^{\text{r}}(\boldsymbol{r}_A) = -\mu_0 \sum_k \Theta(\omega_{nk}) \omega_{nk}^2 \boldsymbol{d}_{nk}\cdot\mathrm{Re}\,{}^{\|}\boldsymbol{G}^{(1)\|}(\boldsymbol{r}_A, \boldsymbol{r}_A, \omega_{nk})\cdot\boldsymbol{d}_{kn}. \tag{3.35}$$

The relevance of the three terms in the interaction Hamiltonian (2.82) in the retarded and non-retarded limits can now be inferred by recalling Eqs. (3.7)–(3.14). The $\hat{\boldsymbol{p}}\cdot\hat{\boldsymbol{A}}$ interaction dominates the CP potential in the retarded limit where the contributions from the other two interaction terms are either exactly cancelled by some parts of the $\hat{\boldsymbol{p}}\cdot\hat{\boldsymbol{A}}$ contribution (as is the case for the off-resonant part of the CP potential, cf. App. D.1) or become negligible (as is obviously true for the resonant part of the CP potential, which only depends on purely transverse fields in this limit). On the contrary, the $\hat{\boldsymbol{d}}\cdot\hat{\boldsymbol{E}}^{\|}$ interaction dominates the potential in the non-retarded limit where all relevant fields are purely longitudinal. Recall that this term is the long wave-length form of the electrostatic Coulomb interaction

$$\hat{H}_{\text{Coulomb}} = \int \mathrm{d}^3 r \, \hat{\rho}_A(\boldsymbol{r}) \hat{\varphi}(\boldsymbol{r}), \tag{3.36}$$

which is why the non-retarded limit is also known as the electrostatic limit. In cases where only the non-retarded CP potential is of interest, calculations can be simplified considerably by restricting the attention to $\hat{H}_{\text{Coulomb}}$ from the very beginning (recall Sec. 1.2.3). The role of the $\hat{\boldsymbol{A}}^2$ interaction is somewhat more subtle. Since it does not give rise to denominators $\omega_{kn}+\omega$, cf. Eq. (3.11), this term does not contribute to the resonant part of the CP potential, as expected (cf. the remark at the end of Sec. 2.2.1). Its contribution to the off-resonant part of the potential is negligible in the non-retarded limit while gaining importance for larger atom–body separations (as stated above, in the retarded limit it is exactly cancelled by a part of the $\hat{\boldsymbol{p}}\cdot\hat{\boldsymbol{A}}$ contribution). Note that our results regarding the relative influence of the interaction terms generalise the findings obtained earlier for the particular case of an atom interacting with a perfectly conducting half space [34, 116, 118, 119].

Finally, let us comment on the potential influence of left-handed material properties on the CP potential (recall Sec. 1.2.2). The off-resonant CP potential (3.22) is not sensitive to left-handed material properties, because it is expressed in terms of the always positive values of the permittivity and the permeability at imaginary frequencies. On the contrary, the resonant CP potential (3.20) present for excited atoms may exhibit unusual features if the bodies are left-handed at one of the resonant transition frequencies.

3.2 Multipolar coupling

The multipolar-coupling Hamiltonian (2.94) consists of two terms which are both linear in the field variables. As already mentioned [recall the discussion below Eq. (3.6)], the contributions from the second term can be neglected for nonrelativistic centre-of-mass motion, so that the leading-order energy shift is given by

$$
\Delta E_n' = \Delta_2 E_n' = -\frac{1}{\hbar} \sum_k \sum_{\lambda=e,m} \int \mathrm{d}^3 r\, \mathcal{P} \int_0^\infty \frac{\mathrm{d}\omega}{\omega_{kn}' + \omega} \left| \langle n' | \langle \{0'\} | -\hat{\boldsymbol{d}}' \cdot \hat{\boldsymbol{E}}'(\boldsymbol{r}_A) | \boldsymbol{1}_\lambda'(\boldsymbol{r},\omega) \rangle | k' \rangle \right|^2
$$

(3.37)

where $|\boldsymbol{1}_\lambda'(\boldsymbol{r},\omega)\rangle = \hat{\boldsymbol{f}}_\lambda'^\dagger(\boldsymbol{r},\omega)|\{0'\}\rangle$ and $\omega_{mn}' = (E_m' - E_n')/\hbar$. Using Eq. (2.23) and applying the commutation relations (2.21) and (2.22), the matrix elements are found to be

$$
\langle n' | \langle \{0'\} | -\hat{\boldsymbol{d}}' \cdot \hat{\boldsymbol{E}}'(\boldsymbol{r}_A) | \boldsymbol{1}_\lambda'(\boldsymbol{r},\omega) \rangle | k' \rangle = -\boldsymbol{d}_{nk}' \cdot \boldsymbol{G}_\lambda(\boldsymbol{r}_A, \boldsymbol{r}, \omega)
$$

(3.38)

where $\boldsymbol{d}_{mn}' = \langle m' | \hat{\boldsymbol{d}}' | n' \rangle$. Substitution of this result into Eq. (3.37) and use of the integral relation (2.26) leads to

$$
\Delta E_n' = -\frac{\mu_0}{\pi} \sum_k \mathcal{P} \int_0^\infty \frac{\mathrm{d}\omega}{\omega_{kn}' + \omega} \, \omega^2 \boldsymbol{d}_{nk}' \cdot \mathrm{Im}\, \boldsymbol{G}(\boldsymbol{r}_A, \boldsymbol{r}_A, \omega) \boldsymbol{d}_{kn}'.
$$

(3.39)

We now apply the same procedure as in Sec. 3.1. Discarding the free-space Lamb shift contributions contained in Eq. (3.39) by replacing the Green tensor with its scattering part and transforming the frequency integral to imaginary frequencies using contour integral techniques, we arrive at [SB1, SB6, SB7, SB8]

$$
U_n'(\boldsymbol{r}_A) = U_n^{\mathrm{or}'}(\boldsymbol{r}_A) + U_n^{\mathrm{r}'}(\boldsymbol{r}_A)
$$

(3.40)

where

$$
U_n^{\mathrm{or}'}(\boldsymbol{r}_A) = \frac{\hbar\mu_0}{2\pi} \int_0^\infty \mathrm{d}\xi\, \xi^2 \mathrm{tr}\left[\boldsymbol{\alpha}_n'(\mathrm{i}\xi) \cdot \boldsymbol{G}^{(1)}(\boldsymbol{r}_A, \boldsymbol{r}_A, \mathrm{i}\xi) \right],
$$

(3.41)

$$
U_n^{\mathrm{r}'}(\boldsymbol{r}_A) = -\mu_0 \sum_k \Theta(\omega_{nk}') \omega_{nk}'^2 \boldsymbol{d}_{nk}' \cdot \mathrm{Re}\, \boldsymbol{G}^{(1)}(\boldsymbol{r}_A, \boldsymbol{r}_A, \omega_{nk}) \cdot \boldsymbol{d}_{kn}'
$$

(3.42)

and

$$
\boldsymbol{\alpha}_n'(\omega) = \lim_{\epsilon \to 0} \frac{1}{\hbar} \sum_k \left[\frac{\boldsymbol{d}_{nk}' \boldsymbol{d}_{kn}'}{\omega_{kn}' - \omega - \mathrm{i}\epsilon} + \frac{\boldsymbol{d}_{kn}' \boldsymbol{d}_{nk}'}{\omega_{kn}' + \omega + \mathrm{i}\epsilon} \right].
$$

(3.43)

Comparing this with the minimal-coupling result, Eq. (3.18) together with Eqs. (3.20) and (3.22), we see that the results are formally the same, but with unperturbed transition frequencies and dipole matrix elements being determined by the atomic Hamiltonians (2.88) and (2.61) in the two cases. Within leading-order perturbation theory, minimal and multipolar coupling schemes thus lead to formally equivalent approximations to the same true

CP potential. Rather remarkably, within the multipolar coupling scheme the entire CP potential is obtained from a single $\hat{\boldsymbol{d}}' \cdot \hat{\boldsymbol{E}}'$ interaction term, which incorporates the interaction of the atom with both longitudinal and transverse degrees of freedom of the body-assisted electromagnetic field. Owing to the resulting greater simplicity of the calculation, the multipolar coupling scheme is almost exclusively used when studying involved problems like higher-order perturbation theory [SB12, SB13] or dynamical calculations (chapter 4).

3.3 Local-field correction

As noted at the beginning of Sec. 1.2, a theory of the CP force based on macroscopic QED is valid provided that the overlap between the electronic wave functions of the atom and the body is negligible. In particular, this implies that the atom must be situated in some free-space region, i.e., $\varepsilon(\boldsymbol{r}_A, \omega) = 1$, $\mu(\boldsymbol{r}_A, \omega) = 1$. When the atom is placed inside a body, the macroscopic electromagnetic field differs from the local field experienced by the atom. This local-field correction can be accounted for by means of the real-cavity model [182], as shall be demonstrated in the following.

According to the real-cavity model, one assumes the atom to be situated at the centre of a spherical free-space cavity of radius R_{cav} inside the host body. As a result, the permittivity $\varepsilon(\boldsymbol{r}, \omega)$ and permeability $\mu(\boldsymbol{r}, \omega)$ describing the body must be replaced with

$$\varepsilon_{\text{loc}}(\boldsymbol{r}, \omega), \mu_{\text{loc}}(\boldsymbol{r}, \omega) = \begin{cases} 1 & \text{if } |\boldsymbol{r} - \boldsymbol{r}_A| < R_{\text{cav}}, \\ \varepsilon(\boldsymbol{r}, \omega), \mu(\boldsymbol{r}, \omega) & \text{if } |\boldsymbol{r} - \boldsymbol{r}_A| \geq R_{\text{cav}}. \end{cases} \tag{3.44}$$

The cavity radius R_{cav} is a model parameter representing an average distance from the guest atom to the nearest neighbouring atoms constituting the host body. Note that the real-cavity model is applicable provided that the unperturbed host body is homogeneous in the region where the atom is situated,

$$\varepsilon(\boldsymbol{r}, \omega) = \varepsilon(\boldsymbol{r}_A, \omega), \ \mu(\boldsymbol{r}, \omega) = \mu(\boldsymbol{r}_A, \omega) \quad \text{for } |\boldsymbol{r} - \boldsymbol{r}_A| \leq (1 + \eta) R_{\text{cav}}, \tag{3.45}$$

with η being some small positive number. In particular, this condition implies that the atom must not be situated on any body surface.

The local-field corrected CP potential can be obtained from Eqs. (3.20) and (3.22) by using the scattering part of the Green tensor $\boldsymbol{G}_{\text{loc}}(\boldsymbol{r}, \boldsymbol{r}', \omega)$ which is defined by Eq. (2.14) with $\varepsilon_{\text{loc}}(\boldsymbol{r}, \omega), \mu_{\text{loc}}(\boldsymbol{r}, \omega)$ instead of $\varepsilon(\boldsymbol{r}, \omega), \mu(\boldsymbol{r}, \omega)$. We assume the cavity radius to be small with respect to the relevant atomic and medium wave lengths, so that one may employ the

expansion (App. C) [SB11, SB15]

$$
\boldsymbol{G}_{\mathrm{loc}}^{(1)}(\boldsymbol{r}_A, \boldsymbol{r}_A, \omega) = \frac{\omega}{6\pi c} \left\{ \frac{3(\varepsilon_A - 1)}{2\varepsilon_A + 1} \frac{c^3}{\omega^3 R_{\mathrm{cav}}^3} + \frac{9[\varepsilon_A^2(5\mu_A - 1) - 3\varepsilon_A - 1]}{5(2\varepsilon_A + 1)^2} \frac{c}{\omega R_{\mathrm{cav}}} \right.
$$

$$
\left. + \mathrm{i}\left[\frac{9\varepsilon_A^{5/2}\mu_A^{3/2}}{(2\varepsilon_A + 1)^2} - 1 \right] \right\} \boldsymbol{I} + \left(\frac{3\varepsilon_A}{2\varepsilon_A + 1} \right)^2 \boldsymbol{G}^{(1)}(\boldsymbol{r}_A, \boldsymbol{r}_A, \omega) + O(\omega R_{\mathrm{cav}}/c) \quad (3.46)
$$

where $\varepsilon_A = \varepsilon_A(\omega) = \varepsilon(\boldsymbol{r}_A, \omega)$ and $\mu_A = \mu_A(\omega) = \mu(\boldsymbol{r}_A, \omega)$. Note that according to condition (3.45) the term in curly brackets does not give rise to a force, so it will be discarded in the following.

Substituting $\boldsymbol{G}_{\mathrm{loc}}^{(1)}$ into Eq. (3.22), we find that the off-resonant part of the CP potential of an atom situated inside a body is given by [SB15]

$$
U_n^{\mathrm{or}}(\boldsymbol{r}_A) = \frac{\hbar\mu_0}{2\pi} \int_0^\infty \mathrm{d}\xi\, \xi^2 \left[\frac{3\varepsilon_A(\mathrm{i}\xi)}{2\varepsilon_A(\mathrm{i}\xi) + 1} \right]^2 \mathrm{tr}\big[\boldsymbol{\alpha}_n(\mathrm{i}\xi) \cdot \boldsymbol{G}^{(1)}(\boldsymbol{r}_A, \boldsymbol{r}_A, \mathrm{i}\xi)\big]. \quad (3.47)
$$

Comparison with Eq. (3.22) reveals that the local-field correction enhances the ξ-dependent contributions to the potential, the factor in square brackets always being greater than unity $[\varepsilon_A(\mathrm{i}\xi) > 1]$. Since the integrand in Eq. (3.47) may have different signs for different values of ξ, the total $U_n^{\mathrm{or}}(\boldsymbol{r}_A)$ may be enhanced or reduced, in general. In the retarded limit where

$$
U_n^{\mathrm{or}}(\boldsymbol{r}_A) = \frac{\hbar\mu_0}{2\pi} \left[\frac{3\varepsilon_A(0)}{2\varepsilon_A(0) + 1} \right]^2 \mathrm{tr}\left[\boldsymbol{\alpha}_n(0) \cdot \int_0^\infty \mathrm{d}\xi\, \xi^2\, \boldsymbol{G}_{\mathrm{zero}}^{(1)}(\boldsymbol{r}_A, \boldsymbol{r}_A, \mathrm{i}\xi) \right] \quad (3.48)
$$

[recall Eq. (3.31)], the local-field effects always lead to an enhancement of $U_n^{\mathrm{or}}(\boldsymbol{r}_A)$ by a simple factor.

Similarly, after substituting Eq. (3.46) into Eq. (3.20), the local-field corrected resonant part of the CP potential reads

$$
U_n^{\mathrm{r}}(\boldsymbol{r}_A) = -\mu_0 \sum_k \Theta(\omega_{nk})\omega_{nk}^2 \boldsymbol{d}_{nk} \cdot \mathrm{Re}\left\{ \left[\frac{3\varepsilon_A(\omega_{nk})}{2\varepsilon_A(\omega_{nk}) + 1} \right]^2 \boldsymbol{G}^{(1)}(\boldsymbol{r}_A, \boldsymbol{r}_A, \omega_{nk}) \right\} \cdot \boldsymbol{d}_{kn}. \quad (3.49)
$$

In the limit of negligible absorption $[\mathrm{Im}\, \varepsilon_A = 0]$, one has

$$
U_n^{\mathrm{r}}(\boldsymbol{r}_A) = -\mu_0 \sum_k \Theta(\omega_{nk})\omega_{nk}^2 \left[\frac{3\varepsilon_A(\omega_{nk})}{2\varepsilon_A(\omega_{nk}) + 1} \right]^2 \boldsymbol{d}_{nk} \cdot \mathrm{Re}\, \boldsymbol{G}^{(1)}(\boldsymbol{r}_A, \boldsymbol{r}_A, \omega_{nk}) \cdot \boldsymbol{d}_{kn}, \quad (3.50)
$$

so the contributions associated with the different transitions ω_{nk} are modified by simple factors due to the influence of the local-field effects. From

$$
\left[\frac{3\varepsilon_A}{2\varepsilon_A + 1} \right]^2 < 1 \quad \Leftrightarrow \quad -\frac{1}{5} < \varepsilon_A < 1 \quad (3.51)
$$

we see that enhancement or reduction may occur, depending on the values of $\varepsilon_A(\omega_{nk})$.

Equations (3.47) and (3.49) extend the free-space results (3.22) and (3.22) for the CP potential to the case of of an atom embedded in a body, hereby fully accounting for local-field effects. It is worth noting that the local-field correction depends only on the electric, and not on the magnetic properties of the host body. This can be understood from the fact that the local-field effects are due to the influence of the neighbouring body atoms on the guest atom, with this influence being dominated by the electrostatic Coulomb interaction.

3.4 Born expansion

In order to apply the general expressions for the CP potential as given by Eqs. (3.18), (3.20) and (3.22) to a specific arrangement of magnetoelectric bodies, the appropriate Green tensor must be obtained by solving the differential equation (2.14) for given functions $\varepsilon(\boldsymbol{r}, \omega)$ and $\mu(\boldsymbol{r}, \omega)$. For many arrangements displaying a high degree of symmetry, e.g., planar, spherical, or cylindrical multilayer systems, the respective Green tensor is available in closed form [183]. For geometries only slightly deviating from such high symmetry, the Born expansion of the Green tensor can be used to develop a systematic approximation to the CP potential, as shall be outlined in the following.

Suppose that for a specific geometry of interest, the permittivity and (inverse) permeability can be decomposed as

$$\varepsilon(\boldsymbol{r}, \omega) = \overline{\varepsilon}(\boldsymbol{r}, \omega) + \chi(\boldsymbol{r}, \omega), \qquad \kappa(\boldsymbol{r}, \omega) = \overline{\kappa}(\boldsymbol{r}, \omega) - \zeta(\boldsymbol{r}, \omega) \tag{3.52}$$

where the Green tensor $\overline{\boldsymbol{G}}(\boldsymbol{r}, \boldsymbol{r}', \omega)$ corresponding to the (background) bodies described by $\overline{\varepsilon}(\boldsymbol{r}, \omega)$ and $\overline{\kappa}(\boldsymbol{r}, \omega) = \overline{\mu}^{-1}(\boldsymbol{r}, \omega)$ is known,

$$\left[\boldsymbol{\nabla} \times \overline{\kappa}(\boldsymbol{r}, \omega) \boldsymbol{\nabla} \times - \frac{\omega^2}{c^2} \overline{\varepsilon}(\boldsymbol{r}, \omega) \right] \overline{\boldsymbol{G}}(\boldsymbol{r}, \boldsymbol{r}', \omega) = \delta(\boldsymbol{r} - \boldsymbol{r}') \boldsymbol{I} \tag{3.53}$$

and $\chi(\boldsymbol{r}, \omega)$ and $\zeta(\boldsymbol{r}, \omega)$ describe some (small) corrections. In this case, the full Green tensor is given by the Dyson equation [SB1]

$$\boldsymbol{G}(\boldsymbol{r}, \boldsymbol{r}', \omega) = \overline{\boldsymbol{G}}(\boldsymbol{r}, \boldsymbol{r}', \omega) + \frac{\omega^2}{c^2} \int \mathrm{d}^3 s\, \overline{\boldsymbol{G}}(\boldsymbol{r}, \boldsymbol{s}, \omega) \cdot \chi(\boldsymbol{s}, \omega) \boldsymbol{G}(\boldsymbol{s}, \boldsymbol{r}', \omega)$$
$$- \int \mathrm{d}^3 s\, \overline{\boldsymbol{G}}(\boldsymbol{r}, \boldsymbol{s}, \omega) \times \overleftarrow{\boldsymbol{\nabla}}_{\boldsymbol{s}} \cdot \zeta(\boldsymbol{s}, \omega) \boldsymbol{\nabla}_{\boldsymbol{s}} \times \boldsymbol{G}(\boldsymbol{s}, \boldsymbol{r}', \omega), \tag{3.54}$$

as can be easily verified by substitution into the differential equation (2.14) and use of Eqs. (3.52) and (3.53). By iterating the Dyson equation, one can obtain an expansion of $\boldsymbol{G}$ in powers of χ and ζ, which is known as the Born expansion (App. D.1). In particular, if the correction is sufficiently small, $|\chi(\boldsymbol{r}, \omega)|, |\zeta(\boldsymbol{r}, \omega)| \ll 1$, then a good approximation to the Green tensor is given by the linear Born expansion

$$\boldsymbol{G}(\boldsymbol{r}, \boldsymbol{r}', \omega) = \overline{\boldsymbol{G}}(\boldsymbol{r}, \boldsymbol{r}', \omega) + \Delta\boldsymbol{G}(\boldsymbol{r}, \boldsymbol{r}', \omega), \tag{3.55}$$

$$\Delta\boldsymbol{G}(\boldsymbol{r}, \boldsymbol{r}', \omega) = \int \mathrm{d}^3 s\, \left\{ \frac{\omega^2}{c^2} \chi(\boldsymbol{s}, \omega) \overline{\boldsymbol{G}}(\boldsymbol{r}, \boldsymbol{s}, \omega) \cdot \overline{\boldsymbol{G}}(\boldsymbol{s}, \boldsymbol{r}', \omega) \right.$$
$$\left. -\zeta(\boldsymbol{s}, \omega) \left[\overline{\boldsymbol{G}}(\boldsymbol{r}, \boldsymbol{s}, \omega) \times \overleftarrow{\boldsymbol{\nabla}}_{\boldsymbol{s}} \right] \cdot \left[\boldsymbol{\nabla}_{\boldsymbol{s}} \times \overline{\boldsymbol{G}}(\boldsymbol{s}, \boldsymbol{r}', \omega) \right] \right\}. \tag{3.56}$$

Use of the Born expansion leads to approximate expressions for the CP potential, where we restrict our attention to the ground-state potential $U(\boldsymbol{r}_A) \equiv U_0(\boldsymbol{r}_A)$ in the following.

Substituting Eqs. (3.55) and (3.56) into Eq. (3.18) [together with Eqs. (3.24) and (3.25)], one finds that to linear order in χ and ζ, the CP potential of an isotropic ground-state atom reads [SB1, SB10]

$$U(\boldsymbol{r}_A) = \overline{U}(\boldsymbol{r}_A) + \Delta U(\boldsymbol{r}_A) \tag{3.57}$$

where

$$\overline{U}(\boldsymbol{r}_A) = \frac{\hbar\mu_0}{2\pi} \int_0^\infty d\xi\, \xi^2 \alpha(i\xi) \mathrm{tr}\, \overline{\boldsymbol{G}}^{(1)}(\boldsymbol{r}_A, \boldsymbol{r}_A, i\xi) \tag{3.58}$$

with $\alpha(\omega) \equiv \alpha_0(\omega)$ is the potential associated with the background bodies $\overline{\varepsilon}(\boldsymbol{r}, \omega)$, $\overline{\mu}(\boldsymbol{r}, \omega)$; and

$$\Delta U(\boldsymbol{r}_A) = -\frac{\hbar\mu_0}{2\pi} \int d^3 s \int_0^\infty d\xi\, \xi^2 \alpha(i\xi) \left\{ \frac{\xi^2}{c^2} \chi(\boldsymbol{s}, i\xi) \mathrm{tr}\left[\overline{\boldsymbol{G}}(\boldsymbol{r}_A, \boldsymbol{s}, i\xi) \cdot \overline{\boldsymbol{G}}(\boldsymbol{s}, \boldsymbol{r}_A, i\xi) \right] \right.$$
$$\left. + \zeta(\boldsymbol{s}, i\xi) \mathrm{tr}\left[\overline{\boldsymbol{G}}(\boldsymbol{r}_A, \boldsymbol{s}, i\xi) \times \overleftarrow{\boldsymbol{\nabla}}_{\boldsymbol{s}} \cdot \boldsymbol{\nabla}_{\boldsymbol{s}} \times \overline{\boldsymbol{G}}(\boldsymbol{s}, \boldsymbol{r}_A, i\xi) \right] \right\} \tag{3.59}$$

is the contribution of the perturbation described by $\chi(\boldsymbol{r}, \omega)$ and $\zeta(\boldsymbol{r}, \omega)$. The linear Born expansion can hence be used to approximate the potential in scenarios where a basic arrangement of magnetoelectric bodies for which the Green tensor is known is weakly disturbed, e.g., by additional bodies, inhomogeneities,[2] or surface roughness. The quality of the approximation can be systematically enhanced by including higher-order terms of the Born expansion (which can be found in App. D.1 or Ref. [SB10]).

The Born expansion, in particular, can be used to evaluate the ground-state CP potential of an atom in the case where only weakly magnetodielectric bodies are present so that we may let $\overline{\varepsilon}(\boldsymbol{r}, \omega) = 1$, $\overline{\mu}(\boldsymbol{r}, \omega) = 1$.[3] In this case, the background Green tensor appearing in Eqs. (3.57)–(3.59) is simply the free-space Green tensor (see, e.g., Ref. [170])

$$\overline{\boldsymbol{G}}(\boldsymbol{r}, \boldsymbol{r}', \omega) = \boldsymbol{G}_{\mathrm{free}}(\boldsymbol{r}, \boldsymbol{r}', \omega) = \frac{1}{4\pi}\left[\boldsymbol{I} + \left(\frac{c}{\omega}\right)^2 \boldsymbol{\nabla}\boldsymbol{\nabla} \right] \frac{e^{i\omega\rho/c}}{\rho}$$
$$= -\tfrac{1}{3}(c/\omega)^2 \delta(\boldsymbol{\rho})\boldsymbol{I} + \boldsymbol{H}_{\mathrm{free}}(\boldsymbol{r}, \boldsymbol{r}', \omega) \tag{3.60}$$

with

$$\boldsymbol{H}_{\mathrm{free}}(\boldsymbol{r}, \boldsymbol{r}', \omega) = -\frac{c^2 e^{i\omega\rho/c}}{4\pi\omega^2\rho^3}\left\{ \left[1 - \frac{i\omega\rho}{c} - \left(\frac{\omega\rho}{c}\right)^2 \right]\boldsymbol{I} - \left[3 - \frac{3i\omega\rho}{c} - \left(\frac{\omega\rho}{c}\right)^2 \right]\boldsymbol{e}_\rho\boldsymbol{e}_\rho \right\}, \tag{3.61}$$

($\boldsymbol{\rho} = \boldsymbol{r} - \boldsymbol{r}'$; $\rho = |\boldsymbol{\rho}|$; $\boldsymbol{e}_\rho = \boldsymbol{\rho}/\rho$) and the CP potential reduces to

$$U(\boldsymbol{r}_A) = \Delta U(\boldsymbol{r}_A). \tag{3.62}$$

---

[2] The example of a ground-state atom interacting with a semi-infinite half space containing an inhomogeneous magnetodielectric is studied in Ref. [SB10].

[3] Recall from Eq. (3.52) that under these assumptions $\chi = \varepsilon - 1$ is nothing but the well-known electric susceptibility and within linear order, $\zeta \simeq \mu - 1$ coincides with the magnetic susceptibility.

Substituting Eqs. (3.60) and (3.61) into Eq. (3.59), one easily finds that weakly dielectric bodies give rise to a potential [SB10]

$$U(\boldsymbol{r}_A) = -\frac{\hbar}{32\pi^3\varepsilon_0} \int \frac{\mathrm{d}^3s}{|\boldsymbol{r}_A - \boldsymbol{s}|^6} \int_0^\infty \mathrm{d}\xi\, \alpha(\mathrm{i}\xi)\chi(\boldsymbol{s},\mathrm{i}\xi)g(\xi|\boldsymbol{r}_A - \boldsymbol{s}|/c), \qquad (3.63)$$

$$g(x) = 2\mathrm{e}^{-2x}(3 + 6x + 5x^2 + 2x^3 + x^4) \qquad (3.64)$$

which is simply a volume integral over attractive central forces, as is seen from

$$\boldsymbol{\nabla}\left[\frac{g(\xi r/c)}{r^6}\right] = -\frac{4\boldsymbol{r}}{r^8}\left[\mathrm{e}^{-2x}(9 + 18x + 16x^2 + 8x^3 + 3x^4 + x^5)\right]_{x=\xi r/c}. \qquad (3.65)$$

In particular, the force is additive in the sense that forces due to two or more weakly dielectric bodies can be simply added in order to obtain the total force. This is only true within linear order in χ; inclusion of higher orders in χ leads to a breakdown of additivity, as illustrated in App. D.2. Equation (3.63) can be further simplified for asymptotically large or small atom–body separations. In the retarded (long-distance) limit, i.e., for $r_{\min} \gg c/\omega_{\min}$ ($r_{\min}$: minimum distance of the atom to any of the bodies; $\omega_{\min}$: minimum of all relevant atomic and medium resonance frequencies), the factor $\mathrm{e}^{-2\xi|\boldsymbol{r}_A - \boldsymbol{s}|/c}$ contained in $g(x)$ effectively limits the ξ-integral in Eq. (3.63) to a range where $\xi \leq c/r_{\min} \ll \omega_{\min}$, so that we may put $\alpha(\mathrm{i}\xi) \simeq \alpha(0)$, $\chi(\boldsymbol{s},\mathrm{i}\xi) \simeq \chi(\boldsymbol{s},0)$, resulting in

$$U(\boldsymbol{r}_A) = -\frac{\hbar c\alpha(0)}{32\pi^3\varepsilon_0} \int \mathrm{d}^3s\, \frac{\chi(\boldsymbol{s},0)}{|\boldsymbol{r}_A - \boldsymbol{s}|^7} \int_0^\infty \mathrm{d}x\, g(x) = -\frac{23\hbar c\alpha(0)}{64\pi^3\varepsilon_0} \int \mathrm{d}^3s\, \frac{\chi(\boldsymbol{s},0)}{|\boldsymbol{r}_A - \boldsymbol{s}|^7}. \qquad (3.66)$$

Note that the retarded limit corresponds to the limit $c \to 0$ in the sense that $c \ll r_{\min}\omega_{\min}$. In the non-retarded (short-distance) limit, i.e., for $r_{\max} \ll c/\omega_{\max}$ ($r_{\max}$: maximum distance of the atom to any body part; $\omega_{\max}$: maximum of all relevant atomic and medium resonance frequencies), the functions $\alpha(\mathrm{i}\xi)$ and $\chi(\boldsymbol{s},\mathrm{i}\xi)$ effectively limit the ξ-integral in Eq. (3.63) to a range where $x = \xi|\boldsymbol{r}_A - \boldsymbol{s}|/c \leq \omega_{\max}r_{\max}/c \ll 1$, so the approximation $g(x) \simeq g(0) = 6$ leads to

$$U(\boldsymbol{r}_A) = -\frac{3\hbar}{16\pi^3\varepsilon_0} \int \frac{\mathrm{d}^3s}{|\boldsymbol{r}_A - \boldsymbol{s}|^6} \int_0^\infty \mathrm{d}\xi\, \alpha(\mathrm{i}\xi)\chi(\boldsymbol{s},\mathrm{i}\xi). \qquad (3.67)$$

The non-retarded limit corresponds to the limit $c \to \infty$ in the sense that $c \gg r_{\max}\omega_{\max}$.

In order to find the CP potential associated with weakly magnetic bodies, we first recall Eq. (3.60) and calculate

$$\boldsymbol{\nabla}\times\boldsymbol{G}_{\mathrm{free}}(\boldsymbol{r},\boldsymbol{r}',\omega) = -\frac{\mathrm{e}^{\mathrm{i}\omega\rho/c}}{4\pi\rho^2}\left(1 - \frac{\mathrm{i}\omega\rho}{c}\right)\boldsymbol{e}_\rho\times\boldsymbol{I}, \quad \text{for } \boldsymbol{r} \neq \boldsymbol{r}', \qquad (3.68)$$

$$\boldsymbol{G}_{\mathrm{free}}(\boldsymbol{r},\boldsymbol{r}',\omega)\times\overleftarrow{\boldsymbol{\nabla}}' = \frac{\mathrm{e}^{\mathrm{i}\omega\rho/c}}{4\pi\rho^2}\left(1 - \frac{\mathrm{i}\omega\rho}{c}\right)\boldsymbol{I}\times\boldsymbol{e}_\rho, \quad \text{for } \boldsymbol{r} \neq \boldsymbol{r}', \qquad (3.69)$$

which upon substitution into Eq. (3.59) results in

$$U(\boldsymbol{r}_A) = \frac{\hbar\mu_0}{32\pi^3} \int \frac{\mathrm{d}^3s}{|\boldsymbol{r}_A - \boldsymbol{s}|^4} \int_0^\infty \mathrm{d}\xi\, \xi^2\alpha(\mathrm{i}\xi)\zeta(\boldsymbol{s},\mathrm{i}\xi)h(\xi|\boldsymbol{r}_A - \boldsymbol{s}|/c), \qquad (3.70)$$

$$h(x) = 2\mathrm{e}^{-2x}(1 + 2x + x^2), \qquad (3.71)$$

where we have used the identity $\mathrm{tr}[\boldsymbol{e}_\rho \times \boldsymbol{I} \times \boldsymbol{e}_\rho] = -2$. As seen from

$$\boldsymbol{\nabla}\left[\frac{h(\xi r/c)}{r^4}\right] = -\frac{4\boldsymbol{r}}{r^6}\left[\mathrm{e}^{-2x}(2 + 4x + 3x^2 + x^3)\right]_{x=\xi r/c}, \tag{3.72}$$

the CP force associated with weakly magnetic bodies is hence a volume integral over repulsive central forces, in contrast to the force created by weakly dielectric bodies.[4] The retarded/non-retarded limits of Eq. (3.70) can be obtained in close analogy to the dielectric case. In the retarded limit, the approximations $\alpha(\mathrm{i}\xi) \simeq \alpha(0)$, $\zeta(\boldsymbol{s}, \mathrm{i}\xi) \simeq \zeta(\boldsymbol{s}, 0)$ can be made, hence we have

$$U(\boldsymbol{r}_A) = \frac{\hbar c\alpha(0)}{32\pi^3\varepsilon_0}\int \mathrm{d}^3 s\, \frac{\zeta(\boldsymbol{s}, 0)}{|\boldsymbol{r}_A - \boldsymbol{s}|^7}\int_0^\infty \mathrm{d}x\, x^2 h(x) = \frac{7\hbar c\alpha(0)}{64\pi^3\varepsilon_0}\int \mathrm{d}^3 s\, \frac{\zeta(\boldsymbol{s}, 0)}{|\boldsymbol{r}_A - \boldsymbol{s}|^7}. \tag{3.73}$$

In the non-retarded limit, one may set $h(x) \simeq h(0) = 2$, resulting in

$$U(\boldsymbol{r}_A) = \frac{\hbar\mu_0}{16\pi^3}\int \frac{\mathrm{d}^3 s}{|\boldsymbol{r}_A - \boldsymbol{s}|^4}\int_0^\infty \mathrm{d}\xi\, \xi^2\alpha(\mathrm{i}\xi)\zeta(\boldsymbol{s}, \mathrm{i}\xi). \tag{3.74}$$

Comparing Eqs. (3.66) and (3.67) with Eqs. (3.73) and (3.74), we note that to leading order, the CP-potential contributions from volume elements possessing dielectric or magnetic properties differ not only in their sign, but they also exhibit different asymptotic distance laws. In the retarded limit, the contributions from magnetic volume elements show the same r^7-dependence as the dielectric-region contributions, but are weaker by factor of $7/23$. In the non-retarded limit, on the contrary, even the asymptotic power laws are different, the r^6-potential due to dielectric volume elements being much stronger than the r^4-potential created by magnetic volume elements for small distances.

To study the influence of material absorption on the ground-state CP potential, we model $\chi(\boldsymbol{r}, \omega)$ and $\zeta(\boldsymbol{r}, \omega)$ by the single-resonance Drude–Lorentz forms

$$\chi(\boldsymbol{r}, \omega) = \frac{\omega_{\mathrm{P}e}^2(\boldsymbol{r})}{\omega_{\mathrm{T}e}^2(\boldsymbol{r}) - \omega^2 - \mathrm{i}\omega\gamma_e(\boldsymbol{r})}, \qquad \zeta(\boldsymbol{r}, \omega) = \frac{\omega_{\mathrm{P}m}^2(\boldsymbol{r})}{\omega_{\mathrm{T}m}^2(\boldsymbol{r}) - \omega^2 - \mathrm{i}\omega\gamma_m(\boldsymbol{r})} \tag{3.75}$$

where $\omega_{\mathrm{P}e}$, $\omega_{\mathrm{P}m}$ are the electric and magnetic plasma frequencies of the medium, $\omega_{\mathrm{T}e}$, $\omega_{\mathrm{T}m}$ are the transverse electric and magnetic resonance frequencies and γ_e, γ_m are the absorption parameters. We have

$$\frac{\partial}{\partial\gamma_e}\chi(\boldsymbol{r}, \mathrm{i}\xi) = -\frac{\xi\omega_{\mathrm{P}e}^2(\boldsymbol{r})}{[\omega_{\mathrm{T}e}^2(\boldsymbol{r}) + \xi^2 + \xi\gamma_e(\boldsymbol{r})]^2} < 0, \tag{3.76}$$

$$\frac{\partial}{\partial\gamma_m}\zeta(\boldsymbol{r}, \mathrm{i}\xi) = -\frac{\xi\omega_{\mathrm{P}m}^2(\boldsymbol{r})}{[\omega_{\mathrm{T}m}^2(\boldsymbol{r}) + \xi^2 + \xi\gamma_m(\boldsymbol{r})]^2} < 0, \tag{3.77}$$

so that Eqs. (3.63) and (3.70) show that an increase of electric or magnetic absorption leads to a decrease of the potential components associated with weakly dielectric or magnetic bodies, with the effect becoming small for large atom–body separations (where only small values

---

[4]This difference will be made plausible in Sec. 3.6.1 by means of a simple physical model.

of ξ contribute). The reduction can be understood by recalling that the ground-state CP potential may be regarded as being due to the fluctuating electromagnetic field inducing an electric dipole of the atomic system and the fluctuating electric dipole moment, inducing an electric field [cf. the remarks below Eq. (3.30)]. Material absorption has the effect of reducing the induced electric field and hence weakening the second source of the CP potential. Note that our conclusions about the role of absorption naturally generalise to multi-resonance media; furthermore, they remain valid for bodies with stronger magnetoelectric properties.

3.5 Microscopic origin

In our description of the CP interaction between a ground-state atom and a macroscopic body, the atom and body properties enter in fundamentally different ways. Whereas the atom is a microscopic, point-like object at position $\boldsymbol{r}_A$ characterised by its polarisability $\alpha(\omega)$, the bodies are described by their macroscopic permittivity $\varepsilon(\boldsymbol{r}, \omega)$ and permeability $\mu(\boldsymbol{r}, \omega)$ which are assumed to be smoothly varying functions of $\boldsymbol{r}$. It is therefore quite natural to address the microscopic origin of the CP potential by investigating how the macroscopic-QED result can be related to a theory of the CP interaction where both atom and bodies are treated in a microscopic way.

Let us focus our attention on a ground-state atom A interacting with a single dielectric body occupying a volume V and being characterised by a susceptibility $\chi(\boldsymbol{r}, \omega)$, where we allow for an arbitrary background of additional magnetoelectric bodies described by $\overline{\varepsilon}(\boldsymbol{r}, \omega)$ and $\overline{\mu}(\boldsymbol{r}, \omega)$. Making use of the Born expansion introduced in the previous section 3.4, one can show that the CP potential associated with the dielectric body of interest can be written in the form (App. D.1)[5]

$$U(\boldsymbol{r}_A) = \sum_{K=1}^{\infty} \Delta_K U(\boldsymbol{r}_A), \tag{3.78}$$

$$\Delta_K U(\boldsymbol{r}_A) = \frac{(-1)^K \hbar \mu_0}{2\pi c^{2K}} \left[\prod_{J=1}^{K} \int_V \mathrm{d}^3 s_J \, \chi(\boldsymbol{s}_J, \mathrm{i}\xi) \right] \int_0^{\infty} \mathrm{d}\xi \, \xi^{2K+2} \alpha_A(\mathrm{i}\xi)$$

$$\times \mathrm{tr} \left[\overline{\boldsymbol{G}}(\boldsymbol{r}_A, \boldsymbol{s}_1, \mathrm{i}\xi) \cdot \overline{\boldsymbol{G}}(\boldsymbol{s}_1, \boldsymbol{s}_2, \mathrm{i}\xi) \cdots \overline{\boldsymbol{G}}(\boldsymbol{s}_K, \boldsymbol{r}_A, \mathrm{i}\xi) \right] \tag{3.79}$$

[recall Eq. (3.53)]. We now assume that the dielectric body consists of polarisable atoms of various species B having polarisabilities $\alpha_B(\omega)$ and number densities $n_B(\boldsymbol{r})$. The gap between the macroscopic and microscopic descriptions of the body can then be bridged by

---

[5]Note that the polarisability of atom A has been denoted by $\alpha_A(\omega)$ to distinguish it from that of the body atoms to be introduced in the following.

means of the Clausius–Mosotti law [171]

$$\chi(\boldsymbol{r},\omega) = \frac{\varepsilon_0^{-1}\sum_B n_B(\boldsymbol{r})\alpha_B(\omega)}{1-(3\varepsilon_0)^{-1}\sum_C n_C(\boldsymbol{r})\alpha_C(\omega)}\,. \tag{3.80}$$

Note that since $\chi(\boldsymbol{r},\omega)$ is the Fourier transform of a linear response function, it must satisfy the condition $\chi(\boldsymbol{r},0)>\chi(\boldsymbol{r},\mathrm{i}\xi)>0$ for $\xi>0$, which implies that the inequality

$$\frac{1}{3\varepsilon_0}\sum_B n_B(\boldsymbol{r})\alpha_B(0) < 1 \tag{3.81}$$

must hold.

Substituting Eq. (3.80) into Eq. (3.79) and taking into account that the unperturbed Green tensor can be decomposed as

$$\overline{\boldsymbol{G}}(\boldsymbol{r},\boldsymbol{r}',\omega) = -\tfrac{1}{3}(c/\omega)^2\delta(\boldsymbol{\rho})\boldsymbol{I} + \overline{\boldsymbol{H}}(\boldsymbol{r},\boldsymbol{r}',\omega) \tag{3.82}$$

[cf. Eq. (3.60)], one may write

$$\Delta_K U(\boldsymbol{r}_A) = \sum_{L=1}^{K}\Delta_K^L U(\boldsymbol{r}_A), \tag{3.83}$$

where

$$\Delta_K^L U(\boldsymbol{r}_A) = \sum_{\substack{\eta_1\geq 0,\ldots,\eta_L\geq 0\\ \eta_1+\ldots+\eta_L=K-L}}\left[\prod_{J=1}^{L}\int_V \mathrm{d}^3 s_J\,\frac{\sum_{B_J} n_{B_J}(\boldsymbol{s}_J)q^{\eta_J}(\boldsymbol{s}_J,\mathrm{i}\xi)}{1-(3\varepsilon_0)^{-1}\sum_{C_J} n_{C_J}(\boldsymbol{s}_J)\alpha_{C_J}(\mathrm{i}\xi)}\right]\int_0^\infty \mathrm{d}\xi$$
$$\times V_{AB_1\ldots B_L}(\boldsymbol{r}_A,\boldsymbol{s}_1,\ldots,\boldsymbol{s}_L,\mathrm{i}\xi) \quad (3.84)$$

with

$$V_{A_1\ldots A_J}(\boldsymbol{r}_1,\ldots,\boldsymbol{r}_J) = \int_0^\infty \mathrm{d}\xi\, V_{A_1\ldots A_J}(\boldsymbol{r}_1,\ldots,\boldsymbol{r}_J,\mathrm{i}\xi)$$
$$= \frac{(-1)^{J-1}\hbar\mu_0^J}{2\pi}\int_0^\infty \mathrm{d}\xi\,\xi^{2J}\alpha_{A_1}(\mathrm{i}\xi)\cdots\alpha_{A_J}(\mathrm{i}\xi)\mathrm{tr}\big[\overline{\boldsymbol{H}}(\boldsymbol{r}_1,\boldsymbol{r}_2,\mathrm{i}\xi)\cdots\overline{\boldsymbol{H}}(\boldsymbol{r}_J,\boldsymbol{r}_1,\mathrm{i}\xi)\big] \quad (3.85)$$

denotes the sum of all L-atom terms that are of order K in χ; and each power of the factor

$$q(\boldsymbol{r},\mathrm{i}\xi) = \frac{-(3\varepsilon_0)^{-1}\sum_B n_B(\boldsymbol{r})\alpha_B(\mathrm{i}\xi)}{1-(3\varepsilon_0)^{-1}\sum_C n_C(\boldsymbol{r})\alpha_C(\mathrm{i}\xi)} \tag{3.86}$$

is due to the integration of one delta function. Summing Eq. (3.82) over K and rearranging the double sum

$$\sum_{K=1}^{\infty}\Delta_K U(\boldsymbol{r}_A) = \sum_{K=1}^{\infty}\sum_{L=1}^{K}\Delta_K^L U(\boldsymbol{r}_A) = \sum_{L=1}^{\infty}\Delta^L U(\boldsymbol{r}_A), \tag{3.87}$$

we find

$$\Delta^L U(\boldsymbol{r}_A) = \left[\prod_{J=1}^{L}\int_V \mathrm{d}^3 s_J\,\frac{\sum_{B_J} n_{B_J}(\boldsymbol{s}_J)}{1-(3\varepsilon_0)^{-1}\sum_{C_J} n_{C_J}(\boldsymbol{s}_J)\alpha_{C_J}(\mathrm{i}\xi)}\sum_{\eta_J=0}^{\infty}q^{\eta_J}(\boldsymbol{s}_J,\mathrm{i}\xi)\right]\int_0^\infty \mathrm{d}\xi$$
$$\times V_{AB_1\ldots B_L}(\boldsymbol{r}_A,\boldsymbol{s}_1,\ldots,\boldsymbol{s}_L,\mathrm{i}\xi)$$
$$= \left[\prod_{J=1}^{L}\int_V \mathrm{d}^3 s_J\sum_{B_J} n_{B_J}(\boldsymbol{s}_J)\right]V_{AB_1\ldots B_L}(\boldsymbol{r}_A,\boldsymbol{s}_1,\ldots,\boldsymbol{s}_L), \tag{3.88}$$

where we have performed the geometric sums

$$\sum_{\eta=0}^{\infty} q^{\eta}(\boldsymbol{r}, \mathrm{i}\xi) = 1 - \frac{1}{3\varepsilon_0} \sum_B n_B(\boldsymbol{r})\alpha_B(\mathrm{i}\xi) \tag{3.89}$$

by means of Eq. (3.86) and recalled Eq. (3.85). Note that convergence of the geometric sums requires $|q(\boldsymbol{r}, \mathrm{i}\xi)| < 1$, which by means of Eq. (3.81) is equivalent to

$$\frac{2}{3\varepsilon_0} \sum_B n_B(\boldsymbol{r})\alpha_B(0) < 1. \tag{3.90}$$

As a last step, we require all many-atom terms to be fully symmetrised with respect to the positions of the atoms. To achieve this, we introduce the symmetrisation operator

$$\mathcal{S}f(\boldsymbol{r}_1, \ldots, \boldsymbol{r}_J) = \frac{1}{(2 - \delta_{2J})J} \sum_{\Pi \in P(J)} f(\boldsymbol{r}_{\Pi(1)}, \ldots, \boldsymbol{r}_{\Pi(J)}) \tag{3.91}$$

where $P(J)$ denotes the permutation group of the numbers $1, \ldots, J$. As a trivial consequence of the cyclic property of the trace as well as the symmetry of the Green tensor, (2.17) together with Eq. (3.82), one easily finds that

$$\mathrm{tr}\Big[\overline{\boldsymbol{H}}(\boldsymbol{r}_1, \boldsymbol{r}_2, \omega)\cdots\overline{\boldsymbol{H}}(\boldsymbol{r}_J, \boldsymbol{r}_1, \omega)\Big] = \mathrm{tr}\Big[\overline{\boldsymbol{H}}(\boldsymbol{r}_{\Pi(1)}, \boldsymbol{r}_{\Pi(2)}, \omega)\cdots\overline{\boldsymbol{H}}(\boldsymbol{r}_{\Pi(J)}, \boldsymbol{r}_{\Pi(1)}, \omega)\Big] \tag{3.92}$$

if Π is either a cyclic permutation or the reverse of a cyclic permutation. With $f(\boldsymbol{r}_1, \ldots, \boldsymbol{r}_J)$ being given by the left hand side of Eq. (3.92), the sum on the right hand side of Eq. (3.91) contains classes of $(2 - \delta_{2J})J$ terms that give the same result. By forming a set $\overline{P}(J) \subsetneq P(J)$ containing exactly one representative of each class, the sum can thus be simplified, leading to

$$\mathcal{S}\mathrm{tr}\Big[\overline{\boldsymbol{H}}(\boldsymbol{r}_1, \boldsymbol{r}_2, \omega)\cdots\overline{\boldsymbol{H}}(\boldsymbol{r}_J, \boldsymbol{r}_1, \omega)\Big] = \sum_{\Pi \in \overline{P}(J)} \mathrm{tr}\Big[\overline{\boldsymbol{H}}(\boldsymbol{r}_{\Pi(1)}, \boldsymbol{r}_{\Pi(2)}, \omega)\cdots\overline{\boldsymbol{H}}(\boldsymbol{r}_{\Pi(J)}, \boldsymbol{r}_{\Pi(1)}, \omega)\Big]. \tag{3.93}$$

Symmetrisation of the many-atom terms in Eq. (3.88) can now easily be achieved by introducing the factor $1/L!$ and summing over all $L!$ possible ways of renaming the variables $\boldsymbol{s}_J$ and B_J. This generates the representative of each class in Eq. (3.93) exactly twice (only once for $J = L+1 = 2$) so that [SB1, SB10, SB13]

$$U(\boldsymbol{r}_A) = \sum_{L=1}^{\infty} \frac{1}{L!} \left[\prod_{J=1}^{L} \int_V \mathrm{d}^3 s_J \sum_{B_J} n_{B_J}(\boldsymbol{s}_J)\right] U_{AB_1\ldots B_L}(\boldsymbol{r}_A, \boldsymbol{s}_1, \ldots, \boldsymbol{s}_L) \tag{3.94}$$

with

$$U_{A_1\ldots A_N}(\boldsymbol{r}_1, \ldots, \boldsymbol{r}_N)$$
$$= \frac{(-1)^{N-1}\hbar\mu_0^N}{(1 + \delta_{2N})\pi} \int_0^{\infty} \mathrm{d}\xi\, \xi^{2N} \alpha_{A_1}(\mathrm{i}\xi)\cdots\alpha_{A_N}(\mathrm{i}\xi)\mathcal{S}\mathrm{tr}\Big[\overline{\boldsymbol{H}}(\boldsymbol{r}_1, \boldsymbol{r}_2, \mathrm{i}\xi)\cdots\overline{\boldsymbol{H}}(\boldsymbol{r}_N, \boldsymbol{r}_1, \mathrm{i}\xi)\Big] \tag{3.95}$$

being the N-atom vdW potential in the presence of arbitrary magnetoelectric bodies char-acterised by $\overline{\varepsilon}(\boldsymbol{r},\omega)$ and $\overline{\mu}(\boldsymbol{r},\omega)$.

Equation (3.94) bridges the gap between the macroscopic and microscopic approaches to the CP potential. It shows that the CP interaction of a single ground-state atom with a macroscopic dielectric body is the result of the microscopic N-atom vdW interactions of the single atom with the atoms contained in the body, provided that the susceptibility is of Clausius–Mosotti type (3.80) and the convergence condition (3.90) holds. Our derivation is valid under very general conditions (i.e., for an atom interacting with an inhomogeneous dielectric body of arbitrary shape containing different atomic species, with additional mag-netoelectric bodies possibly being present); a relation of the type (3.94) was first derived for the special case of a homogeneous dielectric half space filled with harmonic-oscillator atoms [159] and later extended to homogeneous dielectric bodies of arbitrary shapes in free space [161]. Note that the implication of our calculation can be reversed: When Eqs. (3.94) and (3.95) hold and the convergence condition (3.90) is satisfied, then the electric susceptibility must necessarily have the Clausius–Mosotti form.

Obviously the applicability of the microscopic picture depends crucially on the validity of the convergence condition (3.90). To give a physical interpretation, we recall Eq. (3.23) and apply the order-of-magnitude estimate

$$\frac{\alpha_B(0)}{\varepsilon_0} = \frac{2}{3\hbar\varepsilon_0} \sum_k \frac{|\boldsymbol{d}_{0k}^B|^2}{\omega_{k0}^B} \approx \frac{2e^2a_{\mathrm{B}}^2}{3\varepsilon_0 E_{\mathrm{Ry}}} f_B = 4f_B V_{\mathrm{at}} \qquad (3.96)$$

where e is the electron charge; $a_{\mathrm{B}} = \hbar/(\alpha_0 m_e c)$ is the Bohr radius [m_e, electron mass; $\alpha_0 = e^2/(4\pi\varepsilon_0\hbar c)$, fine-structure constant]; $E_{\mathrm{Ry}} = \hbar^2/(2m_e a_{\mathrm{B}}^2)$ is the Rydberg energy; $f_B > 1$ is a factor depending on the atomic species; and $V_{\mathrm{at}} = 4\pi a_{\mathrm{B}}^3/3$ is the volume of an atom the size of a Bohr radius. Furthermore, we write

$$\sum_B n_B(\boldsymbol{r})f_B \approx \frac{f}{V_{\mathrm{sp}}} \qquad (3.97)$$

($f > 1$), where V_{sp} is the volume accessible per atom within the body. Using these estimates, the convergence condition (3.90) can be reformulated as

$$V_{\mathrm{sp}} \gtrsim \tfrac{8}{3} f V_{\mathrm{at}}, \qquad (3.98)$$

which simply states that the atoms must be sufficiently separated within the body, such that their electronic wave functions do not overlap. This condition can be fulfilled for dielectric, but not for metal bodies.

As a side effect, our calculation has delivered the general N-atom vdW potential in the presence of arbitrary magnetoelectric bodies, Eq. (3.95), the derivation being unique

when requiring the vdW potentials to be fully symmetrised. The result for $N = 2$ has been confirmed by extending the perturbative calculation given in Sec. 3.2 to the case of two atoms [SB12, SB13]. For N atoms in free space, $\overline{H}$ in Eq. (3.95) becomes H_{free} [recall Eq. (3.61)], leading to agreement with earlier results [184]. An explicit expression for the two-atom vdW potential in free space can easily be obtained from the results given in Sec. 3.4. From Eqs. (3.63), (3.66) and (3.67) one can infer the well-known Casimir–Polder result [2]

$$U_{AB}(r_{AB}) = -\frac{\hbar}{32\pi^3\varepsilon_0^2 r_{AB}^6}\int_0^\infty d\xi\,\alpha_A(i\xi)\alpha_B(i\xi)g(\xi r_{AB}/c) \tag{3.99}$$

$(r_{AB} = |\mathbf{r}_A - \mathbf{r}_B|)$, recall Eq. (3.64); it reduces to

$$U_{AB}(r_{AB}) = -\frac{23\hbar c\alpha_A(0)\alpha_B(0)}{64\pi^3\varepsilon_0^2 r_{AB}^7} \tag{3.100}$$

in the retarded limit $(r_{AB} \gg c/\omega_{\min})$ and to the London potential [1]

$$U_{AB}(r_{AB}) = -\frac{3\hbar}{16\pi^3\varepsilon_0^2 r_{AB}^6}\int_0^\infty d\xi\,\alpha_A(i\xi)\alpha_B(i\xi) \tag{3.101}$$

in the non-retarded limit $(r_{AB} \ll c/\omega_{\max})$. An explicit expression for the free-space three-atom potential is given in App. D.2 [SB10].

The derivation leading to Eqs. (3.94) and (3.95) has shown that the use of the correct Clausius–Mosotti law (3.80) is crucial for deriving general N-atom vdW potentials from the macroscopic CP potential. On the contrary, the two-atom potential can already be extracted from the leading contribution $\Delta U(\mathbf{r}_A)$ to the CP potential [recall Eq. (3.59)] by assuming the bodies to consist of a single atomic species B and using the linearised version of the Clausius–Mosotti law $\chi(\mathbf{r},\omega) \simeq \varepsilon_0^{-1}n_B(\mathbf{r})\alpha_B(\omega)$ [5, 164, 136, 185]. An analogous statement which holds for magnetic bodies, can be used to derive the vdW potential of a polarisable atom A and a magnetisable atom B. We assume that the body described by ζ contains a single species B of atoms having a (sufficiently small) number density $n_B(\mathbf{r})$ and possessing a magnetisability $\beta_B(\omega)$, such that the linearised Clausius–Mosotti law

$$\zeta(\mathbf{r},\omega) \simeq \mu_0 n_B(\mathbf{r})\beta_B(\omega) \tag{3.102}$$

is valid. Equation (3.102) together with Eq. (3.59) implies that the two-atom potential of a polarisable atom A interacting with a magnetisable atom B in the presence of an arbitrary arrangement of magnetoelectric bodies is given by [SB1, SB14]

$$U_{AB}(\mathbf{r}_A,\mathbf{r}_A) = -\frac{\hbar\mu_0^2}{2\pi}\int_0^\infty d\xi\,\xi^2\alpha_A(i\xi)\beta_B(i\xi)\mathrm{tr}\Big[\overline{\mathbf{G}}(\mathbf{r}_A,\mathbf{r},i\xi)\times\overleftarrow{\boldsymbol{\nabla}}\cdot\boldsymbol{\nabla}\times\overline{\mathbf{G}}(\mathbf{r},\mathbf{r}_A,i\xi)\Big]_{\mathbf{r}=\mathbf{r}_B}. \tag{3.103}$$

As can be seen by combining Eq. (3.70) with Eq. (3.102), this potential reduces to

$$U_{AB}(r_{AB}) = \frac{\hbar\mu_0^2}{32\pi^3 r_{AB}^4}\int_0^\infty d\xi\,\xi^2\alpha_A(i\xi)\beta_B(i\xi)h(\xi r_{AB}/c) \tag{3.104}$$

[recall Eq. (3.71)] for the special case of two atoms placed in free space, in agreement with results found earlier [109, 186]. By recalling Eqs. (3.73) and (3.74), one finds that the free-space potential is approximately given by

$$U_{AB}(r_{AB}) = \frac{7\hbar c \mu_0 \alpha_A(0) \beta_B(0)}{64\pi^3 \varepsilon_0 r_{AB}^7} \tag{3.105}$$

in the retarded limit and by

$$U_{AB}(r_{AB}) = \frac{\hbar \mu_0^2}{16\pi^3 r_{AB}^4} \int_0^\infty \mathrm{d}\xi \, \xi^2 \alpha_A(\mathrm{i}\xi) \beta_B(\mathrm{i}\xi) \tag{3.106}$$

in the non-retarded limit. In contrast to the case of two polarisable atoms, the vdW potential of a polarisable atom and a magnetisable one is hence repulsive. While following a r_{AB}^{-7} power law in the non-retarded limit that is weaker than the corresponding r_{AB}^{-7} vdW potential of two polarisable atoms by a factor of 7/23, the vdW potential of a polarisable and a magnetisable atom exhibits a r_{AB}^{-4} power law in the non-retarded limit that is more weakly diverging than the asymptotic r_{AB}^{-6} potential of two polarisable atoms.

3.6 Applications: Planar systems

The general expressions for the ground-state CP potential[6] obtained in Secs. 3.1–3.4 are valid for atoms placed within arbitrary arrangements of magnetoelectric bodies. For specific geometries, more explicit expressions can be obtained by substitution of the appropriate Green tensors and one can then investigate how the respective CP potentials depend on the atomic position and on the medium and geometry parameters. This will be illustrated in the following by applying the general theory to atoms placed within planar multilayer systems.[7] Note that many geometries studied both theoretically and in experiments belong to this class of systems, examples including idealised model situations like perfectly reflecting plates or semi-infinite half spaces; more realistic cases like plates of finite thickness; and even complex structures like planar cavities.

We first consider the general case of an atom placed inside the gap (of width l) between two planar magnetoelectric multilayer stacks (Fig. 3.1). The left/right stacks are labelled by $\pm$, they consist of $n_\pm$ homogeneous slabs of permittivity $\varepsilon_j^\pm(\omega)$, permeability $\mu_j^\pm(\omega)$ and thickness $d_j^\pm$ $(j = 1, \ldots, n_\pm)$, where $d_{n_\pm}^\pm = \infty$. The z axis is chosen perpendicular to the slab interfaces, extending from $z = 0$ to $z = l$. The scattering part of the Green tensor for $\boldsymbol{r}$ and $\boldsymbol{r}'$ inside the gap is given by [183]

$$\boldsymbol{G}^{(1)}(\boldsymbol{r}, \boldsymbol{r}', \mathrm{i}\xi) = \int \mathrm{d}^2 q \, \mathrm{e}^{\mathrm{i}\boldsymbol{q}\cdot(\boldsymbol{r}-\boldsymbol{r}')} \boldsymbol{G}^{(1)}(\boldsymbol{q}, z, z', \mathrm{i}\xi) \tag{3.107}$$

---

[6]The CP force for atoms initially prepared in an excited state will be discussed in chapter 4.

[7]Examples of other geometries can be found in Refs. [SB5, SB13] and [SB10] where atoms interacting with magnetoelectic spheres and rings are studied, respectively.
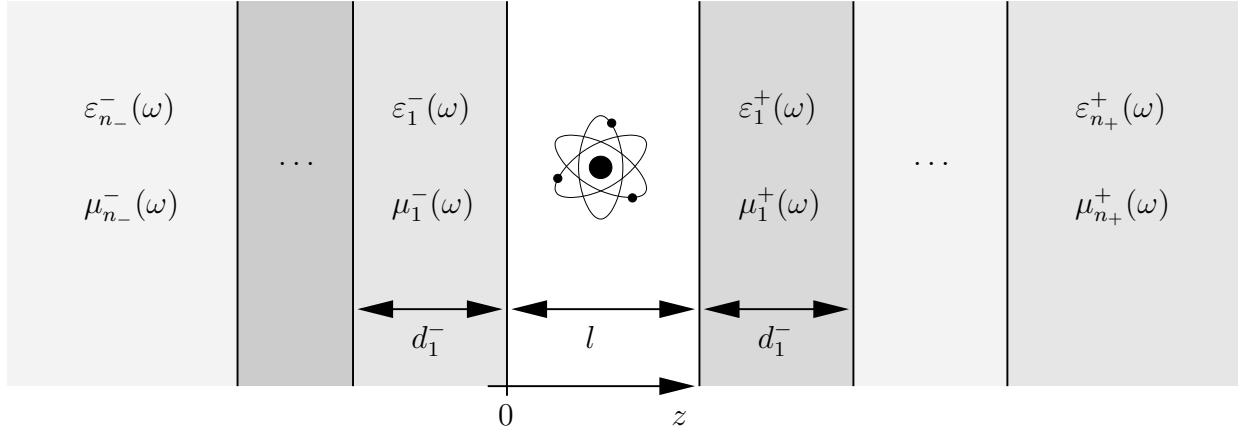
Figure 3.1: An atom within a planar multilayer system is schematically shown.

$(\boldsymbol{q} \perp \boldsymbol{e}_z)$, where

$$\boldsymbol{G}^{(1)}(\boldsymbol{q}, z, z', \mathrm{i}\xi) = \frac{1}{8\pi^2 b} \sum_{\sigma=s,p} \left\{ \frac{r_\sigma^- r_\sigma^+ \mathrm{e}^{-2bl}}{D_\sigma} \left[\boldsymbol{e}_\sigma^+ \boldsymbol{e}_\sigma^+ \mathrm{e}^{-b(z-z')} + \boldsymbol{e}_\sigma^- \boldsymbol{e}_\sigma^- \mathrm{e}^{b(z-z')} \right] \right.$$
$$\left. + \frac{1}{D_\sigma} \left[\boldsymbol{e}_\sigma^+ \boldsymbol{e}_\sigma^- r_\sigma^- \mathrm{e}^{-b(z+z')} + \boldsymbol{e}_\sigma^- \boldsymbol{e}_\sigma^+ r_\sigma^+ \mathrm{e}^{-2bl} e^{b(z+z')} \right] \right\}. \quad (3.108)$$

Here,

$$\boldsymbol{e}_s^\pm = \boldsymbol{e}_q \times \boldsymbol{e}_z, \qquad \boldsymbol{e}_p^\pm = -\frac{c}{\xi} \left(\mathrm{i}q\boldsymbol{e}_z \pm b\boldsymbol{e}_q \right) \quad (3.109)$$

$(q = |\boldsymbol{q}|,\ \boldsymbol{e}_q = \boldsymbol{q}/q)$ are the polarisation vectors for s- and p-polarised waves propagating in the positive and negative z-directions; r_σ^- and r_σ^+ are the generalised coefficients for reflexion at the left/right multilayer stack which are the solutions $r_\sigma^- \equiv r_{\sigma 0}^\pm$ ($\varepsilon_0^\pm \equiv \mu_0^\pm \equiv 1$) of the recursive relations[8]

$$r_{sj}^\pm = r_{sj}^\pm(q, \mathrm{i}\xi) = \frac{(\mu_{j+1}^\pm b_j^\pm - \mu_j^\pm b_{j+1}^\pm) + (\mu_{j+1}^\pm b_j^\pm + \mu_j^\pm b_{j+1}^\pm)\mathrm{e}^{-2b_{j+1}^\pm d_{j+1}^\pm} r_{sj+1}^\pm}{(\mu_{j+1}^\pm b_j^\pm + \mu_j^\pm b_{j+1}^\pm) + (\mu_{j+1}^\pm b_j^\pm - \mu_j^\pm b_{j+1}^\pm)\mathrm{e}^{-2b_{j+1}^\pm d_{j+1}^\pm} r_{sj+1}^\pm}, \quad (3.110)$$

$$r_{pj}^\pm = r_{pj}^\pm(q, \mathrm{i}\xi) = \frac{(\varepsilon_{j+1}^\pm b_j^\pm - \varepsilon_j^\pm b_{j+1}^\pm) + (\varepsilon_{j+1}^\pm b_j^\pm + \varepsilon_j^\pm b_{j+1}^\pm)\mathrm{e}^{-2b_{j+1}^\pm d_{j+1}^\pm} r_{pj+1}^\pm}{(\varepsilon_{j+1}^\pm b_j^\pm + \varepsilon_j^\pm b_{j+1}^\pm) + (\varepsilon_{j+1}^\pm b_j^\pm - \varepsilon_j^\pm b_{j+1}^\pm)\mathrm{e}^{-2b_{j+1}^\pm d_{j+1}^\pm} r_{pj+1}^\pm} \quad (3.111)$$

$(j = 0, \ldots, n_\pm - 1)$ with $r_{\sigma n_\pm}^\pm = 0$;

$$b_j^\pm = b_j^\pm(q, \mathrm{i}\xi) = \sqrt{\frac{\xi^2}{c^2} \varepsilon_j(\mathrm{i}\xi)\mu_j(\mathrm{i}\xi) + q^2}, \qquad b = b(q, \mathrm{i}\xi) \equiv b_0^\pm(q, \mathrm{i}\xi) = \sqrt{\frac{\xi^2}{c^2} + q^2} \quad (3.112)$$

is the imaginary part of the z-component of the wave vector in the respective slab; and the coefficients D_σ are defined by

$$D_\sigma = D_\sigma(q, \mathrm{i}\xi) = 1 - r_\sigma^- r_\sigma^+ \mathrm{e}^{-2bl}. \quad (3.113)$$

---

[8]Note that instead of calculating the reflexion coefficients by means of the recurrence relations, one can determine them via appropriate reflectivity measurements (cf., e.g., Ref. [187]).

To calculate the CP potential, we substitute Eq. (3.107) together with Eq. (3.108) into Eq. (3.24), thereby omitting position-independent terms. Evaluating the trace with the aid of the relations

$$\boldsymbol{e}_s^{\pm}\cdot\boldsymbol{e}_s^{\pm} = \boldsymbol{e}_s^{\pm}\cdot\boldsymbol{e}_s^{\mp} = 1, \qquad \boldsymbol{e}_p^{\pm}\cdot\boldsymbol{e}_p^{\pm} = 1, \qquad \boldsymbol{e}_p^{\pm}\cdot\boldsymbol{e}_p^{\mp} = -1 - 2\,\frac{q^2c^2}{\xi^2} \qquad (3.114)$$

which directly follow from Eqs. (3.109) and (3.112), we realise that the resulting integrand of the **q**-integral only depends on q. Thus after introducing polar coordinates in the $q_x q_y$-plane, we can easily perform the angular integration, leading to [SB1, SB8, SB9]

$$U(z_A) = \frac{\hbar\mu_0}{8\pi^2}\int_0^{\infty}\mathrm{d}\xi\,\xi^2\alpha(\mathrm{i}\xi)\int_0^{\infty}\mathrm{d}q\,\frac{q}{b}\left\{\mathrm{e}^{-2bz_A}\left[\frac{r_s^-}{D_s} - \left(1 + 2\,\frac{q^2c^2}{\xi^2}\right)\frac{r_p^-}{D_p}\right]\right.$$
$$\left. + \,\mathrm{e}^{-2b(l-z_A)}\left[\frac{r_s^+}{D_s} - \left(1 + 2\,\frac{q^2c^2}{\xi^2}\right)\frac{r_p^+}{D_p}\right]\right\}. \quad (3.115)$$

Equation (3.115) together with Eqs. (3.110)–(3.113) gives the CP potential of a ground-state atom placed between two arbitrary magnetoelectric multilayer stacks in terms of the atomic polarisability and the generalised reflexion coefficients of the stacks. Note that the CP potential only depends on z_A, in agreement with the symmetry of the planar multilayer system. If the atom is placed near a single multilayer stack, say the right stack is absent, Eq. (3.115) simplifies to ($r_\sigma \equiv r_\sigma^-$)

$$U(z_A) = \frac{\hbar\mu_0}{8\pi^2}\int_0^{\infty}\mathrm{d}\xi\,\xi^2\alpha(\mathrm{i}\xi)\int_0^{\infty}\mathrm{d}q\,\frac{q}{b}\,\mathrm{e}^{-2bz_A}\left[r_s - \left(1 + 2\,\frac{q^2c^2}{\xi^2}\right)r_p\right]. \qquad (3.116)$$

3.6.1   Perfectly reflecting plate

Let us first consider the idealised example of an atom positioned in front of a perfectly reflecting plate, where $|r_\sigma| = 1$. We begin with the case $r_s = -1$, $r_p = 1$, which corresponds to the limit of a perfectly conducting plate ($\varepsilon_{1-} \to \infty$), as can be seen from Eqs. (3.110)–(3.112). Changing the integration variables in Eq. (3.116) according to

$$\int_0^{\infty}\mathrm{d}\xi\int_0^{\infty}\mathrm{d}q\,\frac{q}{b}\,\mathrm{e}^{-2bz_A}\ldots \mapsto \int_0^{\infty}\mathrm{d}\xi\int_{\xi/c}^{\infty}\mathrm{d}b\,\mathrm{e}^{-2bz_A}\ldots \qquad (3.117)$$

[recall Eq. (3.112)] and carrying out the b-integral, we obtain the attractive CP potential [SB1, SB9]

$$U(z_A) = -\frac{\hbar}{16\pi^2\varepsilon_0 z_A^3}\int_0^{\infty}\mathrm{d}\xi\,\alpha(\mathrm{i}\xi)\,\mathrm{e}^{-2\xi z_A/c}\left[1 + 2\,\frac{\xi z_A}{c} + 2\,\frac{\xi^2 z_A^2}{c^2}\right], \qquad (3.118)$$

in agreement with the famous result found by Casimir and Polder [2]. In the retarded limit ($z_A \gg c/\omega_{\min}$), the ξ-integral is effectively limited to a region where the approximation $\alpha(\mathrm{i}\xi) \simeq \alpha(0)$ is valid, and an evaluation of the ξ-integral results in

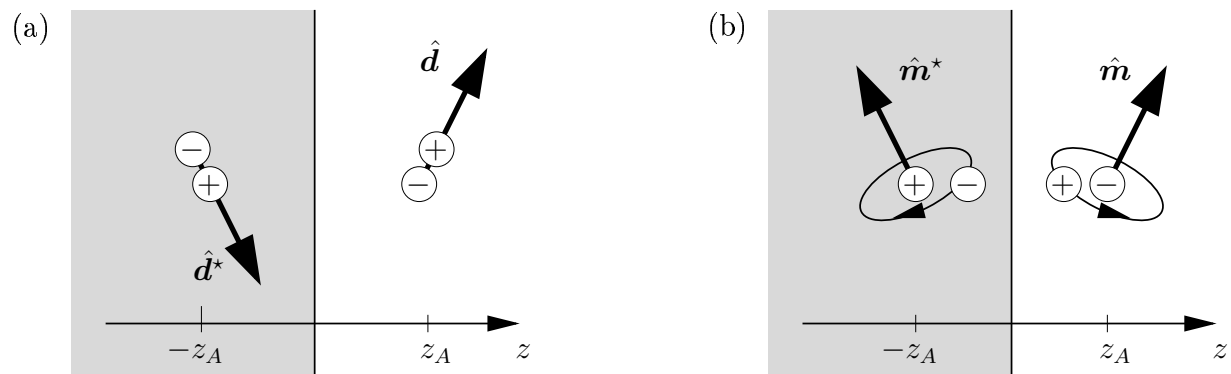$$U(z_A) = -\frac{3\hbar c\alpha(0)}{32\pi^2\varepsilon_0 z_A^4}. \qquad (3.119)$$

Figure 3.2: The image dipole construction for an (a) electric (b) magnetic dipole in front of a perfectly conducting plate, is shown.

In the non-retarded limit ($z_A \ll c/\omega_{\max}$), the factor $\alpha(\mathrm{i}\xi)$ limits the ξ-integral in Eq. (3.118) to a range where we may approximately set $e^{-2\xi z_A/c} \simeq 1$ and neglect the second and third terms in the square brackets to recover the result of Lennard-Jones [3],

$$U(z_A) = -\frac{1}{48\pi\varepsilon_0 z_A^3} \sum_k |\boldsymbol{d}_{0k}|^2 = -\frac{\langle 0|\hat{\boldsymbol{d}}^2|0\rangle}{48\pi\varepsilon_0 z_A^3}, \qquad (3.120)$$

where we have recalled Eq. (3.23).

In contrast, if the plate is infinitely permeable ($\mu_{1-} \to \infty$), Eqs. (3.110)–(3.112) lead to $r_s = 1$, $r_p = -1$ and Eq. (3.116) yields the repulsive CP potential [SB1, SB9]

$$U(z_A) = \frac{\hbar}{16\pi^2\varepsilon_0 z_A^3} \int_0^\infty \mathrm{d}\xi\, \alpha(\mathrm{i}\xi) e^{-2\xi z_A/c} \left[1 + 2\frac{\xi z_A}{c} + 2\frac{\xi^2 z_A^2}{c^2}\right] \qquad (3.121)$$

which reduces to

$$U(z_A) = \frac{3\hbar c\alpha(0)}{32\pi^2\varepsilon_0 z_A^4} \qquad (3.122)$$

and

$$U(z_A) = \frac{\langle 0|\hat{\boldsymbol{d}}^2|0\rangle}{48\pi\varepsilon_0 z_A^3} \qquad (3.123)$$

in the retarded and non-retarded limits, respectively.

The different signs of the non-retarded CP potentials associated with plates possessing perfect electric/magnetic properties can be understood from an image-dipole model. To see this, recall that the non-retarded CP potential is entirely due to the Coulomb interaction of the atom with the plate, which in turn can be modelled by the interaction of the atomic dipole moment with its image in the plate, cf., e.g., Ref. [3]. The image of an electric dipole moment $\hat{\boldsymbol{d}} = (\hat{d}_x, \hat{d}_y, \hat{d}_z)$ situated at a distance z_A from a perfectly conducting plate, is constructed by a reflection at the xy-plane, together with an interchange of positive and negative charges; it is given by $\hat{\boldsymbol{d}}^\star = (-\hat{d}_x, -\hat{d}_y, \hat{d}_z)$, cf. Fig 3.2(a). The average interaction energy of the dipole and its image is hence given by [171]

$$U(z_A) = \frac{1}{2} \frac{\langle 0|\hat{\boldsymbol{d}}\cdot\hat{\boldsymbol{d}}^\star - 3\hat{d}_z\hat{d}_z^\star|0\rangle}{4\pi\varepsilon_0(2z_A)^3} = -\frac{\langle 0|\hat{\boldsymbol{d}}^2 + \hat{d}_z^2|0\rangle}{64\pi\varepsilon_0 z_A^3} = -\frac{\langle 0|\hat{\boldsymbol{d}}^2|0\rangle}{48\pi\varepsilon_0 z_A^3}, \qquad (3.124)$$

reproducing to the attractive potential (3.120), where the factor $1/2$ accounts for the fact that the second dipole is induced by the first one and we have assumed isotropy of the atom, $\langle 0|\hat{d}_z^2|0\rangle = (1/3)\langle 0|\hat{\boldsymbol{d}}^2|0\rangle$.

The interaction of a polarisable atom with an infinitely permeable plate is equivalent to the interaction of a magnetisable one with a perfectly conducting plate by virtue of a duality transformation. We hence consider a magnetic dipole $\hat{\boldsymbol{m}} = (\hat{m}_x, \hat{m}_y, \hat{m}_z)$ in front of a perfect conductor. Since the magnetic dipole moment behaves like a pseudo-vector under reflexion, its image is given by $\hat{\boldsymbol{m}}^\star = (\hat{m}_x, \hat{m}_y, -\hat{m}_z)$, cf. Fig 3.2(b). The interaction energy of the magnetic dipole and its image reads

$$U(z_A) = \frac{1}{2}\frac{\langle 0|\hat{\boldsymbol{m}}\cdot\hat{\boldsymbol{m}}^\star - 3\hat{m}_z\hat{m}_z^\star|0\rangle}{4\pi\varepsilon_0(2z_A)^3} = \frac{\langle 0|\hat{\boldsymbol{m}}^2|0\rangle}{48\pi\varepsilon_0 z_A^3}, \tag{3.125}$$

which by means of a duality transformation, leads to the repulsive CP potential of a polarisable atom in front of an infinitely permeable plate (3.123). The different signs of the CP potential associated with electric/magnetic bodies can thus be understood from the different reflexion behaviour of electric and magnetic dipole moments.

3.6.2 Half space

To study the influence of the medium properties on the CP potential under more realistic conditions, we next consider an atom in front of a semi-infinite magnetoelectric half space of permittivity $\varepsilon(\omega) \equiv \varepsilon_1^-(\omega)$ and permeability $\mu(\omega) \equiv \mu_1^-(\omega)$. Substituting the reflexion coefficients (3.110) and (3.111) into Eq. (3.116), we find [$b_1 \equiv b_1^-$, recall Eq. (3.112)] [SB1, SB7, SB8, SB9]

$$U(z_A) = \frac{\hbar\mu_0}{8\pi^2}\int_0^\infty \mathrm{d}\xi\,\xi^2\alpha(\mathrm{i}\xi)\int_0^\infty \mathrm{d}q\,\frac{q}{b}\,\mathrm{e}^{-2bz_A}$$
$$\times \left[\frac{\mu(\mathrm{i}\xi)b - b_1}{\mu(\mathrm{i}\xi)b + b_1} - \left(1 + 2\frac{q^2c^2}{\xi^2}\right)\frac{\varepsilon(\mathrm{i}\xi)b - b_1}{\varepsilon(\mathrm{i}\xi)b + b_1}\right], \quad (3.126)$$

which agrees with the result derived in Ref. [141] within the frame of linear-response theory and reduces to the well-known Lifshitz formula [5] for the case of a purely electric half space.

To find the asymptotic behaviour of Eq. (3.126) in the retarded limit ($z_A \gg c/\omega_{\min}$), we introduce the new integration variable $v = cb/\xi$ and transform the integral according to

$$\int_0^\infty \mathrm{d}\xi \int_0^\infty \mathrm{d}q\,\frac{q}{b}\,\mathrm{e}^{-2bz_A} \ldots \mapsto \int_1^\infty \mathrm{d}v \int_0^\infty \mathrm{d}\xi\,\frac{\xi}{c}\,\mathrm{e}^{-2v\xi z_A/c} \ldots, \tag{3.127}$$

where b_1 changes to

$$b_1 = \frac{\xi}{c}\sqrt{\varepsilon(\mathrm{i}\xi)\mu(\mathrm{i}\xi) - 1 + v^2}. \tag{3.128}$$

It is then seen that in the retarded limit, the factor $\mathrm{e}^{-2v\xi z_A/c}$ effectively limits the ξ-integral to a range where the approximations $\alpha(\mathrm{i}\xi) \simeq \alpha(0)$, $\varepsilon(\mathrm{i}\xi) \simeq \varepsilon(0)$, $\mu(\mathrm{i}\xi) \simeq \mu(0)$ apply, hence the ξ-integration can be carried out, resulting in

$$U(z_A) = \frac{C_4}{z_A^4}, \tag{3.129}$$

$$C_4 = -\frac{3\hbar c\alpha(0)}{64\pi^2\varepsilon_0} \int_1^\infty \mathrm{d}v \left[\left(\frac{2}{v^2} - \frac{1}{v^4} \right) \frac{\varepsilon(0)v - \sqrt{\varepsilon(0)\mu(0) - 1 + v^2}}{\varepsilon(0)v + \sqrt{\varepsilon(0)\mu(0) - 1 + v^2}} \right.$$
$$\left. - \frac{1}{v^4} \frac{\mu(0)v - \sqrt{\varepsilon(0)\mu(0) - 1 + v^2}}{\mu(0)v + \sqrt{\varepsilon(0)\mu(0) - 1 + v^2}} \right]. \tag{3.130}$$

The nonretarded limit $[n(0)z_A \ll c/\omega_{\max}$ with $n(0) = \sqrt{\varepsilon(0)\mu(0)}\,]$, is conveniently treated by using the integration variables (ξ, b), recall Eq. (3.117), where b_1 becomes

$$b_1 = \sqrt{\frac{\xi^2}{c^2}\left[\varepsilon(\mathrm{i}\xi)\mu(\mathrm{i}\xi) - 1 \right] + b^2}\,. \tag{3.131}$$

For $n(0)z_A \ll c/\omega_{\max}$, the factors $\alpha(\mathrm{i}\xi)$, $\varepsilon(\mathrm{i}\xi)b - b_1$ and $\mu(\mathrm{i}\xi)b - b_1$ limit the ξ-integral in Eq. (3.126) to a range where $(\xi z_A/c)\sqrt{\varepsilon(\mathrm{i}\xi)\mu(\mathrm{i}\xi) - 1} \lesssim (\omega_{\max}z_A/c)n(0) \ll 1$. One may hence apply a Taylor expansion by retaining only the leading-order terms in $\xi\sqrt{\varepsilon(\mathrm{i}\xi)\mu(\mathrm{i}\xi) - 1}/(cb)$, which correspond to the leading-order terms in $\xi z_A\sqrt{\varepsilon(\mathrm{i}\xi)\mu(\mathrm{i}\xi) - 1}/c$. Again discarding higher-order terms in $\xi z_A/c$, this results in

$$U(z_A) = -\frac{C_3}{z_A^3} + \frac{C_1}{z_A}, \tag{3.132}$$

$$C_3 = \frac{\hbar}{16\pi^2\varepsilon_0} \int_0^\infty \mathrm{d}\xi\, \alpha(\mathrm{i}\xi) \frac{\varepsilon(\mathrm{i}\xi) - 1}{\varepsilon(\mathrm{i}\xi) + 1} \geq 0, \tag{3.133}$$

$$C_1 = \frac{\hbar\mu_0}{16\pi^2} \int_0^\infty \mathrm{d}\xi\, \xi^2\alpha(\mathrm{i}\xi) \left\{ \frac{\varepsilon(\mathrm{i}\xi) - 1}{\varepsilon(\mathrm{i}\xi) + 1} + \frac{\mu(\mathrm{i}\xi) - 1}{\mu(\mathrm{i}\xi) + 1} + \frac{2\varepsilon(\mathrm{i}\xi)[\varepsilon(\mathrm{i}\xi)\mu(\mathrm{i}\xi) - 1]}{[\varepsilon(\mathrm{i}\xi) + 1]^2} \right\} \geq 0. \tag{3.134}$$

Let us discuss these results. Equations (3.129) and (3.130) show that in the retarded limit, the CP potential is attractive/repulsive for a purely electric/magnetic half space. As the coefficient C_4 monotonously decreases with increasing $\varepsilon(0)$ and monotonously increases with $\mu(0)$,

$$\frac{\partial C_4}{\partial \varepsilon(0)} < 0, \qquad \frac{\partial C_4}{\partial \mu(0)} > 0, \tag{3.135}$$

the borderline between the attractive and repulsive potentials is given by a unique curve in the $\varepsilon(0)\mu(0)$-plane, which is defined by $C_4 = 0$, Eq. (3.130); this borderline is displayed in Fig. 3.3 on the basis of numerical calculations. In the limits of weak and strong magnetodielectric properties, analytic expressions for the borderline can be obtained. For weak magnetodielectric properties, i.e., $\chi(0) = \varepsilon(0) - 1 \ll 1$ and $\zeta(0) = \mu(0) - 1 \ll 1$, the linear
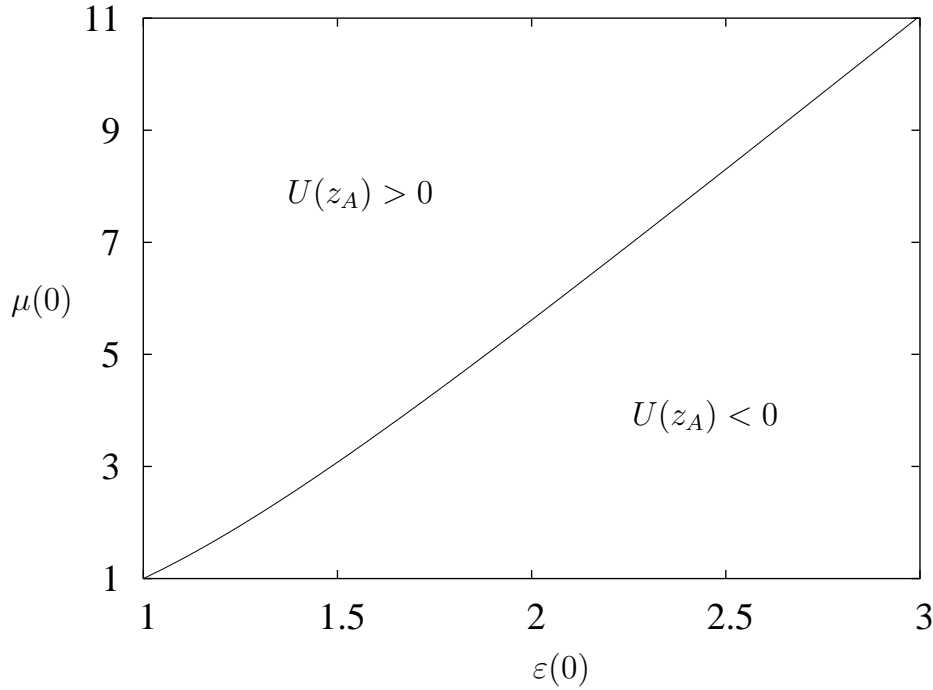
Figure 3.3: The borderline between attractive and repulsive retarded CP potentials of an atom in front of a magnetodielectric half space, is displayed.

expansions

$$\frac{\varepsilon(0)v - \sqrt{\varepsilon(0)\mu(0) - 1 + v^2}}{\varepsilon(0)v + \sqrt{\varepsilon(0)\mu(0) - 1 + v^2}} \simeq \left[\frac{1}{2} - \frac{1}{4v^2}\right]\chi(0) - \frac{1}{4v^2}\zeta(0) \tag{3.136}$$

$$\frac{\mu(0)v - \sqrt{\varepsilon(0)\mu(0) - 1 + v^2}}{\mu(0)v + \sqrt{\varepsilon(0)\mu(0) - 1 + v^2}} \simeq -\frac{1}{4v^2}\chi(0) + \left[\frac{1}{2} - \frac{1}{4v^2}\right]\zeta(0) \tag{3.137}$$

lead to

$$C_4 = -\frac{\hbar c \alpha(0)}{640\pi^2\varepsilon_0}\left[23\chi(0) - 7\zeta(0)\right]. \tag{3.138}$$

For strong magnetodielectric properties, i.e., $\varepsilon(0) \gg 1$ and $\mu(0) \gg 1$, we may approximately set

$$\sqrt{\varepsilon(0)\mu(0) - 1 + v^2} \simeq \sqrt{\varepsilon(0)\mu(0)} \tag{3.139}$$

because large values of v are effectively suppressed in the integral in Eq. (3.130), thus

$$C_4 = -\frac{3\hbar c \alpha(0)}{64\pi^2\varepsilon_0}\left[-\frac{2}{Z^3}\ln(1+Z) + \frac{2}{Z^2} + \frac{4}{Z}\ln(1+Z)\right.$$
$$\left. - \frac{1}{Z} - \frac{4}{3} - Z + 2Z^2 - 2Z^3\ln\left(1 + \frac{1}{Z}\right)\right] \tag{3.140}$$

where $Z = \sqrt{\mu(0)/\varepsilon(0)}$ is the static impedance of the half space. Setting $C_4 = 0$ in Eq. (3.140), it follows that $Z = 2.26$. In conclusion, one can say that in the retarded limit a repulsive CP potential can be realised if the static magnetic properties are stronger than the static electric properties, $\zeta(0)/\chi(0) \geq 23/7 = 3.29$ for weak magnetodielectric properties and $\mu(0)/\varepsilon(0) \geq 2.26^2 = 5.11$ for strong magnetoelectric properties.
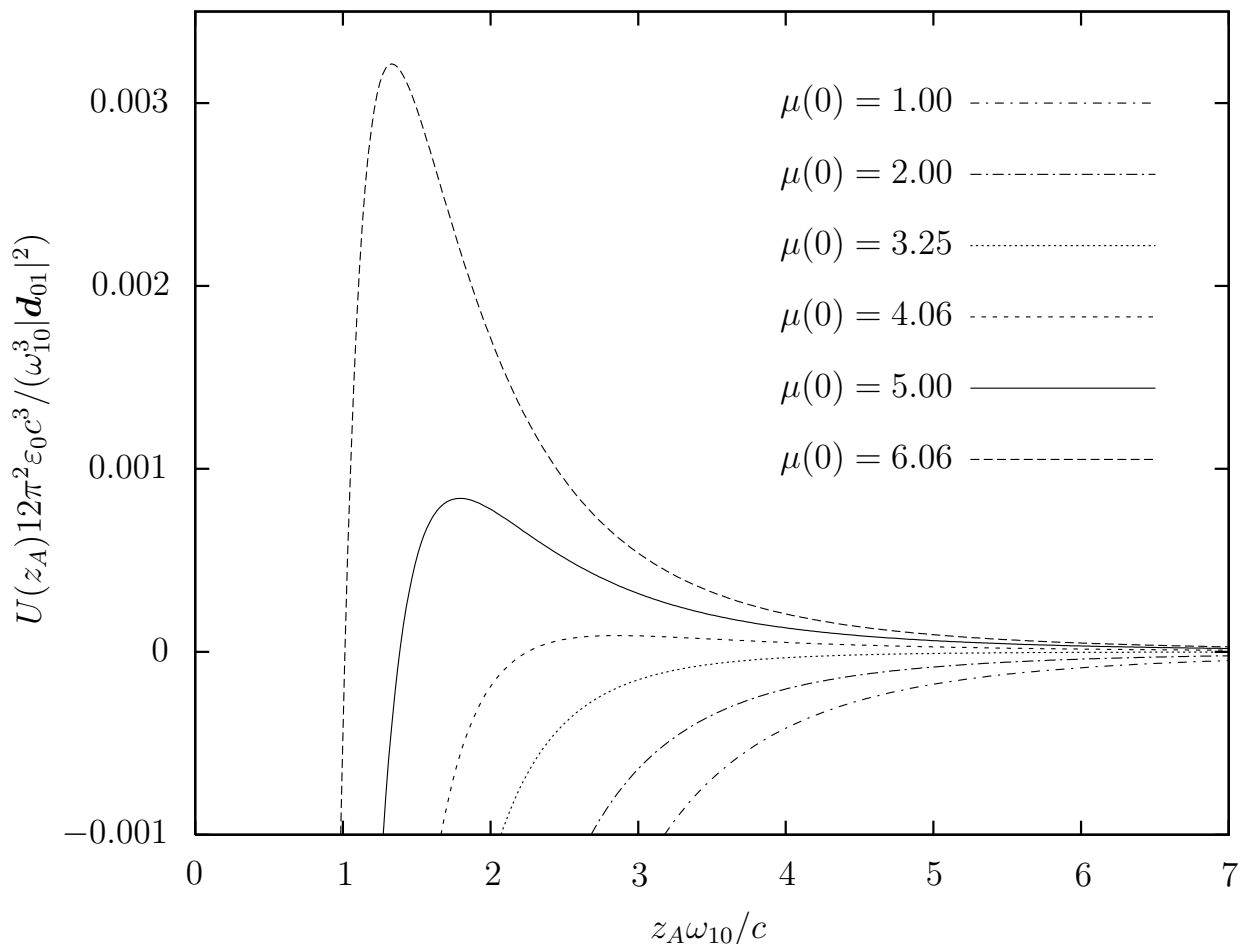
Figure 3.4: The CP potential of a ground-state two-level atom in front of a magnetodielectric half space is shown as a function of the atom–plate separation for different values of $\mu(0)$ ($\omega_{\mathrm{P}e}/\omega_{10} = 0.75$, $\omega_{\mathrm{T}e}/\omega_{10} = 1.03$, $\omega_{\mathrm{T}m}/\omega_{10} = 1$, $\gamma_e/\omega_{10} = \gamma_m/\omega_{10} = 0.001$).

In the non-retarded limit, not only the sign, but also the leading power law of the asymptotic CP potential is affected by the relative strengths of the electric and magnetic properties [$C_3 > 0$ dominant (and $C_1 > 0$) for a purely electric half space, while $C_3 = 0$ and $C_1 > 0$ for a purely magnetic half space, cf. Eqs. (3.132)–(3.134)]. For a genuinely magnetoelectric half space, the attractive $1/z_A^3$ term due to the electric medium properties will always dominate for sufficiently small distances. Hence in cases where the long-distance potential is repulsive due to sufficiently strong magnetic properties, the competing influence of the electric/magnetic medium properties can lead to the formation of a potential barrier at intermediate distances. This is illustrated in Fig. 3.4, where the CP potential of a two-level atom in front of a magnetoelectric half space is displayed, which has been numerically calculated from Eq. (3.126) together with Eqs. (3.23) and (3.112). Here, the single-resonance Drude–Lorentz model has been used for $\varepsilon(\omega)$ and $\mu(\omega)$,

$$\varepsilon(\omega) = 1 + \frac{\omega_{\mathrm{P}e}^2}{\omega_{\mathrm{T}e}^2 - \omega^2 - \mathrm{i}\omega\gamma_e}, \qquad \mu(\omega) = 1 + \frac{\omega_{\mathrm{P}m}^2}{\omega_{\mathrm{T}m}^2 - \omega^2 - \mathrm{i}\omega\gamma_m}, \qquad (3.141)$$

recall Eq. (3.75). The figure shows that the potential is attractive for small $\mu(0)$, as expected. For increasing values of $\mu(0)$, a potential barrier begins to form at intermediate distances which is shifted to smaller distances and increases in height as the value of $\mu(0)$ is further increased. A more detailed discussion of the dependence of the barrier characteristics on the medium parameters can be found in Refs. [SB8, SB9].

3.6.3   Plate of finite thickness

The half-space model studied in the previous section was based on the idealising assumption of an infinitely thick plate. To be more realistic and at the same time investigate under which conditions the semi-infinite half space is a good model, we now consider an atom in front of a magnetoelectric plate of finite thickness $d \equiv d_1^-$, permittivity $\varepsilon(\omega) \equiv \varepsilon_1^-(\omega)$ and permeability $\mu(\omega) \equiv \mu_1^-(\omega)$ [the space behind the plate is assumed to be empty, so that $\varepsilon_2^-(\omega) = \mu_2^-(\omega) = 1$]. Substituting the reflexion coefficients (3.110) and (3.111) into Eq. (3.116), we derive $(b_1 \equiv b_1^-)$ [SB1, SB8, SB9]

$$
U(z_A) = \frac{\hbar\mu_0}{8\pi^2} \int_0^\infty \mathrm{d}\xi\, \xi^2 \alpha(\mathrm{i}\xi) \int_0^\infty \mathrm{d}q\, \frac{q}{b}\, \mathrm{e}^{-2bz_A} \left\{ \frac{[\mu^2(\mathrm{i}\xi)b^2 - b_1^2]\tanh(b_1 d)}{2\mu(\mathrm{i}\xi)bb_1 + [\mu^2(\mathrm{i}\xi)b^2 + b_1^2]\tanh(b_1 d)} \right.
$$
$$
\left. - \left(1 + 2\frac{q^2 c^2}{\xi^2}\right) \frac{[\varepsilon^2(\mathrm{i}\xi)b^2 - b_1^2]\tanh(b_1 d)}{2\varepsilon(\mathrm{i}\xi)bb_1 + [\varepsilon^2(\mathrm{i}\xi)b^2 + b_1^2]\tanh(b_1 d)} \right\}, \quad (3.142)
$$

which reduces to the result given in Ref. [128] for a purely electric plate.

It is obvious that the integration in Eq. (3.142) is effectively limited by the factor e^{-2bz_A} to a circular region where $b \lesssim 1/(2z_A)$. For an asymptotically thick plate, $d \gg z_A$, the estimate $b_1 d \geq bd \simeq d/(2z_A) \gg 1$ [recall Eq. (3.112)] is approximately valid within (the major part of) the effective range of integration. One may hence make the approximation $\tanh(b_1 d) \simeq 1$, leading back to the half-space result (3.126) which demonstrates that the semi-infinite half space is a good model provided that $d \gg z_A$.

On the contrary, in the limit of an asymptotically thin plate, $n(0)d \ll z_A$, we find that the inequalities $b_1 d \leq \sqrt{\varepsilon(\mathrm{i}\xi)\mu(\mathrm{i}\xi)}\, bd \leq \sqrt{\varepsilon(0)\mu(0)}\, bd \leq n(0)d/(2z_A) \ll 1$ hold in the effective region of integration and one may hence perform a linear expansion of the integrand in Eq. (3.142) in terms of $b_1 d$, resulting in [SB1, SB8, SB9]

$$
U(z_A) = \frac{\hbar\mu_0 d}{8\pi^2} \int_0^\infty \mathrm{d}\xi\, \xi^2 \alpha(\mathrm{i}\xi) \int_0^\infty \mathrm{d}q\, \frac{q}{b}\, \mathrm{e}^{-2bz_A} \left[\frac{\mu^2(\mathrm{i}\xi)b^2 - b_1^2}{2\mu(\mathrm{i}\xi)b} \right.
$$
$$
\left. - \left(1 + 2\frac{q^2 c^2}{\xi^2}\right) \frac{\varepsilon^2(\mathrm{i}\xi)b^2 - b_1^2}{2\varepsilon(\mathrm{i}\xi)b} \right]. \quad (3.143)
$$

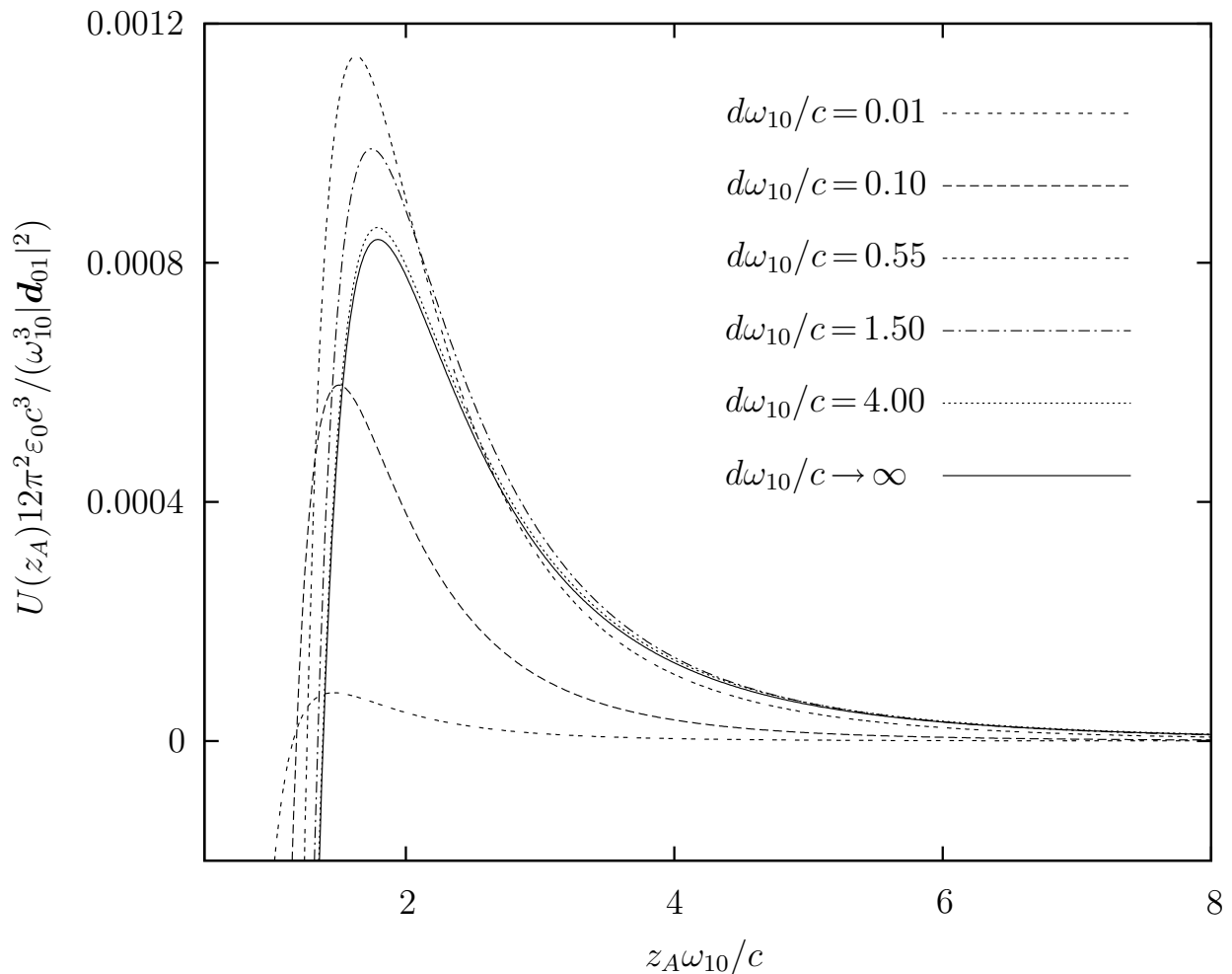Following the steps described above Eqs. (3.129) and (3.132), respectively, it can be

Figure 3.5: The CP potential of a ground-state two-level atom in front of a magnetodielectric plate is shown as a function of the atom–plate separation for different values of the plate thickness d [$\mu(0) = 5$; whereas all other parameters are the same as in Fig. 3.4].

shown that in the retarded limit $(z_A \gg c/\omega_{\min})$, Eq. (3.143) reduces to

$$U(z_A) = \frac{D_5}{z_A^5},\tag{3.144}$$

$$D_5 = -\frac{\hbar c \alpha(0) d}{160\pi^2 \varepsilon_0}\left[\frac{14\varepsilon^2(0) - 9}{\varepsilon(0)} - \frac{6\mu^2(0) - 1}{\mu(0)}\right]\tag{3.145}$$

while in the non-retarded limit $[n(0)z_A \ll c/\omega_{\max}]$, it can be approximated by

$$U(z_A) = -\frac{D_4}{z_A^4} + \frac{D_2}{z_A^2},\tag{3.146}$$

$$D_4 = \frac{3\hbar d}{64\pi^2 \varepsilon_0}\int_0^\infty \mathrm{d}\xi\, \alpha(\mathrm{i}\xi)\frac{\varepsilon^2(\mathrm{i}\xi) - 1}{\varepsilon(\mathrm{i}\xi)} \geq 0,\tag{3.147}$$

$$D_2 = \frac{\mu_0 \hbar d}{64\pi^2}\int_0^\infty \mathrm{d}\xi\, \xi^2 \alpha(\mathrm{i}\xi)\left\{\frac{\varepsilon^2(\mathrm{i}\xi) - 1}{\varepsilon(\mathrm{i}\xi)} + \frac{\mu^2(\mathrm{i}\xi) - 1}{\mu(\mathrm{i}\xi)} + \frac{2[\varepsilon(\mathrm{i}\xi)\mu(\mathrm{i}\xi) - 1]}{\varepsilon(\mathrm{i}\xi)}\right\} \geq 0.\tag{3.148}$$

Comparing the retarded and non-retarded CP potentials of an asymptotically thin plate with those of an infinitely thick plate, Eqs. (3.129) and (3.132), we observe a close similarity. It is therefore natural to expect the formation of a repulsive potential barrier for

plates of finite thickness, provided that the magnetic properties are sufficiently strong. This is confirmed in Fig. 3.5 where the CP potentials of a two-level atom placed in front of plates of various thicknesses are shown which have been obtained by numerical evaluation of Eq. (3.142) [together with Eqs. (3.23), (3.112) and (3.141)]. It is seen that the qualitative behaviour of the CP potential is independent of the plate thickness; all curves in Fig. 3.5 feature a potential barrier at some intermediate distance. However, the barrier height reacts very sensitively as the plate thickness is varied. For a thin plate the barrier is very low; it raises with increasing thickness of the plate, reaches a maximal height for some intermediate thickness and then lowers slowly towards the asymptotic half space value as the thickness is further increased. A more detailed discussion can be found in Refs. [SB9, SB8].

3.6.4   Planar cavity

As a simple model for a planar cavity, consider a free-space region enclosed by two identical magnetodielectric half spaces of permittivity $\varepsilon(\omega) \equiv \varepsilon_1^{\pm}(\omega)$ and permeability $\mu(\omega) \equiv \mu_1^{\pm}(\omega)$ which are separated by a distance l.[9] From Eq. (3.115) together with Eqs. (3.110)–(3.113) it follows that the CP potential of a ground-state atom placed within the planar cavity is given by $(b_1 \equiv b_1^{\pm})$ [SB1, SB8, SB9]

$$U(z_A) = \frac{\hbar\mu_0}{8\pi^2} \int_0^\infty d\xi\, \xi^2 \alpha(i\xi) \int_0^\infty dq\, \frac{q}{b} \Big[e^{-2bz_A} + e^{-2b(l-z_A)} \Big] \Big[\frac{1}{D_s} \frac{\mu(i\xi)b - b_1}{\mu(i\xi)b + b_1}$$
$$- \Big(1 + 2\frac{q^2 c^2}{\xi^2} \Big) \frac{1}{D_p} \frac{\varepsilon(i\xi)b - b_1}{\varepsilon(i\xi)b + b_1} \Big]. \quad (3.149)$$

In general, this potential is not the sum of two separate half-space potentials (3.126). The difference is due to the effect of multiple reflexions between the half spaces, which gives rise to the denominators

$$\frac{1}{D_\sigma} = \frac{1}{1 - r_\sigma^- r_\sigma^+ e^{-2bl}} = \sum_{n=0}^\infty \big(r_\sigma^- e^{-bl} r_\sigma^+ e^{-bl} \big)^n, \quad (3.150)$$

recall Eq. (3.113).

Examples of the CP potentials of an atom in a magnetodielectric, purely electric and purely magnetic cavity are given in Fig. 3.6, which have been obtained by numerical integration of Eq. (3.149), together with Eqs. (3.23), (3.112) and (3.113). For the chosen parameters, multiple reflexions within the cavity do not play a role (i.e., $D_\sigma \simeq 1$ in the effective range of integration),[10] so the cavity potentials reduce to sums of two half-space

---

[9] Note that purely electric planar cavities have been modelled with various degrees of detail, e.g., by two perfectly conducting plates [104, 115, 121, 122, 149], two electric half spaces [149], or even two electric plates of finite thickness [128, 129].

[10] For an example where multiple reflexions must be taken into account, see Ref. [SB9].
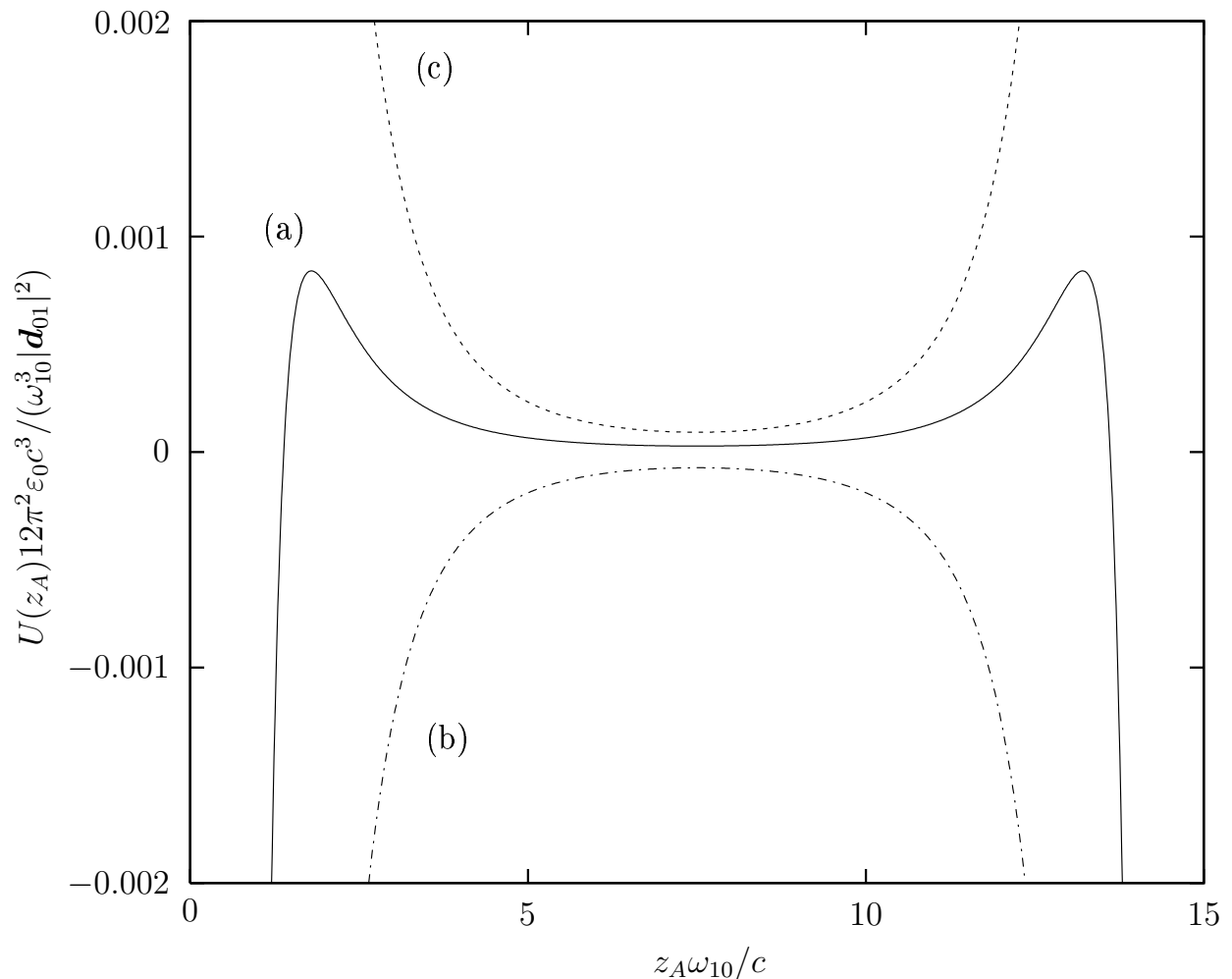
Figure 3.6: The CP potential of a ground-state two-level atom within an (a) magnetodielectric [$\mu(0) = 5$; whereas all other parameters are the same as in Fig. 3.4], (b) purely electric [$\mu(\omega) = 1$, other parameters as in (a)], (c) purely magnetic [$\varepsilon(\omega) = 1$, other parameters as in (a)] cavity of width $l = 15c/\omega_{10}$ is shown as a function of the position of the atom.

potentials. Hence the attractive/repulsive potentials associated with each of two purely electric/magnetic half spaces combine to an infinite potential wall/well at the centre of the cavity, while a potential well of finite depth can be realised within the cavity in the case of two genuinely magnetodielectric plates of sufficiently strong magnetic properties.

3.7   Comparison of dispersion forces

The results of this chapter have revealed that the dispersion forces between various polarisable/magnetisable ground-state objects exhibit a lot of common features; this point will be further elaborated in the following. Table 3.1 summarises the asymptotic retarded and non-retarded dispersion forces that have been found for a ground-state polarisable atom interacting with another ground-state polarisable/magnetisable atom [Eqs. (3.100), (3.101), (3.105) and (3.106)], an electric/magnetic small sphere [SB5, SB13], thin ring [SB10], thin
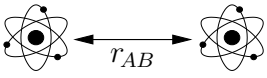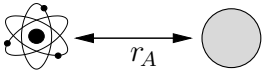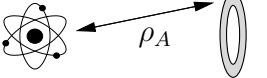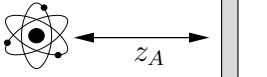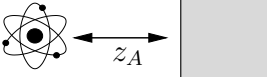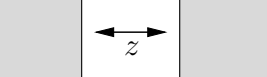
Distance →	Retarded		Nonretarded	
Object type →	$e \leftrightarrow e$	$e \leftrightarrow m$	$e \leftrightarrow e$	$e \leftrightarrow m$
(a) atom ↔ atom, r_{AB}	$-\dfrac{1}{r_{AB}^8}$	$+\dfrac{1}{r_{AB}^8}$	$-\dfrac{1}{r_{AB}^7}$	$+\dfrac{1}{r_{AB}^5}$
(b) atom ↔ sphere, r_A	$-\dfrac{1}{r_A^8}$	$+\dfrac{1}{r_A^8}$	$-\dfrac{1}{r_A^7}$	$+\dfrac{1}{r_A^5}$
(c) atom ↔ ring, ρ_A	$-\dfrac{1}{\rho_A^8}$	$+\dfrac{1}{\rho_A^8}$	$-\dfrac{1}{\rho_A^7}$	$+\dfrac{1}{\rho_A^5}$
(d) atom ↔ plate, z_A	$-\dfrac{1}{z_A^6}$	$+\dfrac{1}{z_A^6}$	$-\dfrac{1}{z_A^5}$	$+\dfrac{1}{z_A^3}$
(e) atom ↔ half space, z_A	$-\dfrac{1}{z_A^5}$	$+\dfrac{1}{z_A^5}$	$-\dfrac{1}{z_A^4}$	$+\dfrac{1}{z_A^2}$
(f) half space ↔ half space, z	$-\dfrac{1}{z^4}$	$+\dfrac{1}{z^4}$	$-\dfrac{1}{z^3}$	$+\dfrac{1}{z}$

Table 3.1: Signs and asymptotic power laws for the dispersion forces between (a) two atoms, (b) an atom and a small sphere, (c) an atom and a thin ring, (d) an atom and a thin plate, (e) an atom and a semi-infinite half space and (f) two semi-infinite half spaces. In the table, e/m stands for polarisable/magnetisable objects and the signs $\pm$ denote repulsive/attractive forces.

plate [Eqs. (3.144) and (3.146)] and semi-infinite half space [Eqs. (3.129) and (3.132)]. In addition, the dispersion force between two semi-infinite half spaces is given [188].

Comparing the dispersion forces between objects of different shapes and sizes, it is seen that the signs are always the same, while the leading inverse powers are the same or changed by some global power when moving from one row of the table to another. This can be understood by assuming that the leading inverse power is determined by the contribution to the force which results from the two-atom interaction [row (a)] by pairwise summation. Obviously, integration of two-atom forces over the (finite) volumes of a small sphere (b) or a thin ring (c) does not change the respective power law, while integration over an infinite volume lowers the leading inverse power according to the number of infinite dimensions. So, the leading inverse powers are lowered by two and three for the interaction of an atom with a thin plate of infinite lateral extension (d) and a half space (e), respectively. The power

laws for the force between two half spaces (f) can then be obtained from the atom–half-space force (e) by integrating over the three infinite dimensions, where integration over z lowers the leading inverse powers by one, while the trivial integrations over x and y yield an infinite force, i.e., a finite force per unit area. It follows from the table that many-atom interactions do not change the leading power laws resulting from the summation of pairwise interactions, but only modify the proportionality factors.

All dispersion forces in Tab. 3.1 are seen to be attractive for two polarisable objects and repulsive for a polarisable object interacting with a magnetisable one. It can further be noted that in the retarded limit the forces decrease more rapidly with increasing distance than might be expected from considering only the non-retarded limit. Finally, the table shows that the retarded dispersion forces between polarisable/polarisable and polarisable/magnetisable objects follow the same power laws, while in the non-retarded limit the forces between polarisable and magnetisable objects are weaker than those between polarisable objects by two powers in the object separation. This can be understood by regarding the forces as being due to the electromagnetic field created by the first object interacting with the second. While the electric and magnetic far fields created by an oscillating electric dipole display the same distance dependence, the electric near field (which can interact with a second polarisable object) is stronger than the magnetic near field (which interacts with a second magnetisable object) by one power in the object separation (giving rise to a difference of two powers in second-order perturbation theory).

Chapter 4

Dynamical Casimir–Polder force

As shown in the previous chapter, time-independent perturbation theory can be used to derive general expressions for the CP potential, which are particularly useful for studying a variety of aspects related to CP forces on ground-state atoms. Nevertheless, the approach leaves some questions unanswered. Firstly, it is known that atomic transitions are shifted and broadened due to the presence of a nearby body, while the transitions entering the perturbative CP potential are unshifted and have a zero line width. Secondly, for atoms initially prepared in an excited state, spontaneous decay is expected to give rise to a dynamics of the CP force which is, of course, beyond the scope of a time-independent theory. In particular, this holds for the Rabi oscillations expected to occur for strong atom–field coupling.

To overcome these deficiencies, we will in this chapter present a genuinely dynamical theory of the CP force. Starting from the operator Lorentz force, we express the CP force in terms of the atomic and field variables [SB1, SB6, SB7, SB8]. For weak atom–field coupling, these results are further evaluated by means of the Markov approximation and the influence of the body-induced shifting and broadening of the atomic transitions on the force, is studied in detail for the example of an excited atom placed near a half space [SB1, SB6, SB7, SB8]. For strong atom–field coupling, we restrict our attention to a two-level atom predominantly interacting with a single quasi-mode of the body-assisted field. The reduced atom–field dynamics can be solved exactly, yielding explicit expressions for the resonant strong-coupling CP force [SB1, SB16], where brief contact is made with the force obtained by means of the well-known dressed-state approach [SB16].

4.1   Lorentz force

A dynamical theory of the CP force can be developed by first calculating the total Lorentz force acting on the atom as given by the Heisenberg equations of motion. The general result for the Lorentz force thus derived, serves as a good basis for calculating the CP force which is simply the special case of the Lorentz force for the body-assisted electromagnetic field initially prepared in its ground state.

4.1.1 Minimal coupling

As shown in Sec. 2.2.1, the Lorentz forces acting on the individual charged particles constituting the atom can be given in the form of Eq. (2.80). Summing this equation over all particles, one obtains

$$m_A \ddot{\hat{r}}_A = \sum_{\alpha \in A} m_\alpha \ddot{\hat{r}}_\alpha = \hat{F} \tag{4.1}$$

[recall Eq. (2.56)], where the Lorentz force acting on the atom is given by

$$\hat{F} = \sum_{\alpha \in A} \left\{ q_\alpha \hat{\mathcal{E}}(r_\alpha) + \frac{q_\alpha}{2} \left[\dot{\hat{r}}_\alpha \times \hat{\mathcal{B}}(r_\alpha) - \hat{\mathcal{B}}(r_\alpha) \times \dot{\hat{r}}_\alpha \right] \right\}. \tag{4.2}$$

Upon substituting the expressions (2.74) for the total electric and induction fields, using the fact that internal forces do not contribute to the net force due to pairwise cancellations,

$$\sum_{\alpha \in A} q_\alpha \nabla \hat{\varphi}_A(r)|_{r=r_\alpha} = 0, \tag{4.3}$$

and recalling definitions (2.51) and (2.55), one obtains

$$\hat{F} = \int \mathrm{d}^3 r \left[\hat{\rho}_A(r) \hat{E}(r) + \hat{j}_A(r) \times \hat{B}(r) \right]. \tag{4.4}$$

Alternatively, the Lorentz force may be expressed in terms of atomic polarisation and magnetisation. This can be achieved by using relations (2.66)–(2.68), leading to

$$\hat{F} = - \int \mathrm{d}^3 r \left[\nabla \cdot \hat{P}_A(r) \right] \hat{E}(r) + \int \mathrm{d}^3 r\, \dot{\hat{P}}_A(r) \times \hat{B}(r)$$
$$+ \int \mathrm{d}^3 r \left(\nabla \times \left\{ \hat{M}_A(r) + \tfrac{1}{2} \left[\hat{P}_A(r) \times \dot{\hat{r}}_A - \dot{\hat{r}}_A \times \hat{P}_A(r) \right] \right\} \right) \times \hat{B}(r). \tag{4.5}$$

Using the rule $a \times (b \times c) = b(a \cdot c) - c(a \cdot b)$ as well as the identities $\nabla \hat{P}_A(r) = -\nabla_A \hat{P}_A(r)$, $\nabla \hat{M}_A(r) = -\nabla_A \hat{M}_A(r)$ [which are direct consequences of definitions (2.62) and (2.63)], one can show that

$$- \int \mathrm{d}^3 r \left[\nabla \cdot \hat{P}_A(r) \right] \hat{E}(r) = \nabla_A \left[\int \mathrm{d}^3 r\, \hat{P}_A(r) \cdot \hat{E}(r) \right] + \int \mathrm{d}^3 r\, \hat{P}_A(r) \times \dot{\hat{B}}(r), \tag{4.6}$$

$$\int \mathrm{d}^3 r \left(\nabla \times \left\{ \hat{M}_A(r) + \frac{1}{2} \left[\hat{P}_A(r) \times \dot{\hat{r}}_A - \dot{\hat{r}}_A \times \hat{P}_A(r) \right] \right\} \right) \times \hat{B}(r)$$
$$= \nabla_A \left\{ \int \mathrm{d}^3 r \left[\hat{M}_A(r) + \hat{P}_A(r) \times \dot{\hat{r}}_A \right] \cdot \hat{B}(r) \right\} \tag{4.7}$$

where we have partially integrated and employed Maxwell equations (2.37) and (2.35), respectively. Substitution of these identities into Eq. (4.5) results in [SB6]

$$\hat{F} = \nabla_A \left\{ \int \mathrm{d}^3 r\, \hat{P}_A(r) \cdot \hat{E}(r) + \int \mathrm{d}^3 r \left[\hat{M}_A(r) + \hat{P}_A(r) \times \dot{\hat{r}}_A \right] \cdot \hat{B}(r) \right\}$$
$$+ \frac{\mathrm{d}}{\mathrm{d}t} \int \mathrm{d}^3 r\, \hat{P}_A(r) \times \hat{B}(r). \tag{4.8}$$

After expanding Eq. (4.8) to leading order in the relative particle coordinates $\hat{\bar{\boldsymbol{r}}}_\alpha$, one finds that the Lorentz force in long wave-length approximation is given by

$$\hat{\boldsymbol{F}} = \boldsymbol{\nabla}_A\Big[\hat{\boldsymbol{d}}\cdot\hat{\boldsymbol{E}}(\hat{\boldsymbol{r}}_A) + \hat{\boldsymbol{m}}\cdot\hat{\boldsymbol{B}}(\hat{\boldsymbol{r}}_A) + \hat{\boldsymbol{d}}\times\dot{\hat{\boldsymbol{r}}}_A\cdot\hat{\boldsymbol{B}}(\hat{\boldsymbol{r}}_A)\Big] + \frac{\mathrm{d}}{\mathrm{d}t}\Big[\hat{\boldsymbol{d}}\times\hat{\boldsymbol{B}}(\hat{\boldsymbol{r}}_A)\Big], \tag{4.9}$$

[recall Eqs. (2.62)–(2.65)] where

$$\frac{\mathrm{d}}{\mathrm{d}t}\Big[\hat{\boldsymbol{d}}\times\hat{\boldsymbol{B}}(\hat{\boldsymbol{r}}_A)\Big] = \dot{\hat{\boldsymbol{d}}}\times\hat{\boldsymbol{B}}(\hat{\boldsymbol{r}}_A) + \hat{\boldsymbol{d}}\times\dot{\hat{\boldsymbol{B}}}(\boldsymbol{r})\big|_{\boldsymbol{r}=\hat{\boldsymbol{r}}_A}$$
$$+ \tfrac{1}{2}\,\hat{\boldsymbol{d}}\times\Big[\big(\dot{\hat{\boldsymbol{r}}}_A\cdot\boldsymbol{\nabla}_A\big)\hat{\boldsymbol{B}}(\hat{\boldsymbol{r}}_A) + \hat{\boldsymbol{B}}(\hat{\boldsymbol{r}}_A)\big(\overleftarrow{\boldsymbol{\nabla}}_A\cdot\dot{\hat{\boldsymbol{r}}}_A\big)\Big], \tag{4.10}$$

recall Eq. (2.34). For a non-magnetic atom and nonrelativistic centre-of-mass motion, we may discard the contribution from magnetic interactions as well as the terms proportional to $\dot{\hat{\boldsymbol{r}}}_A$ so that Eqs. (4.9) and (4.10) reduce to [SB6]

$$\hat{\boldsymbol{F}} = \Big\{\boldsymbol{\nabla}\Big[\hat{\boldsymbol{d}}\cdot\hat{\boldsymbol{E}}(\boldsymbol{r})\Big] + \frac{\mathrm{d}}{\mathrm{d}t}\Big[\hat{\boldsymbol{d}}\times\hat{\boldsymbol{B}}(\boldsymbol{r})\Big]\Big\}_{\boldsymbol{r}=\hat{\boldsymbol{r}}_A}. \tag{4.11}$$

4.1.2   Multipolar coupling

Within the framework of the multipolar coupling scheme, the Lorentz force may be calculated in a similar way by summing Eq. (2.96) over all atomic constituents and using definitions (2.62) and (2.91), leading to

$$m_A\dot{\hat{\boldsymbol{r}}}_A = m_A\dot{\hat{\boldsymbol{r}}}'_A = \sum_{\alpha\in A} m_\alpha\dot{\hat{\boldsymbol{r}}}'_\alpha = \hat{\boldsymbol{p}}'_A + \int \mathrm{d}^3r\,\hat{\boldsymbol{P}}'_A(\boldsymbol{r})\times\hat{\boldsymbol{B}}'(\boldsymbol{r}) \tag{4.12}$$

[recall that $\hat{\boldsymbol{r}}'_A = \hat{\boldsymbol{r}}_A$, Eq. (B.2) and hence also $\dot{\hat{\boldsymbol{r}}}'_A = \dot{\hat{\boldsymbol{r}}}_A$]. Substituting this into the Heisenberg equation of motion (2.34), one finds

$$m_A\ddot{\hat{\boldsymbol{r}}}_A = m_A\ddot{\hat{\boldsymbol{r}}}'_A = \sum_{\alpha\in A} m_\alpha\ddot{\hat{\boldsymbol{r}}}'_\alpha = \hat{\boldsymbol{F}}', \tag{4.13}$$

where the Lorentz force now assumes the form

$$\hat{\boldsymbol{F}}' = \frac{\mathrm{i}}{\hbar}\Big[\hat{H},\hat{\boldsymbol{p}}'_A\Big] + \frac{\mathrm{d}}{\mathrm{d}t}\int \mathrm{d}^3r\,\hat{\boldsymbol{P}}'_A(\boldsymbol{r})\times\hat{\boldsymbol{B}}'(\boldsymbol{r}). \tag{4.14}$$

The different contributions to the first term in Eq. (4.14) can be evaluated by recalling Eq. (2.86) as well as the commutation relations (2.58). Using the identity $\boldsymbol{\nabla}'_A\hat{\boldsymbol{P}}'_A(\boldsymbol{r}) = -\boldsymbol{\nabla}\hat{\boldsymbol{P}}'_A(\boldsymbol{r})$, one can show that

$$\frac{\mathrm{i}}{\hbar}\Big[\frac{1}{2\varepsilon_0}\int \mathrm{d}^3r\,\hat{\boldsymbol{P}}'^2_A(\boldsymbol{r}),\hat{\boldsymbol{p}}'_A\Big] = \frac{1}{2\varepsilon_0}\int \mathrm{d}^3r\,\boldsymbol{\nabla}\big[\hat{\boldsymbol{P}}'_A(\boldsymbol{r})\big]^2 = \boldsymbol{0}, \tag{4.15}$$

and by employing Eq. (2.91) as well as definitions (2.62) and (2.63), we derive

$$\frac{\mathrm{i}}{\hbar}\Big[\sum_{\alpha\in A}\frac{1}{2m_\alpha}\Big\{\hat{\boldsymbol{p}}'_\alpha + \int \mathrm{d}^3r\,\hat{\boldsymbol{\Xi}}'_\alpha(\boldsymbol{r})\times\hat{\boldsymbol{B}}'(\boldsymbol{r})\Big\}^2,\hat{\boldsymbol{p}}'_A\Big]$$
$$= \boldsymbol{\nabla}_A\Big\{\int \mathrm{d}^3r\,\Big[\hat{\boldsymbol{M}}'_A(\boldsymbol{r}) + \hat{\boldsymbol{P}}'_A(\boldsymbol{r})\times\dot{\hat{\boldsymbol{r}}}_A\Big]\cdot\hat{\boldsymbol{B}}'(\boldsymbol{r})\Big\}. \tag{4.16}$$

Substituting Eqs. (4.15) and (4.16) into Eq. (4.14), we find that within the multipolar coupling scheme the Lorentz force reads [SB1, SB6]

$$\hat{\boldsymbol{F}}' = \boldsymbol{\nabla}_A \left\{ \int \mathrm{d}^3 r \, \hat{\boldsymbol{P}}'_A(\boldsymbol{r}) \cdot \hat{\boldsymbol{E}}'(\boldsymbol{r}) + \int \mathrm{d}^3 r \left[\hat{\boldsymbol{M}}'_A(\boldsymbol{r}) + \hat{\boldsymbol{P}}'_A(\boldsymbol{r}) \times \dot{\hat{\boldsymbol{r}}}_A \right] \cdot \hat{\boldsymbol{B}}'(\boldsymbol{r}) \right\}$$
$$+ \frac{\mathrm{d}}{\mathrm{d}t} \int \mathrm{d}^3 r \, \hat{\boldsymbol{P}}'_A(\boldsymbol{r}) \times \hat{\boldsymbol{B}}'(\boldsymbol{r}). \quad (4.17)$$

As is obvious from Eqs. (4.1) and (4.13), the expressions found for the Lorentz force in minimal (4.8) and multipolar coupling schemes must agree: $\hat{\boldsymbol{F}} = \hat{\boldsymbol{F}}'$. This can be verified explicitly by using the transformation rules (B.1), (B.3) and (2.97) and noting that

$$\boldsymbol{\nabla}_A \int \mathrm{d}^3 r \left[\hat{\boldsymbol{P}}_A^\perp(\boldsymbol{r}) \right]^2 = - \int \mathrm{d}^3 r \, \boldsymbol{\nabla} \left[\hat{\boldsymbol{P}}_A^\perp(\boldsymbol{r}) \right]^2 = \boldsymbol{0}. \quad (4.18)$$

In close analogy to the minimal-coupling case, the Lorentz force reduces to

$$\hat{\boldsymbol{F}}' = \boldsymbol{\nabla}_A \left[\hat{\boldsymbol{d}}' \cdot \hat{\boldsymbol{E}}'(\hat{\boldsymbol{r}}_A) + \hat{\boldsymbol{m}}' \cdot \hat{\boldsymbol{B}}'(\hat{\boldsymbol{r}}_A) + \hat{\boldsymbol{d}}' \times \dot{\hat{\boldsymbol{r}}}_A \cdot \hat{\boldsymbol{B}}'(\hat{\boldsymbol{r}}_A) \right] + \frac{\mathrm{d}}{\mathrm{d}t} \left[\hat{\boldsymbol{d}}' \times \hat{\boldsymbol{B}}'(\hat{\boldsymbol{r}}_A) \right] \quad (4.19)$$

in the long wave-length approximation and simplifies further to [SB1, SB6, SB7, SB8]

$$\hat{\boldsymbol{F}}' = \left\{ \boldsymbol{\nabla} \left[\hat{\boldsymbol{d}}' \cdot \hat{\boldsymbol{E}}'(\boldsymbol{r}) \right] + \frac{\mathrm{d}}{\mathrm{d}t} \left[\hat{\boldsymbol{d}}' \times \hat{\boldsymbol{B}}'(\boldsymbol{r}) \right] \right\}_{\boldsymbol{r} = \hat{\boldsymbol{r}}_A} \quad (4.20)$$

for a non-magnetic atom and nonrelativistic centre-of-mass motion. Equations (4.11) and (4.20) are a generalisation of the free-space result for the QED Lorentz force [175, 179] to the case of magnetoelectric bodies being present. According to Eqs. (2.23) and (2.27), they express the Lorentz force acting on the atom in terms of the dynamical variables of the atom–field system in minimal and multipolar coupling, respectively. Explicit expressions for the time-dependent force can be found by solving the (internal) atomic and field dynamics, which will be done in the following. For simplicity, we will exclusively work within the multipolar coupling scheme throughout the remainder of this chapter.[1]

Let us first address the dynamics of the body-assisted electromagnetic field. In the presence of an electric-dipole atom with nonrelativistic centre-of-mass motion, the Heisenberg equations of motion (2.34) for the dynamical field variables are governed by the multipolar Hamiltonian (2.86) [together with Eqs. (2.87), (2.88) and (2.94)] and by recalling definitions (2.23)–(2.25) and making use of the commutation relations (2.21) and (2.22), one obtains

$$\dot{\hat{\boldsymbol{f}}}_\lambda(\boldsymbol{r}, \omega) = \mathrm{i}\hbar^{-1} \left[\hat{H}, \hat{\boldsymbol{f}}_\lambda(\boldsymbol{r}, \omega) \right] = -\mathrm{i}\omega \hat{\boldsymbol{f}}_\lambda(\boldsymbol{r}, \omega) + \mathrm{i}\hbar^{-1} \hat{\boldsymbol{d}} \cdot \boldsymbol{G}_\lambda^*(\hat{\boldsymbol{r}}_A, \boldsymbol{r}, \omega). \quad (4.21)$$

The formal solution to this equation is given by

$$\hat{\boldsymbol{f}}_\lambda(\boldsymbol{r}, \omega, t) = \hat{\boldsymbol{f}}_{\lambda\mathrm{free}}(\boldsymbol{r}, \omega, t) + \hat{\boldsymbol{f}}_{\lambda\mathrm{source}}(\boldsymbol{r}, \omega, t) \quad (4.22)$$

---

[1]Note that the primes distinguishing the multipolar-coupling variables from the minimal-coupling ones will be omitted for brevity.

where

$$\hat{\boldsymbol{f}}_{\lambda\text{free}}(\boldsymbol{r},\omega,t) = \mathrm{e}^{-\mathrm{i}\omega(t-t_0)}\,\hat{\boldsymbol{f}}_\lambda(\boldsymbol{r},\omega) \tag{4.23}$$

and

$$\hat{\boldsymbol{f}}_{\lambda\text{source}}(\boldsymbol{r},\omega,t) = \frac{\mathrm{i}}{\hbar}\int_{t_0}^t \mathrm{d}\tau\,\mathrm{e}^{-\mathrm{i}\omega(t-\tau)}\hat{\boldsymbol{d}}(\tau)\!\cdot\!\boldsymbol{G}_\lambda^*[\hat{\boldsymbol{r}}_A(\tau),\boldsymbol{r},\omega] \tag{4.24}$$

determine the free and source parts of the electromagnetic field and where t_0 denotes the initial time. Upon substituting Eqs. (4.22)–(4.24) into Eq. (4.20) together with Eqs. (2.23) and (2.27), using identity (2.26) and taking the average with respect to the body-assisted field and the internal state of the atom, one finds that the mean force[2] is given by

$$\boldsymbol{F}(t) = \boldsymbol{F}_{\text{free}}(t) + \boldsymbol{F}_{\text{source}}(t), \tag{4.25}$$

where

$$\begin{aligned}
\boldsymbol{F}_{\text{free}}(t) = \sum_{\lambda=e,m}\int \mathrm{d}^3r'\int_0^\infty \mathrm{d}\omega\,\Big\{ &\boldsymbol{\nabla}\big\langle\hat{\boldsymbol{d}}(t)\!\cdot\!\boldsymbol{G}_\lambda(\boldsymbol{r},\boldsymbol{r}',\omega)\!\cdot\!\hat{\boldsymbol{f}}_\lambda(\boldsymbol{r}',\omega)\big\rangle\mathrm{e}^{-\mathrm{i}\omega(t-t_0)} \\
&+\frac{1}{\mathrm{i}\omega}\frac{\mathrm{d}}{\mathrm{d}t}\Big[\big\langle\hat{\boldsymbol{d}}(t)\!\times\!\big[\boldsymbol{\nabla}\!\times\!\boldsymbol{G}_\lambda(\boldsymbol{r},\boldsymbol{r}',\omega)\big]\!\cdot\!\hat{\boldsymbol{f}}_\lambda(\boldsymbol{r}',\omega)\big\rangle\mathrm{e}^{-\mathrm{i}\omega(t-t_0)}\Big]\Big\}_{\boldsymbol{r}=\hat{\boldsymbol{r}}_A(t)} + \text{C.c.} \quad (4.26)
\end{aligned}$$

and

$$\boldsymbol{F}_{\text{source}}(t) = \boldsymbol{F}_{\text{source}}^{\text{el}}(t) + \boldsymbol{F}_{\text{source}}^{\text{mag}}(t) \tag{4.27}$$

with the components

$$\begin{aligned}
\boldsymbol{F}_{\text{source}}^{\text{el}}(t) = \Big\{&\frac{\mathrm{i}\mu_0}{\pi}\int_0^\infty \mathrm{d}\omega\,\omega^2\int_{t_0}^t \mathrm{d}\tau\,\mathrm{e}^{-\mathrm{i}\omega(t-\tau)} \\
&\times\boldsymbol{\nabla}\big\langle\hat{\boldsymbol{d}}(t)\!\cdot\!\text{Im}\,\boldsymbol{G}[\boldsymbol{r},\hat{\boldsymbol{r}}_A(\tau),\omega]\!\cdot\!\hat{\boldsymbol{d}}(\tau)\big\rangle\Big\}_{\boldsymbol{r}=\hat{\boldsymbol{r}}_A(t)} + \text{C.c.}, \quad (4.28)
\end{aligned}$$

$$\begin{aligned}
\boldsymbol{F}_{\text{source}}^{\text{mag}}(t) = \Big\{&\frac{\mu_0}{\pi}\int_0^\infty \mathrm{d}\omega\,\omega\,\frac{\mathrm{d}}{\mathrm{d}t}\int_{t_0}^t \mathrm{d}\tau\,\mathrm{e}^{-\mathrm{i}\omega(t-\tau)} \\
&\times\big\langle\hat{\boldsymbol{d}}(t)\!\times\!\big(\boldsymbol{\nabla}\!\times\!\text{Im}\,\boldsymbol{G}[\boldsymbol{r},\hat{\boldsymbol{r}}_A(\tau),\omega]\big)\!\cdot\!\hat{\boldsymbol{d}}(\tau)\big\rangle\Big\}_{\boldsymbol{r}=\hat{\boldsymbol{r}}_A(t)} + \text{C.c.} \quad (4.29)
\end{aligned}$$

being due to the source parts of the electric and the induction fields, respectively. Equations (4.25)–(4.29) can be used to determine the radiation force on an atom for arbitrary atomic and field states. The CP force is obtained when the body-assisted field is initially prepared in its ground state so that the density matrix of the system at initial time reads

$$\hat{\varrho}(t_0) = |\{0\}\rangle\langle\{0\}|\hat{\sigma}(t_0), \tag{4.30}$$

with $\hat{\sigma}$ being the density matrix that defines the internal state of the atom. This obviously implies that $\boldsymbol{F}_{\text{free}}(t) = \boldsymbol{0}$ so that the CP force is given by

$$\boldsymbol{F}(t) = \boldsymbol{F}_{\text{source}}(t). \tag{4.31}$$

---

[2] For a discussion of force fluctuations, see Ref. [113].

4.2 Weak atom–field coupling

According to Eq. (4.31) together with Eqs. (4.27)–(4.29), an explicit expression for the dynamical CP force can be obtained by solving the internal dynamics of the atom which is coupled to the body-assisted electromagnetic field. In this section, we assume that the atom–field coupling is weak, which is typically the case if the resonances of the field do not coincide with any of the atomic transitions or if the field spectrum is broad with respect to the atomic line widths.

4.2.1 Markov approximation

In particular, we are interested in the dipole–dipole correlation function

$$\big\langle \hat{\boldsymbol{d}}(t)\hat{\boldsymbol{d}}(\tau)\big\rangle = \sum_{m,n}\sum_{m',n'} \boldsymbol{d}_{mn}\boldsymbol{d}_{m'n'}\big\langle \hat{A}_{mn}(t)\hat{A}_{m'n'}(\tau)\big\rangle \tag{4.32}$$

$[\hat{A}_{mn} = |m\rangle\langle n|$, recall Eq. (2.88)] which appears in Eqs. (4.28) and (4.29). For weak atom–field coupling, the Markov approximation can by used to considerably simplify the calculation, where in addition we assume that the internal atomic motion is fast with respect to the centre-of-mass motion, so that the Born–Oppenheimer approximation applies (cf. the discussion at the beginning of chapter 3).[3] Provided that the relevant atomic transition frequencies are well separated from one another so that diagonal and off-diagonal density matrix elements evolve independently, application of the quantum-regression theorem [189] leads to (App. E)

$$\big\langle \hat{A}_{mn}(t)\hat{A}_{m'n'}(\tau)\big\rangle = \delta_{nm'}\big\langle \hat{A}_{mn'}(\tau)\big\rangle \mathrm{e}^{\{\mathrm{i}\tilde{\omega}_{mn}(\boldsymbol{r}_A)-[\Gamma_m(\boldsymbol{r}_A)+\Gamma_n(\boldsymbol{r}_A)]/2\}(t-\tau)} \tag{4.33}$$

$(t \geq \tau,\, m \neq n)$. Here,

$$\tilde{\omega}_{mn}(\boldsymbol{r}_A) = \omega_{mn} + \delta\omega_m(\boldsymbol{r}_A) - \delta\omega_n(\boldsymbol{r}_A) \tag{4.34}$$

are the atomic transition frequencies including the position-dependent energy-level shifts[4]

$$\delta\omega_n(\boldsymbol{r}_A) = \sum_k \delta\omega_n^k(\boldsymbol{r}_A), \tag{4.35}$$

$$\begin{aligned}
\delta\omega_n^k(\boldsymbol{r}_A) &= \frac{\mu_0}{\pi\hbar}\mathcal{P}\int_0^\infty \frac{\mathrm{d}\omega}{\tilde{\omega}_{nk}(\boldsymbol{r}_A)-\omega}\,\omega^2\boldsymbol{d}_{nk}\!\cdot\!\mathrm{Im}\,\boldsymbol{G}^{(1)}(\boldsymbol{r}_A,\boldsymbol{r}_A,\omega)\!\cdot\!\boldsymbol{d}_{kn} \\
&= -\frac{\mu_0}{\hbar}\sum_k \Theta[\tilde{\omega}_{nk}(\boldsymbol{r}_A)]\tilde{\omega}_{nk}^2(\boldsymbol{r}_A)\boldsymbol{d}_{nk}\!\cdot\!\mathrm{Re}\,\boldsymbol{G}^{(1)}[\boldsymbol{r}_A,\boldsymbol{r}_A,\tilde{\omega}_{nk}(\boldsymbol{r}_A)]\!\cdot\!\boldsymbol{d}_{kn} \\
&\quad +\frac{\mu_0}{\pi\hbar}\sum_k \int_0^\infty \mathrm{d}\xi\,\frac{\tilde{\omega}_{kn}(\boldsymbol{r}_A)\xi^2}{\tilde{\omega}_{kn}^2(\boldsymbol{r}_A)+\xi^2}\,\boldsymbol{d}_{nk}\!\cdot\!\boldsymbol{G}^{(1)}(\boldsymbol{r}_A,\boldsymbol{r}_A,\mathrm{i}\xi)\!\cdot\!\boldsymbol{d}_{kn},
\end{aligned} \tag{4.36}$$

---

[3]Note that again there is no need to distinguish between the cases of quantum and classical centre-of-mass motion, so that we drop the operator hat, $\hat{\boldsymbol{r}}_A \mapsto \boldsymbol{r}_A$.

[4]Note that the free-space Lamb shifts associated with $\boldsymbol{G}^{(0)}$ [recall Eq. (3.16) and the remarks thereafter] are thought of as being already included in the frequencies ω_{mn}. The second equality in Eq. (4.36) is obtained via the procedure outlined above Eq. (3.18).

which are due to the interaction of the atom with the body-assisted electromagnetic field, and similarly,

$$\Gamma_n(\boldsymbol{r}_A) = \sum_k \Gamma_n^k(\boldsymbol{r}_A), \tag{4.37}$$

$$\Gamma_n^k(\boldsymbol{r}_A) = \frac{2\mu_0}{\hbar}\,\Theta[\tilde{\omega}_{nk}(\boldsymbol{r}_A)]\tilde{\omega}_{nk}^2(\boldsymbol{r}_A)\boldsymbol{d}_{nk}\cdot\mathrm{Im}\,\boldsymbol{G}[\boldsymbol{r}_A,\boldsymbol{r}_A,\tilde{\omega}_{nk}(\boldsymbol{r}_A)]\cdot\boldsymbol{d}_{kn} \tag{4.38}$$

are the position-dependent level widths. Note that due to the appearance of the shifted frequencies on the right hand side of Eq. (4.36), this equation determines the shift only implicitly (cf. also Ref. [181]). The effect can be ignored for sufficiently small frequency shifts, in which case the position-dependent energy shifts $\hbar\delta\omega_n(\boldsymbol{r}_A)$ reduce to those obtained by leading-order perturbation theory, recall Eqs. (3.39)–(3.43).

In order to calculate the CP force, we substitute our results (4.32) and (4.33) into Eq. (4.31) together with Eqs. (4.27)–(4.29) and evaluate the time integrals with the aid of the Born–Oppenheimer and Markov approximations by putting $\boldsymbol{r}_A(\tau) \simeq \boldsymbol{r}_A(t)$ and $\langle \hat{A}_{mn}(\tau)\rangle \simeq \mathrm{e}^{-\mathrm{i}\tilde{\omega}_{mn}(\boldsymbol{r}_A)(t-\tau)}\langle\hat{A}_{mn}(t)\rangle$ and letting the lower integration limit tend to $t_0 \to -\infty$. As a result, the CP force can be written in the form

$$\boldsymbol{F}(\boldsymbol{r}_A,t) = \sum_{m,n} \sigma_{nm}(t)\boldsymbol{F}_{mn}(\boldsymbol{r}_A) \tag{4.39}$$

where the atomic density matrix elements $\sigma_{nm}(t) = \langle n|\hat{\sigma}(t)|m\rangle = \langle\hat{A}_{mn}(t)\rangle$ solve the intra-atomic master equation and the associated force components read

$$\boldsymbol{F}_{mn}(\boldsymbol{r}_A) = \boldsymbol{F}_{mn}^{\mathrm{el}}(\boldsymbol{r}_A) + \boldsymbol{F}_{mn}^{\mathrm{mag}}(\boldsymbol{r}_A), \tag{4.40}$$

$$\boldsymbol{F}_{mn}^{\mathrm{el}}(\boldsymbol{r}_A) = \frac{\mu_0}{\pi}\sum_k \int_0^\infty \mathrm{d}\omega\,\omega^2\,\frac{\boldsymbol{\nabla}\boldsymbol{d}_{mk}\cdot\mathrm{Im}\,\boldsymbol{G}^{(1)}(\boldsymbol{r},\boldsymbol{r}_A,\omega)\cdot\boldsymbol{d}_{kn}\big|_{\boldsymbol{r}=\boldsymbol{r}_A}}{\omega - \tilde{\omega}_{nk}(\boldsymbol{r}_A) - \mathrm{i}[\Gamma_k(\boldsymbol{r}_A)+\Gamma_m(\boldsymbol{r}_A)]/2} + \mathrm{C.c.}, \tag{4.41}$$

$$\boldsymbol{F}_{mn}^{\mathrm{mag}}(\boldsymbol{r}_A) = \frac{\mu_0}{\pi}\sum_k \int_0^\infty \mathrm{d}\omega\,\omega\tilde{\omega}_{mn}(\boldsymbol{r}_A)\,\frac{\boldsymbol{d}_{mk}\times\big[\boldsymbol{\nabla}\times\mathrm{Im}\,\boldsymbol{G}^{(1)}(\boldsymbol{r},\boldsymbol{r}_A,\omega)\big]\cdot\boldsymbol{d}_{kn}\big|_{\boldsymbol{r}=\boldsymbol{r}_A}}{\omega - \tilde{\omega}_{nk}(\boldsymbol{r}_A) - \mathrm{i}[\Gamma_k(\boldsymbol{r}_A)+\Gamma_m(\boldsymbol{r}_A)]/2} + \mathrm{C.c.} \tag{4.42}$$

Note that the bulk part $\boldsymbol{G}^{(1)}$ of the Green tensor does not contribute to the force [recall the discussion below Eq. (3.16)]. By applying the procedure outlined above Eq. (3.18), the force components $\boldsymbol{F}_{mn}(\boldsymbol{r}_A)$ can be rewritten as [SB1, SB6, SB7, SB8]

$$\boldsymbol{F}_{mn}(\boldsymbol{r}_A) = \boldsymbol{F}_{mn}^{\mathrm{el,or}}(\boldsymbol{r}_A) + \boldsymbol{F}_{mn}^{\mathrm{el,r}}(\boldsymbol{r}_A) + \boldsymbol{F}_{mn}^{\mathrm{mag,or}}(\boldsymbol{r}_A) + \boldsymbol{F}_{mn}^{\mathrm{mag,r}}(\boldsymbol{r}_A), \tag{4.43}$$

with the electric/magnetic, off-resonant/resonant force components being given by

$$\boldsymbol{F}_{mn}^{\mathrm{el,or}}(\boldsymbol{r}_A) = -\frac{\hbar\mu_0}{2\pi}\int_0^\infty \mathrm{d}\xi\,\xi^2\boldsymbol{\nabla}\mathrm{tr}\big\{[\boldsymbol{\alpha}_{mn}(\boldsymbol{r}_A,\mathrm{i}\xi) + \boldsymbol{\alpha}_{mn}(\boldsymbol{r}_A,-\mathrm{i}\xi)]\cdot\boldsymbol{G}^{(1)}(\boldsymbol{r}_A,\boldsymbol{r},\mathrm{i}\xi)\big\}\big|_{\boldsymbol{r}=\boldsymbol{r}_A}, \tag{4.44}$$

$$\boldsymbol{F}_{mn}^{\mathrm{el,r}}(\boldsymbol{r}_A) = \mu_0\sum_k \Theta[\tilde{\omega}_{nk}(\boldsymbol{r}_A)]\Omega_{mnk}^2(\boldsymbol{r}_A)\boldsymbol{\nabla}\boldsymbol{d}_{mk}\cdot\boldsymbol{G}^{(1)}[\boldsymbol{r},\boldsymbol{r}_A,\Omega_{mnk}(\boldsymbol{r}_A)]\cdot\boldsymbol{d}_{kn}\big|_{\boldsymbol{r}=\boldsymbol{r}_A} + \mathrm{C.c.}, \tag{4.45}$$

$$\boldsymbol{F}_{mn}^{\mathrm{mag,or}}(\boldsymbol{r}_A) = \frac{\hbar\mu_0}{2\pi} \int_0^\infty \mathrm{d}\xi\, \xi^2\, \mathrm{tr}\Bigg\{ \Bigg[\frac{\tilde{\omega}_{mn}(\boldsymbol{r}_A)}{\mathrm{i}\xi}\, \boldsymbol{\alpha}_{mn}^{\mathrm{T}}(\boldsymbol{r}_A, \mathrm{i}\xi) - \frac{\tilde{\omega}_{mn}(\boldsymbol{r}_A)}{\mathrm{i}\xi}\, \boldsymbol{\alpha}_{mn}^{\mathrm{T}}(\boldsymbol{r}_A, -\mathrm{i}\xi) \Bigg]$$

$$\times \Big[\boldsymbol{\nabla} \times \boldsymbol{G}^{(1)}(\boldsymbol{r}, \boldsymbol{r}_A, \mathrm{i}\xi) \Big] \Bigg\}_{\boldsymbol{r}=\boldsymbol{r}_A} , \quad (4.46)$$

$$\boldsymbol{F}_{mn}^{\mathrm{mag,r}}(\boldsymbol{r}_A) = \mu_0 \sum_k \Theta[\tilde{\omega}_{nk}(\boldsymbol{r}_A)]\tilde{\omega}_{mn}(\boldsymbol{r}_A)\Omega_{mnk}(\boldsymbol{r}_A)$$

$$\times \boldsymbol{d}_{mk} \times \Big\{ \boldsymbol{\nabla} \times \boldsymbol{G}^{(1)}[\boldsymbol{r}, \boldsymbol{r}_A, \Omega_{mnk}(\boldsymbol{r}_A)]\cdot\boldsymbol{d}_{kn} \Big\}_{\boldsymbol{r}=\boldsymbol{r}_A} + \mathrm{C.c.} \quad (4.47)$$

$[(\mathrm{tr}\,\boldsymbol{T})_j = T_{ljl}]$. Here, we have introduced the complex atomic transition frequencies

$$\Omega_{mnk}(\boldsymbol{r}_A) = \tilde{\omega}_{nk}(\boldsymbol{r}_A) + \mathrm{i}[\Gamma_m(\boldsymbol{r}_A) + \Gamma_k(\boldsymbol{r}_A)]/2 \qquad (4.48)$$

and the generalised polarisability tensor

$$\boldsymbol{\alpha}_{mn}(\boldsymbol{r}_A, \omega) = \frac{1}{\hbar} \sum_k \Bigg[\frac{\boldsymbol{d}_{mk}\boldsymbol{d}_{kn}}{-\Omega_{mnk}(\boldsymbol{r}_A) - \omega} + \frac{\boldsymbol{d}_{kn}\boldsymbol{d}_{mk}}{-\Omega_{nmk}^*(\boldsymbol{r}_A) + \omega} \Bigg]. \qquad (4.49)$$

Under the assumptions made, the temporal evolution of the intra-atomic density matrix elements entering Eq. (4.39) is governed by the equations (App. E)

$$\dot{\sigma}_{nn}(t) = -\Gamma_n(\boldsymbol{r}_A)\sigma_{nn}(t) + \sum_k \Gamma_k^n(\boldsymbol{r}_A)\sigma_{kk}(t), \qquad (4.50)$$

$$\sigma_{nm}(t) = \mathrm{e}^{\{\mathrm{i}\tilde{\omega}_{mn}(\boldsymbol{r}_A) - [\Gamma_m(\boldsymbol{r}_A) + \Gamma_n(\boldsymbol{r}_A)]/2\}(t-t_0)}\sigma_{nm}(t_0) \quad \text{for } m \neq n. \qquad (4.51)$$

Equation (4.39) together with Eqs. (4.34)–(4.38) as well as Eqs. (4.43)–(4.49) determines the dynamical CP force acting on an atom prepared in an arbitrary initial state $\hat{\sigma}(t_0)$ and placed within an arbitrary arrangement of magnetoelectric bodies under the condition of weak atom–field coupling. It is seen that the force is a superposition of different force components $\boldsymbol{F}_{mn}(\boldsymbol{r}_A)$ which are weighted by the respective time-dependent atomic density matrix elements $\sigma_{nm}(t)$. As expected, the force is influenced by the body-induced shifts (4.35) and widths (4.37) of the atomic transitions which sensitively depend on the atomic position.

Let us discuss the general result in more detail, considering first the situation studied in chapter 3 where an atom is initially prepared in an energy eigenstate $|n\rangle$, i.e., $\hat{\sigma}(t_0) = |n\rangle\langle n|$. For times that are short with respect to the relevant decay rate $\Gamma_n(\boldsymbol{r}_A)$, the CP force in this case is given by

$$\boldsymbol{F}(\boldsymbol{r}_A, t) \simeq \boldsymbol{F}(\boldsymbol{r}_A, t_0) = \boldsymbol{F}_{nn}(\boldsymbol{r}_A) \quad \text{for } (t - t_0)\Gamma_n(\boldsymbol{r}_A) \ll 1. \qquad (4.52)$$

Using the fact that $\boldsymbol{F}_{nn}^{\mathrm{mag,or}}(\boldsymbol{r}_A) = \boldsymbol{F}_{nn}^{\mathrm{mag,r}}(\boldsymbol{r}_A) = \boldsymbol{0}$ [cf. Eqs. (4.46) and (4.47)] and assuming real dipole matrix elements so that the symmetry of the Green tensor (2.17) allows for

the replacement $\boldsymbol{\nabla}\boldsymbol{G}^{(1)}(\boldsymbol{r},\boldsymbol{r}_A,\omega)|_{\boldsymbol{r}=\boldsymbol{r}_A} \mapsto \frac{1}{2}\boldsymbol{\nabla}\boldsymbol{G}^{(1)}(\boldsymbol{r},\boldsymbol{r},\omega)|_{\boldsymbol{r}=\boldsymbol{r}_A}$, the relevant diagonal force component can be written as

$$\boldsymbol{F}_{nn}(\boldsymbol{r}_A) = \boldsymbol{F}^{\mathrm{or}}_{nn}(\boldsymbol{r}_A) + \boldsymbol{F}^{\mathrm{r}}_{nn}(\boldsymbol{r}_A), \tag{4.53}$$

$$\boldsymbol{F}^{\mathrm{or}}_{nn}(\boldsymbol{r}_A) = -\frac{\hbar\mu_0}{4\pi}\int_0^\infty \mathrm{d}\xi\,\xi^2\boldsymbol{\nabla}\mathrm{tr}\big\{[\boldsymbol{\alpha}_{nn}(\boldsymbol{r}_A,\mathrm{i}\xi) + \boldsymbol{\alpha}_{nn}(\boldsymbol{r}_A,-\mathrm{i}\xi)]\cdot\boldsymbol{G}^{(1)}(\boldsymbol{r},\boldsymbol{r},\mathrm{i}\xi)\big\}\big|_{\boldsymbol{r}=\boldsymbol{r}_A}, \tag{4.54}$$

$$\boldsymbol{F}^{\mathrm{r}}_{nn}(\boldsymbol{r}_A) = \frac{\mu_0}{2}\sum_k \Theta[\tilde{\omega}_{nk}(\boldsymbol{r}_A)]\Omega^2_{nnk}(\boldsymbol{r}_A)\boldsymbol{\nabla}\boldsymbol{d}_{nk}\cdot\boldsymbol{G}^{(1)}[\boldsymbol{r},\boldsymbol{r},\Omega_{nnk}(\boldsymbol{r}_A)]\cdot\boldsymbol{d}_{kn}\big|_{\boldsymbol{r}=\boldsymbol{r}_A} + \mathrm{C.c.} \tag{4.55}$$

When neglecting the level shifts and widths, Eqs. (4.52)–(4.55) obviously reduce to the results found in chapter 3, Eq. (3.5) together with Eqs. (3.40)–(3.42). The static perturbative CP force is hence seen to be an approximation to the dynamical CP force that is valid on sufficiently short time scales and ignores the influence of shifts and widths. In particular, these effects introduce an additional position dependence, so that the dynamical CP force cannot be derived from a potential in the usual way.

Let us return to the temporal evolution of the CP force. When the initial atomic state $|n\rangle$ is not the ground state, then spontaneous decay as described by the balance equations (4.50) leads to a populating of the lower lying states $|k\rangle$ ($k < n$). As time proceeds, the state of the atom thus evolves into an incoherent superposition of energy eigenstates and the force is given by a superposition of the respective diagonal force components which are all of the form of Eq. (4.53) together with Eqs. (4.54) and (4.55). In the long-time limit, the atom will always decay to its ground state, with the CP force reducing to the ground-state force:

$$\boldsymbol{F}(\boldsymbol{r}_A, t \to \infty) = \boldsymbol{F}_{00}(\boldsymbol{r}_A). \tag{4.56}$$

The off-diagonal density matrix elements may become relevant if the atom is initially prepared in a coherent superposition of energy eigenstates. According to Eq. (4.51), these matrix elements are transient and they lead to oscillating force components. Recalling Eqs. (4.43)–(4.47), we see that these force components are due to the influence of both electric and induction fields; they hence display a vector structure that is entirely different from the (purely electric) diagonal force components.

4.2.2 Application: Half space

In order to illustrate the effect of the body-induced level shifting and broadening on the force, let us consider an two-level atom prepared in its upper state which is placed in front of a dielectric half space of permittivity $\varepsilon(\omega)$, where we restrict our attention to the non-retarded limit $[n(0)z_A \ll c/\omega_{\mathrm{max}}]$. Recalling Eqs. (3.107)–(3.112), one may easily verify that the relevant Green tensor for this arrangement reads

$$\boldsymbol{G}^{(1)}(\boldsymbol{r},\boldsymbol{r},\omega) \simeq \frac{c^2}{32\pi\omega^2 z^3}\frac{\varepsilon(\omega)-1}{\varepsilon(\omega)+1}(\boldsymbol{e}_x\boldsymbol{e}_x + \boldsymbol{e}_y\boldsymbol{e}_y + 2\boldsymbol{e}_z\boldsymbol{e}_z) \quad \text{for } |\omega|z/c \ll 1. \tag{4.57}$$
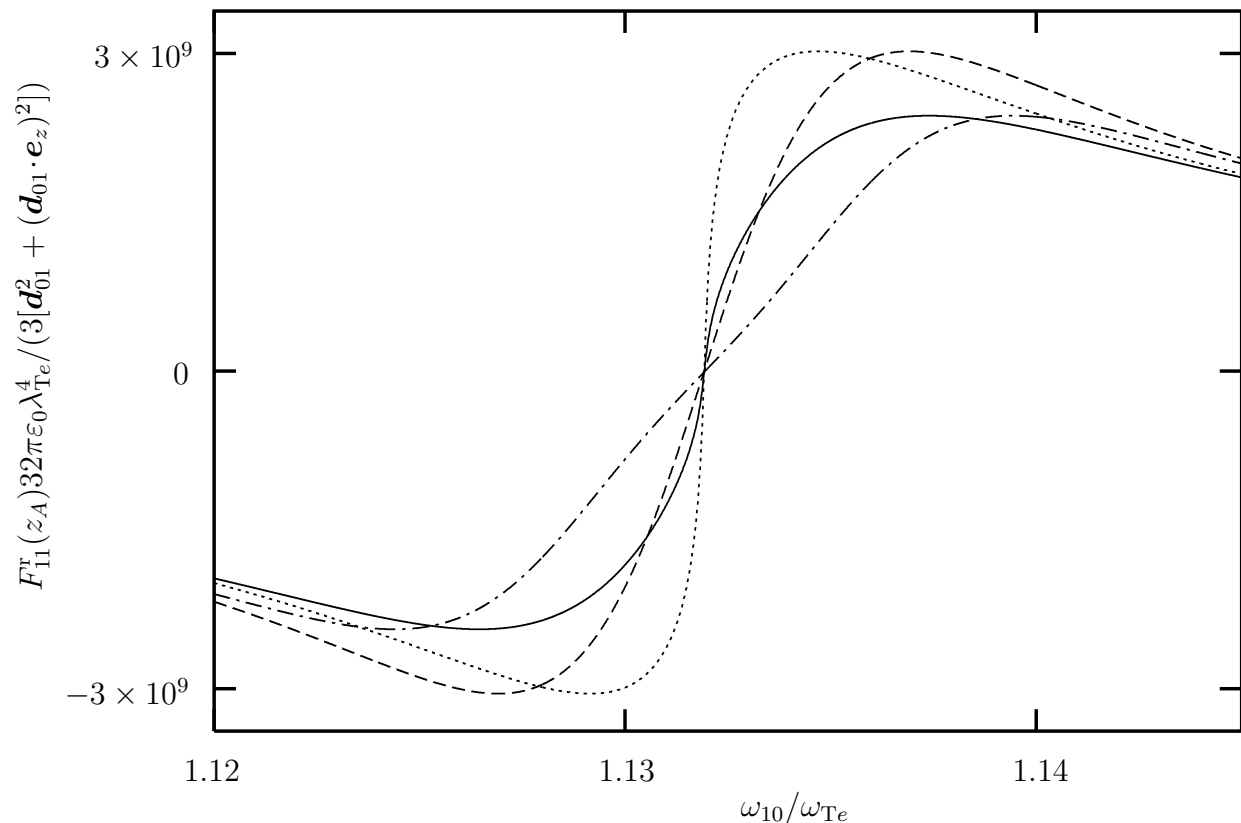
Figure 4.1: The resonant part of the CP force on a two-level atom in the upper state placed in front of a dielectric half space is shown as a function of the unperturbed transition frequency ω_{10} (solid line) ($\omega_{Pe}/\omega_{Te} = 0.75$, $\gamma_e/\omega_{Te} = 0.01$, $\omega_{Te}^2[\boldsymbol{d}_{01}^2 + (\boldsymbol{d}_{01}\cdot\boldsymbol{e}_z)^2]/3\pi\hbar\varepsilon_0 c^3 = 10^{-7}$, $z_A/\lambda_{Te} = 0.0075$, $\lambda_{Te} = 2\pi c/\omega_{Te}$). For comparison, the result without shifting and broadening of the atomic transition (dashed lines) and the separate effects of shifting (dotted lines) and broadening (dash-dotted lines), are also shown.

After substituting Eq. (4.57) into Eqs. (4.34)–(4.38), it is found that in the non-retarded limit, the shift and width of the transition frequency are given by

$$\delta\omega(z_A) = \delta\omega_1(z_A) - \delta\omega_0(z_A) = -\frac{\boldsymbol{d}_{01}^2 + (\boldsymbol{d}_{01}\cdot\boldsymbol{e}_z)^2}{32\pi\hbar\varepsilon_0 z_A^3}\frac{|\varepsilon[\omega_{10} + \delta\omega(z_A)]|^2 - 1}{|\varepsilon[\omega_{10} + \delta\omega(z_A)] + 1|^2}, \tag{4.58}$$

$$\Gamma(z_A) = \Gamma_1(z_A) = \frac{\boldsymbol{d}_{01}^2 + (\boldsymbol{d}_{01}\cdot\boldsymbol{e}_z)^2}{8\pi\hbar\varepsilon_0 z_A^3}\frac{\operatorname{Im}\varepsilon[\omega_{10} + \delta\omega(z_A)]}{|\varepsilon[\omega_{10} + \delta\omega(z_A)] + 1|^2} \tag{4.59}$$

where the transition-dipole matrix element has been assumed to be real and the (small) off-resonant contribution to the frequency shift has been omitted.

With these preparations at hand, let us consider the component of the CP force that is relevant when the atom is prepared in the upper state, starting with the dominant resonant contribution. Substituting Eq. (4.57) into Eq. (4.55), one obtains [SB1, SB6, SB7, SB8]

$$\boldsymbol{F}_{11}^{r}(z_A) = F_{11}^{r}(z_A)\boldsymbol{e}_z = -\frac{3[\boldsymbol{d}_{01}^2 + (\boldsymbol{d}_{01}\cdot\boldsymbol{e}_z)^2]}{32\pi\hbar\varepsilon_0 z_A^4}\frac{|\varepsilon[\Omega_{110}(z_A)]|^2 - 1}{|\varepsilon[\Omega_{110}(z_A)] + 1|^2}\boldsymbol{e}_z \tag{4.60}$$

where, according to Eq. (4.48),

$$\Omega_{110}(z_A) = \tilde{\omega}_{10}(z_A) + \mathrm{i}\Gamma(z_A)/2 = \omega_{10} + \delta\omega(z_A) + \mathrm{i}\Gamma(z_A)/2. \tag{4.61}$$
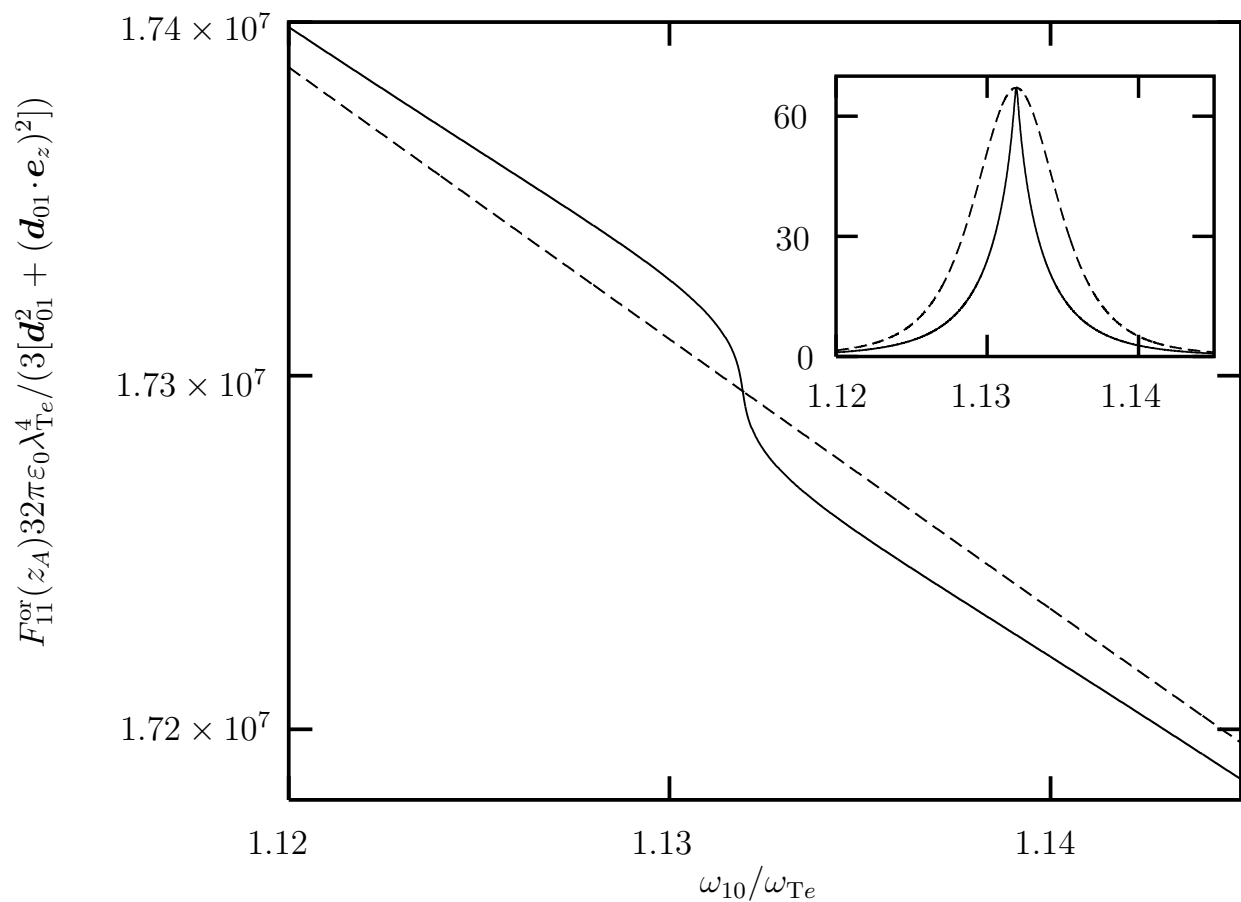
Figure 4.2: The off-resonant part of the CP force on a two-level atom in the upper state placed in front of a dielectric half space is shown as a function of the unperturbed transition frequency (solid line), the parameters being the same as in Fig. 4.1. For comparison, the result without shifting and broadening of the atomic transition is also shown (dashed lines). The inset displays the difference between the force with and without consideration of broadening (solid lines), where the same difference is displayed when the shifting is ignored (dashed lines).

In particular, when using the single-resonance Drude–Lorentz model (3.141) for the permittivity of the half space, one has

$$\varepsilon[\Omega_{110}(z_A)] = 1 + \frac{\omega_{Pe}^2}{\omega_{Te}^2 - \tilde{\omega}_{10}^2(z_A) - i[\Gamma(z_A) + \gamma_e]\tilde{\omega}_{10}(z_A)} \quad \text{for } \gamma_e, \Gamma(z_A) \ll \omega_{Te}, \qquad (4.62)$$

demonstrating that the absorption parameter γ_e of the half-space medium is replaced with the total absorption parameter, i.e., the sum of γ_e and the decay rate $\Gamma(z_A)$ of the atom. Figure 4.1 displays $F_{11}^r(z_A)$ [Eq. (4.60) together with Eqs. (3.141), (4.58), (4.59) and (4.61)] as a function of the unperturbed transition frequency ω_{10}. It is seen that in the vicinity of the (surface-plasmon) frequency $\omega_S = \sqrt{\omega_{Te}^2 + \omega_{Pe}^2/2}$, an enhanced force is observed which is attractive/repulsive for $\omega_{10} \lessgtr \omega_S$ – a result already known from perturbation theory [152]. The figure, however, shows that due to the body-induced level shifting and broadening, the absolute value of the force can be noticeably reduced. Interestingly, the positions of the extrema of the force remain nearly unchanged, because level shifting and broadening give

rise to competing effects that almost cancel.

The off-resonant contribution to the force (4.54) can also be calculated with the aid of the Green tensor (4.57), where after recalling Eq. (3.23) one finds [SB1, SB6, SB7, SB8]

$$\boldsymbol{F}_{11}^{\mathrm{or}}(z_A) = F_{11}^{\mathrm{or}}(z_A)\boldsymbol{e}_z = \frac{3[\boldsymbol{d}_{01}^2 + (\boldsymbol{d}_{01}\cdot\boldsymbol{e}_z)^2]}{32\pi^2\hbar\varepsilon_0 z_A^4} \int_0^\infty \mathrm{d}\xi \, \frac{\varepsilon(\mathrm{i}\xi) - 1}{\varepsilon(\mathrm{i}\xi) + 1} \frac{\tilde{\omega}_{10}(z_A)}{\tilde{\omega}_{10}^2(z_A) + [\xi + \Gamma(z_A)/2]^2}$$
$$\times \frac{\tilde{\omega}_{10}^2(z_A) + \xi^2 + \Gamma^2(z_A)/4}{\tilde{\omega}_{10}^2(z_A) + [\xi - \Gamma(z_A)/2]^2} \, \boldsymbol{e}_z. \quad (4.63)$$

One sees that the off-resonant component of the force is only weakly influenced by level broadening [the leading-order dependence being $O(\Gamma^2)$], which is in agreement with the physical requirement that the virtual emission and absorption processes governing the off-resonant component should be only weakly affected by decay-induced broadening. Formally, the absence of a linear-order term $O(\Gamma)$ is due to the fact that the atomic polarisability enters the off-resonant force components (4.54) only in the combination $\boldsymbol{\alpha}_{nn}(\boldsymbol{r}_A, \mathrm{i}\xi) + \boldsymbol{\alpha}_{nn}(\boldsymbol{r}_A, -\mathrm{i}\xi)$. The effects of level shifting and broadening are illustrated in Fig. 4.2, where $F_{11}^{\mathrm{or}}(z_A)$ [Eqs. (4.63) together with Eqs. (3.141), (4.58) and (4.59)] is displayed as a function of the unperturbed transition frequency ω_{10}. It is seen that the frequency shifting has the effect of raising/lowering the force for $\omega_{10} \lessgtr \omega_{\mathrm{S}}$, whereas the effect of broadening is not visible in the curves. Only by plotting the difference between the results with and without broadening, a slight reduction of the force becomes visible in the vicinity of ω_{S}, where Γ is largest. Note that our results for the off-resonant CP force hold similarly for an atom in the lower state, because for a two-level atom we have $\boldsymbol{F}_{00}(z_A) = \boldsymbol{F}_{00}^{\mathrm{or}}(z_A) = -\boldsymbol{F}_{11}^{\mathrm{or}}(z_A)$.

The results of this section and the preceding Sec. 4.2.1 have well illustrated the validity limits of the time-independent perturbative approach to the CP force. In Sec. 4.2.1, we have seen that due to the decay-induced dynamics of the CP force, the static results are valid only for atoms initially prepared in their ground state (or, for sufficiently short times, also for atoms in metastable states). The results of this section further stress that the perturbative result should not be applied to excited atoms in general, because the arising resonant force components can be strongly affected by level broadening, which is not included in the perturbative approach.

4.3 Strong atom–field coupling

As seen in the previous section, an initially excited atom that is weakly coupled to the body-assisted electromagnetic field will undergo irreversible spontaneous decay where the excitation is permanently lost from the atom. Qualitatively different phenomena may arise when the near-resonant interaction of an atom with a narrow quasi-mode of the body-assisted

electromagnetic field leads to strong atom–field coupling – which is typically realised when an excited atom is placed within a cavity or another resonator-like geometry. Strong coupling is ususally accompanied by Rabi oscillations, i.e., a periodic exchange of the excitation between the atom and the field.

4.3.1 Atom–field interaction

The atom–field dynamics for strong coupling cannot be described within the Markov approximation. Instead, one may use the two-level model for the atom and treat the interaction in rotating-wave approximation [189], since strong coupling typically arises via the resonant interaction of a single atomic transition with a single quasi-mode of the field. Combining Eqs. (2.23)–(2.25) and (2.94), one finds that for sufficiently slow centre-of-mass motion, the interaction Hamiltonian can be written in the form [SB16]

$$\hat{H}_{AF} = \hbar \int_0^\infty \mathrm{d}\omega\, g(\boldsymbol{r}_A, \omega)\hat{a}(\boldsymbol{r}_A, \omega)|1\rangle\langle 0| + \text{H.c.} \tag{4.64}$$

where the atom–field coupling strength is given by

$$g(\boldsymbol{r}, \omega) = \sqrt{\frac{\mu_0}{\pi\hbar}\, \omega^2 \boldsymbol{d}_{10}{\cdot}\mathrm{Im}\,\boldsymbol{G}(\boldsymbol{r}, \boldsymbol{r}, \omega){\cdot}\boldsymbol{d}_{01}}\,, \tag{4.65}$$

and $\hat{a}(\boldsymbol{r}, \omega)$ and $\hat{a}^\dagger(\boldsymbol{r}, \omega)$ are photon-like annihilation and creation operators, which are defined according to

$$\hat{a}(\boldsymbol{r}, \omega) = -\frac{1}{\hbar g(\boldsymbol{r}, \omega)}\sum_{\lambda=e,m}\int \mathrm{d}^3r'\, \boldsymbol{d}_{10}{\cdot}\boldsymbol{G}_\lambda(\boldsymbol{r}, \boldsymbol{r}', \omega){\cdot}\hat{\boldsymbol{f}}_\lambda(\boldsymbol{r}', \omega). \tag{4.66}$$

The commutation relations

$$[\hat{a}(\boldsymbol{r}, \omega), \hat{a}(\boldsymbol{r}, \omega')] = 0, \qquad \big[\hat{a}(\boldsymbol{r}, \omega), \hat{a}^\dagger(\boldsymbol{r}', \omega')\big] = \frac{g(\boldsymbol{r}, \boldsymbol{r}', \omega)}{g(\boldsymbol{r}, \omega)g(\boldsymbol{r}', \omega)}\, \delta(\omega - \omega') \tag{4.67}$$

with

$$g(\boldsymbol{r}, \boldsymbol{r}', \omega) = \frac{\mu_0}{\pi\hbar}\, \omega^2 \boldsymbol{d}_{10}{\cdot}\mathrm{Im}\,\boldsymbol{G}(\boldsymbol{r}, \boldsymbol{r}', \omega){\cdot}\boldsymbol{d}_{01} \tag{4.68}$$

immediately follow from those of $\hat{\boldsymbol{f}}_\lambda(\boldsymbol{r}, \omega)$ and $\hat{\boldsymbol{f}}_\lambda^\dagger(\boldsymbol{r}, \omega)$ [Eqs. (2.21) and (2.22)] upon using the identity (2.26). In combination with Eq. (2.95), the definition (4.66) shows that $\hat{a}(\boldsymbol{r}, \omega)$ is indeed an annihilation operator:

$$\hat{a}(\boldsymbol{r}, \omega)|\{0\}\rangle = 0 \quad \forall\ \boldsymbol{r}, \omega; \tag{4.69}$$

while $\hat{a}^\dagger(\boldsymbol{r}, \omega)$ can be used to construct single-excitation states of the body-assisted electromagnetic field:

$$|1(\boldsymbol{r}, \omega)\rangle = \hat{a}^\dagger(\boldsymbol{r}, \omega)|\{0\}\rangle. \tag{4.70}$$

According to Eq. (4.64), the relevant Hilbert space of singly excited atom–field states is spanned by states of the form $|1\rangle|\{0\}\rangle$ and $|0\rangle|1(\boldsymbol{r}_A,\omega)\rangle$, so it is useful for the following to determine the action of the total Hamiltonian (2.86) [together with Eqs. (2.87), (2.88) and (4.64)] on these states. Making use of the commutation relations (2.22), (2.21) and (4.67), one calculates

$$\hat{H}|1\rangle|\{0\}\rangle = E_1|1\rangle|\{0\}\rangle + \hbar \int_0^\infty \mathrm{d}\omega\, g(\boldsymbol{r}_A,\omega)|0\rangle|1(\boldsymbol{r}_A,\omega)\rangle, \tag{4.71}$$

$$\hat{H}|0\rangle|1(\boldsymbol{r}_A,\omega)\rangle = (E_0 + \hbar\omega)|0\rangle|1(\boldsymbol{r}_A,\omega)\rangle + \hbar g(\boldsymbol{r}_A,\omega)|1\rangle|\{0\}\rangle. \tag{4.72}$$

In the following, we will assume that the part of the field excitation spectrum which may give rise to strong atom–field coupling can be assigned to a single Lorentzian quasi-mode ν of mid-frequency ω_ν and width $\gamma_\nu/2 \ll \omega_\nu$:

$$g^2(\boldsymbol{r},\omega) = g^2(\boldsymbol{r},\omega_\nu) \frac{\gamma_\nu^2/4}{(\omega - \omega_\nu)^2 + \gamma_\nu^2/4} + g'^2(\boldsymbol{r},\omega), \tag{4.73}$$

where the residual part of the field spectrum $g'^2(\boldsymbol{r},\omega)$ is only weakly coupled to the atom. The single-excitation state associated with the quasi-mode ν may be introduced as

$$|1_\nu\rangle = \sqrt{\frac{\gamma_\nu}{2\pi}} \int_0^\infty \frac{\mathrm{d}\omega}{\sqrt{(\omega - \omega_\nu)^2 + \gamma_\nu^2/4}} |1(\boldsymbol{r}_A,\omega)\rangle; \tag{4.74}$$

it is normalised to unity, as can be easily verified by recalling Eq. (4.70) [together with Eqs. (4.65), (4.67) and (4.68)] and noting that

$$\int_0^\infty \frac{\mathrm{d}\omega}{(\omega - \omega_\nu)^2 + \gamma_\nu^2/4} = \frac{2\pi}{\gamma_\nu} \quad \text{for } \gamma_\nu/2 \ll \omega_\nu. \tag{4.75}$$

4.3.2 Rabi dynamics

With the preparations of the previous section, we can now study the CP force for strong atom–field coupling. Starting again from the Lorentz force (4.20), the dynamical CP force for the atom–field system being in state $|\psi(t)\rangle$ can be written as

$$\boldsymbol{F}(\boldsymbol{r}_A,t) = \left\{ \langle\psi(t)|\boldsymbol{\nabla}\big[\hat{\boldsymbol{d}}\cdot\hat{\boldsymbol{E}}(\boldsymbol{r})\big]|\psi(t)\rangle \right\}_{\boldsymbol{r}=\boldsymbol{r}_A} + \left\{ \frac{\mathrm{d}}{\mathrm{d}t}\big[\langle\psi(t)|\hat{\boldsymbol{d}}\times\hat{\boldsymbol{B}}(\boldsymbol{r})|\psi(t)\rangle\big] \right\}_{\boldsymbol{r}=\boldsymbol{r}_A}$$
$$= \boldsymbol{F}^{\mathrm{el}}(\boldsymbol{r}_A,t) + \boldsymbol{F}^{\mathrm{mag}}(\boldsymbol{r}_A,t) \tag{4.76}$$

where we work again within the Born–Oppenheimer approximation and where the force has been separated into its electric and magnetic parts. Since the treatment of electric and magnetic parts of the force is completely analogous, we will only present the calculation of the electric part in detail while the magnetic part is derived in App. F. Upon using Eqs. (2.23) and (4.66), we may write

$$\boldsymbol{F}^{\mathrm{el}}(\boldsymbol{r}_A,t) = -\hbar \int_0^\infty \mathrm{d}\omega\, \langle\psi(t)|\big[\boldsymbol{\nabla}g(\boldsymbol{r},\omega)\hat{a}(\boldsymbol{r},\omega)|1\rangle\langle 0|\big]_{\boldsymbol{r}=\boldsymbol{r}_A}|\psi(t)\rangle + \mathrm{C.c.} \tag{4.77}$$

for a two-level atom treated within rotating-wave approximation. We assume that the system is initially prepared in a superposition (i) of excited atom with ground-state field and (ii) ground-state atom with (singly) excited quasi-mode:

$$|\psi(t_0)\rangle = |\theta\rangle = \cos\theta\,|1\rangle|\{0\}\rangle + \sin\theta\,|0\rangle|1_\nu\rangle, \quad \theta \in [0,\pi]; \tag{4.78}$$

hence $|\psi(t)\rangle$ can be given in the form

$$|\psi(t)\rangle = \psi_1(t)|1\rangle|\{0\}\rangle + \int_0^\infty d\omega\,\psi_0(\omega,t)|0\rangle|1(\boldsymbol{r}_A,\omega)\rangle \tag{4.79}$$

with initial conditions

$$\psi_1(t_0) = \cos\theta, \qquad \psi_0(\omega,t_0) = \sqrt{\frac{\gamma_\nu}{2\pi}}\,\frac{\sin\theta}{\sqrt{(\omega-\omega_\nu)^2 + \gamma_\nu^2/4}}, \tag{4.80}$$

recall Eq. (4.74). Substituting Eq. (4.79) into Eq. (4.77), recalling definition (4.70) and using the commutation relations (4.67), we obtain

$$\boldsymbol{F}^{\mathrm{el}}(\boldsymbol{r}_A, t) = -\hbar \int_0^\infty d\omega\,\frac{\left[\boldsymbol{\nabla}g(\boldsymbol{r},\boldsymbol{r}_A,\omega)\right]_{\boldsymbol{r}=\boldsymbol{r}_A}}{g(\boldsymbol{r}_A,\omega)}\,\psi_1^*(t)\psi_0(\omega,t) + \mathrm{C.c.} \tag{4.81}$$

In order to proceed, we must solve the Schrödinger equation

$$i\hbar\frac{\partial}{\partial t}|\psi(t)\rangle = \hat{H}|\psi(t)\rangle, \tag{4.82}$$

which by virtue of Eqs. (4.71) and (4.72) is equivalent to the system of equations

$$\dot{\psi}_1(t) = -i(E_1/\hbar)\psi_1(t) - i\int_0^\infty d\omega\,g(\boldsymbol{r}_A,\omega)\psi_0(\omega,t), \tag{4.83}$$

$$\dot{\psi}_0(\omega,t) = -i(E_0/\hbar + \omega)\psi_0(\omega,t) - ig(\boldsymbol{r}_A,\omega)\psi_1(t). \tag{4.84}$$

Equation (4.84) together with the initial condition (4.80) is formally solved by

$$\psi_0(\omega,t) = \sqrt{\frac{\gamma_\nu}{2\pi}}\,\frac{\sin\theta\,e^{-i(E_0/\hbar+\omega)(t-t_0)}}{\sqrt{(\omega-\omega_\nu)^2 + \gamma_\nu^2/4}} - ig(\boldsymbol{r}_A,\omega)\int_{t_0}^t d\tau\,e^{-i(E_0/\hbar+\omega)(t-\tau)}\psi_1(\tau). \tag{4.85}$$

Using this result, the force (4.81) can be expressed entirely in terms of $\psi_1(t)$:

$$\boldsymbol{F}^{\mathrm{el}}(\boldsymbol{r}_A, t) = -\pi\hbar[\gamma_\nu/\Omega_{\mathrm{R}}(\boldsymbol{r}_A)]\left[\boldsymbol{\nabla}g(\boldsymbol{r},\boldsymbol{r}_A,\omega_\nu)\right]_{\boldsymbol{r}=\boldsymbol{r}_A}\sin\theta\,e^{[-i(E_0/\hbar+\omega_\nu)-\gamma_\nu/2](t-t_0)}\psi_1^*(t)$$
$$+ i\hbar\int_0^\infty d\omega\,\left[\boldsymbol{\nabla}g(\boldsymbol{r},\boldsymbol{r}_A,\omega)\right]_{\boldsymbol{r}=\boldsymbol{r}_A}\int_{t_0}^t d\tau\,e^{-i(E_0/\hbar+\omega)(t-\tau)}\psi_1^*(t)\psi_1(\tau) + \mathrm{C.c.} \tag{4.86}$$

with $\Omega_{\mathrm{R}}(\boldsymbol{r}_A) = \sqrt{2\pi\gamma_\nu g^2(\boldsymbol{r}_A,\omega_\nu)}$ denoting the vacuum Rabi frequency. Note that the first term of Eq. (4.86) has been obtained by using the single-resonance form (4.73) of the field spectrum $g^2(\boldsymbol{r},\omega)$ [hereby neglecting the residual field continuum $g'^2(\boldsymbol{r},\omega)$] and an analogeous relation for $g(\boldsymbol{r},\boldsymbol{r}',\omega)$ and by evaluating the frequency integral by means of the relation

$$\int_0^\infty d\omega\,\frac{e^{-i\omega x}}{(\omega-\omega_\nu)^2 + \gamma_\nu^2/4} = \frac{2\pi}{\gamma_\nu}\,e^{-i\omega_\nu x - \gamma_\nu|x|/2} \quad \text{for } \gamma_\nu/2 \ll \omega_\nu. \tag{4.87}$$

In complete analogy, by substituting Eq. (4.85) into Eq. (4.83), one obtains

$$\dot{\psi}_1(t) = -\mathrm{i}(E_1/\hbar)\psi_1(t) - \tfrac{1}{2}\,\mathrm{i}\Omega_\mathrm{R}(\boldsymbol{r}_A)\sin\theta\,\mathrm{e}^{[-\mathrm{i}(E_0/\hbar+\omega_\nu)-\gamma_\nu/2](t-t_0)}$$
$$- \int_0^\infty \mathrm{d}\omega\, g^2(\boldsymbol{r}_A,\omega)\int_{t_0}^t \mathrm{d}\tau\, \mathrm{e}^{-\mathrm{i}(E_0/\hbar+\omega)(t-\tau)}\psi_1(\tau). \quad (4.88)$$

Using Eq. (4.73) and treating the (weakly coupled) residual field spectrum $g'^2(\boldsymbol{r},\omega)$ according to the Markov approximation, one can then show that (App. E)

$$\psi_1(t) = \mathrm{e}^{[-\mathrm{i}E_1/\hbar-\mathrm{i}\delta\omega_1'(\boldsymbol{r}_A)-\Gamma_1'(\boldsymbol{r}_A)/2](t-t_0)}\phi_1(t), \quad (4.89)$$

where $\phi_1(t)$ is the solution to the differential equation

$$\ddot{\phi}_1(t) + \big\{\mathrm{i}\Delta(\boldsymbol{r}_A) + [\gamma_\nu - \Gamma_1'(\boldsymbol{r}_A)]/2\big\}\dot{\phi}_1(t) + \tfrac{1}{4}\,\Omega_\mathrm{R}^2(\boldsymbol{r}_A)\phi_1(t) = 0 \quad (4.90)$$

together with the initial conditions

$$\phi_1(t_0) = \cos\theta, \qquad \dot{\phi}_1(t_0) = -\tfrac{1}{2}\,\mathrm{i}\Omega_\mathrm{R}(\boldsymbol{r}_A)\sin\theta. \quad (4.91)$$

Here,

$$\delta\omega_1'(\boldsymbol{r}_A) = \frac{\mu_0}{\pi\hbar}\,\mathcal{P}\int_0^\infty \mathrm{d}\omega\,\omega^2\,\frac{\boldsymbol{d}_{10}\cdot\mathrm{Im}\,\boldsymbol{G}^{(1)}(\boldsymbol{r}_A,\boldsymbol{r}_A,\omega)\cdot\boldsymbol{d}_{01}}{\tilde{\omega}_{10}'(\boldsymbol{r}_A) - \omega} + \frac{\Omega_\mathrm{R}^2(\boldsymbol{r}_A)}{4}\,\frac{\Delta(\boldsymbol{r}_A)}{\Delta^2(\boldsymbol{r}_A) + \gamma_\nu^2/4} \quad (4.92)$$

and

$$\Gamma_1'(\boldsymbol{r}_A) = \frac{2\mu_0}{\hbar}\big[\tilde{\omega}_{10}'(\boldsymbol{r}_A)\big]^2\boldsymbol{d}_{01}\cdot\mathrm{Im}\,\boldsymbol{G}\big[\boldsymbol{r}_A,\boldsymbol{r}_A,\tilde{\omega}_{10}'(\boldsymbol{r}_A)\big]\cdot\boldsymbol{d}_{10} - \frac{\Omega_\mathrm{R}^2(\boldsymbol{r}_A)}{4}\,\frac{\gamma_\nu}{\Delta^2(\boldsymbol{r}_A) + \gamma_\nu^2/4} \quad (4.93)$$

are the shift[5] and width of the upper level associated with the residual field continuum; $\tilde{\omega}_{10}(\boldsymbol{r}_A) = [\tilde{E}_1(\boldsymbol{r}_A) - E_0]/\hbar = \omega_{10}' + \delta\omega_1'(\boldsymbol{r}_A)$ is the respective shifted atomic transition frequency; and $\Delta(\boldsymbol{r}_A) = \omega_\nu - \tilde{\omega}_{10}'(\boldsymbol{r}_A)$ is the (shifted) resonator–atom detuning. Writing the general solution to the second-order differential equation (4.90) in the form

$$\phi_1(t) = c_+(\boldsymbol{r}_A)\mathrm{e}^{\Omega_+(\boldsymbol{r}_A)(t-t_0)} + c_-(\boldsymbol{r}_A)\mathrm{e}^{\Omega_-(\boldsymbol{r}_A)(t-t_0)}, \quad (4.94)$$

we find that

$$\Omega_\pm(\boldsymbol{r}_A) = -\tfrac{1}{2}\big\{\mathrm{i}\Delta(\boldsymbol{r}_A) + [\gamma_\nu - \Gamma_1'(\boldsymbol{r}_A)]/2\big\} \mp \tfrac{1}{2}\sqrt{\big\{\mathrm{i}\Delta(\boldsymbol{r}_A) + [\gamma_\nu - \Gamma_1'(\boldsymbol{r}_A)]/2\big\}^2 - \Omega_\mathrm{R}^2(\boldsymbol{r}_A)} \quad (4.95)$$

where the initial conditions (4.91) imply

$$c_\pm(\boldsymbol{r}_A) = \frac{\Omega_\mp(\boldsymbol{r}_A)\cos\theta + \tfrac{1}{2}\mathrm{i}\Omega_\mathrm{R}(\boldsymbol{r}_A)\sin\theta}{\Omega_\mp(\boldsymbol{r}_A) - \Omega_\pm(\boldsymbol{r}_A)}. \quad (4.96)$$

---

[5] Note that the free-space Lamb shift contribution to the level shift has again been absorbed in the bare transition frequency ω_{10} by making the replacement $\boldsymbol{G} \mapsto \boldsymbol{G}^{(1)}$.

After substitution of Eqs. (4.89) and (4.94), the electric part of the CP force, Eq. (4.86), takes the explicit form [SB16]

$$
\boldsymbol{F}^{\mathrm{el}}(\boldsymbol{r}_A, t) = -\pi\hbar[\gamma_\nu/\Omega_{\mathrm{R}}(\boldsymbol{r}_A)]\big[\boldsymbol{\nabla}g(\boldsymbol{r}, \boldsymbol{r}_A, \omega_\nu)\big]_{\boldsymbol{r}=\boldsymbol{r}_A} \sin\theta\, q(\boldsymbol{r}_A, t-t_0)
$$
$$
+ \hbar\int_0^\infty \mathrm{d}\omega\,\big[\boldsymbol{\nabla}g(\boldsymbol{r}, \boldsymbol{r}_A, \omega)\big]_{\boldsymbol{r}=\boldsymbol{r}_A} s(\boldsymbol{r}_A, \omega, t-t_0) + \mathrm{C.c.} \quad (4.97)
$$

where

$$
q(\boldsymbol{r}_A, t) = \mathrm{e}^{\{-\mathrm{i}\Delta(\boldsymbol{r}_A)-[\gamma_\nu+\Gamma_1'(\boldsymbol{r}_A)]/2\}t}\Big[c_+^*(\boldsymbol{r}_A)\mathrm{e}^{\Omega_+^*(\boldsymbol{r}_A)t} + c_-^*(\boldsymbol{r}_A)\mathrm{e}^{\Omega_-^*(\boldsymbol{r}_A)t}\Big] \quad (4.98)
$$

and

$$
\begin{aligned}
s(\boldsymbol{r}_A, \omega, t) ={}& |c_+(\boldsymbol{r}_A)|^2 \frac{\mathrm{e}^{[-\Gamma_1'(\boldsymbol{r}_A)+\Omega_+^*(\boldsymbol{r}_A)+\Omega_+(\boldsymbol{r}_A)]t} - \mathrm{e}^{\{\mathrm{i}[\tilde\omega_{10}'(\boldsymbol{r}_A)-\omega]-\Gamma_1'(\boldsymbol{r}_A)/2+\Omega_+^*(\boldsymbol{r}_A)\}t}}{\omega - \tilde\omega_{10}'(\boldsymbol{r}_A) + \mathrm{i}\Gamma_1'(\boldsymbol{r}_A)/2 - \mathrm{i}\Omega_+(\boldsymbol{r}_A)} \\
&+ c_+^*(\boldsymbol{r}_A)c_-(\boldsymbol{r}_A) \frac{\mathrm{e}^{[-\Gamma_1'(\boldsymbol{r}_A)+\Omega_+^*(\boldsymbol{r}_A)+\Omega_-(\boldsymbol{r}_A)]t} - \mathrm{e}^{\{\mathrm{i}[\tilde\omega_{10}'(\boldsymbol{r}_A)-\omega]-\Gamma_1'(\boldsymbol{r}_A)/2+\Omega_+^*(\boldsymbol{r}_A)\}t}}{\omega - \tilde\omega_{10}'(\boldsymbol{r}_A) + \mathrm{i}\Gamma_1'(\boldsymbol{r}_A)/2 - \mathrm{i}\Omega_-(\boldsymbol{r}_A)} \\
&+ c_-^*(\boldsymbol{r}_A)c_+(\boldsymbol{r}_A) \frac{\mathrm{e}^{[-\Gamma_1'(\boldsymbol{r}_A)+\Omega_-^*(\boldsymbol{r}_A)+\Omega_+(\boldsymbol{r}_A)]t} - \mathrm{e}^{\{\mathrm{i}[\tilde\omega_{10}'(\boldsymbol{r}_A)-\omega]-\Gamma_1'(\boldsymbol{r}_A)/2+\Omega_-^*(\boldsymbol{r}_A)\}t}}{\omega - \tilde\omega_{10}'(\boldsymbol{r}_A) + \mathrm{i}\Gamma_1'(\boldsymbol{r}_A)/2 - \mathrm{i}\Omega_+(\boldsymbol{r}_A)} \\
&+ |c_-(\boldsymbol{r}_A)|^2 \frac{\mathrm{e}^{[-\Gamma_1'(\boldsymbol{r}_A)+\Omega_-^*(\boldsymbol{r}_A)+\Omega_-(\boldsymbol{r}_A)]t} - \mathrm{e}^{\{\mathrm{i}[\tilde\omega_{10}'(\boldsymbol{r}_A)-\omega]-\Gamma_1'(\boldsymbol{r}_A)/2+\Omega_-^*(\boldsymbol{r}_A)\}t}}{\omega - \tilde\omega_{10}'(\boldsymbol{r}_A) + \mathrm{i}\Gamma_1'(\boldsymbol{r}_A)/2 - \mathrm{i}\Omega_-(\boldsymbol{r}_A)} \quad (4.99)
\end{aligned}
$$

have been defined. As shown in App. F, the respective magnetic part of the force is given by

$$
\boldsymbol{F}^{\mathrm{mag}}(\boldsymbol{r}_A, t) = \frac{\mathrm{i}\mu_0\omega_\nu\gamma_\nu}{\Omega_{\mathrm{R}}(\boldsymbol{r}_A)}\,\boldsymbol{d}_{10}\times\big[\boldsymbol{\nabla}\times\mathrm{Im}\,\boldsymbol{G}(\boldsymbol{r}, \boldsymbol{r}_A, \omega_\nu)\cdot\boldsymbol{d}_{01}\big]_{\boldsymbol{r}=\boldsymbol{r}_A}\sin\theta\,\frac{\mathrm{d}}{\mathrm{d}t}\,q(\boldsymbol{r}_A, t-t_0)
$$
$$
- \frac{\mathrm{i}\mu_0}{\pi}\int_0^\infty \mathrm{d}\omega\,\omega\boldsymbol{d}_{10}\times\big[\boldsymbol{\nabla}\times\mathrm{Im}\,\boldsymbol{G}(\boldsymbol{r}, \boldsymbol{r}_A, \omega)\cdot\boldsymbol{d}_{01}\big]_{\boldsymbol{r}=\boldsymbol{r}_A}\frac{\mathrm{d}}{\mathrm{d}t}\,s(\boldsymbol{r}_A, \omega, t-t_0) + \mathrm{C.c.} \quad (4.100)
$$

Equations (4.97) and (4.100) determine the (resonant part of the) dynamical CP force on a two-level atom for arbitrary strength of the atom–field coupling, with the system initially being prepared in state $|\theta\rangle$, Eq. (4.78). In the following, we consider the two limiting cases of weak and strong atom–field coupling.

Weak atom–field coupling is realised if the quasi-mode ν is very broad, $\gamma_\nu \gg 2\Omega_{\mathrm{R}}(\boldsymbol{r}_A)$, or far detuned from the atomic transition frequency, $|\Delta(\boldsymbol{r}_A)| \gg 2\Omega_{\mathrm{R}}^2(\boldsymbol{r}_A)/\gamma_\nu$. In both cases, the first term under the square root in Eq. (4.95) is much larger than the second one and a Taylor expansion yields

$$
\Omega_\pm(\boldsymbol{r}_A) = \begin{cases} -\mathrm{i}\Delta(\boldsymbol{r}_A) - [\gamma_\nu - \Gamma_1'(\boldsymbol{r}_A)]/2 \\[2mm] \dfrac{\mathrm{i}\Omega_{\mathrm{R}}^2(\boldsymbol{r}_A)}{4}\dfrac{\Delta(\boldsymbol{r}_A)}{\Delta^2(\boldsymbol{r}_A)+\gamma_\nu^2/4} - \dfrac{\Omega_{\mathrm{R}}^2(\boldsymbol{r}_A)}{8}\dfrac{\gamma_\nu}{\Delta^2(\boldsymbol{r}_A)+\gamma_\nu^2/4} \end{cases}. \quad (4.101)
$$

For the system initially being prepared in the state $|1\rangle|\{0\}\rangle$ [i.e., $\theta = 0$, recall Eq. (4.78)], the coefficients (4.96) approximate to $c_+(\boldsymbol{r}_A) = 0$, $c_-(\boldsymbol{r}_A) = 1$, so Eq. (4.89) [together with Eq. (4.94)] reduces to

$$
\psi_1(t) = \mathrm{e}^{[-\mathrm{i}E_1/\hbar-\mathrm{i}\delta\omega_1'(\boldsymbol{r}_A)-\Gamma_1'(\boldsymbol{r}_A)/2+\Omega_-(\boldsymbol{r}_A)](t-t_0)} = \mathrm{e}^{[-\mathrm{i}E_1/\hbar-\mathrm{i}\delta\omega_1(\boldsymbol{r}_A)-\Gamma_1(\boldsymbol{r}_A)/2](t-t_0)}. \quad (4.102)
$$

Here, $\delta\omega_1(\boldsymbol{r}_A)$ and $\Gamma_1(\boldsymbol{r}_A)$ are the shift (4.35) and width (4.37) of the upper level associated with the total field spectrum (4.73), including both the quasi-mode ν and the residual continuum. Note that the absence of the lower-level shift is due to the rotating-wave approximation. In order to find the CP force in the weak-coupling limit, we substitute Eq. (4.102) into Eq. (4.86). Evaluating the time integral in the spirit of the Markov approximation by putting $|\psi_1(\tau)|^2 \mapsto |\psi_1(t)|^2$ and letting the lower integration limit tend to $-\infty$, one arrives at [SB1, SB16]

$$\boldsymbol{F}(\boldsymbol{r}_A, t) = \boldsymbol{F}^{\text{el}}(\boldsymbol{r}_A, t) = \mathrm{e}^{-\Gamma_1(\boldsymbol{r}_A)(t-t_0)}\boldsymbol{F}_{11}(\boldsymbol{r}_A) \tag{4.103}$$

where

$$\boldsymbol{F}_{11}(\boldsymbol{r}_A) = \frac{\mu_0}{\pi}\int_0^\infty \mathrm{d}\omega\,\omega^2\,\frac{\left[\boldsymbol{\nabla}\boldsymbol{d}_{10}\!\cdot\!\mathrm{Im}\,\boldsymbol{G}^{(1)}(\boldsymbol{r}, \boldsymbol{r}_A, \omega)\!\cdot\!\boldsymbol{d}_{01}\right]_{\boldsymbol{r}=\boldsymbol{r}_A}}{\omega - \tilde{\omega}_{10}(\boldsymbol{r}_A) - \mathrm{i}\Gamma_1(\boldsymbol{r}_A)/2} + \mathrm{C.c.}$$

$$\simeq \mu_0\Omega_{110}^2(\boldsymbol{r}_A)\big\{\boldsymbol{\nabla}\boldsymbol{d}_{10}\!\cdot\!\boldsymbol{G}^{(1)}[\boldsymbol{r}, \boldsymbol{r}_A, \Omega_{110}(\boldsymbol{r}_A)]\!\cdot\!\boldsymbol{d}_{01}\big\}_{\boldsymbol{r}=\boldsymbol{r}_A} + \mathrm{C.c.} \tag{4.104}$$

with $\Omega_{110}(\boldsymbol{r}_A) = \tilde{\omega}_{10}(\boldsymbol{r}_A) + \mathrm{i}\Gamma_1(\boldsymbol{r}_A)/2$. Note that the magnetic part of the force does not contribute under the conditions considered, $\boldsymbol{F}^{\text{mag}}(\boldsymbol{r}_A, t) = \boldsymbol{0}$ (App. F). As expected, we have thus recovered the (two-level case of the) result (4.39) derived in Sec. 4.2, by assuming that the body-assisted field is initially prepared in its ground state and the atom–field coupling is sufficiently weak. In addition, the calculation has explicitly shown that weak–atom field coupling is realised (and the Markov approximation is applicable) if all atomic transitions are sufficiently far detuned from the field resonances, or if those (quasi-)modes of the field which interact near-resonantly with the atom are sufficiently broad, recall the two conditions above Eq. (4.101).

Next, we consider the case of strong atom–field coupling, which is realised if the quasi-mode ν is both sufficiently narrow, $\gamma_\nu \leq 2\Omega_{\text{R}}(\boldsymbol{r}_A)$ and near-resonant with the atomic transition, $|\Delta(\boldsymbol{r}_A)| \ll 2\Omega_{\text{R}}^2(\boldsymbol{r}_A)/\gamma_\nu$. In this case, the real part of the square root in Eq. (4.95) becomes negligible, so that we have

$$\Omega_\pm(\boldsymbol{r}_A) = -\tfrac{1}{2}\big\{\mathrm{i}\Delta(\boldsymbol{r}_A) + [\gamma_\nu - \Gamma_1'(\boldsymbol{r}_A)]/2\big\} \mp \tfrac{1}{2}\mathrm{i}\Omega(\boldsymbol{r}_A), \tag{4.105}$$

with

$$\Omega(\boldsymbol{r}_A) = \sqrt{\Omega_{\text{R}}^2(\boldsymbol{r}_A) + \Delta^2(\boldsymbol{r}_A) - \big[\gamma_\nu - \Gamma_1'(\boldsymbol{r}_A)\big]^2/4} \tag{4.106}$$

being the shifted Rabi frequency; and the coefficients (4.96) reduce to

$$c_\pm(\boldsymbol{r}_A) = \frac{\big\{\Omega(\boldsymbol{r}_A) \mp \Delta(\boldsymbol{r}_A) \pm \mathrm{i}[\gamma_\nu - \Gamma_1'(\boldsymbol{r}_A)]/2\big\}\cos\theta}{2\Omega(\boldsymbol{r}_A)} \pm \frac{\Omega_{\text{R}}(\boldsymbol{r}_A)\sin\theta}{2\Omega(\boldsymbol{r}_A)}. \tag{4.107}$$

Substituting these results into Eq. (4.89) [together with Eq. (4.94)], one obtains

$$\psi_1(t) = \mathrm{e}^{-\gamma(\boldsymbol{r}_A)(t-t_0)/2}\Big[c_+(\boldsymbol{r}_A)\mathrm{e}^{-\mathrm{i}E_+(\boldsymbol{r}_A)(t-t_0)/\hbar}c_-(\boldsymbol{r}_A)\mathrm{e}^{-\mathrm{i}E_-(\boldsymbol{r}_A)(t-t_0)/\hbar}\Big] \tag{4.108}$$

where

$$\gamma(\boldsymbol{r}_A) = \frac{\gamma_\nu}{2} - \frac{\Omega_{\mathrm{R}}^2(\boldsymbol{r}_A)}{8} \frac{\gamma_\nu}{\Delta^2(\boldsymbol{r}_A) + \gamma_\nu^2/4} + \frac{\mu_0}{\hbar}\big[\tilde{\omega}_{10}'(\boldsymbol{r}_A)\big]^2 \boldsymbol{d}_{01}\!\cdot\!\mathrm{Im}\,\boldsymbol{G}\big[\boldsymbol{r}_A,\boldsymbol{r}_A,\tilde{\omega}_{10}'(\boldsymbol{r}_A)\big]\!\cdot\!\boldsymbol{d}_{10}$$

$$\simeq \begin{cases} \gamma_\nu/2 & \text{for } |\Delta(\boldsymbol{r}_A)| \ll \gamma_\nu/2, \\ \Gamma_1(\boldsymbol{r}_A)/2 & \text{for } \gamma_\nu/2 \ll |\Delta(\boldsymbol{r}_A)| \ll 2\Omega_{\mathrm{R}}^2(\boldsymbol{r}_A)/\gamma_\nu \end{cases} \tag{4.109}$$

is the total damping rate [which has been found by using Eq. (4.93)] and

$$E_\pm(\boldsymbol{r}_A) = \tfrac{1}{2}[E_0 + E_1 + \hbar\delta\omega_1'(\boldsymbol{r}_A) + \hbar\omega_\nu] \pm \tfrac{1}{2}\hbar\Omega(\boldsymbol{r}_A) \tag{4.110}$$

are the (approximate) eigenenergies of the system, with

$$\delta\omega_1'(\boldsymbol{r}_A) = \frac{\mu_0}{\pi\hbar}\mathcal{P}\int_0^\infty \mathrm{d}\omega\,\omega^2 \frac{\boldsymbol{d}_{10}\!\cdot\!\mathrm{Im}\,\boldsymbol{G}^{(1)}(\boldsymbol{r}_A,\boldsymbol{r}_A,\omega)\!\cdot\!\boldsymbol{d}_{01}}{\tilde{\omega}_{10}'(\boldsymbol{r}_A) - \omega} + \frac{\Omega_{\mathrm{R}}^2(\boldsymbol{r}_A)}{4}\frac{\Delta(\boldsymbol{r}_A)}{\Delta^2(\boldsymbol{r}_A) + \gamma_\nu^2/4}$$

$$\simeq \begin{cases} \Omega_{\mathrm{R}}^2(\boldsymbol{r}_A)\Delta(\boldsymbol{r}_A)/\gamma_\nu^2 & \text{for } |\Delta(\boldsymbol{r}_A)| \ll \gamma_\nu/2, \\ \delta\omega_1(\boldsymbol{r}_A) & \text{for } \gamma_\nu/2 \ll |\Delta(\boldsymbol{r}_A)| \ll 2\Omega_{\mathrm{R}}^2(\boldsymbol{r}_A)/\gamma_\nu \end{cases} \tag{4.111}$$

being the level shift associated with the residual field spectrum [recall Eq. (4.92)]. To find the electric part of the CP force for strong coupling, we substitute Eq. (4.105) into Eqs. (4.97)–(4.99) and evaluate the frequency integral by means of Eq. (4.73), where we neglect the contribution from the residual field continuum $g'^2(\boldsymbol{r},\omega)$. Using relations that are analogous to Eqs. (4.75) and (4.87), one finds [SB16]

$$\boldsymbol{F}^{\mathrm{el}}(\boldsymbol{r}_A,t) = -\mathrm{e}^{-\gamma(\boldsymbol{r}_A)(t-t_0)}\Bigg[\frac{|c_+(\boldsymbol{r}_A)|^2 + c_-^*(\boldsymbol{r}_A)c_+(\boldsymbol{r}_A)\mathrm{e}^{-\mathrm{i}\Omega(\boldsymbol{r}_A)(t-t_0)}}{\Delta(\boldsymbol{r}_A) - \Omega(\boldsymbol{r}_A) - \mathrm{i}\big[\gamma_\nu - \Gamma_1'(\boldsymbol{r}_A)\big]/2}$$

$$+ \frac{|c_-(\boldsymbol{r}_A)|^2 + c_+^*(\boldsymbol{r}_A)c_-(\boldsymbol{r}_A)\mathrm{e}^{\mathrm{i}\Omega(\boldsymbol{r}_A)(t-t_0)}}{\Delta(\boldsymbol{r}_A) + \Omega(\boldsymbol{r}_A) - \mathrm{i}\big[\gamma_\nu - \Gamma_1'(\boldsymbol{r}_A)\big]/2}\Bigg]\pi\hbar\gamma_\nu\big[\boldsymbol{\nabla}g(\boldsymbol{r},\boldsymbol{r}_A,\omega_\nu)\big]_{\boldsymbol{r}=\boldsymbol{r}_A} + \mathrm{C.c.} \tag{4.112}$$

where the respective magnetic part of the force is given in App. F. To make the spatial and temporal dependence of the force more explicit, we discuss some special cases in the following.

Again, we first consider the case of the system initially being prepared in state $|1\rangle|\{0\}\rangle$ (i.e., $\theta = 0$), where the coefficients (4.107) in Eq. (4.112) assume a simpler form. For real dipole matrix elements, the symmetry property (2.17) implies that $\boldsymbol{\nabla}g(\boldsymbol{r},\boldsymbol{r}_A,\omega_\nu)|_{\boldsymbol{r}=\boldsymbol{r}_A}$ is real; in addition, one may make the replacement

$$\frac{\gamma_\nu g(\boldsymbol{r},\boldsymbol{r}',\omega_\nu)}{\omega_\nu - \omega + \mathrm{i}\gamma_\nu/2} \mapsto \frac{2\mu_0}{\pi\hbar}\,\omega^2\boldsymbol{d}_{10}\!\cdot\!\boldsymbol{G}(\boldsymbol{r},\boldsymbol{r}',\omega)\!\cdot\!\boldsymbol{d}_{01}, \tag{4.113}$$

since we have assumed that the interaction is dominated by the single quasi-mode ν, recall Eq. (4.73). Following these steps, the electric force (4.112) can be written in the form [SB1, SB16]

$$\boldsymbol{F}^{\mathrm{el}}(\boldsymbol{r}_A,t) = 2\mathrm{e}^{-\gamma(\boldsymbol{r}_A)(t-t_0)}\sin^2[\Omega(\boldsymbol{r}_A)(t-t_0)/2]C(\boldsymbol{r}_A)\boldsymbol{F}_{11}(\boldsymbol{r}_A), \tag{4.114}$$

where $\boldsymbol{F}_{11}(\boldsymbol{r}_A)$ is given by Eq. (4.104) with $\Omega'_{110}(\boldsymbol{r}_A){=}\tilde{\omega}'_{10}(\boldsymbol{r}_A){+}\mathrm{i}\Gamma'_1(\boldsymbol{r}_A)/2$ in place of $\Omega_{110}(\boldsymbol{r}_A)$ and the factor $C(\boldsymbol{r}_A)$ reads

$$C(\boldsymbol{r}_A) = \frac{\Delta^2(\boldsymbol{r}_A) - [\gamma_\nu - \Gamma'_1(\boldsymbol{r}_A)/2]^2/4}{\Delta^2(\boldsymbol{r}_A) - [\gamma_\nu - \Gamma'_1(\boldsymbol{r}_A)/2]^2/4 + \Omega_\mathrm{R}^2(\boldsymbol{r}_A)}$$
$$\simeq \begin{cases} \dfrac{\gamma_\nu^2/4}{\gamma_\nu^2/4 - \Omega_\mathrm{R}^2(\boldsymbol{r}_A)} & \text{for } |\Delta(\boldsymbol{r}_A)| \ll \gamma_\nu/2, \\[3mm] \dfrac{\Delta^2(\boldsymbol{r}_A)}{\Delta^2(\boldsymbol{r}_A) + \Omega_\mathrm{R}^2(\boldsymbol{r}_A)} & \text{for } \gamma_\nu/2 \ll |\Delta(\boldsymbol{r}_A)| \ll 2\Omega_\mathrm{R}^2(\boldsymbol{r}_A)/\gamma_\nu. \end{cases} \tag{4.115}$$

A principal difference between the weak and strong-coupling CP forces is the fact that for strong coupling the magnetic part of force (4.100) does not vanish, in general [see also Eq. (4.124) below]. Even the electric part of the CP force, however, differs from the weak-coupling force (4.103) [together with Eq. (4.104)] in several respects. Firstly, the shift and width of the excited atomic level relevant for determining $\boldsymbol{F}_{11}(\boldsymbol{r}_A)$ are now only those associated with the residual field continuum, in contrast to the full shift and width appearing in the weak-coupling force. Secondly, the strength of the strong-coupling force is modified with respect to the weak-coupling result by the factor $C(\boldsymbol{r}_A)$. Thirdly, and most strikingly, the dynamics of the force is not given by an exponential decay, but by damped oscillations with a (shifted) Rabi frequency $\Omega(\boldsymbol{r}_A)$ and a damping rate $\gamma(\boldsymbol{r}_A)$. Note that only the magnitude and not the sign of the force, is oscillating. As seen from Eq. (4.109), the damping is dominated by irreversible decay of the field excitation for small detuning, while irreversible spontaneous decay of the atomic excitation is the dominant loss mechanism for larger detuning, where in both limits the losses are characterised by one half the respective damping rates, γ_ν and $\Gamma_1(\boldsymbol{r}_A)$, respectively. This can easily be understood from the fact that in the strong coupling limit the states affected by these losses, $|0\rangle|1_\nu\rangle$ and $|1\rangle|\{0\}\rangle$, are both occupied to one half on average.

We now return to the case of an arbitrary initial state $|\theta\rangle$, Eq. (4.78) and assume that $\gamma_\nu \ll 2\Omega_\mathrm{R}(\boldsymbol{r}_A)$, which is often true for strong atom–field coupling. In this case, terms of the form $[\gamma_\nu - \Gamma'_1(\boldsymbol{r}_A)]/2$ can be neglected, hence the shifted Rabi frequency (4.106) reduces to

$$\Omega(\boldsymbol{r}_A) = \sqrt{\Omega_\mathrm{R}^2(\boldsymbol{r}_A) + \Delta^2(\boldsymbol{r}_A)}\,. \tag{4.116}$$

In the same approximation, the coefficients (4.107) can be written as

$$c_+(\boldsymbol{r}_A) = \cos[\theta_\mathrm{c}(\boldsymbol{r}_A)]\cos[\theta - \theta_\mathrm{c}(\boldsymbol{r}_A)], \qquad c_-(\boldsymbol{r}_A) = -\sin[\theta_\mathrm{c}(\boldsymbol{r}_A)]\sin[\theta - \theta_\mathrm{c}(\boldsymbol{r}_A)] \tag{4.117}$$

where we have introduced the coupling angle $\theta_\mathrm{c}(\boldsymbol{r}_A)$ via

$$\tan[2\theta_\mathrm{c}(\boldsymbol{r}_A)] = -\Omega_\mathrm{R}(\boldsymbol{r}_A)/\Delta(\boldsymbol{r}_A), \quad \theta_\mathrm{c}(\boldsymbol{r}_A) \in (0, \pi/2) \tag{4.118}$$

and used the identities [190]

$$\frac{1}{\sqrt{1+\tan^2(\alpha)}} = \begin{cases} \cos(\alpha) & \text{for } \alpha \in (0, \pi/2), \\ -\cos(\alpha) & \text{for } \alpha \in (\pi/2, \pi), \end{cases} \qquad \frac{1}{\sqrt{1+\cot^2(\alpha)}} = \sin(\alpha) \quad \text{for } \alpha \in (0, \pi).$$

(4.119)

Accordingly, after using the additional relations

$$\frac{\Omega_{\mathrm{R}}(\boldsymbol{r}_A)}{\Delta(\boldsymbol{r}_A) \pm \Omega(\boldsymbol{r}_A)} = \begin{cases} \cot\theta_{\mathrm{c}}(\boldsymbol{r}_A) \\ -\tan\theta_{\mathrm{c}}(\boldsymbol{r}_A) \end{cases} \tag{4.120}$$

[which follow from Eqs. (4.116), (4.118) and (4.119)], the electric part of the CP force (4.112) simplifies to [SB16]

$$\boldsymbol{F}^{\mathrm{el}}(\boldsymbol{r}_A, t) = \mathrm{e}^{-\gamma(\boldsymbol{r}_A)(t-t_0)}\Big(\cos\big\{2[\theta-\theta_{\mathrm{c}}(\boldsymbol{r}_A)]\big\} + \cot[2\theta_{\mathrm{c}}(\boldsymbol{r}_A)]\sin\big\{2[\theta-\theta_{\mathrm{c}}(\boldsymbol{r}_A)]\big\}$$
$$\times \cos[\Omega(\boldsymbol{r}_A)(t-t_0)]\Big)\boldsymbol{F}_+(\boldsymbol{r}_A) \quad (4.121)$$

with

$$\boldsymbol{F}_+(\boldsymbol{r}_A) = -\tfrac{1}{2}\hbar\boldsymbol{\nabla}\sqrt{\Omega_{\mathrm{R}}^2(\boldsymbol{r}) + \Delta^2(\boldsymbol{r}_A)}\,\Big|_{\boldsymbol{r}=\boldsymbol{r}_A}, \tag{4.122}$$

where we have assumed real dipole matrix elements, so that the symmetry property of the Green tensor (2.17), together with definitions (4.65) and (4.68) implies

$$\pi\gamma_\nu\boldsymbol{\nabla}g(\boldsymbol{r},\boldsymbol{r}_A,\omega_\nu)|_{\boldsymbol{r}=\boldsymbol{r}_A} = \pi\gamma_\nu g(\boldsymbol{r}_A,\omega_\nu)\boldsymbol{\nabla}_A\,g(\boldsymbol{r}_A,\omega_\nu) = \tfrac{1}{2}\Omega_{\mathrm{R}}(\boldsymbol{r}_A)\boldsymbol{\nabla}_A\,\Omega_{\mathrm{R}}(\boldsymbol{r}_A)$$
$$= \frac{\Omega_{\mathrm{R}}(\boldsymbol{r}_A)\boldsymbol{\nabla}\sqrt{\Omega_{\mathrm{R}}^2(\boldsymbol{r}) + \Delta^2(\boldsymbol{r}_A)}\,\big|_{\boldsymbol{r}=\boldsymbol{r}_A}}{2\sin[2\theta_{\mathrm{c}}(\boldsymbol{r}_A)]}. \quad (4.123)$$

Equations (4.121) and (4.122) can be used to study the electric part of the dynamical resonant force on an atom placed within an arbitrary resonator under the conditions of sufficiently strong atom–field coupling [so that the inequalities above Eqs. (4.105) and (4.116) hold], with the system initially being prepared in state $|\theta\rangle$, Eq. (4.78). Whereas the spatial dependence of the force strongly depends on the particular geometry of the system [which enters via the Green tensor, recall Eq. (4.65)], the temporal behaviour is quite generic and can be investigated regardless of the specific resonator in which the atom is placed. From Eq. (4.121), one sees that the force is always exponentially damped with a damping rate $\gamma(\boldsymbol{r}_A)$ and that it contains a non-oscillating part and a component that oscillates with the shifted Rabi frequency $\Omega(\boldsymbol{r}_A)$. The relative strengths of the constant and oscillating parts depend on both the coupling angle $\theta_{\mathrm{c}}(\boldsymbol{r}_A)$ and the inital state of the system $|\theta\rangle$. This is illustrated in Fig. 4.3, where the time dependence of the force is displayed for various initial states $|\theta\rangle$ and fixed coupling angle $2\theta_{\mathrm{c}}(\boldsymbol{r}_A) = 3\pi/8$. We first observe that the curves may be grouped in pairs of curves differing only by their sign; each of these pairs corresponds to
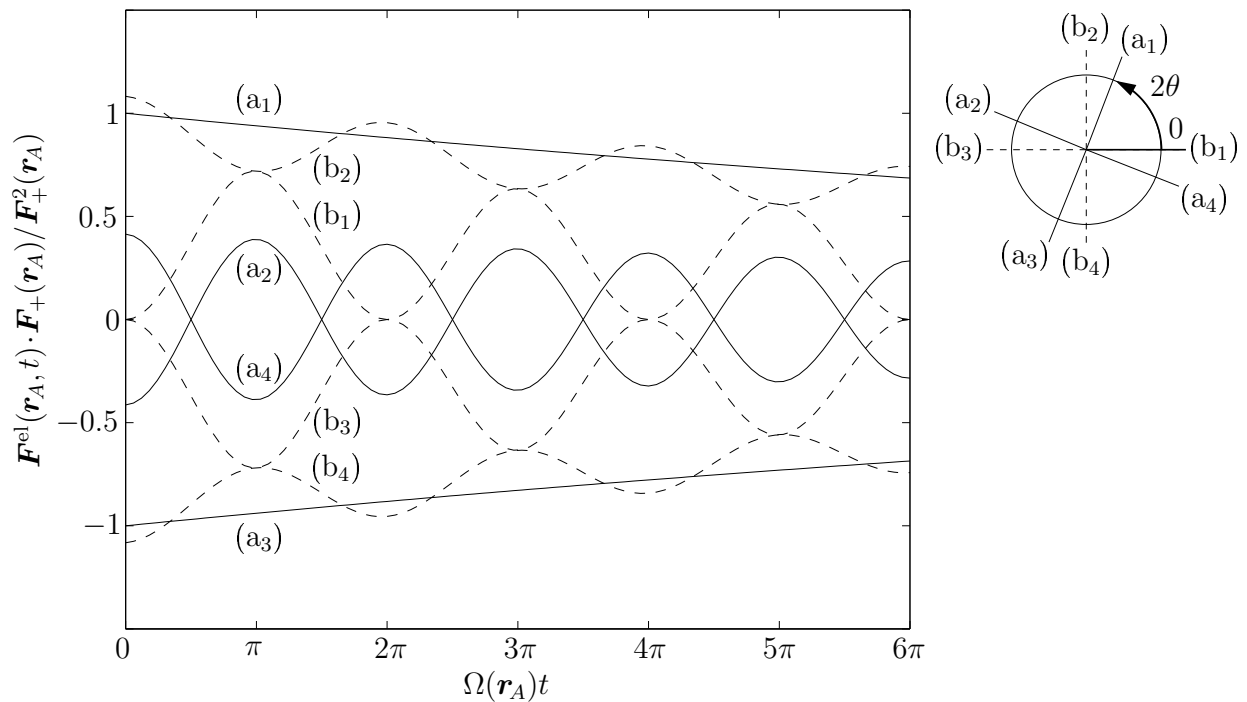
Figure 4.3: The time dependence of the electric part of the resonant CP force for strong atom–field coupling is displayed for different values of θ, i.e., $2\theta = 2\theta_c(\boldsymbol{r}_A)$ (a$_1$), $2\theta_c(\boldsymbol{r}_A)+\pi/2$ (a$_2$), $2\theta_c(\boldsymbol{r}_A)+\pi$ (a$_3$), $2\theta_c(\boldsymbol{r}_A)+3\pi/2$ (a$_4$), 0 (b$_1$), $\pi/2$ (b$_2$), π (b$_3$), $3\pi/2$ (b$_4$), with parameters $2\theta_c(\boldsymbol{r}_A) = 3\pi/8$ and $\gamma(\boldsymbol{r}_A) = 0.05\,\Omega(\boldsymbol{r}_A)$. The angles 2θ for the various curves are indicated in the small polar diagram.

values of θ which differ by $2\Delta\theta = \pi$. The existence of such pairs is an obvious consequence of Eq. (4.121). The figure further reveals that there are two extremes of behaviour; while for the initial states with $2\theta = 2\theta_c(\boldsymbol{r}_A)$, $2\theta_c(\boldsymbol{r}_A)+\pi$, the force shows no oscillations and is purely exponentially damped as a function of time [curves (a$_1$) and (a$_3$)], the initial states $2\theta = 2\theta_c(\boldsymbol{r}_A)+\pi/2$, $2\theta_c(\boldsymbol{r}_A)+3\pi/2$ lead to oscillations of maximal amplitude around a zero mean value [curves (a$_2$) and (a$_4$)]. For other values of θ, the temporal behaviour of the force is a combination of oscillating and non-oscillating components [curves (b$_1$)–(b$_4$)]. Note that in particular for $2\theta = 0$ which corresponds to the initial state $|1\rangle|\{0\}\rangle$, oscillating and non-oscillating parts combine in such a way that the sign of the force remains invariant for all times [curve (b$_1$)] – in agreement with Eq. (4.114).

As shown in App. F, the magnetic part of the resonant CP force for strong atom–field coupling can be given as

$$\boldsymbol{F}^{\mathrm{mag}}(\boldsymbol{r}_A, t) = \mathrm{e}^{-\gamma(\boldsymbol{r}_A)(t-t_0)}\, \frac{\sin\{2[\theta - \theta_c(\boldsymbol{r}_A)]\}}{\sin[2\theta_c(\boldsymbol{r}_A)]}\, \cos[\Omega(\boldsymbol{r}_A)(t-t_0)]$$

$$\times\, \mu_0\omega_\nu\gamma_\nu\boldsymbol{d}_{10}\times\left[\boldsymbol{\nabla}\times\boldsymbol{G}^{(1)}(\boldsymbol{r}, \boldsymbol{r}_A, \omega_\nu)\cdot\boldsymbol{d}_{01}\right]_{\boldsymbol{r}=\boldsymbol{r}_A}. \quad (4.124)$$

Comparing this with the electric part (4.121), we see that the magnetic part has a different vector structure. Its order of magnitude is roughly $\Omega(\boldsymbol{r}_A)/\omega_\nu$ times that of the electric

part of the force, indicating that it might become relevant in the context of the recently considered superstrong coupling regime [191] (where $\Omega(\boldsymbol{r}_A)/\omega_\nu$ might be comparable to, or even greater then unity).[6] In contrast to the electric part, $\boldsymbol{F}^{\mathrm{mag}}(\boldsymbol{r}_A, t)$ is always purely oscillating around a zero mean value. In particular, it vanishes for those initial states $|\theta = \theta_{\mathrm{c}}(\boldsymbol{r}_A)\rangle$ and $|\theta = \theta_{\mathrm{c}}(\boldsymbol{r}_A) + \pi/2\rangle$ for which the electric part of the force is non-oscillating.

4.3.3 Dressed states

The results of the previous section have shown that for certain initial states $|\theta = \theta_{\mathrm{c}}(\boldsymbol{r}_A)\rangle$ and $|\theta = \theta_{\mathrm{c}}(\boldsymbol{r}_A) + \pi/2\rangle$, the strong-coupling CP force is quasi-stationary with the only time dependence being exponential damping due to irreversible losses of the excitation from the strongly coupled system of atom and quasi-mode. By neglecting these losses, one may develop an intuitive static approach to the force which is valid on time scales that are short with respect to the typical inverse loss rate $\gamma^{-1}(\boldsymbol{r}_A)$. As demonstrated in the following, the states $|\theta = \theta_{\mathrm{c}}(\boldsymbol{r}_A)\rangle$ and $|\theta = \theta_{\mathrm{c}}(\boldsymbol{r}_A) + \pi/2\rangle$, commonly known as dressed states, turn out to be the approximate eigenstates of the system, and the CP force can be derived from the position-dependent part of the associated eigenenergies – in straightforward generalisation of the approach employed in chapter 3.

We start by returning to Eq. (4.71) which in conjunction with Eq. (4.73) states that an initially excited atom is coupled to a single quasi-mode ν plus a continuum of additional field excitations. As seen in the previous section, the coupling to the residual field continuum leads to irreversible spontaneous decay and a (small) shift of the atomic transition frequency. For sufficiently short times, we may neglect both effects by discarding the residual field continuum so that Eq. (4.71) can be written in the form

$$\hat{H}|1\rangle|\{0\}\rangle = E_1|1\rangle|\{0\}\rangle + \hbar\sqrt{\pi\gamma_\nu/2}\, g(\boldsymbol{r}_A, \omega_\nu)|0\rangle|1_\nu\rangle, \tag{4.125}$$

recall definition (4.74). Similarly, we neglect the coupling of the quasi-mode ν to the residual field continuum by combining Eqs. (4.71) and (4.74) and neglecting the width γ_ν,

$$\hat{H}|0\rangle|1_\nu\rangle = (E_0 + \hbar\omega_\nu)|0\rangle|1_\nu\rangle + \hbar\sqrt{\pi\gamma_\nu/2}\, g(\boldsymbol{r}_A, \omega_\nu)|1\rangle|\{0\}\rangle. \tag{4.126}$$

As seen in the previous section, γ_ν is associated with damping of the quasi-mode so that Eq. (4.126) may again be justified for sufficiently short times. We have thus constructed a reduced, two-dimensional Hilbert space (spanned by the states $|1\rangle|\{0\}\rangle$ and $|0\rangle|1_\nu\rangle$) which is invariant under $\hat{H}$ within the approximations made. On this subspace, $\hat{H}$ obviously takes

---

[6]Note, however, that the scenario considered in Ref. [191] involves quite a large number of atoms.

the Jaynes–Cummings form [123]

$$H_{\alpha\beta} = E_1 \mathbf{I}_2 + \frac{\hbar}{2} \begin{pmatrix} 0 & \Omega_{\mathrm{R}}(\mathbf{r}_A) \\ \Omega_{\mathrm{R}}(\mathbf{r}_A) & 2\Delta \end{pmatrix} \tag{4.127}$$

($\mathbf{I}_2$: two-dimensional unit matrix) where $\Delta = \omega_\nu - \omega_{10}$ is the (unshifted) resonator–atom detuning. Straightforward diagonalisation of $\hat{H}$ yields the two eigenenergies

$$E_\pm = \tfrac{1}{2}(E_0 + E_1 + \hbar\omega_\nu) \pm \tfrac{1}{2}\hbar\Omega(\mathbf{r}_A) \quad \text{with } \Omega(\mathbf{r}_A) = \sqrt{\Omega_{\mathrm{R}}^2(\mathbf{r}_A) + \Delta^2} \tag{4.128}$$

and the corresponding eigenstates (the dressed states)

$$|\pm\rangle = \begin{cases} |\theta = \theta_{\mathrm{c}}(\mathbf{r}_A)\rangle = \cos[\theta_{\mathrm{c}}(\mathbf{r}_A)]\,|1\rangle|\{0\}\rangle + \sin[\theta_{\mathrm{c}}(\mathbf{r}_A)]\,|0\rangle|1_\nu\rangle, \\ |\theta = \theta_{\mathrm{c}}(\mathbf{r}_A) + \pi/2\rangle = -\sin[\theta_{\mathrm{c}}(\mathbf{r}_A)]\,|1\rangle|\{0\}\rangle + \cos[\theta_{\mathrm{c}}(\mathbf{r}_A)]\,|0\rangle|1_\nu\rangle \end{cases} \tag{4.129}$$

where the (unshifted) coupling angle $\theta_{\mathrm{c}}(\mathbf{r}_A)$ is given by

$$\tan[2\theta_{\mathrm{c}}(\mathbf{r}_A)] = -\Omega_{\mathrm{R}}(\mathbf{r}_A)/\Delta, \quad \theta_{\mathrm{c}}(\mathbf{r}_A) \in (0, \pi/2) \tag{4.130}$$

and where the identities (4.119) have been used.

In generalisation of the perturbative approach employed in chapter 3, we now identify the CP potential with the position-dependent part of the atom–field coupling energy, recall Eqs. (3.5) and (3.6). From Eq. (4.128), we hence conclude that for the system being prepared in state $|+\rangle$ or $|-\rangle$, respectively, the CP potential is given by [SB16]

$$U_\pm(\mathbf{r}_A) = \pm\tfrac{1}{2}\hbar\Omega(\mathbf{r}_A) \tag{4.131}$$

and the associated CP force reads

$$\mathbf{F}_\pm(\mathbf{r}_A) = -\boldsymbol{\nabla}_A U_\pm(\mathbf{r}_A). \tag{4.132}$$

We have thus obtained the strong-coupling CP force in a very simple way by finding the eigenstates (dressed states) and eigenenergies of the two-dimensional Hamiltonian (4.127). Comparison with Eqs. (4.121) and (4.122) confirms that the dynamical CP force indeed reduces to the static result (4.132) when the system is initially prepared in one of the dressed states; and if one neglects losses $[\gamma(\mathbf{r}_A) \to 0]$ as well as the frequency shift associated with the residual field continuum $[\delta\omega_1'(\mathbf{r}_A) \to 0$ and hence $\Delta(\mathbf{r}_A) \to \Delta]$. Note that the dressed-state approach has first been applied to an atom placed within an idealised standing-wave resonator [119, 124].

By means of the dressed-state picture, an intuitive insight to the spatial dependence of the strong-coupling CP force can be given as follows: One first recalls that according to

Eq. (2.32) together with Eqs. (4.65), (4.73) and (4.75), the vacuum fluctuations associated with the quasi-mode ν are given by $\frac{1}{2}\hbar\mu_0\gamma_\nu\omega_\nu^2\text{Im}\big[\text{tr}\,\boldsymbol{G}(\boldsymbol{r},\boldsymbol{r},\omega_\nu)\big] \propto \Omega_\text{R}(\boldsymbol{r})$. One then sees that for a system in state $|+\rangle$, the atom is repelled from regions of high vacuum fluctuations (i.e., the antinodes of the quasi-mode) while for a system in state $|-\rangle$, the atom is attracted towards regions of high vacuum fluctuations.

Chapter 5

Summary and outlook

In this work, macroscopic quantum electrodynamics (QED) in linear media has been employed to develop a unified theory of the Casimir–Polder (CP) force experienced by a single atom when placed within an arbitrary environment of dispersing and absorbing magneto-electric bodies. The theory has been demonstrated to cover a broad variety of aspects, including inter alia the dependence of the force on the atomic and body properties; its modification due to local-field effects; its microscopic orgin; and its dynamical behaviour for both weak and strong atom–field coupling.

To provide for a sufficiently general framework, we have first extended an existing quantisation scheme for the electromagnetic field in the presence of linearly responding electric bodies to the magnetoelectric case, proceeding in the following steps: One starts from the macroscopic Maxwell equations in the presence of dispersing and absorbing magnetoelectric media, including the noise polarisation and magnetisation associated with the absorptive medium properties. These equations are solved by expressing the electromagnetic field in terms of the noise sources with the aid of the classical Green tensor. Explicit quantisation is then performed by relating the noise terms to the Bosonic dynamical variables of the system, whose dynamics in the absence of free charges or currents is determined by a harmonic-oscillator Hamiltonian. Finally, atom–field interactions are introduced in a canonical way according to the minimal or multipolar coupling schemes. As verified, the macroscopic QED hence obtained fulfills all necessary requirements of an exact quantum theory for the electromagnetic field; in particular, the field obeys the correct equal-time commutation relations and the Heisenberg equations of motion generate the Maxwell equations for the body-assisted field as well as the Newton equations for the charged particles constituting the atom. Note that while the response of the present bodies has been assumed to be linear, local and isotropic, the formalism can be extended to account for anisotropic, non-local and even non-linear medium properties. In addition, it is an almost trivial step to include the interaction of more than one atom with the body-assisted field.

Based on the presented macroscopic QED, a theory of CP forces has been developed in two major stages. In the first stage, we have chosen a static approach to the CP force by employing the well-known idea of identifying the CP potential of an atom in an energy eigenstate with the position-dependent atom–field coupling energy. Calculating this potential within leading-order perturbation theory, we have obtained general formulae which are

valid for atoms in energy eigestates that are placed within arbitrary environments of magnetoelectric bodies. For ground-state atoms, the CP potential is a purely off-resonant, integral effect that can be expressed in terms of the atomic polarisability and the scattering Green tensor associated with the bodies, both taken at imaginary frequencies. For excited atoms, resonant potential components occur which are associated with possible transitions to lower atomic levels and depend of the respective atomic transition frequencies and dipole matrix elements on the one hand and the real part of the scattering Green tensor on the other hand. Note that all information on the position, shape and magnetoelectric properties of the bodies is contained in the Green tensor. We have explicitly verified the formal equivalence of minimal and multipolar coupling schemes. Our general formulae are the natural generalisation of the (geometry-dependent) normal-mode results; in addition, our calculation may be regarded as the justification of similar findings obtained on the basis of linear-response theory. Note in this context that the fluctuation–dissipation theorem which is a central assumption of linear-response theory, is explicitly valid in our quantisation scheme. By using more general realisations of macroscopic QED, one could extend our results to the case of anisotropic or non-local response of the bodies where non-local properties are expected to play an important role when atoms are placed in the close vicinity of metal bodies. The influence of finite field temperature could be included by replacing ground-state by thermal averages at the beginning of the perturbative calculations. Such an extension may become imperative in the near future in view of the improved experimental sensitivity. Furthermore, finite temperature is known to lead to interesting effects in non-equilibrium situations of different bodies being held at different temperatures – a scenario that is well-accessible by means of our approach.

The perturbative results have been used to discuss a variety of issues that have never been addressed so far. By employing the real-cavity model to account for local-field effects, we have extended the range of applicability of our theory to atoms embedded in bodies. It has been found that the local-field effects manifest themselves via a frequency-dependent factor, which exclusively depends on the electric properties of the atom's local environment. In addition, we have made use of the Born expansion of the Green tensor to develop an approximation scheme for calculating CP potentials of atoms placed near weakly magnetodielectric bodies. Such potentials have been shown to be obtainable from volume integrals over central forces which are repulsive/attractive for dielectric/magnetic bodies. The microscopic origin of the CP potential has been illuminated by combining the Born expansion with the Clausius–Mosotti law, leading to a proof that under very general conditions the CP interaction of a single ground-state atom with a dielectric body is due to its van der

Waals (vdW) interactions with the body atoms. The body-assisted N-atom vdW potentials occuring in this relation are a generalisation of the well-known free-space potentials.

The use of the general formulae for the static CP potential has been illustrated by applying them to ground-state atoms interacting with a variety of planar systems, extending prominent results for purely electric systems to the magnetoelectric case. It has been found that an infinitely permeable plate gives rise to a CP potential that is exactly opposite to the well-known attractive potential associated with a perfectly conducting plate, where the different sign can be understood from the opposite reflexion behaviours of electric and magnetic dipoles. For more realistic medium properties, the situation becomes more involved. It turns out that the attractive potential components associated with the permittivity always dominate for asymptotically small atom–plate separations, while sufficiently large permeabilities can lead to the formation of a repulsive potential wall at some intermediate distance. For a planar cavity, a trapping potential well may thus be realised. Note that the possible repulsive CP forces associated with magnetic bodies which have been predicted for the first time within the context of the current work, have not yet been verified experimentally. A promising setup for their observation would be quantum reflexion of atoms from surfaces of Mumetal where a theoretical understanding of the scattering process requires the calculation of atomic reflexion amplitudes from the potentials presented here. Repulsive CP force components would open interesting possibilities of reducing or even eliminating the disturbing effect of CP forces in modern applications.

A comparison of dispersion forces between objects of different natures and shapes has revealed a lot of common features. In particular, forces between two polarisable objects are attractive while those between polarisable and magnetisable objects, are repulsive. Furthermore, for asymptotically small/large object separations, the distance dependence of the force is given by simple asymptotic power laws. As these observations are essentially due to the common microscopic origin of all dispersion forces, one might heuristically extend them beyond the specific examples considered; however, it would be more satisfying to prove their validity on basis of general properties of the Green tensor.

In the second major stage of developing a theory of the CP force, the dynamics of the force has been addressed for the first time. Abandoning the potential approach, the calculations were based on the operator Lorentz force appearing in the Heisenberg equations for the atomic centre-of-mass motion. It has been found that the Lorentz force in electric-dipole approximation can be expressed in a simple way in terms of the body-assisted electromagnetic field and the electric dipole moment of the atom, with minimal and multipolar coupling schemes leading to identical results. The CP force then follows by taking expectation values

with respect to the field (initially prepared in its ground state) and the internal atomic state. To obtain explicit expressions for the time-dependent CP force, the coupled atom–field dynamics must be solved where we have distinguished between the cases of weak and strong atom–field coupling.

For weak atom–field coupling, we have used the Markov approximation to show that the CP force can be written as a superposition of force components that are weighted by the respective internal atomic density-matrix elements. For an atom initially prepared in an energy eigenstate, only the diagonal density matrix elements come into play, whose dynamics is governed by spontaneous decay to the lower energy levels. The initial excited-state force thus decays to the ground-state one in an intuitive way. The spatial structure of the associated force components is a generalisation of the perturbative result, where now the relevant atomic transitions exhibit a body-assisted shifting and broadening. Due to the introduced additional position dependence, the CP force cannot be written as a potential force in the usual way. The off-diagonal density-matrix elements become relevant when the atom is initially prepared in a coherent superposition of energy eigenstates in which case, oscillating force components appear which display an entirely new vector structure. By considering the example of an atom placed in the vicinity of a dielectric half space that is initially prepared in an excited energy eigenstate, we have shown that the dominant resonant force components can be noticeably reduced by the combined effect of level shifting and broadening, while the off-resonant components are only weakly effected by the broadening. In particular, it was found that the level broadening combines with the material damping constant to a new total absorption coefficient. In future, it would be interesting to investigate in detail the spatial and temporal dependence of the weak-coupling force on excited atoms placed within more complex geometries.

The strong atom–field coupling that may arise if an initially excited atom is placed in a resonator-like environment, is due to the near-resonant interaction of a single atomic transition with a narrow quasi-mode of the electromagnetic field – a phenomenon that can best be studied by employing the model of a two-level atom predominantly interacting with this mode and working within the rotating-wave approximation. By separating the field spectrum into a strongly coupled Lorentzian mode and a weakly coupled residual continuum, we have obtained a detailed picture of the strongly coupled dynamics that arises when the atom–mode system initially carries a single excitation. It has been seen that the residual field continuum gives rise to shifts and broadenings of the atomic transition in close analogy to the weak-coupling case, while the resonant exchange of energy between the atom and the mode manifests in (damped) Rabi oscillations. Here, the amplitude and mean value of

the oscillating force delicately depends on the initial distribution of the excitation between the atom and the mode. For certain initial states the force does not oscillate, and it has been shown that these quasi-stationary states correspond to the well-known dressed states. The associated CP force at initial time reduces to the dressed-state result for the CP force, when the influence of the residual field spectrum is neglected; so the atom is attracted to, or repelled from the nodes of the resonator mode, depending on the chosen dressed state. A detailed analysis of the spatial structure of the strong-coupling force acting on atoms placed within specific resonators would be an important task for future investigations.

In conclusion, the developed unified theory of CP forces is at the very edge of both requirements and possibilities associated with current experimental techniques; hence it forms a solid basis for addressing a wide range of questions that arise in the context of modern applications such as atomic manipulation and control. In particular, the predictions of our macroscopic theory apply as long as atom–body separations remain sufficiently large with respect to the typical length scales associated with the microscopic structure of the bodies. In addition to the possible further investigations and extensions mentioned above, directions of future research could include studying the CP interaction of excited atoms with bodies exhibiting left-handed properties or adapting the theory to scenarios such as evanescent-wave mirrors, where an interplay of the CP force with interactions due to excited fields needs to be taken into account.

Bibliography

[1] F. London, Z. Phys. **63**, 245 (1930).

[2] H. B. G. Casimir and D. Polder, Phys. Rev. **73**, 360 (1948).

[3] J. E. Lennard-Jones, Trans. Faraday Society **28**, 333 (1932).

[4] H. B. G. Casimir, Proc. K. Ned. Akad. Wet. **51**, 793 (1948).

[5] E. M. Lifshitz, Sov. Phys. JETP **2**, 73 (1956).

[6] Y. Kim and H. Meyer, Int. Rev. Phys. Chem. **20**, 219 (2001).

[7] M. C. Heaven, Int. Rev. Phys. Chem. **24**, 375 (2005).

[8] J. N. Israelachvili, *Intermolecular and Surface Forces*, 2nd edn. (Academic Press, London, 1991).

[9] R. H. French, J. Am. Ceram. Soc. **83**, 2117 (2000).

[10] P. I. C. Teixeira, J. M. Tavares and M. M. Telo da Gama, J. Phys. Condens. Mat. **12**, R411 (2000).

[11] U. Tartaglino, T. Zykova-Timan, F. Ercolessi and E. Tosatti, Phys. Rep. **411**, 291 (2005).

[12] R. Schmid, Monatsh. Chem. **132**, 1295 (2001).

[13] Y. A. Freiman and H. J. Jodl, Phys. Rep. **401**, 1 (2004).

[14] L. W. Bruch, Surf. Sci. **125**, 194 (1983); G. P. Brivio and M. I. Trioni, Rev. Mod. Phys. **71**, 231 (1999).

[15] L. W. Bruch, M. W. Cole and E. Zaremba, *Physical Adsorption: Forces and Phenomena* (Clarendon Press, Oxford, 1997).

[16] D. Bonn, Curr. Opin. Colloid In. **6**, 22, (2001); D. Bonn and D. Ross, Rep. Prog. Phys. **64**, 1085 (2001).

[17] J. R. Henderson, Heterogen. Chem. Rev. **2**, 233 (1995).

[18] B. V. Derjaguin, Prog. Surf. Sci. **45**, 223 (1994).

[19] T. F. Tadros, Adv. Colloid Interfac. **46**, 1 (1993); J. Gregory, Water Sci. Technol. **27**, 1 (1993).

[20] D. F. Lawler, Water Sci. Technol. **27**, 165 (1993); D. N. Thomas, S. J. Judd and N. Fawcett, Water Res. **33**, 1579 (1999).

[21] T. Poppe, J. Blum and T. Henning, Adv. Space Res. **23**, 1197 (1999).

[22] M. V. Volkenstein, *Molecular Biophysics* (Academic Press, New York, 1977).

[23] J. N. Israelachvili, Q. Rev. Biophys. **6**, 341 (1974).

[24] P. C. W. Davies, Biosystems **78**, 69 (2004).

[25] S. Nir, Prog. Surf. Sci. **8**, 1 (1976).

[26] K. Autumn, M. Sitti, Y. A. Liang, A. M. Peattie, W. R. Hansen, S. Sponberg, T. W. Kenny, R. Fearing, J. N. Israelachvili and R. J. Full, P. Natl. Acad. Sci. USA **99**, 12252 (2002).

[27] A. B. Kesel, A. Martin and T. Seidl, Smart Mater. Struct. **13**, 512 (2004).

[28] W. G. Pollard, Phys. Rev. **60**, 578 (1941); E. Zaremba and W. Kohn, Phys. Rev. B **15**, 1769 (1977).

[29] D. Raskin and P. Kusch, Phys. Rev. **179**, 712 (1969); A. Shih, D. Raskin and P. Kusch, Phys. Rev. A **9**, 652 (1974); A. Shih, Phys. Rev. A **9**, 1507 (1974); A. Shih and V. A. Parsegian, Phys. Rev. A **12**, 835 (1975).

[30] A. Anderson, S. Haroche, E. A. Hinds, W. Jhe and D. Meschede, Phys. Rev. A **37**, 3594 (1988).

[31] E. A. Hinds, C. I. Sukenik, M. G. Boshier and D. Cho, in *Atomic Physics 12*, edited by J. C. Zorn and R. R. Lewis, p. 283 (American Institute of Physics, New York, 1991); C. I. Sukenik, M. G. Boshier, D. Cho, V. Sandoghdar and E. A. Hinds, Phys. Rev. Lett. **70**, 560 (1993).

[32] E. A. Hinds, K. S. Lai and M. Schnell, Phil. Trans Soc. London, Ser. A **355**, 2353 (1997).

[33] E. A. Hinds, Adv. Atom. Mol. Opt. Phy. **28**, 237 (1991).

[34] E. A. Hinds, Adv. Atom. Mol. Opt. Phy. Supp. **2**, 1 (1994).

[35] J. P. Dowling and J. Gea-Banacloche, Adv. Atom. Mol. Opt. Phy. **37**, 1 (1996); A. M. Guzmán, in *Frontiers in Optics 2004* (The Optical Society of America, Washington, 2004).

[36] M. Kasevich, K. Moler, E. Riis, E. Sundermann, D. Weiss and S. Chu, in *Atomic Physics 12*, edited by J. C. Zorn and R. R. Lewis, p. 47 (American Insitute of Physics, New York, 1991); A. Landragin, J.-Y. Courtois, G. Labeyrie, N. Vansteenkiste, C. I. Westbrook and A. Aspect, Phys. Rev. Lett. **77**, 1464 (1996); N. Westbrook, C. I. Westbrook, A. Landragin, G. Labeyrie, L. Cognet, V. Savalli, G. Horvath, A. Aspect, C. Hendel, K. Moelmer, J. Y. Courtois, W. Phillips, R. Kaiser and V. Bagnato, Phys. Scripta **T78**, 7 (1998); D. Voigt, B. T. Wolschrijn, R. A. Cornelussen, R. Janssen, N. Bhattacharya, H. B. V. van Linden van den Heuvell and R. J. C. Spreeuw, C. R. Acad. Sci. IV Phys. **2**, 619 (2001).

[37] A. K. Mohapatra and C. S. Unnikrishnan, Europhys. Lett. **73**, 839 (2006).

[38] P. Bushev, A. Wilson, J. Eschner, C. Raab, F. Schmidt-Kaler, C. Becher and R. Blatt, Phys. Rev. Lett. **92**, 223602 (2004).

[39] D. M. Harber, J. M. Obrecht, J. M. McGuirk and E. A. Cornell, Phys. Rev. A **72**, 033610 (2005).

[40] I. Carusotto, L. Pitaevskii, S. Stringari, G. Modugno and M. Inguscio, Phys. Rev. Lett. **95**, 093202 (2005).

[41] H. Friedrich, G. Jacobi and C. G. Meister, Phys. Rev. A **65**, 032902 (2002).

[42] D. O. Edwards, P. Fatouros, G. G. Ihas, P. Mrozinski and S. Y. Shen, Phys. Rev. Lett. **34**, 1153 (1975); A. Anderson, S. Haroche, E. A. Hinds, W. Jhe, D. Meschede and L. Moi, Phys. Rev. A **34**, 3513 (1986); J. J. Berkhout, O. J. Luiten, I. D. Setija, T. W. Hijmans and T. Mizusaki, Phys. Rev. Lett. **63**, 1689 (1989); J. J. Berkhout and J. T. M. Walraven, Phys. Rev. B **47**, 8886 (1993); I. A. Yu, J. M. Doyle, J. C. Sandberg, C. L. Cesar, D. Kleppner and T. J. Greytak, Phys. Rev. Lett. **71**, 1589 (1993).

[43] V. U. Nayak, D. O. Edwards and N. Masuhara, Phys. Rev. Lett. **50**, 990 (1983); V. Druzhinina and M. DeKieviet, Phys. Rev. Lett. **91**, 193202 (2003); T. A. Pasquini, Y. Shin, C. Sanner, M. Saba, A. Schirotzek, D. E. Pritchard and W. Ketterle, Phys. Rev. Lett. **93**, 223201 (2004), T. A. Pasquini, G. Jo, M. Saba, Y. Shin, S. Will, D. E. Pritchard and W. Ketterle, J. Phys. Conf. Ser. **19**, 139 (2005).

[44] F. Shimizu, Phys. Rev. Lett. **86**, 987 (2001); H. Oberst, Y. Tashiro, K. Shimizu and F. Shimizu, Phys. Rev. A **71**, 052901 (2005).

[45] R. E. Grisenti, W. Schöllkopf, J. P. Toennies, G. C. Hegerfeldt and T. Köhler, Phys. Rev. Lett. **83**, 1755 (1999); A. Cronin and J. D. Perreault, Phys. Rev. A **70**, 043607 (2004); J. D. Perreault, A. P. Cronin and T. A. Savas, Phys. Rev. A **71**, 053612 (2005).

[46] J. D. Perreault and A. D. Cronin, Phys. Rev. Lett. **95**, 133201 (2005).

[47] R. Brühl, P. Fouquet, R. E. Grisenti, J. P. Toennies, G. C. Hegerfeldt, T. Köhler, M. Stoll and C. Walter, Europhys. Lett. **59**, 357 (2002); W. Schöllkopf, R. E. Grisenti and J. P. Toennies, Eur. Phys. J. D **28**, 125 (2004); J.-C. Karam, N. Wipf, J. Grucker, F. Perales, M. Boustimi, G. Vassilev, V. Bocvarski, C. Mainos, J. Baudon and J. Robert, J. Phys. B: At. Mol. Opt. Phys. **38**, 2691 (2005).

[48] V. Sandoghdar, C. I. Sukenik, E. A. Hinds and S. Haroche, Phys. Rev. Lett. **68**, 3432 (1992); V. Sandoghdar, C. I. Sunenik, S. Haroche and E. A. Hinds, Phys. Rev. A **53**, 1919 (1996); M. Marrocco, M. Weidinger, R. T. Sang and H. Walther, Phys. Rev. Lett. **81**, 5784 (1998).

[49] H. Walther, B. T. H. Varcoe, B.-G. Englert and T. Becker, Rep. Prog. Phys. **69**, 1325 (2006).

[50] D. J. Heinzen and M. S. Feld, Phys. Rev. Lett. **59**, 2623 (1987); M. Brune, P. Nussenzveig, F. Schmidt-Kaler, F. Bernadot, A. Maali, J. M. Raimond and S. Haroche, Phys. Rev. Lett. **72**, 3339 (1994).

[51] V. V. Ivanov, R. A. Cornelussen, H. B. van Linden van den Heuvell and R. J. C. Spreeuw, J. Opt. B: Quantum Semiclass. Opt. **6**, 454 (2004); R. J. C. Spreeuw, V. V. Ivanov, R. A. Cornelussen and H. B. van Linden van den Heuvell, Opt. Spectrosc. (USSR) **99**, 477 (2005).

[52] M. A. Wilson, P. Bushev, J. Eschner, F. Schmidt-Kaler, C. Becher, R. Blatt and U. Dorner, Phys. Rev. Lett. **91**, 213602 (2003).

[53] M. Ducloy and M. Fichet, J. Phys. II **1**, 1429 (1991).

[54] M. Oria, M. Chevrollier, D. Bloch, M. Fichet and M. Ducloy, Europhys. Lett. **14**, 527 (1991); M. Chevrollier, D. Bloch, G. Rahmat and M. Ducloy, Opt. Lett. **16**, 1879 (1991); M. Chevrollier, M. Fichet, M. Oria, G. Rahmat, D. Bloch and M. Ducloy, J. Phys. II **2**, 631 (1992); J. Guo, J. Cooper and A. Gallagher, Phys. Rev. A **53**, 1130 (1996); P. Wang, A. Gallagher and J. Cooper, Phys. Rev. A **56**, 1598 (1997); M. Gorri-Neveux, P. Monnot, M. Fichet, M. Ducloy, R. Barbé and J. C. Keller, Opt. Commun. **134**, 85 (1997); I. Hamdi, M.-P. Gorza, P. Segundo, G. Dutier, P. Valente, J. R. R. Leite, M. Fichet, D. Bloch and M. Ducloy, J. Phys. IV **119**, 187 (2004).

[55] M. Chevrollier, M. Oria, J. G. de Souza, D. Bloch, M. Fichet and M. Ducloy, Phys. Rev. E **63**, 046610 (2001).

[56] H. Failache, S. Saltiel, M. Fichet, D. Bloch and M. Ducloy, Phys. Rev. Lett. **83**, 5467 (1999); H. Failache, S. Saltiel, M. Fichet, D. Bloch and M. Ducloy, Eur. Phys. J. D **23**, 237 (2003).

[57] P. Münstermann, T. Fischer, P. Maunz, P. W. H. Pinkse and G. Rempe, Phys. Rev. Lett. **82**, 3791 (1999); P. W. H. Pinkse, T. Fischer, P. Maunz, T. Puppe and G. Rempe, J. Mod. Opt. **47**, 2769 (2000); P. H. W. Pinkse, T. Fischer, P. Maunz and G. Rempe, Nature **404**, 365 (2000); C. J. Hood, T. W. Lynn, A. C. Doherty, A. S. Parkins and H. J. Kimble, Science **287**, 1447 (2000); C. J. Hood, T. W. Lynn,

A. C. Doherty, D. W. Vernooy, J. Ye and H. J. Kimble, Laser Phys. **11**, 1190 (2001); T. Fischer, P. Maunz, P. H. W. Pinkse, T. Puppe and G. Rempe, Phys. Rev. Lett. **88**, 163002 (2002).

[58] M. Chevrollier, E. G. Lima, O. Di Lorenzo, A. Lezama and M. Oria, Opt. Commun. **136**, 22 (1997); Y.-j. Lin, I. Teper, C. Chin and V. Vuletić, Phys. Rev. Lett. **92**, 050404 (2004).

[59] C. G. Aminoff, A. M. Steane, P. Bouyer, P. Desbiolles, J. Dalibard and C. Cohen-Tannoudji, Phys. Rev. Lett. **71**, 3083 (1993); P. Desbiolles, M. Arndt, P. Szriftgiser and J. Dalibard, Phys. Rev. A **54**, 4292 (1996); Y. B. Ovchinnikov, I. Manek and R. Grimm, Phys. Rev. Lett. **79**, 2225 (1997); M. Hammes, D. Rychtarik, V. Druzhin-ina, U. Moslener, I. Manek-Hönninger and R. Grimm, J. Mod. Opt. **47**, 2755 (2000); M. Hammes, D. Rychtarik and R. Grimm, C. R. Acad. Sci. IV Phys. **2**, 625 (2001); M. Hammes, D. Rychtarik, B. Engeser, H.-C. Nägerl and R. Grimm, Phys. Rev. Lett. **90**, 173001 (2003); Y. Colombe, D. Kadio, M. Olshanii, B. Mercier, V. Lorent and H. Perrin, J. Opt. B: Quantum Semiclass. Opt. **5**, S155 (2003).

[60] R. Folman, P. Krüger, J. Schmiedmayer, J. Denschlag and C. Henkel, Adv. Atom. Mol. Opt. Phy. **48**, 263 (2002).

[61] J. Denschlag, D. Cassettari, A. Chenet, S. Schneider and J. Schmiedmayer, Appl. Phys. B **69**, 291 (1999).

[62] M. J. Renn, E. A. Donley, E. A. Cornell, C. E. Wieman and D. Z. Anderson, Phys. Rev. A **53**, R648 (1996); H. Ito, K. Sakaki, W. Jhe and M. Ohtsu, Opt. Commun. **141**, 43 (1997); H. Ito, K. Sakawi, W. Jhe and M. Ohtsu, Phys. Rev. A **56**, 712 (1997); A. Takamizawa, H. Ito and M. Ohtsu, Jpn. J. Appl. Phys. 1 **41**, 6215 (2002); F. L. Kien, V. I. Balykin and K. Hakuta, Phys. Rev. A **70**, 063403 (2004).

[63] H. Ito, K. Sakaki, M. Ohstu and W. Jhe, Appl. Phys. Lett. **70**, 2496 (1997).

[64] C. S. Adams, M. Sigel and J. Mlynek, Phys. Rep. **240**, 143 (1994).

[65] H. Oberst, M. Morinaga, F. Shimizu and K. Shimizu, Appl. Phys. B **76**, 801 (2003).

[66] J. Fujita and F. Shimizu, Mat. Sci. Eng. B Solid **96**, 159 (2002); F. Shimizu and J.-i. Fujita, J. Phys. Soc. Jpn. **71**, 5 (2002); H. Oberst, D. Kouznetsov, K. Shimizu, J.-i. Fujita and F. Shimizu, Phys. Rev. Lett. **94**, 013203 (2005).

[67] T. Kohno, F. Shimizu, J.-i. Fujita and K. Shimizu, J. Phys. Soc. Jpn. **72**, 461 (2003).

[68] F. Shimizu and J.-i. Fujita, Phys. Rev. Lett. **88**, 123201 (2002).

[69] V. I. Balykin, V. S. Letokhov, Y. B. Ovchinnikov and A. I. Sidorov, Phys. Rev. Lett. **60**, 2137 (1988); W. Seifert, R. Kaiser, A. Aspect and J. Mlynek, Opt. Commun. **111**, 566 (1994); Y. B. Ovchinnikov, D. V. Laryushin, V. Balykin and V. S. Letokhov, Laser Phys. **6**, 264 (1996); H. Oberst, S. Kasashima, V. I. Balykin and F. Shimizu, Phys. Rev. A **68**, 013606 (2003).

[70] R. G. Scott, A. M. Martin, T. M. Fromhold and F. W. Sheard, Phys. Rev. Lett. **95**, 073201 (2005).

[71] M. Naraschewski, H. Wallis, A. Schenzle, J. I. Cirac and P. Zoller, Phys. Rev. A **54**, 2185 (1996); M. Naraschewski, A. Röhrl, H. Wallis and A. Schenzle, Mat. Sci. Eng. B Solid **48**, 1 (1997); A. Röhrl, M. Naraschewski, A. Schenzle and H. Wallis, Phys. Rev. Lett. **78**, 4143 (1997); H. Wallis, A. Röhrl, M. Naraschewski and A. Schenzle, Phys. Rev. A **55**, 2109 (1997).

[72] J. B. Pendry, A. J. Holden, D. J. Robbins and W. J. Stewart, IEEE Trans. Microwave Theory Tech. **47**, 2075 (1999).

[73] D. R. Smith, W. J. Padilla, D. C. Vier, S. C. Nemat-Nasser and S. Schultz, Phys. Rev. Lett. **84**, 4184 (2000); S. Linden, C. Enrich, M. Wegener, J. Zhou, T. Koschny and C. M. Soukoulis, Science **306**, 1351 (2004); C. Enrich, M. Wegener, S. Linden, S. Burger, L. Zschiedrich, F. Schmidt, J. F. Zhou, T. Koschny and C. M. Soukoulis, Phys. Rev. Lett. **95**, 203901 (2005); G. Dolling, C. Enrich, M. Wegener, J. F. Zhou, C. M. Soukoulis and S. Linden, Opt. Lett. **30**, 3198 (2005); A. N. Grigorenko, A. K. Geim, H. F. Gleeson, Y. Zhang, A. A. Firsov, I. Y. Khrushchev and J. Petrovic, Nature **438**, 335 (2005); S. Zhang, W. Fan, N. C. Panoiu, K. J. Malloy, R. M. Osgood and S. R. J. Brueck, Phys. Rev. Lett. **95**, 137404 (2005).

[74] J. Kästel, M. Fleischhauer, S. F. Yelin and R. L. Walsworth, *Tunable negative refraction without absorption in the optical regime*, submitted to Nature (2006).

[75] V. G. Veselago, Sov. Phys. Uspekhi **10**, 509 (1968); J. B. Pendry, Phys. Rev. Lett. **85**, 3966 (2000); J. Kästel and M. Fleischhauer, Phys. Rev. A **71**, 011804(R) (2005); J. Kästel and M. Fleischhauer, Laser Phys. **15**, 135 (2005).

[76] R. M. Bozorth, *Ferromagnetism* (D. Van Nostrand Company, Inc., New York, 1951); R. C. O'Handley, *Modern Magnetic Materials* (Wiley, New York, 2000).

[77] D. J. Snee, J. Appl. Phys. **38**, 1172 (1967).

[78] W. G. Pollard and H. Margenau, Phys. Rev. **57**, 557 (1940); E. J. R. Prosen, R. G. Sachs and E. Teller, Phys. Rev. **57**, 1066 (1940); H. Margenau and W. G. Pollard, Phys. Rev. **60**, 128 (1941); E. J. R. Prosen and R. G. Sachs, Phys. Rev. **61**, 65 (1942).

[79] J. Bardeen, Phys. Rev. **57**, 1066 (1940); J. Bardeen, Phys. Rev. **58**, 727 (1940).

[80] X.-P. Jiang, F. Toigo and M. W. Cole, Chem. Phys. Lett. **101**, 159 (1983).

[81] C. Holmberg and P. Apell, Phys. Rev. B **30**, 5721 (1984).

[82] P. Apell and C. Holmberg, Solid State Commun. **49**, 1059 (1984); K. Ganesan and K. T. Taylor, J. Phys. B: At. Mol. Opt. Phys. **29**, 1293 (1996).

[83] C. Mavroyannis and D. A. Hutchinson, Solid State Commun. **23**, 463 (1977).

[84] J.-Y. Courtois, J.-M. Courty and J. C. Mertz, Phys. Rev. A **53**, 1862 (1996).

[85] F. Schuller, G. Nienhuis and M. Ducloy, Mol. Phys. **104**, 229 (2006); note that the result is very similar to the dispersion potential of a small metal sphere placed near a dielectric half space, cf. C. E. Romàn-Velàzquez, C. Noguez, C. Víllarreal and R. Esquivel-Sirvent, Phys. Rev. A **69**, 042109 (2004).

[86] F. Schuller, Z. Naturforsch. A **49a**, 885 (1994).

[87] E. Zaremba and W. Kohn, Phys. Rev. B **13**, 2270 (1976).

[88] C. Girard, J. Chem. Phys. **85**, 6750 (1986).

[89] P. Nordlander and J. Harris, J. Phys. C: Solid State **17**, 1141 (1984); J. F. Annett and P. M. Echenique, Phys. Rev. B **34**, 6853 (1986); S. Das Sarma and S.-M. Paik, Chem. Phys. Lett. **126**, 526 (1986).

[90] C. Holmberg, P. Apell and J. Giraldo, Phys. Scripta **33**, 173 (1986).

[91] D. Chan and P. Richmond, J. Phys. C: Solid State **9**, 163 (1976).

[92] G. Mukhopadhyay and J. Mahanty, Solid State Commun. **16**, 597 (1975); J. Mahanty and B. V. Paranjape, Solid State Commun. **24**, 651 (1977); G. Barton, Rep. Prog. Phys. **42**, 963 (1979); P. R. Rao and G. Mukhopadhyay, Solid State Commun. **52**, 697 (1984).

[93] Y. C. Cheng and K. C. Lin, Chinese J. Phys. **26**, 212 (1988).

[94] G. Mukhopadhyay, Phys. Scripta **36**, 676 (1987); Y.-C. Cheng and H.-T. Huang, Chinese J. Phys. **31**, 137 (1993).

[95] J. Harris and P. J. Feibelman, Surf. Sci. **115**, L133 (1982).

[96] A. Bambini and E. J. Robinson, Phys. Rev. A **45**, 4661 (1992).

[97] M. Fichet, F. Schuller, D. Bloch and M. Ducloy, Phys. Rev. A **51**, 1553 (1995).

[98] N. J. M. Horing and S. Silverman, Nuovo Cim. B **38**, 396 (1977); N. J. M. Horing and L. Y. Chen, Phys. Rev. A **66**, 042905 (2002).

[99] M. S. Tomassone and A. Widom, Phys. Rev. B **56**, 4938 (1997).

[100] T. L. Ferrell and R. H. Ritchie, Phys. Rev. A **21**, 1305 (1980).

[101] B. Labani, C. Girard, and S. Maghezzi, Mol. Phys. **69**, 85 (1990); C. Girard, S. Marghezzi, and F. Hache, J. Chem. Phys. **91**, 5509 (1989).

[102] Y.-C. Cheng and J. S. Yang, Phys. Rev. B **41**, 1196 (1990).

[103] M. Boustimi, J. Baudon, P. Candori and J. Robert, Phys. Rev. B **65**, 155402 (2002); M. Boustimi, J. Baudon and J. Robert, Phys. Rev. B **67**, 045407 (2003).

[104] P. V. Panat and V. V. Paranjape, Solid State Commun. **110**, 443 (1999).

[105] B. Labani, M. Boustimi and J. Baudon, Phys. Rev. B **55**, 4745 (1997); M. Boustimi, J. Baudon, J. Robert, A. Semali and B. Labani, Phys. Rev. B **62**, 7593 (2000).

[106] E. A. Power, *Introductory Quantum Electrodynamics* (Longmans, London, 1964); M. J. Renne, Physica **53**, 193 (1971); T. H. Boyer, Phys. Rev. A **5**, 1799 (1972); T. H. Boyer, Phys. Rev. A **6**, 314 (1972); T. H. Boyer, Phys. Rev. A **7**, 1832 (1973); P. W. Milonni, Phys. Rev. A **25**, 1315 (1982); P. W. Milonni and M.-L. Shih, Phys. Rev. A **45**, 4241 (1992).

[107] P. W. Milonni, *The Quantum Vacuum* (Academic Press, New York, 1994).

[108] C. A. Lütken and F. Ravndal, Phys. Rev. A **31**, 2082 (1985).

[109] T. H. Boyer, Phys. Rev. **180**, 19 (1969).

[110] M. Babiker and G. Barton, Proc. R. Soc. London, Ser. A **326**, 255 (1972); T. Datta and L. H. Ford, Phys. Lett. A **83**, 314 (1981).

[111] I.-T. Cheon, Phys. Rev. A **37**, 2785 (1988).

[112] R. Blanco, K. Dechoum, H. M. França and E. Santos, Phys. Rev. A **57**, 724 (1998).

[113] C.-H. Wu, C.-I. Kuo and L. H. Ford, Phys. Rev. A **65**, 062102 (2002).

[114] T. H. Boyer, Phys. Rev. A **11**, 1650 (1975).

[115] T. Nakajima, P. Lambropoulos and H. Walther, Phys. Rev. A **56**, 5100 (1997).

[116] G. Barton, J. Phys. B: At. Mol. Opt. Phys. **7**, 2134 (1974).

[117] E. A. Power and Thirunamachandran, Phys. Rev. A **25**, 2473 (1982); A. O. Barut and J. P. Dowling, Phys. Rev. A **36**, 2550 (1987).

[118] D. Meschede, W. Jhe and E. A. Hinds, Phys. Rev. A **41**, 1587 (1990).

[119] S. Haroche, in *Fundamental Systems in Quantum Optics, Les Houches Summer School Session LIII*, edited by J. Dalibard, J. M. Raimond and J. Zinn-Justin, p. 767 (North-Holland, Amsterdam, 1992).

[120] L. H. Ford and N. F. Svaiter, Phys. Rev. A **62**, 062105 (2000); L. H. Ford and N. F. Svaiter, Phys. Rev. A **66**, 062106 (2002).

[121] L. H. Ford, Proc. R. Soc. London, Ser. A **362**, 559 (1978);

[122] G. Barton, Proc. R. Soc. London, Ser. A **320**, 251 (1970); G. Barton, Proc. R. Soc. London, Ser. A **367**, 117 (1979); G. Barton, Proc. R. Soc. London, Ser. A **410**, 141 (1987); G. Barton, Phys. Scripta **T21**, 11 (1988); W. Jhe, Phys. Rev. A **43**, 5795 (1991); W. Jhe, Phys. Rev. A **44**, 5932 (1991).

[123] E. T. Jaynes and F. W. Cummings, Proc. IEEE **51**, 89 (1963).

[124] S. Haroche, M. Brune and J. M. Raimond, Europhys. Lett. **14**, 19 (1991); B.-G. Englert, J. Schwinger, A. O. Barut and M. O. Scully, Europhys. Lett. **14**, 25 (1991).

[125] M. Babiker and G. Barton, J. Phys. A: Math. Gen. **9**, 129 (1976).

[126] C. Mavroyannis, Mol. Phys. **6**, 593 (1963); L. Spruch and Y. Tikochinsky, Phys. Rev. A **48**, 4213 (1993); Y. Tikochinsky and L. Spruch, Phys. Rev. A **48**, 4223 (1993).

[127] Y. Tikochinsky and L. Spruch, Phys. Rev. A **48**, 4236 (1993).

[128] F. Zhou and L. Spruch, Phys. Rev. A **52**, 297 (1995).

[129] M. Boström and B. E. Sernelius, Phys. Rev. A **61**, 052703 (2000).

[130] S.-T. Wu and C. Eberlein, Proc. R. Soc. London, Ser. A **455**, 2487 (1999); S.-T. Wu and C. Eberlein, Proc. R. Soc. London, Ser. A **456**, 1931 (2000); H. F. Arnoldus, Surf. Sci. **444**, 221 (2000); C. Eberlein and S.-T. Wu, Phys. Rev. A **68**, 033813 (2003).

[131] P. Horak, P. Domokos and H. Ritsch, Europhys. Lett. **61**, 459 (2003).

[132] J.-M. Daul and P. Grangier, Eur. Phys. J. D **32**, 195 (2005).

[133] A. D. McLachlan, Proc. R. Soc. London, Ser. A **271**, 387 (1963).

[134] A. D. McLachlan, Mol. Phys. **7**, 381 (1964).

[135] G. S. Agarwal, Phys. Rev. A **11**, 243 (1975).

[136] J. Schwinger, L. L. DeRaad Jr. and K. A. Milton, Ann. Phys. **115**, 1 (1978).

[137] M. J. Mehl and W. L. Schaich, Surf. Sci. **99**, 553 (1980).

[138] J. M. Wylie and J. E. Sipe, Phys. Rev. A **30**, 1185 (1984).

[139] J. Mahanty and B. W. Ninham, *Dispersion Forces* (Academic Press, London, 1976).

[140] A. M. Marvin and F. Toigo, Phys. Rev. A **25**, 782 (1982).

[141] S. Kryszewski, Mol. Phys. **78**, 1225 (1993).

[142] J. Mahanty, P. Summerside and B. V. Paranjape, Phys. Rev. B **18**, 5174 (1978); P. Apell, Phys. Scripta **24**, 795 (1981).

[143] C. Schwartz, J. Chem. Phys. **83**, 437 (1985).

[144] W. Jhe and J. W. Kim, Phys. Lett. A **197**, 192 (1995).

[145] W. Jhe and J. W. Kim, Phys. Rev. A **51**, 1150 (1995).

[146] I. Brevik, M. Lygren and V. N. Marachevsky, Ann. Phys. **267**, 134 (1998); V. N. Marachevsky, Theor. Math. Phys. **131**, 468 (2002).

[147] A. M. Marvin and F. Toigo, Phys. Rev. A **25**, 803 (1982); D. P. Fussell, R. C. McPhedran and C. M. de Sterke, Phys. Rev. A **71**, 013815 (2005).

[148] H. Nha and W. Jhe, Phys. Rev. A **56**, 2213 (1997).

[149] H. Nha and W. Jhe, Phys. Rev. A **54**, 3505 (1996).

[150] W. Jhe and K. Jang, Phys. Rev. A **53**, 1126 (1996).

[151] G. S. Agarwal, Phys. Rev. Lett. **32**, 703 (1974).

[152] J. M. Wylie and J. E. Sipe, Phys. Rev. A **32**, 2030 (1985).

[153] M.-P. Gorza, S. Saltiel, H. Failache and M. Ducloy, Eur. Phys. J. D **15**, 113 (2001).

[154] C. Henkel and V. Sandoghdar, Opt. Commun. **158**, 250 (1998).

[155] A. D. McLachlan, Proc. R. Soc. London, Ser. A **274**, 80 (1963); M. Antezza, L. P. Pitaevskii and S. Stringari, Phys. Rev. Lett. **95**, 113202 (2005).

[156] G. V. Dedkov and A. A. Kyasov, Phys. Solid State **44**, 1809 (2002).

[157] C. Henkel, K. Joulain, J.-P. Mulet and J.-J. Greffet, J. Opt. A: Pure Appl. Opt. **4**, S109 (2002).

[158] H. Imura and K. Okano, J. Chem. Phys. **58**, 2763 (1973).

[159] M. J. Renne and B. R. A. Nijboer, Chem. Phys. Lett. **1**, 317 (1967); M. J. Renne and B. R. A. Nijboer, Chem. Phys. Lett. **2**, 35 (1968); M. J. Renne, Physica **56**, 125 (1971).

[160] J. Mahanty and B. W. Ninham, J. Chem. Phys. **59**, 6157 (1973).

[161] P. W. Milonni and P. B. Lerner, Phys. Rev. A **46**, 1185 (1992).

[162] G. Barton, Proc. R. Soc. London, Ser. A **453**, 2461 (1997); C. Eberlein and M. Janowicz, Phys. Rev. A **67**, 063816 (2003).

[163] Y. Sherkunov, Phys. Rev. A **72**, 052703 (2005); Y. Sherkunov, *Casimir interaction between excited media in electromagnetic field*, eprint `quant-ph/0604046` (2006); Y. Sherkunov, Phys. Rev. A **75** 012705 (2007).

[164] I. E. Dzyaloshinskii, E. M. Lifshitz and L. P. Pitaevskii, Avd. Phys. **10**, 165 (1961).

[165] M. Antezza, L. P. Pitaevskii and S. Stringari, Phys. Rev. A **70**, 053619 (2004).

[166] V. B. Bezerra, G. L. Klimchitskaya and C. Romero, Phys. Rev. A **61**, 022115 (2000).

[167] E. V. Blagov, G. L. Klimchitskaya and V. M. Mostepanenko, Phys. Rev. B **71**, 235401 (2005).

[168] M. S. Tomaš, Phys. Rev. A **72**, 034104 (2005).

[169] V. M. Nabutovskiǐ, V. R. Belosludov and A. M. Korotkikh, Sov. Phys. JETP **50**, 352 (1979).

[170] L. Knöll, S. Scheel and D.-G. Welsch, in *Coherence and Statistics of Photons and Atoms*, edited by J. Peřina, p. 1 (Wiley, New York, 2001).

[171] J. D. Jackson, *Classical Electrodynamics*, 3rd edn. (Wiley, New York, 1998).

[172] A. A. Abrikosov, L. P. Gor'kov and I. E. Dzjalosinskij, *Methods of Quantum Field Theory in Statistical Physics*, revised edn. (Dover, New York, 1975).

[173] R. Matloob, R. Loudon, S. M. Barnett and J. Jeffers, Phys. Rev. A **52**, 4823 (1995); A. Tip, Phys. Rev. A **57**, 4818 (1998); R. Matloob, Phys. Rev. A **69**, 052110 (2004); R. Matloob, Phys. Rev. A **70**, 022108 (2004).

[174] B. Huttner and S. M. Barnett, Phys. Rev. A **46**, 4306 (1992); M. Wubs and L. G. Suttorp, Phys. Rev. A **63**, 043809 (2001); L. G. Suttorp and M. Wubs, Phys. Rev. A **70**, 013816 (2004); L. G. Suttorp and A. J. van Wonderen, Europhys. Lett. **67**, 766 (2004).

[175] C. Baxter, M. Babiker and R. Loudon, Phys. Rev. A **47**, 1278 (1993).

[176] D. P. Craig and T. Thirunamachandran, *Molecular Quantum Electrodynamics* (Dover, New York, 1998).

[177] E. A. Power and S. Zienau, Phil. Trans. R. Soc. London Ser. A **251**, 427 (1959); R. G. Woolley, Proc. R. Soc. London, Ser. A **321**, 557 (1971); C. Cohen-Tannoudji, J. Dupont-Roc and G. Grynberg, *Photons and Atoms* (Wiley, New York, 1989).

[178] W. P. Healy, J. Phys. A: Math. Gen. **10**, 279 (1977); J.-C. Guillot and J. Robert, J. Phys. A: Math. Gen. **35**, 5023 (2002).

[179] V. E. Lembessis, M. Babiker, C. Baxter and R. Loudon, Phys. Rev. A **48**, 1594 (1993).

[180] V. M. Fain and Y. I. Khanin, *Quantum Electronics* (Cambridge, MA, MIT Press, 1969).

[181] I. V. Bondarev and P. Lambin, Opt. Spectrosc. (USSR) **99**, 475 (2005); I. V. Bondarev and P. Lambin, Phys. Rev. B **72**, 035451 (2005); I. V. Bondarev and P. Lambin, in *Trends in Nanotubes Research*, edited by D. A. Martin, p. 139 (Nova Science Publishers, New York, 2006).

[182] L. Onsager, J. Am. Chem. Soc. **58**, 1486 (1936).

[183] W. C. Chew, *Waves and Fields in Inhomogeneous Media* (IEEE, New York, 1995).

[184] E. A. Power and T. Thirunamachandran, Proc. R. Soc. London, Ser. A **401**, 267 (1985); E. A. Power and T. Thirunamachandran, Phys. Rev. A **50**, 3929 (1994).

[185] V. A. Parsegian, Mol. Phys. **27**, 1503 (1974).

[186] G. Feinberg and J. Sucher, Phys. Rev. A **2**, 2395 (1970).

[187] K. P. Thakur and W. S. Holmes, IEEE Trans. Microwave Theory Tech. **52**, 76 (2004).

[188] M. S. Tomaš, Phys. Lett. A **342**, 381 (2005); C. Henkel and K. Joulain, Europhys. Lett. **72**, 929 (2005).

[189] W. Vogel and D.-G. Welsch, *Quantum Optics*, 3rd edn. (Wiley-VCH, Berlin, 2006).

[190] I. N. Bronstein, K. A. Semendjajew, G. Musiol and H. Mühlig, *Taschenbuch der Mathematik* (Harri Deutsch, Frankfurt am Main, 1995).

[191] D. Meiser and P. Meystre, Phys. Rev. A **74**, 065801 (2006).

[192] L.-W. Li, P.-S. Kooi, M.-S. Leong and T.-S. Yeo, IEEE Trans. Microwave Theory Tech. **42**, 2302 (1994).

[193] M. R. Aub and S. Zienau, Proc. R. Soc. London, Ser. A **257**, 464 (1960).

[194] B. M. Axilrod and E. Teller, J. Chem. Phys. **11**, 299 (1943).

List of publications

Review article

[SB1]   *Dispersion forces in macroscopic quantum electrodynamics*, S. Y. Buhmann and D.-G. Welsch, Prog. Quantum Electron. **31**, 51 (2007).

Regular articles and preprints

[SB2]   *Enhancement of the electron electric dipole moment in Gd^{3+}*, S. Y. Buhmann, V. A. Dzuba and O. P. Sushkov, Phys. Rev. A **66**, 042109 (2002).

[SB3]   *Electromagnetic-field quantization and spontaneous decay in left-handed media*, D. T. Ho, S. Y. Buhmann, L. Knöll, D.-G. Welsch, S. Scheel and J. Kästel, Phys. Rev. A **68**, 043816 (2003).

[SB4]   *Spontaneous decay in left-handed material*, S. Y. Buhmann, D. T. Ho, L. Knöll, S. Scheel and D.-G. Welsch, in *Proceedings of the 8th International Conference on Squeezed States and Uncertainty Relations*, edited by H. Moya-Cessa, R. Jáuregui, S. Hacyan and O. Castaños, p. 110 (Rinton Press, Princeton, New Jersey, 2003).

[SB5]   *The van der Waals energy of atomic systems near absorbing and dispersing bodies*, S. Y. Buhmann, D. T. Ho and D.-G. Welsch, J. Opt. B: Quantum Semiclass. Opt. **6**, S127 (2004); note erratum: J. Phys. B: Atomic and Molecular Physics **39**, 3145 (2006).

[SB6]   *Casimir–Polder forces: A nonperturbative approach*, S. Y. Buhmann, L. Knöll, D.-G. Welsch and D. T. Ho, Phys. Rev. A **70**, 052117 (2004).

[SB7]   *Atoms near magnetodielectric bodies: van der Waals energy and the Casimir–Polder force*, S. Y. Buhmann, D. T. Ho, T. Kampf, L. Knöll and D.-G. Welsch, Opt. Spectrosc. (USSR) **99**, 466 (2005).

[SB8]   *Casimir–Polder interaction of atoms with magnetodielectric bodies*, S. Y. Buhmann, D. T. Ho, T. Kampf and D.-G. Welsch, Eur. Phys. J. D **35**, 15 (2005).

[SB9]   *Ground-state van der Waals forces in planar multilayer magnetodielectrics*, S. Y. Buhmann, T. Kampf and D.-G. Welsch, Phys. Rev. A **72**, 032112 (2005).

[SB10] *Born expansion of the Casimir–Polder interaction of a ground-state atom with dielectric bodies*, S. Y. Buhmann and D.-G. Welsch, Appl. Phys. B **82**, 189 (2006).

[SB11] *Local-field correction to the spontaneous decay rate of atoms embedded in bodies of finite size*, D. T. Ho, S. Y. Buhmann and D.-G. Welsch, Phys. Rev. A **74**, 023803 (2006).

[SB12] *Body-assisted van der Waals interaction between two atoms*, H. Safari, S. Y. Buhmann, D.-G. Welsch and D. T. Ho, Phys. Rev. A **74**, 042101 (2006).

[SB13] *Microscopic origin of Casimir–Polder forces*, S. Y. Buhmann, H. Safari, D.-G. Welsch and D. T. Ho, Open Sys. Inf. Dyn. **13**, 427 (2006).

[SB14] *Two-atom van der Waals interaction between polarizable/magnetizable atoms near magnetodielectric bodies*, S. Y. Buhmann, H. Safari, D. T. Ho and D.-G. Welsch, submitted to Opt. Spectrosc. (USSR); eprint `quant-ph/0606232` (2006).

[SB15] *Local-field correction to one- and two-atom van der Waals interactions*, A. Sambale, S. Y. Buhmann, D.-G. Welsch and M. S. Tomaš, Phys. Rev. A **75**, 042109 (2007).

[SB16] *Casimir–Polder forces for strong atom–field coupling*, S. Y. Buhmann and D.-G. Welsch, eprint `quant-ph/0701151` (2007).

List of presentations

(1) *Casimir–Polder-Kräfte auf Atome bei Anwesenheit absorptiver Körper*, short talk (67$^\text{th}$ Annual Meeting of the German Physical Society, Hannover, 2003).

(2) *Dynamical theory of Casimir–Polder forces on excited atoms*, talk (10$^\text{th}$ Young Atom Opticians Conference, Innsbruck, 2004).

(3) *Dynamical theory of Casimir–Polder forces on excited atoms*, group report (68$^\text{th}$ Annual Meeting of the German Physical Society, München, 2004).

(4) *Casimir–Polder forces – a dynamical approach*, invited talk (X$^\text{th}$ International Conference on Quantum Optics, Minsk, 2004).

(5) *Casimir–Polder forces – a dynamical approach*, seminar talk (Joint Institute for Nuclear Research, Dubna, 2004).

(6) *Where light travels backwards – electromagnetic field quantization and spontaneous decay in left-handed media*, seminar talk (Friedrich-Schiller-University Jena, 2004).

(7) *QED in linear, causal media: A novel approach to the Casimir–Polder force*, poster (333$^\text{rd}$ WEH seminar New Frontiers in Quantum Theory and Measurement, Reisensburg, 2004).

(8) *Dynamical theory of van der Waals forces*, invited talk (Quantum Optics II, Cozumel, 2004).

(9) *The Casimir–Polder force: A manifestation of the QED vacuum*, seminar talk (Imperial College London, 2005).

(10) *Van der Waals potential and Casimir–Polder force*, poster (11$^\text{th}$ Young Atom Opticians Conference, Hannover, 2005).

(11) *Casimir–Polder forces in multilayer magnetodielectrics*, group report (69$^\text{th}$ Annual Meeting of the German Physical Society, Berlin, 2005).

(12) *Casimir–Polder interaction between atoms and magnetodielectric bodies*, talk (QED, Quantum Vacuum and the Search for New Forces, Les Houches, 2005).

(13) *Van der Waals potential and Casimir–Polder force*, poster (QED, Quantum Vacuum and the Search for New Forces, Les Houches, 2005).

(14) *On the search for nothing: Vacuum birefringence and Casimir–Polder forces*, seminar talk (Friedrich-Schiller-University Jena, 2005).

(15) *Born expansion of the Casimir–Polder potential*, talk (New Trends in Quantum Mechanics: Fundamental Aspects and Applications, Palermo, 2005).

(16) *Microscopic origin of Casimir–Polder forces*, group report (Spring meeting of the German Physical Society, Section Atoms, Molecules, Quantum Optics, and Plasmas, Frankfurt, 2006).

(17) *One-, two-, and many-atom Casimir–Polder forces*, seminar talk (University of Heidelberg, 2006).

(18) *Microscopic origin of Casimir–Polder forces*, invited talk (XI$^\text{th}$ International Conference on Quantum Optics, Minsk, 2006).

(19) *Casimir–Polder forces on atoms in the presence of magnetodielectric bodies*, seminar talk (University of Duisburg–Essen, 2006).

(20) *Casimir–Polder forces in macroscopic quantum electrodynamics*, seminar talk (Friedrich-Schiller-University Jena, 2007).

Appendix A

Commutators and equations of motion

In this appendix, the commutators and equations of motion stated in chapter 2 are derived. After calculating the relevant field commutators, the results are used to obtain the equations of motion for both the body-assisted field and the charged particles interacting with this field.

A.1   Calculation of some field commutators

All field commutators given in Sec. 2.1 can be derived from the commutators of $\hat{\boldsymbol{E}}$ and $\hat{\boldsymbol{A}}$. Use of definition (2.23) together with the basic commutations relations (2.21) and (2.22) leads to

$$\left[\underline{\hat{E}}_i(\boldsymbol{r},\omega),\underline{\hat{E}}_j(\boldsymbol{r}',\omega')\right] = 0 = \left[\underline{\hat{E}}_i^\dagger(\boldsymbol{r},\omega),\underline{\hat{E}}_j^\dagger(\boldsymbol{r}',\omega')\right], \tag{A.1}$$

$$\left[\underline{\hat{E}}_i(\boldsymbol{r},\omega),\underline{\hat{E}}_j^\dagger(\boldsymbol{r}',\omega')\right] = \frac{\hbar\mu_0\omega^2}{\pi}\,\mathrm{Im}\,G_{ij}(\boldsymbol{r},\boldsymbol{r}',\omega)\delta(\omega-\omega') = -\left[\underline{\hat{E}}_i^\dagger(\boldsymbol{r},\omega),\underline{\hat{E}}_j(\boldsymbol{r}',\omega')\right] \tag{A.2}$$

where we have used identity (2.26) in order to derive Eq. (A.2) and where the right hand side equalities follow via

$$\left[\hat{O}^\dagger,\hat{P}^\dagger\right] = -\left[\hat{O},\hat{P}\right]^\dagger. \tag{A.3}$$

Similarly, by using definition (2.44), we find

$$\left[\underline{\hat{A}}_i(\boldsymbol{r},\omega),\underline{\hat{A}}_j(\boldsymbol{r}',\omega')\right] = 0 = \left[\underline{\hat{A}}_i^\dagger(\boldsymbol{r},\omega),\underline{\hat{A}}_j^\dagger(\boldsymbol{r}',\omega')\right], \tag{A.4}$$

$$\left[\underline{\hat{A}}_i(\boldsymbol{r},\omega),\underline{\hat{A}}_j^\dagger(\boldsymbol{r}',\omega')\right] = \frac{\hbar\mu_0}{\pi}\,\mathrm{Im}\,{}^\perp G_{ij}^\perp(\boldsymbol{r},\boldsymbol{r}',\omega)\delta(\omega-\omega') = -\left[\underline{\hat{A}}_i^\dagger(\boldsymbol{r},\omega),\underline{\hat{A}}_j(\boldsymbol{r}',\omega')\right], \tag{A.5}$$

recall Eq. (2.45). The commutation relations (2.28) and (2.47) immediately follow from these results upon expressing the fields in terms of their frequency components according to Eq. (2.1) and recalling definitions (2.40) and (2.46).

The non-trivial commutator of $\hat{\boldsymbol{E}}$ and $\hat{\boldsymbol{A}}$ can be found by combining Eqs. (2.21)–(2.23), (2.26), (2.44) and (A.3), yielding

$$\left[\underline{\hat{E}}_i(\boldsymbol{r},\omega),\underline{\hat{A}}_j(\boldsymbol{r}',\omega')\right] = 0 = \left[\underline{\hat{E}}_i^\dagger(\boldsymbol{r},\omega),\underline{\hat{A}}_j^\dagger(\boldsymbol{r}',\omega')\right], \tag{A.6}$$

$$\left[\underline{\hat{E}}_i(\boldsymbol{r},\omega),\underline{\hat{A}}_j^\dagger(\boldsymbol{r}',\omega')\right] = \frac{i\hbar\omega}{\pi\varepsilon_0 c^2}\,\mathrm{Im}\,G_{ij}^\perp(\boldsymbol{r},\boldsymbol{r}',\omega)\delta(\omega-\omega') = \left[\underline{\hat{E}}_i^\dagger(\boldsymbol{r},\omega),\underline{\hat{A}}_j(\boldsymbol{r}',\omega')\right] \tag{A.7}$$

for the frequency components, so application of Eq. (2.1) results in

$$\left[\hat{E}_i(\boldsymbol{r}),\hat{A}_j(\boldsymbol{r}')\right] = \frac{2i\hbar}{\pi\varepsilon_0}\int_0^\infty \mathrm{d}\omega\,\frac{\omega}{c^2}\,\mathrm{Im}\,G_{ij}^\perp(\boldsymbol{r},\boldsymbol{r}',\omega). \tag{A.8}$$

In order to evaluate the frequency integral, we write $\operatorname{Im} z = (z - z^*)/(2\mathrm{i})$ and make use of Eq. (2.16), leading to

$$
\int_0^\infty \mathrm{d}\omega \, \frac{\omega}{c^2} \operatorname{Im} \boldsymbol{G}^\perp(\boldsymbol{r}, \boldsymbol{r}', \omega) = -\frac{\mathrm{i}}{2} \mathcal{P} \int_{-\infty}^\infty \mathrm{d}\omega \, \frac{\omega}{c^2} \, \boldsymbol{G}^\perp(\boldsymbol{r}, \boldsymbol{r}', \omega)
$$

$$
= \frac{1}{2} \lim_{|\omega| \to 0} \int_0^\pi \mathrm{d}\phi \, \frac{\omega^2}{c^2} \, \boldsymbol{G}^\perp(\boldsymbol{r}, \boldsymbol{r}', \omega) - \frac{1}{2} \lim_{|\omega| \to \infty} \int_0^\pi \mathrm{d}\phi \, \frac{\omega^2}{c^2} \, \boldsymbol{G}^\perp(\boldsymbol{r}, \boldsymbol{r}'\omega) \quad \text{(A.9)}
$$

($\mathcal{P}$: principal value). The second line in Eq. (A.9) was obtained by transforming the principal value integral into an integral along an infinitely small half circle around the origin plus an integral along an infinitely large half circle via contour integral techniques (where we have introduced polar coordinates $\omega = |\omega| \mathrm{e}^{\mathrm{i}\phi}$, $\mathrm{d}\omega = \mathrm{i}\omega \mathrm{d}\phi$), which is always possible since the Green tensor is analytic in the upper half of the complex frequency plane [170, SB3]. The integral along the small half circle vanishes since [SB3]

$$
\lim_{|\omega| \to 0} \frac{\omega^2}{c^2} \, \boldsymbol{G}^\perp(\boldsymbol{r}, \boldsymbol{r}', \omega) = \lim_{|\omega| \to 0} \frac{\omega^2}{c^2} {}^\perp \boldsymbol{G}(\boldsymbol{r}, \boldsymbol{r}', \omega) = \boldsymbol{0} \quad \text{(A.10)}
$$

whereas the integral along the large half circle can be calculated by means of [SB3]

$$
\lim_{|\omega| \to \infty} \frac{\omega^2}{c^2} \, \boldsymbol{G}(\boldsymbol{r}, \boldsymbol{r}', \omega) = -\delta(\boldsymbol{r} - \boldsymbol{r}')\boldsymbol{I}, \quad \text{(A.11)}
$$

hence

$$
\int_0^\infty \mathrm{d}\omega \, \frac{\omega}{c^2} \operatorname{Im} \boldsymbol{G}^\perp(\boldsymbol{r}, \boldsymbol{r}', \omega) = \int_0^\infty \mathrm{d}\omega \, \frac{\omega}{c^2} \operatorname{Im} {}^\perp \boldsymbol{G}(\boldsymbol{r}, \boldsymbol{r}', \omega) = \frac{\pi}{2} \, \boldsymbol{\delta}^\perp(\boldsymbol{r} - \boldsymbol{r}'). \quad \text{(A.12)}
$$

Substitution of this result into Eq. (A.8) leads to

$$
\left[\hat{E}_i(\boldsymbol{r}), \hat{A}_j(\boldsymbol{r}') \right] = \mathrm{i}\hbar \varepsilon_0^{-1} \delta_{ij}^\perp(\boldsymbol{r} - \boldsymbol{r}') \quad \text{(A.13)}
$$

which upon recalling definitions Eq. (2.40) and (2.46), respectively, results in the commutation relations (2.29) and (2.48). Furthermore, the vacuum fluctuations of the electric field (2.32) immediately follow from the commutator (A.2) together with Eq. (2.1) upon noting that $\underline{\hat{\boldsymbol{E}}}(\boldsymbol{r}, \omega)|\{0\}\rangle = \boldsymbol{0}$.

Next, we derive some commutation relations that are needed for the evaluation of the Heisenberg equations of motion in App. A.2. Using definitions (2.43) and (2.44), recalling that $\hat{\boldsymbol{D}}(\boldsymbol{r})$ is given according to Eqs. (2.6), (2.8), (2.19) and (2.23) and employing the basic commutation relations (2.21) and (2.22) as well as identity (2.26), one finds that

$$
\left[\underline{\hat{D}}_i(\boldsymbol{r}, \omega), \underline{\hat{A}}_j(\boldsymbol{r}', \omega') \right] = 0 = \left[\underline{\hat{D}}_i^\dagger(\boldsymbol{r}, \omega), \underline{\hat{A}}_j^\dagger(\boldsymbol{r}', \omega') \right], \quad \text{(A.14)}
$$

$$
\left[\underline{\hat{D}}_i(\boldsymbol{r}, \omega), \underline{\hat{A}}_j^\dagger(\boldsymbol{r}', \omega') \right] = \frac{\mathrm{i}\hbar\omega}{\pi c^2} \operatorname{Im}\left[\varepsilon(\boldsymbol{r}, \omega) G_{ij}^\perp(\boldsymbol{r}, \boldsymbol{r}', \omega) \right] \delta(\omega - \omega')
$$

$$
= \left[\underline{\hat{D}}_i^\dagger(\boldsymbol{r}, \omega), \underline{\hat{A}}_j(\boldsymbol{r}', \omega') \right], \quad \text{(A.15)}
$$

$$\left[\underline{\hat{\boldsymbol{A}}}(\boldsymbol{r},\omega),\underline{\hat{\varphi}}(\boldsymbol{r}',\omega')\right] = \boldsymbol{0} = \left[\underline{\hat{\boldsymbol{A}}}^{\dagger}(\boldsymbol{r},\omega),\underline{\hat{\varphi}}^{\dagger}(\boldsymbol{r}',\omega')\right], \tag{A.16}$$

$$\left[\underline{\hat{\boldsymbol{A}}}(\boldsymbol{r},\omega),\underline{\hat{\varphi}}^{\dagger}(\boldsymbol{r}',\omega')\right] = \frac{\mathrm{i}\hbar\omega}{\pi\varepsilon_0 c^2}\int_{\boldsymbol{r}_0}^{\boldsymbol{r}'} \mathrm{Im}\,{}^{\perp}\boldsymbol{G}^{\parallel}(\boldsymbol{r},\boldsymbol{s},\omega)\cdot\mathrm{d}\boldsymbol{s}\,\delta(\omega-\omega')$$

$$= \left[\underline{\hat{\boldsymbol{A}}}^{\dagger}(\boldsymbol{r},\omega),\underline{\hat{\varphi}}(\boldsymbol{r}',\omega')\right], \tag{A.17}$$

$$\left[\underline{\hat{\boldsymbol{D}}}(\boldsymbol{r},\omega),\underline{\hat{\varphi}}(\boldsymbol{r}',\omega')\right] = \boldsymbol{0} = \left[\underline{\hat{\boldsymbol{D}}}^{\dagger}(\boldsymbol{r},\omega),\underline{\hat{\varphi}}^{\dagger}(\boldsymbol{r}',\omega')\right], \tag{A.18}$$

$$\left[\underline{\hat{\boldsymbol{D}}}(\boldsymbol{r},\omega),\underline{\hat{\varphi}}^{\dagger}(\boldsymbol{r}',\omega')\right] = -\frac{\hbar\omega^2}{\pi c^2}\int_{\boldsymbol{r}_0}^{\boldsymbol{r}'} \mathrm{Im}\left[\varepsilon(\boldsymbol{r},\omega)\boldsymbol{G}^{\parallel}(\boldsymbol{r},\boldsymbol{s},\omega)\right]\cdot\mathrm{d}\boldsymbol{s}\,\delta(\omega-\omega')$$

$$= -\left[\underline{\hat{\boldsymbol{D}}}^{\dagger}(\boldsymbol{r},\omega),\underline{\hat{\varphi}}(\boldsymbol{r}',\omega')\right]. \tag{A.19}$$

Upon using Eq. (2.1), Eqs. (A.18) and (A.19) imply that

$$\left[\hat{\boldsymbol{D}}(\boldsymbol{r}),\hat{\varphi}(\boldsymbol{r}')\right] = \boldsymbol{0}, \tag{A.20}$$

while we proceed with Eqs. (A.14)–(A.17) in a similar way as given below Eq. (A.8). Using the properties $\varepsilon^*(\boldsymbol{r},\omega)=\varepsilon(\boldsymbol{r},-\omega^*)$ and $\lim_{|\omega|\to\infty}\varepsilon(\boldsymbol{r},\omega)=1$, we find

$$\left[\hat{D}_i(\boldsymbol{r}),\hat{A}_j(\boldsymbol{r}')\right] = \frac{\hbar}{\pi}\mathcal{P}\int_{-\infty}^{\infty}\mathrm{d}\omega\,\frac{\omega}{c^2}\,\varepsilon(\boldsymbol{r},\omega)\boldsymbol{G}^{\perp}(\boldsymbol{r},\boldsymbol{r}',\omega) = \mathrm{i}\hbar\delta_{ij}^{\perp}(\boldsymbol{r}-\boldsymbol{r}'), \tag{A.21}$$

$$\left[\hat{\boldsymbol{A}}(\boldsymbol{r}),\hat{\varphi}(\boldsymbol{r}')\right] = \frac{\hbar}{\pi\varepsilon_0}\mathcal{P}\int_{-\infty}^{\infty}\mathrm{d}\omega\,\frac{\omega}{c^2}\int_{\boldsymbol{r}_0}^{\boldsymbol{r}'} {}^{\perp}\boldsymbol{G}^{\parallel}(\boldsymbol{r},\boldsymbol{s},\omega)\cdot\mathrm{d}\boldsymbol{s} = \boldsymbol{0} \tag{A.22}$$

where the last equality follows from Eq. (A.11) and the property

$$\int \mathrm{d}^3 s\,\boldsymbol{\delta}^{\perp}(\boldsymbol{r}-\boldsymbol{s})\cdot\boldsymbol{\delta}^{\parallel}(\boldsymbol{s}-\boldsymbol{r}') = \boldsymbol{0}. \tag{A.23}$$

A.2   Derivation of Maxwell and Newton equations

We first demonstrate the validity of the Maxwell equations in the absence of free charges and currents as given in Sec. 2.1. As seen from Eq. (2.40) and Eq. (2.5), respectively, both $\hat{\boldsymbol{B}}(\boldsymbol{r})$ and $\hat{\boldsymbol{D}}(\boldsymbol{r})$ can be written as the curl of a vector field, so Maxwell equations (2.35) and (2.36) are trivially fulfilled. The dynamic Maxwell equations (2.37) and (2.38) follow from Hamiltonian (2.33) which according the commutation relations (2.21) and (2.22) generates the Heisenberg equation of motion

$$\dot{\hat{\boldsymbol{f}}}_{\lambda}(\boldsymbol{r},\omega) = \mathrm{i}\hbar^{-1}\left[\hat{H}_{\mathrm{F}},\hat{\boldsymbol{f}}_{\lambda}(\boldsymbol{r},\omega)\right] = -\mathrm{i}\omega\hat{\boldsymbol{f}}_{\lambda}(\boldsymbol{r},\omega). \tag{A.24}$$

Together with Eqs. (2.1), (2.4) and (2.5), this implies

$$\dot{\boldsymbol{B}}(\boldsymbol{r}) = i\hbar^{-1}\left[\hat{H}_{\mathrm{F}}, \hat{\boldsymbol{B}}(\boldsymbol{r})\right] = -\int_0^\infty d\omega\, i\omega\underline{\hat{\boldsymbol{B}}}(\boldsymbol{r}, \omega) + \mathrm{H.c.}$$

$$= -\int_0^\infty d\omega\, \boldsymbol{\nabla}\times\underline{\hat{\boldsymbol{E}}}(\boldsymbol{r}, \omega) + \mathrm{H.c.} = -\boldsymbol{\nabla}\times\hat{\boldsymbol{E}}(\boldsymbol{r}), \qquad (A.25)$$

$$\dot{\boldsymbol{D}}(\boldsymbol{r}) = i\hbar^{-1}\left[\hat{H}_{\mathrm{F}}, \hat{\boldsymbol{D}}(\boldsymbol{r})\right] = -\int_0^\infty d\omega\, i\omega\underline{\hat{\boldsymbol{D}}}(\boldsymbol{r}, \omega) + \mathrm{H.c.}$$

$$= \int_0^\infty d\omega\, \boldsymbol{\nabla}\times\underline{\hat{\boldsymbol{H}}}(\boldsymbol{r}, \omega) + \mathrm{H.c.} = \boldsymbol{\nabla}\times\hat{\boldsymbol{H}}(\boldsymbol{r}). \qquad (A.26)$$

Next, we turn to the Maxwell equations in the presence of an atom (Sec. 2.2.1). Maxwell equation (2.76) follows trivially from the corresponding Eq. (2.35) via Eq. (2.74), while Eq. (2.75) shows that Eq. (2.36) together with Eq. (2.53) implies Maxwell equation (2.77). Similarly, the dynamic Maxwell equation (2.78) follows from the corresponding Eq. (2.37) because the atom does not contribute, $\boldsymbol{\nabla}\times\boldsymbol{\nabla}\hat{\varphi}_A(\boldsymbol{r}) = \boldsymbol{0}$. The only non-trivial change with respect to the Maxwell equations in the absence of free charges and currents, occurs in the second dynamical Maxwell equation (2.79). Combining Eqs. (2.34) and (2.75), we now have

$$\dot{\boldsymbol{\mathcal{D}}}(\boldsymbol{r}) = i\hbar^{-1}\left[\hat{H}_{\mathrm{F}}, \hat{\boldsymbol{D}}(\boldsymbol{r})\right] + i\hbar^{-1}\left[\hat{H}_{AF}, \hat{\boldsymbol{D}}(\boldsymbol{r})\right] - i\hbar^{-1}\left[\hat{H}_A, \varepsilon_0\boldsymbol{\nabla}\hat{\varphi}_A(\boldsymbol{r})\right] - i\hbar^{-1}\left[\hat{H}_{AF}, \varepsilon_0\boldsymbol{\nabla}\hat{\varphi}_A(\boldsymbol{r})\right].$$
$$(A.27)$$

Recalling the interaction Hamiltonian (2.73), the commutation relations (A.20) and (A.21) imply that

$$i\hbar^{-1}\left[\hat{H}_{AF}, \hat{\boldsymbol{D}}(\boldsymbol{r})\right] = -\sum_{\alpha\in A}\frac{q_\alpha}{m_\alpha}\left[\hat{\boldsymbol{p}}_\alpha - q_\alpha\hat{\boldsymbol{A}}(\hat{\boldsymbol{r}}_\alpha)\right]\cdot\boldsymbol{\delta}^\perp(\boldsymbol{r} - \hat{\boldsymbol{r}}_\alpha) = -\hat{\boldsymbol{j}}_A^\perp(\boldsymbol{r}) \qquad (A.28)$$

where we have used Eqs. (2.55) and (2.81). With the atomic Hamiltonian being given by Eq. (2.50), use of definition (2.52) as well as the commutation relations (2.49), results in

$$-i\hbar^{-1}\left[\hat{H}_A, \varepsilon_0\boldsymbol{\nabla}\hat{\varphi}_A(\boldsymbol{r})\right] = -\sum_{\alpha\in A}\left[\frac{\hat{\boldsymbol{p}}_\alpha}{2m_\alpha}\cdot\boldsymbol{\delta}^\parallel(\boldsymbol{r} - \hat{\boldsymbol{r}}_\alpha) + \boldsymbol{\delta}^\parallel(\boldsymbol{r} - \hat{\boldsymbol{r}}_\alpha)\cdot\frac{\hat{\boldsymbol{p}}_\alpha}{2m_\alpha}\right], \qquad (A.29)$$

where we have employed Eq. (2.42); and similarly, with the interaction Hamiltonian (2.73) one may obtain

$$-i\hbar^{-1}\left[\hat{H}_{AF}, \varepsilon_0\boldsymbol{\nabla}\hat{\varphi}_A(\boldsymbol{r})\right] = \sum_{\alpha\in A}\frac{q_\alpha}{m_\alpha}\,\hat{\boldsymbol{A}}(\hat{\boldsymbol{r}}_\alpha)\cdot\boldsymbol{\delta}^\parallel(\boldsymbol{r} - \hat{\boldsymbol{r}}_\alpha), \qquad (A.30)$$

so that

$$-i\hbar^{-1}\left[\hat{H}_A, \varepsilon_0\boldsymbol{\nabla}\hat{\varphi}_A(\boldsymbol{r})\right] - i\hbar^{-1}\left[\hat{H}_{AF}, \varepsilon_0\boldsymbol{\nabla}\hat{\varphi}_A(\boldsymbol{r})\right] = -\hat{\boldsymbol{j}}_A^\parallel(\boldsymbol{r}). \qquad (A.31)$$

Substituting Eqs. (A.26), (A.28) and (A.31) into Eq. (A.27) and recalling Eq. (2.75), one arrives at Maxwell equation (2.79).

The Newton equation is verified by considering the Heisenberg equations of motion for the charged particles. Hence, by using Eqs. (2.50) and (2.73) together with the commutation

relations (2.49), the Heisenberg equations of motion (2.34) for the particle coordinates take the form of Eq. (2.81) which leads to

$$
m_\alpha \ddot{\hat{\boldsymbol{r}}}_\alpha = \mathrm{i}\hbar^{-1}\big[\hat{H}_A, \hat{\boldsymbol{p}}_\alpha\big] + \mathrm{i}\hbar^{-1}\big[\hat{H}_{AF}, \hat{\boldsymbol{p}}_\alpha\big] - \mathrm{i}\hbar^{-1}\big[\hat{H}_{\mathrm{F}}, q_\alpha \hat{\boldsymbol{A}}(\hat{\boldsymbol{r}}_\alpha)\big] - \mathrm{i}\hbar^{-1}\big[\hat{H}_A, q_\alpha \hat{\boldsymbol{A}}(\hat{\boldsymbol{r}}_\alpha)\big]
$$
$$
- \mathrm{i}\hbar^{-1}\big[\hat{H}_{AF}, q_\alpha \hat{\boldsymbol{A}}(\hat{\boldsymbol{r}}_\alpha)\big]. \quad \text{(A.32)}
$$

Using definitions (2.50) and (2.73) as well as the commutation relations (2.49), one may easily find

$$
\mathrm{i}\hbar^{-1}\big[\hat{H}_A, \hat{\boldsymbol{p}}_\alpha\big] = -q_\alpha \boldsymbol{\nabla} \hat{\varphi}_A(\hat{\boldsymbol{r}}_\alpha), \tag{A.33}
$$

$$
\mathrm{i}\hbar^{-1}\big[\hat{H}_{AF}, \hat{\boldsymbol{p}}_\alpha\big] = q_\alpha \hat{\boldsymbol{E}}^{\parallel}(\hat{\boldsymbol{r}}_\alpha) + q_\alpha \big[\boldsymbol{\nabla}\hat{\boldsymbol{A}}(\hat{\boldsymbol{r}}_\alpha)\big]\cdot\dot{\hat{\boldsymbol{r}}}_\alpha, \tag{A.34}
$$

$$
-\mathrm{i}\hbar^{-1}\big[\hat{H}_A, q_\alpha \hat{\boldsymbol{A}}(\hat{\boldsymbol{r}}_\alpha)\big] = -\frac{q_\alpha}{m_\alpha}\Big\{\hat{\boldsymbol{p}}_\alpha\cdot\big[\boldsymbol{\nabla}\hat{\boldsymbol{A}}(\hat{\boldsymbol{r}}_\alpha)\big] + \big[\boldsymbol{\nabla}\hat{\boldsymbol{A}}(\hat{\boldsymbol{r}}_\alpha)\big]^{\mathrm{T}}\cdot\hat{\boldsymbol{p}}_\alpha\Big\}, \tag{A.35}
$$

$$
-\mathrm{i}\hbar^{-1}\big[\hat{H}_{AF}, q_\alpha \hat{\boldsymbol{A}}(\hat{\boldsymbol{r}}_\alpha)\big] = \frac{q_\alpha^2}{m_\alpha}\,\hat{\boldsymbol{A}}(\hat{\boldsymbol{r}}_\alpha)\cdot\big[\boldsymbol{\nabla}\hat{\boldsymbol{A}}(\hat{\boldsymbol{r}}_\alpha)\big] \tag{A.36}
$$

where we have employed Eqs. (2.43) and (2.81) in order to derive Eq. (A.34) and where Eq. (A.36) is based on Eq. (A.22). Equations (A.34)–(A.36) can be combined by using Eq. (2.81) as well as the rule $\boldsymbol{a}\times(\boldsymbol{b}\times\boldsymbol{c})=\boldsymbol{b}(\boldsymbol{a}\cdot\boldsymbol{c})-\boldsymbol{c}(\boldsymbol{a}\cdot\boldsymbol{b})$ and recalling Eq. (2.40), leading to

$$
q_\alpha\big[\boldsymbol{\nabla}\hat{\boldsymbol{A}}(\hat{\boldsymbol{r}}_\alpha)\big]\cdot\dot{\hat{\boldsymbol{r}}}_\alpha - \frac{q_\alpha}{m_\alpha}\Big\{\hat{\boldsymbol{p}}_\alpha\cdot\big[\boldsymbol{\nabla}\hat{\boldsymbol{A}}(\hat{\boldsymbol{r}}_\alpha)\big] + \big[\boldsymbol{\nabla}\hat{\boldsymbol{A}}(\hat{\boldsymbol{r}}_\alpha)\big]^{\mathrm{T}}\cdot\hat{\boldsymbol{p}}_\alpha\Big\} + \frac{q_\alpha^2}{m_\alpha}\,\hat{\boldsymbol{A}}(\hat{\boldsymbol{r}}_\alpha)\cdot\big[\boldsymbol{\nabla}\hat{\boldsymbol{A}}(\hat{\boldsymbol{r}}_\alpha)\big]
$$
$$
= \frac{q_\alpha}{2}\Big[\dot{\hat{\boldsymbol{r}}}_\alpha\times\hat{\boldsymbol{B}}(\hat{\boldsymbol{r}}_\alpha) - \hat{\boldsymbol{B}}(\hat{\boldsymbol{r}}_\alpha)\times\dot{\hat{\boldsymbol{r}}}_\alpha\Big]. \quad \text{(A.37)}
$$

The remaining third term on the right hand side of Eq. (A.32) follows trivially from (A.24) [recall Eq. (2.44)], yielding

$$
-\mathrm{i}\hbar^{-1}\big[\hat{H}_{\mathrm{F}}, q_\alpha \hat{\boldsymbol{A}}(\hat{\boldsymbol{r}}_\alpha)\big] = q_\alpha \hat{\boldsymbol{E}}^{\perp}(\hat{\boldsymbol{r}}_\alpha). \tag{A.38}
$$

Substituting Eqs. (A.33)–(A.38) into Eq. (A.32) and recalling the definitions (2.74), we finally arrive at Eq. (2.80).

Appendix B

Power–Zienau–Woolley transformation

In this appendix, the Power–Zienau–Woolley transformation is used to derive the multipolar Hamiltonian (2.86) given in Sec. 2.2.2. We first calculate the transformed variables. From Eqs. (2.83) and (2.84) one can conclude that the following quantities remain unchanged, because they commute with both $\hat{\boldsymbol{r}}_\alpha$ [and hence with $\hat{\boldsymbol{P}}_A$, recall Eq. (2.62)] and $\hat{\boldsymbol{A}}$ [recall Eqs. (2.40), (2.47) and (A.22)]:

$$\hat{\boldsymbol{B}}'(\boldsymbol{r}) = \hat{\boldsymbol{B}}(\boldsymbol{r}), \qquad \hat{\boldsymbol{A}}'(\boldsymbol{r}) = \hat{\boldsymbol{A}}(\boldsymbol{r}), \qquad \hat{\varphi}'(\boldsymbol{r}) = \hat{\varphi}(\boldsymbol{r}), \tag{B.1}$$

$$\hat{\boldsymbol{r}}'_\alpha = \hat{\boldsymbol{r}}_\alpha, \qquad \hat{\rho}'_A(\boldsymbol{r}) = \hat{\rho}_A(\boldsymbol{r}), \qquad \hat{\varphi}'_A(\boldsymbol{r}) = \hat{\varphi}_A(\boldsymbol{r}), \qquad \hat{\boldsymbol{r}}'_A = \hat{\boldsymbol{r}}_A, \qquad \hat{\bar{\boldsymbol{r}}}'_\alpha = \hat{\bar{\boldsymbol{r}}}_\alpha, \tag{B.2}$$

$$\hat{\boldsymbol{P}}'_A(\boldsymbol{r}) = \hat{\boldsymbol{P}}_A(\boldsymbol{r}), \qquad \hat{\boldsymbol{M}}'_A(\boldsymbol{r}) = \hat{\boldsymbol{M}}_A(\boldsymbol{r}), \qquad \hat{\boldsymbol{\Theta}}'_\alpha(\boldsymbol{r}) = \hat{\boldsymbol{\Theta}}_\alpha(\boldsymbol{r}), \qquad \hat{\boldsymbol{\Xi}}'_\alpha(\boldsymbol{r}) = \hat{\boldsymbol{\Xi}}_\alpha(\boldsymbol{r}). \tag{B.3}$$

The transformed electric field can be found by combining Eqs. (2.83) and (2.84) and recalling the commutation relation (A.13), resulting in Eq. (2.97). Similarly, upon recalling definition (2.62), the commutation relations (2.58)–(2.60) lead to

$$
\begin{aligned}
\hat{\boldsymbol{p}}'_\alpha = {}& \hat{\boldsymbol{p}}_\alpha - \sum_{\beta \in A} q_\beta \left(\delta_{\alpha\beta} - \frac{m_\alpha}{m_A} \right) \int_0^1 \mathrm{d}\sigma \, \hat{\boldsymbol{A}}(\hat{\boldsymbol{r}}_A + \sigma\hat{\bar{\boldsymbol{r}}}_\beta) \\
& + \int \mathrm{d}^3 r \sum_{\beta \in A} q_\beta \int_0^1 \mathrm{d}\sigma \left[\sigma\delta_{\alpha\beta} + (1-\sigma)\frac{m_\alpha}{m_A} \right] \hat{\boldsymbol{A}}(\hat{\boldsymbol{r}}) \big(\hat{\bar{\boldsymbol{r}}}_\beta \cdot \boldsymbol{\nabla} \big) \delta\big(\boldsymbol{r} - \hat{\boldsymbol{r}}_A - \sigma\hat{\bar{\boldsymbol{r}}}_\beta \big) \\
& - \int \mathrm{d}^3 r \sum_{\beta \in A} q_\beta \int_0^1 \mathrm{d}\sigma \left[\sigma\delta_{\alpha\beta} + (1-\sigma)\frac{m_\alpha}{m_A} \right] \delta\big(\boldsymbol{r} - \hat{\boldsymbol{r}}_A - \sigma\hat{\bar{\boldsymbol{r}}}_\beta \big) \hat{\bar{\boldsymbol{r}}}_\beta \times \hat{\boldsymbol{B}}(\hat{\boldsymbol{r}}) \\
= {}& \hat{\boldsymbol{p}}_\alpha - q_\alpha \hat{\boldsymbol{A}}(\hat{\boldsymbol{r}}_\alpha) - \int \mathrm{d}^3 r \, \hat{\boldsymbol{\Xi}}_\alpha(\boldsymbol{r}) \times \hat{\boldsymbol{B}}(\boldsymbol{r})
\end{aligned}
\tag{B.4}
$$

where we have used the rule $\boldsymbol{a} \times (\boldsymbol{b} \times \boldsymbol{c}) = \boldsymbol{b}(\boldsymbol{a} \cdot \boldsymbol{c}) - \boldsymbol{c}(\boldsymbol{a} \cdot \boldsymbol{b})$ and where the last equality follows by partially integrating with respect to σ and exploiting the fact that the atom is neutral, with $\hat{\boldsymbol{\Xi}}_\alpha$ being defined as in Eq. (2.91). Note that upon using Eqs. (2.34) and (2.86), Eq. (B.4) leads to Eq. (2.96).

With these preparations at hand, the minimal-coupling Hamiltonian (2.72) can be expressed in terms of the transformed variables. Upon recalling definition (2.23) and the identities (2.26) and (A.12), the transformation rule (2.85) implies

$$
\begin{aligned}
\sum_{\lambda=e,m} \int \mathrm{d}^3 r \int_0^\infty \mathrm{d}\omega \, \hbar\omega \, \hat{\boldsymbol{f}}_\lambda^\dagger(\boldsymbol{r}, \omega) \cdot \hat{\boldsymbol{f}}_\lambda(\boldsymbol{r}, \omega) = {}& \sum_{\lambda=e,m} \int \mathrm{d}^3 r \int_0^\infty \mathrm{d}\omega \, \hbar\omega \, \hat{\boldsymbol{f}}_\lambda'^\dagger(\boldsymbol{r}, \omega) \cdot \hat{\boldsymbol{f}}_\lambda'(\boldsymbol{r}, \omega) \\
& - \int \mathrm{d}^3 r \, \hat{\boldsymbol{P}}_A'^\perp(\boldsymbol{r}) \cdot \hat{\boldsymbol{E}}'(\boldsymbol{r}) + \frac{1}{2\varepsilon_0} \int \mathrm{d}^3 r \left[\hat{\boldsymbol{P}}_A'^\perp(\boldsymbol{r}) \right]^2 ; \tag{B.5}
\end{aligned}
$$

and similarly Eqs. (B.1) and (B.2) result in

$$\frac{1}{2}\int \mathrm{d}^3r\, \hat{\rho}_A(\boldsymbol{r})\hat{\varphi}_A(\boldsymbol{r}) = \frac{1}{2\varepsilon_0}\int \mathrm{d}^3r\left[\hat{\boldsymbol{P}}_A'^{\|}(\boldsymbol{r})\right]^2, \tag{B.6}$$

$$\int \mathrm{d}^3r\, \hat{\rho}_A(\boldsymbol{r})\hat{\varphi}(\boldsymbol{r}) = -\int \mathrm{d}^3r\, \hat{\boldsymbol{P}}_A'^{\|}(\boldsymbol{r})\cdot\hat{\boldsymbol{E}}'^{\|}(\boldsymbol{r}) \tag{B.7}$$

where we have used the identity (2.53), partially integrated, and recalled Eqs. (2.43) and (2.69). Substituting Eqs. (B.4)–(B.7) into Eq. (2.72) and noting that integrals over mixed scalar products of longitudinal and transverse vector fields vanish, we arrive at the multipolar-coupling Hamiltonian (2.86).

Appendix C

Green tensor for the real-cavity model

In this appendix, we present a proof of Eq. (3.46) (given in Sec. 3.3) which relates the scattering Green tensors $\boldsymbol{G}_{\mathrm{loc}}^{(1)}(\boldsymbol{r}_A, \boldsymbol{r}_A, \omega)$ and $\boldsymbol{G}^{(1)}(\boldsymbol{r}_A, \boldsymbol{r}_A, \omega)$ for an atom placed inside a host body with and without taking into account the local-field correction by means of the real-cavity model. We begin with the case of an atom embedded in a homogeneous host body in which case the permittivities $\varepsilon_{\mathrm{loc}}(\boldsymbol{r}, \omega)$, $\varepsilon(\boldsymbol{r}, \omega)$ and permeabilities $\mu_{\mathrm{loc}}(\boldsymbol{r}, \omega)$, $\mu(\boldsymbol{r}, \omega)$ belonging to $\boldsymbol{G}_{\mathrm{loc}}(\boldsymbol{r}_A, \boldsymbol{r}_A, \omega)$ and $\boldsymbol{G}(\boldsymbol{r}_A, \boldsymbol{r}_A, \omega)$ are illustrated in Figs. C.1(a) and (b).

We first recall from Eqs. (2.15) and (3.16) that $\boldsymbol{G}_{\mathrm{loc}}^{(1)}(\boldsymbol{r}_A, \boldsymbol{r}_A, \omega)$ determines the electric field originated by a source at $\boldsymbol{r}_A$ that reaches the same point $\boldsymbol{r}_A$ after being scattered at the surfaces of inhomogeneity. In the following, we distinguish three classes of scattering processes where class (i) includes only (multiple) scattering at the inner surface of the cavity; class (ii) subsumes processes involving transmission to the outside of the cavity, (multiple) reflexion at the body surface and retransmission into the cavity (without scattering at the cavity surface from the outside); and class (iii) accounts for all remaining processes (where backscattering at the cavity surface from the outside occurs at least once). Simple examples of processes belonging to the three classes are sketched in Fig. C.1(a).

Processes of type (i) do not depend on the outer boundaries of the host body, so they can be characterised by considering the simplified arrangement

$$\varepsilon_{\mathrm{cav}}(\boldsymbol{r}, \omega) = \begin{cases} 1 & \text{if } |\boldsymbol{r} - \boldsymbol{r}_A| < R_{\mathrm{cav}}, \\ \varepsilon_A(\omega) & \text{if } |\boldsymbol{r} - \boldsymbol{r}_A| \geq R_{\mathrm{cav}} \end{cases} \tag{C.1}$$

of a cavity embedded in an infinitely extended homogeneous body as depicted in Fig. C.1(c). All class (i) processes are hence contained in the corresponding scattering Green tensor $\boldsymbol{G}_{\mathrm{cav}}^{(1)}$, which reads [192, SB3, SB15]

$$\boldsymbol{G}_{\mathrm{cav}}^{(1)}(\boldsymbol{r}_A, \boldsymbol{r}_A, \omega) = \frac{\omega}{6\pi c} \left\{ \frac{3(\varepsilon_A - 1)}{2\varepsilon_A + 1} \frac{c^3}{\omega^3 R_{\mathrm{cav}}^3} + \frac{9[\varepsilon_A^2(5\mu_A - 1) - 3\varepsilon_A - 1]}{5(2\varepsilon_A + 1)^2} \frac{c}{\omega R_{\mathrm{cav}}} \right.$$
$$\left. + \mathrm{i} \left[\frac{9\varepsilon_A^{5/2} \mu_A^{3/2}}{(2\varepsilon_A + 1)^2} - 1 \right] \right\} \boldsymbol{I} + O(\omega R_{\mathrm{cav}}/c). \tag{C.2}$$

Next, we determine the contribution from class (ii) processes which involve transmission to the cavity exterior. In an infinitely extended body, the field transmitted to a point $\boldsymbol{r}$ outside the cavity would be given by $\boldsymbol{G}_{\mathrm{cav}}(\boldsymbol{r}, \boldsymbol{r}_A, \omega)$ [Fig. C.1(c)]. It can be shown that [SB11, SB15]

$$\boldsymbol{G}_{\mathrm{cav}}(\boldsymbol{r}, \boldsymbol{r}_A, \omega) = \frac{3\varepsilon_A}{2\varepsilon_A + 1} \boldsymbol{G}_{\mathrm{inf}}(\boldsymbol{r}, \boldsymbol{r}_A, \omega) + O(\omega R_{\mathrm{cav}}/c) \tag{C.3}$$
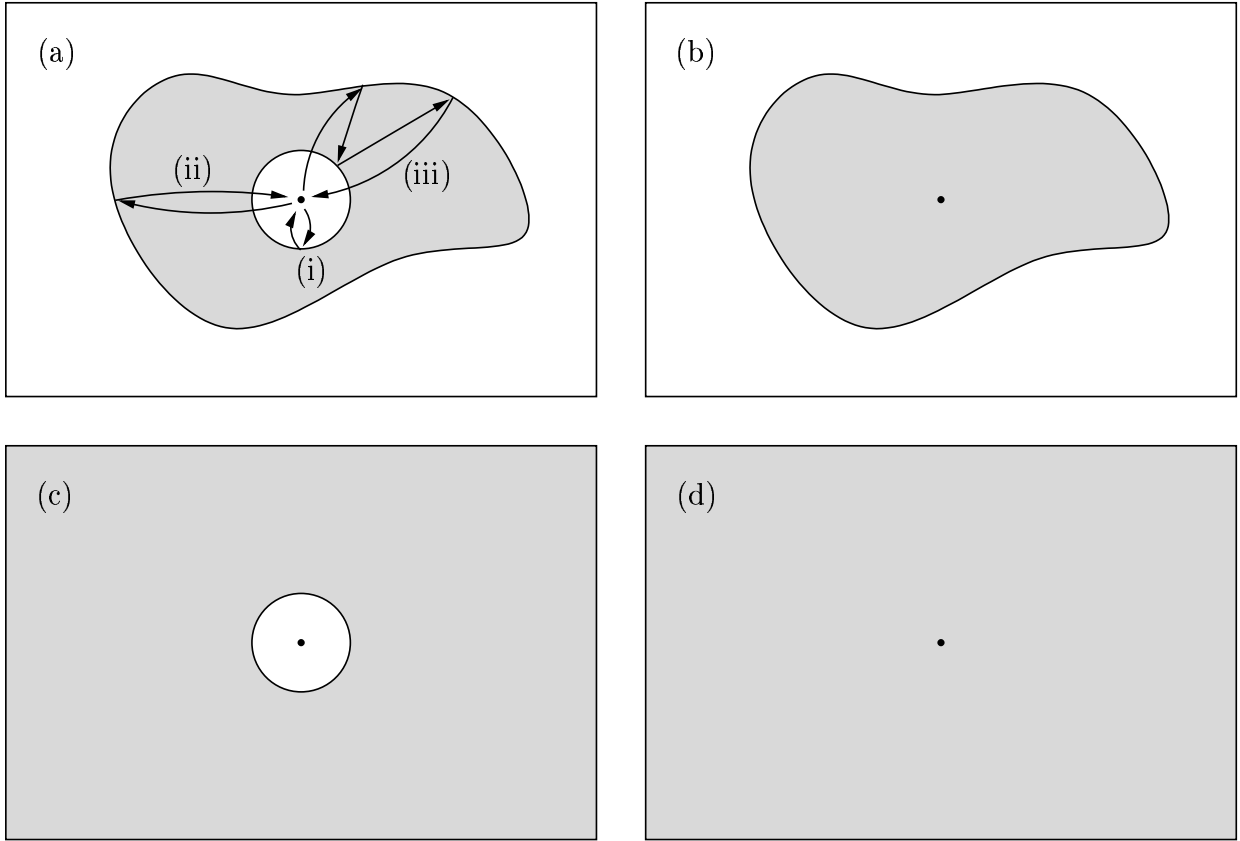
Figure C.1: Schematic illustration of the permittivities and permeabilities corresponding to (a) $\boldsymbol{G}_{\mathrm{loc}}(\boldsymbol{r}_A, \boldsymbol{r}_A, \omega)$, (b) $\boldsymbol{G}(\boldsymbol{r}_A, \boldsymbol{r}_A, \omega)$, (c) $\boldsymbol{G}_{\mathrm{cav}}(\boldsymbol{r}_A, \boldsymbol{r}_A, \omega)$ and (d) $\boldsymbol{G}_{\mathrm{inf}}(\boldsymbol{r}_A, \boldsymbol{r}_A, \omega)$; the dot indicates the position of the guest atom $\boldsymbol{r}_A$. Examples of scattering processes of types (i), (ii) and (iii) are also sketched.

where $\boldsymbol{G}_{\mathrm{inf}}(\boldsymbol{r}, \boldsymbol{r}_A, \omega)$ is the Green tensor for an infinitely extended homogeneous body without the cavity, $\varepsilon_{\mathrm{inf}}(\boldsymbol{r}, \omega) = \varepsilon_A(\omega)$ as depicted in Fig. C.1(d). In other words, the electric field transmitted through the cavity surface to a point outside the cavity is equal to the field that would be transmitted to the same point in the absence of the cavity, multiplied by a global factor. By means of the general symmetry property (2.17), we also have

$$\boldsymbol{G}_{\mathrm{cav}}(\boldsymbol{r}_A, \boldsymbol{r}, \omega) = \frac{3\varepsilon_A}{2\varepsilon_A + 1} \, \boldsymbol{G}_{\mathrm{inf}}(\boldsymbol{r}_A, \boldsymbol{r}, \omega) + O(\omega R_{\mathrm{cav}}/c), \qquad (\text{C.4})$$

i.e., the electric field transmitted through the cavity surface from an arbitrary point outside the cavity is also equal to the corresponding result in the absence of the cavity, multiplied by the same factor. For a finite body, the electric field transmitted to the exterior of the cavity will be (multiply) reflected from the body's outer surface and retransmitted into the cavity, eventually giving rise to a field at $\boldsymbol{r}_A$. Without the cavity, processes of this kind are taken into account by replacing the infinite-body Green tensor $\boldsymbol{G}_{\mathrm{inf}}$ [Fig. C.1(d)] with its finite-body counterpart $\boldsymbol{G}$ [Fig. C.1(b)]. Combining this observation with Eqs. (C.3) and (C.4) and taking advantage of the linearity of the differential equation (2.14), we conclude

that the contribution from the class (ii) processes can be described by

$$\left(\frac{3\varepsilon_A}{2\varepsilon_A + 1}\right)^2 \boldsymbol{G}^{(1)}(\boldsymbol{r}_A, \boldsymbol{r}_A, \omega) + O(\omega R_{\text{cav}}/c). \tag{C.5}$$

Finally, we consider processes of type (iii), which involve at least one scattering event at the cavity surface from the outside. Single scattering at the cavity surface can be characterised by $\boldsymbol{G}^{(1)}_{\text{cav}}(\boldsymbol{r}, \boldsymbol{r}', \omega)$ [Fig. C.1(c)] with both $\boldsymbol{r}$ and $\boldsymbol{r}'$ outside the cavity. One can show that [192, SB11, SB15]

$$\boldsymbol{G}^{(1)}_{\text{cav}}(\boldsymbol{r}, \boldsymbol{r}', \omega) = O\big[(\omega R_{\text{cav}}/c)^3\big] \tag{C.6}$$

so that the contribution of the class (iii) processes is of order $O[(\omega R_{\text{cav}}/c)^3]$ and hence negligible for sufficiently small R_{cav}. Combining this with Eqs. (C.2) and (C.5), we arrive at Eq. (3.46).

The arguments given above can be extended to inhomogeneous bodies in a straightforward way. If the condition (3.45) is satisfied, one can divide such a body into a more or less small homogeneous part containing the cavity plus an inhomogeneous rest. Equations (C.3), (C.4) and (C.6) then still describe the propagation of the electric field inside the homogeneous part of the body and the effect of the inhomogeneous part can be taken into account by the scattering at the (fictitious) surface dividing the two parts. Consequently, we again find that Eq. (3.46) holds.

Appendix D

Born expansion of the Green tensor

First, the Born expansion of the Green tensor is given to arbitrary order in χ and ζ (see Sec. 3.4) and the result is used to derive general forms of the CP potential in retarded and non-retarded limits given in Sec. 3.1. Thereafter, we will provide explicit expressions for the contributions to the ground-state CP potential that are quadratic in χ and infer the free-space three-atom vdW potential from these contributions.

D.1   Expansion to arbitrary order

Provided that Eqs. (3.52) and (3.53) hold, one can make iterative use of the Dyson equation (3.54) to derive the Born expansion of the Green tensor [SB1, SB10]

$$\boldsymbol{G}(\boldsymbol{r}, \boldsymbol{r}', \omega) = \overline{\boldsymbol{G}}(\boldsymbol{r}, \boldsymbol{r}', \omega) + \sum_{K=1}^{\infty} \Delta_K \boldsymbol{G}(\boldsymbol{r}, \boldsymbol{r}', \omega) \tag{D.1}$$

where

$$\Delta_K \boldsymbol{G}(\boldsymbol{r}, \boldsymbol{r}', \omega) = \sum_{\lambda_1 \ldots \lambda_K = e, m} \left[\prod_{J=1}^{K} \int \mathrm{d}^3 s_J \, f_{\lambda_J}(\boldsymbol{s}_J, \omega) \right]$$
$$\times \, \boldsymbol{G}_{0\lambda_1}(\boldsymbol{r}, \boldsymbol{s}_1, \omega) \cdot \boldsymbol{G}_{\lambda_1\lambda_2}(\boldsymbol{s}_1, \boldsymbol{s}_2, \omega) \cdots \boldsymbol{G}_{\lambda_K 0}(\boldsymbol{s}_K, \boldsymbol{r}', \omega) \tag{D.2}$$

denotes the contribution that is of order K in χ, ζ and the definitions

$$f_e(\boldsymbol{r}, \omega) = \chi(\boldsymbol{r}, \omega), \qquad f_m(\boldsymbol{r}, \omega) = -\zeta(\boldsymbol{r}, \omega) \tag{D.3}$$

and

$$\boldsymbol{G}_{0e}(\boldsymbol{r}, \boldsymbol{r}', \omega) = \overline{\boldsymbol{G}}(\boldsymbol{r}, \boldsymbol{r}', \omega) \frac{\omega}{c}, \qquad \boldsymbol{G}_{e0}(\boldsymbol{r}, \boldsymbol{r}', \omega) = \frac{\omega}{c} \overline{\boldsymbol{G}}(\boldsymbol{r}, \boldsymbol{r}', \omega), \tag{D.4}$$

$$\boldsymbol{G}_{0m}(\boldsymbol{r}, \boldsymbol{r}', \omega) = \overline{\boldsymbol{G}}(\boldsymbol{r}, \boldsymbol{r}', \omega) \times \overleftarrow{\boldsymbol{\nabla}}', \qquad \boldsymbol{G}_{m0}(\boldsymbol{r}, \boldsymbol{r}', \omega) = \boldsymbol{\nabla} \times \overline{\boldsymbol{G}}(\boldsymbol{r}, \boldsymbol{r}', \omega), \tag{D.5}$$

$$\boldsymbol{G}_{ee}(\boldsymbol{r}, \boldsymbol{r}', \omega) = \frac{\omega}{c} \overline{\boldsymbol{G}}(\boldsymbol{r}, \boldsymbol{r}', \omega) \frac{\omega}{c}, \qquad \boldsymbol{G}_{em}(\boldsymbol{r}, \boldsymbol{r}', \omega) = \frac{\omega}{c} \overline{\boldsymbol{G}}(\boldsymbol{r}, \boldsymbol{r}', \omega) \times \overleftarrow{\boldsymbol{\nabla}}', \tag{D.6}$$

$$\boldsymbol{G}_{me}(\boldsymbol{r}, \boldsymbol{r}', \omega) = \boldsymbol{\nabla} \times \overline{\boldsymbol{G}}(\boldsymbol{r}, \boldsymbol{r}', \omega) \frac{\omega}{c}, \qquad \boldsymbol{G}_{mm}(\boldsymbol{r}, \boldsymbol{r}', \omega) = \boldsymbol{\nabla} \times \overline{\boldsymbol{G}}(\boldsymbol{r}, \boldsymbol{r}', \omega) \times \overleftarrow{\boldsymbol{\nabla}}', \tag{D.7}$$

have been introduced. In particular, within linear order in χ, ζ, Eqs. (D.1)–(D.7) reduce to Eqs. (3.55) and (3.56).

The full Born expansion can be used to derive the general retarded and non-retarded limits of the CP potential presented at the end of Sec. 3.1. To that end, we set $\varepsilon(\boldsymbol{r}, \omega)$

$= 1 + \chi(\boldsymbol{r}, \omega)$ and $\kappa(\boldsymbol{r}, \omega) = 1 - \zeta(\boldsymbol{r}, \omega)$ so that $\overline{\varepsilon}(\boldsymbol{r}, \omega) = 1$, $\overline{\mu}(\boldsymbol{r}, \omega) = 1$, recall Eq. (3.52), and consequently the unperturbed Green tensor $\overline{\boldsymbol{G}}$ entering the Born expansion is just the free-space Green tensor $\boldsymbol{G}_{\text{free}}$. After substituting Eqs. (D.1) and (D.2) into Eq. (3.20), the resonant part of the CP potential can be written in the form

$$U_n^{\text{r}}(\boldsymbol{r}_A) = \sum_{K=1}^{\infty} \Delta_K U_n^{\text{r}}(\boldsymbol{r}_A), \tag{D.8}$$

$$\Delta_K U_n^{\text{r}}(\boldsymbol{r}_A) = -\mu_0 \sum_k \Theta(\omega_{nk}) \omega_{nk}^2 \boldsymbol{d}_{nk} \sum_{\lambda_1 \ldots \lambda_K = e,m} \text{Re} \left\{ \left[\prod_{J=1}^{K} \int \mathrm{d}^3 s_J \, f_{\lambda_J}(\boldsymbol{s}_J, \omega_{nk}) \right] \right.$$
$$\left. \cdot \boldsymbol{G}_{0\lambda_1}(\boldsymbol{r}_A, \boldsymbol{s}_1, \omega_{nk}) \cdots \boldsymbol{G}_{\lambda_K 0}(\boldsymbol{s}_K, \boldsymbol{r}_A, \omega_{nk}) \right\} \cdot \boldsymbol{d}_{kn}, \tag{D.9}$$

where we have used the fact that $\boldsymbol{G}_{\text{free}}^{(1)}(\boldsymbol{r}, \boldsymbol{r}', \omega) = \boldsymbol{0}$, recall Eq. (3.16). As a preparation, note that the free-space Green tensor (3.60) may be decomposed into its longitudinal and transverse components according to [170]

$$^{\parallel}\boldsymbol{G}_{\text{free}}^{\parallel}(\boldsymbol{r}, \boldsymbol{r}', \omega) = -\frac{1}{3} \frac{c^2}{\omega^2} \delta(\boldsymbol{\rho}) \boldsymbol{I} - \frac{c^2}{4\pi\omega^2\rho^3} (\boldsymbol{I} - 3\boldsymbol{e}_\rho \boldsymbol{e}_\rho), \tag{D.10}$$

$$^{\perp}\boldsymbol{G}_{\text{free}}^{\perp}(\boldsymbol{r}, \boldsymbol{r}', \omega) = \frac{c^2}{4\pi\omega^2\rho^3} \left([\boldsymbol{I} - 3\boldsymbol{e}_\rho \boldsymbol{e}_\rho] - \left\{ \left[1 - \frac{\mathrm{i}\omega\rho}{c} - \left(\frac{\omega\rho}{c}\right)^2 \right] \boldsymbol{I} \right. \right.$$
$$\left. \left. - \left[3 - \frac{3\mathrm{i}\omega\rho}{c} - \left(\frac{\omega\rho}{c}\right)^2 \right] \boldsymbol{e}_\rho \boldsymbol{e}_\rho \right\} \mathrm{e}^{\mathrm{i}\omega\rho/c} \right), \tag{D.11}$$

implying that

$$\boldsymbol{G}_{\text{free}}(\boldsymbol{r}, \boldsymbol{r}', \omega) \simeq {}^{\parallel}\boldsymbol{G}_{\text{free}}^{\parallel}(\boldsymbol{r}, \boldsymbol{r}', \omega) \quad \text{for } |\omega|\rho/c \ll 1, \tag{D.12}$$

$$\boldsymbol{G}_{\text{free}}(\boldsymbol{r}, \boldsymbol{r}', \omega) \simeq {}^{\perp}\boldsymbol{G}_{\text{free}}^{\perp}(\boldsymbol{r}, \boldsymbol{r}', \omega) \quad \text{for } \omega\rho/c \gg 1 \ (\omega \text{ real}). \tag{D.13}$$

The asymptotic expressions (3.33) and (3.35) for the resonant part of the CP potential follow immediately. In the retarded limit, we have $r_{\min} \gg c/\omega_{\min}$ ($r_{\min}$, minimum distance of the atom to any of the bodies; $\omega_{\min}$, minimum of all relevant atomic and medium resonance frequencies) so that according to Eq. (D.13), the first factor $\boldsymbol{G}_{0\lambda_1}(\boldsymbol{r}_A, \boldsymbol{s}_1, \omega_{nk})$ and the last factor $\boldsymbol{G}_{\lambda_K 0}(\boldsymbol{s}_K, \boldsymbol{r}_A, \omega_{nk})$ appearing in each term of Eq. (D.9) become purely transverse, leading to Eq. (3.33) after recalling Eq. (2.45). Simlarly, Eq. (D.12) shows that in the non-retarded limit, where $r_{\max} \ll c/\omega_{\max}$ ($r_{\max}$, maximum distance of the atom to any body part; $\omega_{\max}$, maximum of all relevant atomic and medium resonance frequencies), the factors $\boldsymbol{G}_{0\lambda_1}(\boldsymbol{r}_A, \boldsymbol{s}_1, \omega_{nk})$ and $\boldsymbol{G}_{\lambda_K 0}(\boldsymbol{s}_K, \boldsymbol{r}_A, \omega_{nk})$ become purely longitudinal, implying Eq. (3.35).

Next, we consider the off-resonant CP potential (3.22) which by means of the Born

expansion (D.1) [together with Eq. (D.2)] can be written in the form [SB10]

$$U_n^{\text{or}}(\boldsymbol{r}_A) = \sum_{K=1}^{\infty} \Delta_K U_n^{\text{or}}(\boldsymbol{r}_A), \tag{D.14}$$

$$\Delta_K U_n^{\text{or}}(\boldsymbol{r}_A) = \frac{\hbar\mu_0}{2\pi} \sum_{\lambda_1\ldots\lambda_K=e,m} \left[\prod_{J=1}^{K} \int \mathrm{d}^3 s_J\, f_{\lambda_J}(\boldsymbol{s}_J, \mathrm{i}\xi)\right] \int_0^{\infty} \mathrm{d}\xi\, \xi^2$$

$$\times \operatorname{tr}\left[\boldsymbol{\alpha}_n(\mathrm{i}\xi)\cdot\boldsymbol{G}_{0\lambda_1}(\boldsymbol{r}_A, \boldsymbol{s}_1, \mathrm{i}\xi)\cdots\boldsymbol{G}_{\lambda_K 0}(\boldsymbol{s}_K, \boldsymbol{r}_A, \mathrm{i}\xi)\right]. \tag{D.15}$$

In the non-retarded limit, the functions $\boldsymbol{\alpha}_n(\mathrm{i}\xi)$ and $f_{\lambda_J}(\boldsymbol{s}_J, \mathrm{i}\xi)$ effectively limit the ξ-integral to a range where $\xi|\boldsymbol{r}_A - \boldsymbol{s}_1|/c,\, \xi|\boldsymbol{s}_K - \boldsymbol{r}_A|/c \leq \omega_{\max} r_{\max}/c \ll 1$, so that the first and last factors of each term (D.15) become purely longitudinal by virtue of Eq. (D.12), leading to the asymptotic form (3.34) of the off-resonant CP potential. In the retarded limit, the condition $\xi|\boldsymbol{r}_A - \boldsymbol{s}_1|/c,\, \xi|\boldsymbol{s}_K - \boldsymbol{r}_A|/c \ll 1$ is violated for the major part of the ξ-integral. As seen from Eqs. (D.10) and (D.11), the contribution from $^{\|}\boldsymbol{G}_{\text{free}}^{\|}$ is then entirely cancelled by a similar term in $^{\perp}\boldsymbol{G}_{\text{free}}^{\perp}$ (implying that the contribution from the $\hat{\boldsymbol{d}}\cdot\hat{\boldsymbol{E}}^{\|}$-interaction is cancelled by a part of the $\hat{\boldsymbol{p}}\cdot\hat{\boldsymbol{A}}$-contribution in this limit) and the ξ-integral over the remaining terms is restricted by the factors $\mathrm{e}^{-\xi|\boldsymbol{r}_A-\boldsymbol{s}_1|/c}$ and $\mathrm{e}^{-\xi|\boldsymbol{s}_K-\boldsymbol{r}_A|/c}$ to a range where $\xi \leq c/r_{\min} \ll \omega_{\min}$, so that one may put

$$\boldsymbol{\alpha}_n(\mathrm{i}\xi) \simeq \boldsymbol{\alpha}_n(0), \qquad f_{\lambda_J}(\boldsymbol{s}_J, \mathrm{i}\xi) \simeq f_{\lambda_J}(\boldsymbol{s}_J, 0) \tag{D.16}$$

which upon recalling Eq. (D.3) leads to the retarded limit of the off-resonant CP potential, Eqs. (3.31) and (3.32). In this limit, the contribution from the $\hat{\boldsymbol{A}}^2$-interaction reads

$$\frac{\mu_0}{\pi} \sum_k \omega_{kn} \int_0^{\infty} \mathrm{d}\xi\, \boldsymbol{d}_{nk}\cdot{}^{\perp}\boldsymbol{G}_{\text{zero}}^{(1)\perp}(\boldsymbol{r}_A, \boldsymbol{r}_A, \mathrm{i}\xi)\cdot\boldsymbol{d}_{kn}; \tag{D.17}$$

it is completely cancelled by the $\hat{\boldsymbol{p}}\cdot\hat{\boldsymbol{A}}$-contribution

$$\frac{\mu_0}{\pi} \sum_k \omega_{kn} \int_0^{\infty} \mathrm{d}\xi \left(-1 + \frac{\xi^2}{\omega_{kn}^2 + \xi^2}\right) \boldsymbol{d}_{nk}\cdot{}^{\perp}\boldsymbol{G}_{\text{zero}}^{(1)\perp}(\boldsymbol{r}_A, \boldsymbol{r}_A, \mathrm{i}\xi)\cdot\boldsymbol{d}_{kn}. \tag{D.18}$$

D.2 Contributions quadratic in χ

The limits of validity of the linear Born expansion to the ground-state potential can best be probed by considering the second-order corrections, where for the sake of simplicity, we restrict our attention to the case of purely dielectric bodies. In this case, the quadratic correction $\Delta_2 U(\boldsymbol{r}_A)$, as given by Eq. (D.15) together with Eqs. (D.3)–(D.7), can be separated into a single-point term and a two-point term,

$$\Delta_2 U(\boldsymbol{r}_A) = \Delta_2^1 U(\boldsymbol{r}_A) + \Delta_2^2 U(\boldsymbol{r}_A) \tag{D.19}$$

where the single-point term

$$\Delta_2^1 U(\boldsymbol{r}_A) = \frac{\hbar}{96\pi^3\varepsilon_0} \int \frac{\mathrm{d}^3 s}{|\boldsymbol{r}_A - \boldsymbol{s}|^6} \int_0^\infty \mathrm{d}\xi\, \alpha(\mathrm{i}\xi)\chi^2(\boldsymbol{s}, \mathrm{i}\xi)g(\xi|\boldsymbol{r}_A - \boldsymbol{s}|/c) \tag{D.20}$$

which arises from the δ-function in Eq. (3.60), can be obtained from the linear contribution (3.63) by making the replacement

$$\chi(\boldsymbol{r}, \omega) \mapsto -\frac{1}{3}\,\chi^2(\boldsymbol{r}, \omega). \tag{D.21}$$

Its asymptotic retarded and non-retarded forms can hence be obtained by applying the same replacement to Eqs. (3.66) and (3.67), respectively.

Recalling Eq. (3.61), the two-point term is derived to be [SB10]

$$\Delta_2^2 U(\boldsymbol{r}_A) = \frac{\hbar}{128\pi^4\varepsilon_0} \int \mathrm{d}^3 s_1\, \chi(\boldsymbol{s}_1, \mathrm{i}\xi) \int \mathrm{d}^3 s_2\, \chi(\boldsymbol{s}_2, \mathrm{i}\xi) \int_0^\infty \mathrm{d}\xi\, \alpha(\mathrm{i}\xi) \frac{g(\xi, \boldsymbol{\alpha}, \boldsymbol{\beta}, \boldsymbol{\gamma})}{\alpha^3\beta^3\gamma^3} \tag{D.22}$$

where

$$\begin{aligned}
g(\xi, \boldsymbol{\alpha}, \boldsymbol{\beta}, \boldsymbol{\gamma}) = \mathrm{e}^{-\xi(\alpha+\beta+\gamma)/c}\Bigg[&3a\left(\frac{\xi\alpha}{c}\right)a\left(\frac{\xi\beta}{c}\right)a\left(\frac{\xi\gamma}{c}\right) - b\left(\frac{\xi\alpha}{c}\right)a\left(\frac{\xi\beta}{c}\right)a\left(\frac{\xi\gamma}{c}\right) \\
&- a\left(\frac{\xi\alpha}{c}\right)b\left(\frac{\xi\beta}{c}\right)a\left(\frac{\xi\gamma}{c}\right) - a\left(\frac{\xi\alpha}{c}\right)a\left(\frac{\xi\beta}{c}\right)b\left(\frac{\xi\gamma}{c}\right) + b\left(\frac{\xi\alpha}{c}\right)b\left(\frac{\xi\beta}{c}\right)a\left(\frac{\xi\gamma}{c}\right)(\boldsymbol{e}_\alpha\cdot\boldsymbol{e}_\beta)^2 \\
&+ a\left(\frac{\xi\alpha}{c}\right)b\left(\frac{\xi\beta}{c}\right)b\left(\frac{\xi\gamma}{c}\right)(\boldsymbol{e}_\beta\cdot\boldsymbol{e}_\gamma)^2 + b\left(\frac{\xi\alpha}{c}\right)a\left(\frac{\xi\beta}{c}\right)b\left(\frac{\xi\gamma}{c}\right)(\boldsymbol{e}_\gamma\cdot\boldsymbol{e}_\alpha)^2 \\
&- b\left(\frac{\xi\alpha}{c}\right)b\left(\frac{\xi\beta}{c}\right)b\left(\frac{\xi\gamma}{c}\right)(\boldsymbol{e}_\alpha\cdot\boldsymbol{e}_\beta)(\boldsymbol{e}_\beta\cdot\boldsymbol{e}_\gamma)(\boldsymbol{e}_\gamma\cdot\boldsymbol{e}_\alpha)\Bigg],
\end{aligned} \tag{D.23}$$

with the definitions

$$a(x) = 1 + x + x^2, \qquad b(x) = 3 + 3x + x^2, \tag{D.24}$$

and

$$\boldsymbol{\alpha} = \boldsymbol{r}_A - \boldsymbol{s}_1, \qquad \alpha = |\boldsymbol{\alpha}|, \qquad \boldsymbol{e}_\alpha = \boldsymbol{\alpha}/\alpha, \tag{D.25}$$

$$\boldsymbol{\beta} = \boldsymbol{s}_1 - \boldsymbol{s}_2, \qquad \beta = |\boldsymbol{\beta}|, \qquad \boldsymbol{e}_\beta = \boldsymbol{\beta}/\beta, \tag{D.26}$$

$$\boldsymbol{\gamma} = \boldsymbol{s}_2 - \boldsymbol{r}_A, \qquad \gamma = |\boldsymbol{\gamma}|, \qquad \boldsymbol{e}_\gamma = \boldsymbol{\gamma}/\gamma \tag{D.27}$$

having been introduced. Note that the two-point contribution to the CP potential is a double spatial integral, the integrand of which can be attractive or repulsive, depending on the angles in the triangle formed by the vectors $\boldsymbol{\alpha}$, $\boldsymbol{\beta}$ and $\boldsymbol{\gamma}$. Obviously, the double spatial integral leads to a breakdown of the additivity of CP forces so that within quadratic (or higher) order in χ, the force due to two or more bodies, is not simply the sum of the forces due to the individual bodies.

In the retarded limit, we apply the approximations $\alpha(\mathrm{i}\xi) \simeq \alpha(0)$, $\chi(\boldsymbol{s}, \mathrm{i}\xi) \simeq \chi(\boldsymbol{s}, 0)$, so that Eq. (D.22) reduces to

$$\Delta_2^2 U(\boldsymbol{r}_A) = \frac{\hbar\alpha(0)}{128\pi^4\varepsilon_0} \int \mathrm{d}^3 s_1 \int \mathrm{d}^3 s_2 \frac{\chi(\boldsymbol{s}_1, 0)\chi(\boldsymbol{s}_2, 0)}{\alpha^3\beta^3\gamma^3} \int_0^\infty \mathrm{d}\xi\, g(\xi, \boldsymbol{\alpha}, \boldsymbol{\beta}, \boldsymbol{\gamma}). \tag{D.28}$$

We introduce the notation

$$\sigma_i = \alpha^i + \beta^i + \gamma^i, \quad \text{for } i = 1, 2, 3 \tag{D.29}$$

and perform the ξ-integral with the aid of the relation

$$\int_0^\infty \mathrm{d}\xi \left(\frac{\xi}{c}\right)^j \mathrm{e}^{-\xi\sigma_1/c} = \frac{j!\, c}{\sigma_1^{j+1}}. \tag{D.30}$$

Exploiting the triangle formula

$$a_\bigtriangledown \equiv 1 - (\boldsymbol{e}_\alpha \cdot \boldsymbol{e}_\beta)^2 - (\boldsymbol{e}_\beta \cdot \boldsymbol{e}_\gamma)^2 - (\boldsymbol{e}_\gamma \cdot \boldsymbol{e}_\alpha)^2 + 2(\boldsymbol{e}_\alpha \cdot \boldsymbol{e}_\beta)(\boldsymbol{e}_\beta \cdot \boldsymbol{e}_\gamma)(\boldsymbol{e}_\gamma \cdot \boldsymbol{e}_\alpha) = 0 \tag{D.31}$$

[which is a trivial consequence of Eqs. (D.25)–(D.27)] by adding the expression

$$6a_\bigtriangledown + \frac{6a_\bigtriangledown}{\sigma_1^6} \left\{ \left[\alpha^5(\beta + \gamma) + \beta^5(\gamma + \alpha) + \gamma^5(\alpha + \beta)\right] + 7\left[\alpha^4(\beta^2 + \gamma^2) + \beta^4(\gamma^2 + \alpha^2)\right. \right.$$
$$\left. + \gamma^4(\alpha^2 + \beta^2)\right] + 12(\alpha^3\beta^3 + \beta^3\gamma^3 + \gamma^3\alpha^3) + 12\alpha\beta\gamma(\alpha^3 + \beta^3 + \gamma^3)$$
$$\left. + 52\alpha\beta\gamma\left[\alpha\beta(\alpha + \beta) + \beta\gamma(\beta + \gamma) + \gamma\alpha(\gamma + \alpha)\right] + 138\alpha^2\beta^2\gamma^2 \right\} \tag{D.32}$$

to Eq. (D.28), the result may be written in the form

$$\Delta_2^2 U(\boldsymbol{r}_A) = \frac{\hbar c\alpha(0)}{32\pi^4\varepsilon_0} \int \mathrm{d}^3 s_1 \int \mathrm{d}^3 s_2 \frac{\chi(\boldsymbol{s}_1, 0)\chi(\boldsymbol{s}_2, 0)}{\alpha^3\beta^3\gamma^3(\alpha + \beta + \gamma)} \left[f_1(\alpha, \beta, \gamma) + f_2(\gamma, \alpha, \beta)(\boldsymbol{e}_\alpha \cdot \boldsymbol{e}_\beta)^2 \right.$$
$$\left. + f_2(\alpha, \beta, \gamma)(\boldsymbol{e}_\beta \cdot \boldsymbol{e}_\gamma)^2 + f_2(\beta, \gamma, \alpha)(\boldsymbol{e}_\gamma \cdot \boldsymbol{e}_\alpha)^2 + f_3(\alpha, \beta, \gamma)(\boldsymbol{e}_\alpha \cdot \boldsymbol{e}_\beta)(\boldsymbol{e}_\beta \cdot \boldsymbol{e}_\gamma)(\boldsymbol{e}_\gamma \cdot \boldsymbol{e}_\alpha)\right] \tag{D.33}$$

where

$$f_1(\alpha, \beta, \gamma) = 9 - \frac{39\sigma_2}{\sigma_1^2} + 22\frac{\sigma_3}{\sigma_1^3} + \frac{54\sigma_2^2}{\sigma_1^4} - \frac{65\sigma_2\sigma_3}{\sigma_1^5} + \frac{20\sigma_3^2}{\sigma_1^6}, \tag{D.34}$$

$$f_2(\alpha, \beta, \gamma) = 3\left[\frac{\alpha^2}{\sigma_1^2} + \frac{3\alpha^2(\beta + \gamma)}{\sigma_1^3} + \frac{4\beta\gamma(3\alpha^2 - \beta\gamma)}{\sigma_1^4} - \frac{20\alpha\beta^2\gamma^2}{\sigma_1^5}\right], \tag{D.35}$$

$$f_3(\alpha, \beta, \gamma) = -1 - \frac{39\sigma_2}{\sigma_1^2} + \frac{17\sigma_3}{\sigma_1^3} + \frac{72\sigma_2^2}{\sigma_1^4} - \frac{75\sigma_2\sigma_3}{\sigma_1^5} + \frac{20\sigma_3^2}{\sigma_1^6}. \tag{D.36}$$

In the non-retarded limit, we may approximate

$$g(\xi, \boldsymbol{\alpha}, \boldsymbol{\beta}, \boldsymbol{\gamma}) \simeq g(0, \boldsymbol{\alpha}, \boldsymbol{\beta}, \boldsymbol{\gamma}) = 3\left[1 - 3(\boldsymbol{e}_\alpha \cdot \boldsymbol{e}_\beta)(\boldsymbol{e}_\beta \cdot \boldsymbol{e}_\gamma)(\boldsymbol{e}_\gamma \cdot \boldsymbol{e}_\alpha)\right] \tag{D.37}$$

[recall Eq. (D.31)], so Eq. (D.22) reduces to

$$\Delta_2^2 U(\boldsymbol{r}_A) = \frac{3\hbar}{128\pi^4\varepsilon_0} \int \mathrm{d}^3 s_1 \int \mathrm{d}^3 s_2 \int_0^\infty \mathrm{d}\xi\, \alpha(\mathrm{i}\xi)\chi(\boldsymbol{s}_1, \mathrm{i}\xi)\chi(\boldsymbol{s}_2, \mathrm{i}\xi)$$
$$\times \frac{1 - 3(\boldsymbol{e}_\alpha \cdot \boldsymbol{e}_\beta)(\boldsymbol{e}_\beta \cdot \boldsymbol{e}_\gamma)(\boldsymbol{e}_\gamma \cdot \boldsymbol{e}_\alpha)}{\alpha^3\beta^3\gamma^3}. \tag{D.38}$$

Note that by using the general relation (3.94), the above results can be used to infer general expressions for the three-atom potential $U_{ABC}(\boldsymbol{r}_{AB}, \boldsymbol{r}_{BC}, \boldsymbol{r}_{CA})$ of polarisable ground-state atoms in free space. Thus, Eq. (D.22) implies that [SB10]

$$U_{ABC}(\boldsymbol{r}_{AB}, \boldsymbol{r}_{BC}, \boldsymbol{r}_{CA}) = \frac{\hbar}{64\pi^4\varepsilon_0^3} \int_0^\infty \mathrm{d}\xi\, \alpha_A(\mathrm{i}\xi)\alpha_B(\mathrm{i}\xi)\alpha_C(\mathrm{i}\xi) \frac{g(\xi, \boldsymbol{r}_{AB}, \boldsymbol{r}_{BC}, \boldsymbol{r}_{CA})}{r_{AB}^3 r_{BC}^3 r_{CA}^3} \quad \text{(D.39)}$$

[recall Eqs. (D.23) and (D.24), where $\boldsymbol{r}_{ij} = \boldsymbol{r}_i - \boldsymbol{r}_j$, $r_{ij} = |\boldsymbol{r}_{ij}|$, $\boldsymbol{e}_{ij} = \boldsymbol{r}_{ij}/r_{ij}$ for $i, j = A, B, C$] which is in agreement with the result found in Refs. [184, 193]. Equations (D.33) and (D.38) show that the three-atom potential simplifies to

$$U_{ABC}(\boldsymbol{r}_{AB}, \boldsymbol{r}_{BC}, \boldsymbol{r}_{CA}) = \frac{\hbar c \alpha_A(0)\alpha_B(0)\alpha_C(0)}{16\pi^4\varepsilon_0^3 r_{AB}^3 r_{BC}^3 r_{CA}^3 (r_{AB}+r_{BC}+r_{CA})} \big[f_1(r_{AB}, r_{BC}, r_{CA})$$

$$+ f_2(r_{CA}, r_{AB}, r_{BC})(\boldsymbol{e}_{AB}\!\cdot\!\boldsymbol{e}_{BC})^2 + f_2(r_{AB}, r_{BC}, r_{CA})(\boldsymbol{e}_{BC}\!\cdot\!\boldsymbol{e}_{CA})^2 + f_2(r_{BC}, r_{CA}, r_{AB})$$

$$\times (\boldsymbol{e}_{CA}\!\cdot\!\boldsymbol{e}_{AB})^2 + f_3(r_{AB}, r_{BC}, r_{CA})(\boldsymbol{e}_{AB}\!\cdot\!\boldsymbol{e}_{BC})(\boldsymbol{e}_{BC}\!\cdot\!\boldsymbol{e}_{CA})(\boldsymbol{e}_{CA}\!\cdot\!\boldsymbol{e}_{AB}) \big] \quad \text{(D.40)}$$

[recall Eqs. (D.34)–(D.36) where $\sigma_i = r_{AB}^i + r_{BC}^i + r_{CA}^i$] in the retarded limit (defined by $r_{AB}+r_{BC}+r_{CA} \gg c/\omega_{\min}$) and reduces to the Axilrod–Teller potential [194]

$$U_{ABC}(\boldsymbol{r}_{AB}, \boldsymbol{r}_{BC}, \boldsymbol{r}_{CA}) = \frac{3\hbar\big[1 - 3(\boldsymbol{e}_{AB}\!\cdot\!\boldsymbol{e}_{BC})(\boldsymbol{e}_{BC}\!\cdot\!\boldsymbol{e}_{CA})(\boldsymbol{e}_{CA}\!\cdot\!\boldsymbol{e}_{AB})\big]}{64\pi^4\varepsilon_0^3 r_{AB}^3 r_{BC}^3 r_{CA}^3}$$

$$\times \int_0^\infty \mathrm{d}\xi\, \alpha_A(\mathrm{i}\xi)\alpha_B(\mathrm{i}\xi)\alpha_C(\mathrm{i}\xi) \quad \text{(D.41)}$$

in the non-retarded limit (where $r_{AB}+r_{BC}+r_{CA} \ll c/\omega_{\max}$).

Appendix E

Atom–field dynamics

In this appendix, we address some aspects of the atom–field dynamics which are relevant for calculating the time-dependent CP force in Secs. 4.2.1 and 4.3.2. Let us begin with the Heisenberg equations of motion for the operators $\hat{A}_{mn}$ which are relevant for finding the dipole–dipole correlation function (4.32) in Sec. 4.2.1. Using Hamiltonian (2.86) together with Eqs. (2.87), (2.88) and (2.94), one finds that for nonrelativistic centre-of-mass motion[1]

$$\dot{\hat{A}}_{mn} = \frac{\mathrm{i}}{\hbar}\big[\hat{H},\hat{A}_{mn}\big] = \mathrm{i}\omega_{mn}\hat{A}_{mn} + \frac{\mathrm{i}}{\hbar}\sum_k \int_0^\infty \mathrm{d}\omega \bigg[\big(\boldsymbol{d}_{nk}\hat{A}_{mk} - \boldsymbol{d}_{km}\hat{A}_{kn}\big)\cdot\underline{\hat{\boldsymbol{E}}}(\hat{\boldsymbol{r}}_A,\omega)$$
$$+ \underline{\hat{\boldsymbol{E}}}^\dagger(\hat{\boldsymbol{r}}_A,\omega)\cdot\big(\boldsymbol{d}_{nk}\hat{A}_{mk} - \boldsymbol{d}_{km}\hat{A}_{kn}\big)\bigg]. \quad (\mathrm{E}.1)$$

Recalling Eq. (2.23) as well as Eqs. (4.22)–(4.24), the frequency components of the electric field can be written as

$$\underline{\hat{\boldsymbol{E}}}[\hat{\boldsymbol{r}}_A(t),\omega,t] = \underline{\hat{\boldsymbol{E}}}_{\mathrm{free}}[\hat{\boldsymbol{r}}_A(t),\omega,t] + \underline{\hat{\boldsymbol{E}}}_{\mathrm{source}}[\hat{\boldsymbol{r}}_A(t),\omega,t] \quad (\mathrm{E}.2)$$

with

$$\underline{\hat{\boldsymbol{E}}}_{\mathrm{free}}[\hat{\boldsymbol{r}}_A(t),\omega,t] = \mathrm{e}^{-\mathrm{i}\omega(t-t_0)}\sum_{\lambda=e,m}\int \mathrm{d}^3 r\, \boldsymbol{G}_\lambda[\hat{\boldsymbol{r}}_A(t),\boldsymbol{r},\omega]\cdot\hat{\boldsymbol{f}}_\lambda(\boldsymbol{r},\omega) \quad (\mathrm{E}.3)$$

$$\underline{\hat{\boldsymbol{E}}}_{\mathrm{source}}[\hat{\boldsymbol{r}}_A(t),\omega,t] = \frac{\mathrm{i}\mu_0}{\pi}\,\omega^2\int_{t_0}^t \mathrm{d}\tau\, \mathrm{e}^{-\mathrm{i}\omega(t-\tau)}\sum_{k,l}\mathrm{Im}\,\boldsymbol{G}[\hat{\boldsymbol{r}}_A(t),\hat{\boldsymbol{r}}_A(\tau),\omega]\cdot\boldsymbol{d}_{kl}\hat{A}_{kl}(\tau). \quad (\mathrm{E}.4)$$

We substitute Eqs. (E.2)–(E.4) into Eq. (E.1). We assume sufficiently slow centre-of-mass motion and weak–atom field coupling so that the time integral can then be evaluated using the Born–Oppenheimer and Markov approximations, i.e., by putting $\hat{\boldsymbol{r}}_A(\tau)\simeq\hat{\boldsymbol{r}}_A(t)\mapsto\boldsymbol{r}_A$ and $\langle\hat{A}_{mn}(\tau)\rangle\simeq\mathrm{e}^{-\mathrm{i}\tilde{\omega}_{mn}(\boldsymbol{r}_A)(t-\tau)}\langle\hat{A}_{mn}(t)\rangle$ and letting the lower integration limit tend to $t_0\to-\infty$,

$$\int_{-\infty}^t \mathrm{d}\tau\, \mathrm{e}^{-\mathrm{i}[\omega-\tilde{\omega}_{nm}(\boldsymbol{r}_A)](t-\tau)} = \pi\delta[\omega-\tilde{\omega}_{nm}(\boldsymbol{r}_A)] + \mathrm{i}\mathcal{P}\,\frac{1}{\tilde{\omega}_{nm}(\boldsymbol{r}_A)-\omega}\,. \quad (\mathrm{E}.5)$$

As a result, we obtain

$$\dot{\hat{A}}_{mn} = \mathrm{i}\omega_{mn}\hat{A}_{mn} + \frac{\mathrm{i}}{\hbar}\sum_k \int_0^\infty \mathrm{d}\omega \bigg[\big(\boldsymbol{d}_{nk}\hat{A}_{mk} - \boldsymbol{d}_{km}\hat{A}_{kn}\big)\cdot\underline{\hat{\boldsymbol{E}}}_{\mathrm{free}}(\hat{\boldsymbol{r}}_A,\omega)$$
$$+ \underline{\hat{\boldsymbol{E}}}^\dagger_{\mathrm{free}}(\hat{\boldsymbol{r}}_A,\omega)\cdot\big(\boldsymbol{d}_{nk}\hat{A}_{mk} - \boldsymbol{d}_{km}\hat{A}_{kn}\big)\bigg] + \sum_{k,l}\big[\boldsymbol{d}_{km}\cdot\boldsymbol{C}_{nl}(\boldsymbol{r}_A)\hat{A}_{kl} - \boldsymbol{d}_{nk}\cdot\boldsymbol{C}_{kl}(\boldsymbol{r}_A)\hat{A}_{ml}$$
$$+ \boldsymbol{d}_{nk}\cdot\boldsymbol{C}^*_{ml}(\boldsymbol{r}_A)\hat{A}_{lk} - \boldsymbol{d}_{km}\cdot\boldsymbol{C}^*_{kl}(\boldsymbol{r}_A)\hat{A}_{ln}\big] \quad (\mathrm{E}.6)$$

---

[1] Note that as in Secs. 4.2 and 4.3 we drop the primes identifying the operators in the multipolar scheme; this will be done throughout this appendix.

where we have defined

$$
\begin{aligned}
\boldsymbol{C}_{kn}(\boldsymbol{r}_A) = {} & \frac{\mu_0}{\hbar}\,\Theta[\tilde{\omega}_{nk}(\boldsymbol{r}_A)]\,\tilde{\omega}_{nk}^2(\boldsymbol{r}_A)\,\mathrm{Im}\,\boldsymbol{G}\left[\boldsymbol{r}_A, \boldsymbol{r}_A, \tilde{\omega}_{nk}(\boldsymbol{r}_A)\right]\!\cdot\!\boldsymbol{d}_{kn} \\
& + \frac{\mathrm{i}\mu_0}{\pi\hbar}\,\mathcal{P}\int_0^\infty \mathrm{d}\omega\,\omega^2 \frac{\mathrm{Im}\,\boldsymbol{G}(\boldsymbol{r}_A, \boldsymbol{r}_A, \omega)\!\cdot\!\boldsymbol{d}_{kn}}{\tilde{\omega}_{nk}(\boldsymbol{r}_A) - \omega}\,. \quad (\mathrm{E}.7)
\end{aligned}
$$

Taking expectation values of Eq. (E.6), we note that the free fields do not contribute according to Eq. (4.30), recall Eq. (2.95). Assuming that the relevant atomic transition frequencies are well-separated from one another, the resulting differential equations for the off-diagonal density matrix elements decouple from one another as well as from the diagonal ones. By using the identities

$$
\boldsymbol{d}_{nk}\!\cdot\!\boldsymbol{C}_{kn}(\boldsymbol{r}_A) = \mathrm{i}\delta\omega_n^k(\boldsymbol{r}_A) + \Gamma_n^k(\boldsymbol{r}_A)/2, \qquad \boldsymbol{d}_{kn}\!\cdot\!\boldsymbol{C}_{kn}^*(\boldsymbol{r}_A) = -\mathrm{i}\delta\omega_n^k(\boldsymbol{r}_A) + \Gamma_n^k(\boldsymbol{r}_A)/2, \quad (\mathrm{E}.8)
$$

[which are a direct consequence of definitions (4.36), (4.38) and (E.7)], one hence arrives at Eqs. (4.50) and (4.51). Equation (4.33) follows after employing the quantum regression theorem.

The Markov approximation can also be used to determine the effect of the residual field continuum in the Schrödinger equation (4.88) which appears in Sec. 4.3.2. Using the steps outlined above Eq. (E.5), one calculates

$$
\begin{aligned}
\int_0^\infty \mathrm{d}\omega\, g'^2(\boldsymbol{r}_A, \omega) &\int_{t_0}^t \mathrm{d}\tau\, \mathrm{e}^{-\mathrm{i}(E_0/\hbar + \omega)(t-\tau)}\psi_1(\tau) \\
&\simeq \psi_1(t)\int_0^\infty \mathrm{d}\omega\, g'^2(\boldsymbol{r}_A, \omega)\int_{-\infty}^t \mathrm{d}\tau\, \mathrm{e}^{-\mathrm{i}[\hbar\omega - \tilde{E}_1(\boldsymbol{r}_A) + E_0](t-\tau)/\hbar} \\
&= \left[\mathrm{i}\delta\omega_1'(\boldsymbol{r}_A) + \Gamma_1'(\boldsymbol{r}_A)/2\right]\psi_1(t) \quad (\mathrm{E}.9)
\end{aligned}
$$

where we have recalled Eq. (4.73) and introduced Eqs. (4.92) and (4.93). Substituting Eqs. (4.73) and (E.9) into Eq. (4.88) and using Eq. (4.87), one finds

$$
\begin{aligned}
\dot{\psi}_1(t) = {} & \left[-\mathrm{i}E_1/\hbar - \mathrm{i}\delta\omega_1'(\boldsymbol{r}_A) - \Gamma_1'(\boldsymbol{r}_A)/2\right]\psi_1(t) - \tfrac{1}{2}\mathrm{i}\Omega_\mathrm{R}(\boldsymbol{r}_A)\sin\theta\, \mathrm{e}^{[-\mathrm{i}(E_0/\hbar + \omega_\nu) - \gamma_\nu/2](t-t_0)} \\
& - \tfrac{1}{4}\Omega_\mathrm{R}^2(\boldsymbol{r}_A)\int_{t_0}^t \mathrm{d}\tau\, \mathrm{e}^{[-\mathrm{i}(E_0/\hbar + \omega_\nu) - \gamma_\nu/2](t-\tau)}\psi_1(\tau). \quad (\mathrm{E}.10)
\end{aligned}
$$

By writing $\psi_1(t)$ in the form of Eq. (4.89), this result is transformed to

$$
\begin{aligned}
\dot{\phi}_1(t) = {} & -\tfrac{1}{2}\mathrm{i}\Omega_\mathrm{R}(\boldsymbol{r}_A)\sin\theta\, \mathrm{e}^{\{-\mathrm{i}\Delta(\boldsymbol{r}_A) - [\gamma_\nu - \Gamma_1'(\boldsymbol{r}_A)]/2\}(t-t_0)} \\
& - \tfrac{1}{4}\Omega_\mathrm{R}^2(\boldsymbol{r}_A)\int_{t_0}^t \mathrm{d}\tau\, \mathrm{e}^{\{-\mathrm{i}\Delta(\boldsymbol{r}_A) - [\gamma_\nu - \Gamma_1'(\boldsymbol{r}_A)]/2\}(t-\tau)}\phi_1(\tau), \quad (\mathrm{E}.11)
\end{aligned}
$$

and after differentiating with respect to t, we arrive at Eq. (4.90).

Appendix F

Magnetic part of the Casimir–Polder force

In this appendix, the magnetic part of the CP force that appears in Sec. 4.3.2, is provided. Upon using Eq. (2.27), $\boldsymbol{F}^{\mathrm{mag}}(\boldsymbol{r}_A, t)$ as defined in Eq. (4.76) can for a two-level atom in rotating-wave approximation be written in the form

$$\boldsymbol{F}^{\mathrm{mag}}(\boldsymbol{r}_A, t) = \left\{ \frac{\mathrm{d}}{\mathrm{d}t} \sum_{\lambda=e,m} \int \mathrm{d}^3 r' \int_0^\infty \frac{\mathrm{d}\omega}{\mathrm{i}\omega} \langle \psi(t)| \boldsymbol{d}_{10} \times \left[\boldsymbol{\nabla} \times \boldsymbol{G}_\lambda(\boldsymbol{r}, \boldsymbol{r}', \omega) \right] \cdot \hat{\boldsymbol{f}}_\lambda(\boldsymbol{r}', \omega) |1\rangle\langle 0| \right.$$
$$\left. \times |\psi(t)\rangle \right\}_{\boldsymbol{r}=\boldsymbol{r}_A} + \mathrm{C.c.} \quad (\mathrm{F.1})$$

and substitution of Eq. (4.79) for $|\psi(t)\rangle$ results in

$$\boldsymbol{F}^{\mathrm{mag}}(\boldsymbol{r}_A, t) = \frac{\mathrm{i}\mu_0}{\pi} \int_0^\infty \mathrm{d}\omega \, \omega \, \frac{\boldsymbol{d}_{10} \times \left[\boldsymbol{\nabla} \times \mathrm{Im}\,\boldsymbol{G}(\boldsymbol{r}, \boldsymbol{r}_A, \omega) \cdot \boldsymbol{d}_{01} \right]_{\boldsymbol{r}=\boldsymbol{r}_A}}{g(\boldsymbol{r}_A, \omega)} \frac{\mathrm{d}}{\mathrm{d}t} \left[\psi_1^*(t) \psi_0(\omega, t) \right] + \mathrm{C.c.}$$
$$(\mathrm{F.2})$$

In close analogy to the derivation of Eq. (4.97), we next eliminate $\psi_0(\omega, t)$ by means of Eq. (4.85) and make use of the solution (4.89) [together with Eq. (4.94)] for $\psi_1(t)$, leading to Eq. (4.100).

Next, we consider the limiting cases of weak and strong atom–field coupling. The magnetic part of the CP force for weak coupling follows from Eq. (F.2) after use of Eqs. (4.85) and (4.102). Carrying out the time derivative and evaluating the time integral in the spirit of the Markov approximation by putting $|\psi_1(\tau)|^2 \mapsto |\psi_1(t)|^2$ and letting the lower integration limit tend to $-\infty$, one finds that the magnetic part of the CP force vanishes for weak atom–field coupling, when the system is initially prepared in the state $|1\rangle|\{0\}\rangle$.

For strong atom–field coupling, Eq. (4.100) may be simplified by means of Eq. (4.105). Following the steps outline above Eq. (4.112) and discarding terms of order $O[\gamma(\boldsymbol{r}_A)/\omega_\nu]$, one obtains

$$\boldsymbol{F}^{\mathrm{mag}}(\boldsymbol{r}_A, t) = \mathrm{e}^{-\gamma(\boldsymbol{r}_A)(t-t_0)} \left[\frac{c_-^*(\boldsymbol{r}_A) c_+(\boldsymbol{r}_A) \mathrm{e}^{-\mathrm{i}\Omega(\boldsymbol{r}_A)(t-t_0)}}{\Delta(\boldsymbol{r}_A) - \Omega(\boldsymbol{r}_A) - \mathrm{i}\left[\gamma_\nu - \Gamma_1'(\boldsymbol{r}_A)\right]/2} \right.$$
$$\left. - \frac{c_+^*(\boldsymbol{r}_A) c_-(\boldsymbol{r}_A) \mathrm{e}^{\mathrm{i}\Omega(\boldsymbol{r}_A)(t-t_0)}}{\Delta(\boldsymbol{r}_A) + \Omega(\boldsymbol{r}_A) - \mathrm{i}\left[\gamma_\nu - \Gamma_1'(\boldsymbol{r}_A)\right]/2} \right]$$
$$\times \mu_0 \omega_\nu \gamma_\nu \Omega_{\mathrm{R}}(\boldsymbol{r}_A) \boldsymbol{d}_{10} \times \left[\boldsymbol{\nabla} \times \mathrm{Im}\,\boldsymbol{G}(\boldsymbol{r}, \boldsymbol{r}_A, \omega_\nu) \cdot \boldsymbol{d}_{01} \right]_{\boldsymbol{r}=\boldsymbol{r}_A} + \mathrm{C.c.} \quad (\mathrm{F.3})$$

which after neglecting terms of the form $[\gamma_\nu - \Gamma_1'(\boldsymbol{r}_A)]/2$ further simplifies to Eq. (4.124).

Acknowledgements

Zusammenfassung

Casimir–Polder-Kräfte zwischen einzelnen Atomen und makroskopischen Körpern sind langreichweitige effektive elektromagnetische Kräfte zwischen neutralen, (elektrisch und magnetisch) unpolarisierten Objekten, und als solche ein Spezialfall der sogenannten Dispersionskräfte. Alle Dispersionskräfte haben ihren gemeinsamen physikalischen Ursprung in den quantenmechanischen Grundzustandsfluktuationen, die gemäß der Heisenbergschen Unschärferelation ein absolutes Verschwinden der Polarisation und Magnetisierung der beteiligten Objekte einerseits sowie des elektromagnetischen Feldes andererseits verhindern und über die Wechselwirkung von Polarisation und Feld letztlich zur besagten Kraft führen. Sie spielen eine wesentliche Rolle in den verschiedensten Feldern, wie z. B. in den Materialwissenschaften, in der physikalischen Chemie und in der Biologie. Die Erforschung der Casimir–Polder-Kräfte hat in jüngerer Zeit aufgrund fortgeschrittener Techniken zur Manipulation und Kontrolle einzelner Atome eine neue und verstärkte Aktualität erhalten. In Folge der resultierenden Präzisionsmessungen von Casimir–Polder-Kräften hat sich die Perspektive einer gezielten Kontrolle oder sogar Nutzung des Phänomens eröffnet. So muss der Einfluss von Casimir–Polder-Kräften in modernen Anwendungen der Nanotechnologie wie z. B. der Konstruktion von atomaren Fallen mit fortschreitender Miniaturisierung zunehmend berücksichtigt werden. Speziell die Rolle magnetischer Körpereigenschaften beim Zustandekommen Casimir–Polder-Kraft hat durch die kürzlich gelungene Entwicklung von Metamaterialien mit kontrollierbaren magnetoelektrischen Eigenschaften zusätzlich an Relevanz gewonnen.

Der Vielzahl an praktisch relevanten Szenarien steht eine ebenso große Vielfalt theoretischer Methoden gegenüber, die in der Vergangenheit entwickelt worden sind und jeweils ihre eigenen Vor- und Nachteile sowie intrinsischen Gültigkeitsbereiche mitbringen. Speziell liefert die Normalmoden-Quantenelektrodynamik einen exakten Zugang, der jedoch den Nachteil hat, dass jedes neue Szenario eine neue Rechnung erforderlich macht. Demgegenüber liefern auf der Theorie der linearen Antwort basierende Zugänge universell anwendbare Resultate, deren Gültigkeit allerdings bislang nur semiphänomenologisch gezeigt werden konnte. Der Großteil der durchgeführten Untersuchungen beschränkt sich zudem auf eine rein statische Beschreibung der Casimir–Polder-Kräfte.

Vor diesem Hintergrund ist eine exakte Theorie wünschenswert, die einen vereinheitlichten Zugang liefert und zugleich den Anforderungen und Möglichkeiten moderner Experimente und Anwendungen Rechenschaft trägt. Im Rahmen der vorliegenden Dissertation wird eine solche Theorie der Casimir–Polder-Kräfte auf einzelne Atome bei Anwesenheit makroskopischer Körper entwickelt. Ziel sind dabei insbesondere universelle, leicht auf spe-

zielle Geometrien anwendbare Ergebnisse, welche

- sowohl für elektrische als auch für magnetische Körper gültig sind,
- die dispersiven und absorptiven Eigenschaften der Körper angemessen berücksichtigen,
- Lokalfeldeffekte mit einbeziehen,
- eine Beziehung zu mikroskopischen van-der-Waals-Kräften herstellen lassen,
- den Einfluss der atomaren Linienbreiten und -verschiebungen transparent machen,
- die zeitliche Abhängigkeit der Kräfte korrekt wiedergeben,
- sowohl für starke als auch für schwache Atom–Feld-Kopplung anwendbar sind.

Als Grundlage für die Untersuchungen wurde im Rahmen der vorliegenden Arbeit eine makroskopische Quantenelektrodynamik in linearen Elektrika auf den magnetoelektrischen Fall erweitert. Ausgangspunkt ist eine makroskopische Beschreibung der vorhandenen Körper mittels ihrer elektrischen Permittivität und magnetischen Permeabilität – ein Ansatz, dessen Gültigkeitsbereich sich bis hin zu mikroskopischen Atom–Körper-Abständen reicht. Die Feldquantisierung beruht im Wesentlichen auf dem Lösen einer verallgemeinerten Helmholtzgleichung für das elektromagnetische Feld im Medium mit Hilfe des Greentensors, unter Berücksichtigung der bei absorptiven Medien zwangsläufig auftretenden Rauschterme. Die Wechselwirkung des quantisierten elektromagnetischen Feldes mit einem einzelnen Atom wird in kanonischer Weise über die minimale oder multipolare Kopplung eingeführt. Die so gewonnene makroskopische Quantenelektrodynamik bei Anwesenheit magnetoelektrischer Körper erfüllt alle Voraussetzungen an eine exakten Quantentheorie; inbesondere kann gezeigt werden, dass der Hamiltonoperator des Gesamtsystems die Gültigkeit der Maxwellgleichungen sowie der Newtonschen Bewegungsgleichungen für die geladenen Bestandteile des Atoms impliziert. Die der Einfachheit halber gemachten Voraussetzungen linearer, lokaler und isotroper Körpereigenschaften und die Beschränkung auf ein einzelnes Atom sind hierbei nicht zwingend, wie durch geeignete Erweiterung des Ansatzes gezeigt werden kann.

Aufbauend auf der bereitgestellten makroskopischen Quantenelektrodynamik erfolgt die Entwicklung einer Theorie der Casimir–Polder-Kräfte in zwei Teilen. Im ersten Teil werden die zeitunabhängigen Aspekte der Kraft beleuchtet. Hierzu wird die Kraft aus dem zugehörigen Casimir–Polder-Potential hergeleitet, welches als positionsabhängiger Teil der Atom–Feld-Kopplungsenergie gewonnen wird. Durch störungstheoretische Berechnung dieser Energie erhält man allgemeine Ausdrücke für das Casimir–Polder-Potential eines Atoms in einem Energieeigenzustand bei Anwesenheit einer beliebigen Anordnung magnetoelektrischer Körper. Hierbei gehen die atomspezifischen Eigenschaften über die atomaren Dipolmatrixelemente und entsprechenden Übergangsfrequenzen sowie die atomare Polarisierbarkeit ein,

wohingegen alle Informationen über Form, elektromagnetische Eigenschaften und Anordnung der Körper in Gestalt des Greentensors für das elektromagnetische Feld zum Ausdruck kommen. Die erhaltenen Formeln verallgemeinern die in früheren Arbeiten mittels Normalmoden-Quantisierung gewonnenen geometrieabhängigen Ergebnisse auf den Fall beliebiger Anordnungen von Körpern und stellen zugleich die erste exakte Herleitung der im Rahmen der Theorie der linearen Antwort postulierten Ergebnisse für den Fall dispersiver und absorptiver magnetoelektrischer Körper dar. Insbesondere wird nachgewiesen, dass minimale und multipolare Kopplung zu formal äquivalenten Ausdrücken führen.

Die störungstheoretischen Ergebnisse bilden den Ausgangspunkt für umfangreiche weitergehende Untersuchungen. Erstens wird die Anwendbarkeit der allgemeinen Formeln durch Berücksichtigung von Lokalfeldeffekten auf den Fall in einen Körper eingebetteter Atome erweitert. Es stellt sich heraus, dass die Lokalfeldkorrektur der Kraft allein von den elektrischen Eigenschaften des Körpers am Ort des Gastatoms abhängt. Zweitens wird mit Hilfe einer Bornreihe für den Greentensor ein Näherungsverfahren zur Berechnung von Potentialen für schwach magnetodielektrische Körper entwickelt. Insbesondere wird gezeigt, dass sich in linearer Näherung die Kraft durch Volumenintegration über Zentralkräfte gewinnen lässt, welche für rein dielektrische/magnetische Körper anziehend bzw. abstoßend sind. Drittens wird durch Kombination der Bornreihe mit dem Clausius–Mosotti-Gesetz der mikroskopische Ursprung der Casimir–Polder-Kraft erörtert. Es wird bewiesen, dass sich die Casimir–Polder Wechselwirkung eines einzelnen Atoms mit einem dielektrischen Körper unter sehr allgemeinen Bedingungen stets auf seine mikroskopischen van-der-Waals-Wechselwirkungen mit den Körperatomen zurückführen lässt. Die in dieser Beziehung auftretenden N-Atom-Potentiale sind eine Verallgemeinerung bekannter Freiraumresultate auf den Fall einer beliebigen Umgebung magnetoelektrischer Körper.

Um die Diskussion der statischen Theorie der Casimir–Polder-Kräfte abzurunden, werden anschließend die allgemeinen Formeln für Grundzustandsatome exemplarisch auf einige konkrete planare Geometrien angewandt, wodurch bekannte Resultate für rein elektrische Körper auf den magnetoelektrischen Fall erweitert werden. So wird z. B. gezeigt, dass die Kraft zwischen einem Atom und einer perfekt permeablen Platte genau entgegengesetzt zu der wohlbekannten anziehenden Kraft zwischen einem Atom und einer perfekt leitenden Platte ist – ein Befund, der im Rahmen einer Spiegelladungsmethode mit der unterschiedlichen Parität elektrischer und magnetischer Dipole anschaulich gemacht wird. Für realistischere Szenarien diktiert ein kompliziertes Wechselspiel von elektrischen und magnetischen Körpereigenschaften das Verhalten der Casimir–Polder-Kraft. Es zeigt sich am Fall einer Platte, dass die dominanten elektrischen Eigenschaften für asymptotisch kleine

Abstände des Atoms stets zu einem anziehenden Potential führen, wohingegen bei hinreichend starken magnetischen Eignschaften ein abstoßendes Potential bei mittleren Abständen beobachtet werden kann. Durch Kombination zweier Platten kann so ein Fallenpotential zwischen diesen realisiert werden. Man beachte, dass die neuartige Vorhersage von magnetischen Materialeigenschaften hervorgerufener abstoßender Kraftkomponenten noch ihrer experimentellen Bestätigung harrt, ein aussichtsreiches Szenario hierfür wäre die Quantenreflexion langsamer Atome an Platten aus extrem weichmagnetischem Mü-Metall. Eine anschließende Gegenüberstellung der Dispersionskräfte zwischen verschiedenen Grundzustandsobjekten legt den Schluss nahe, dass das in den Beispielen gefundene anziehende und abstoßende Verhalten der Kräfte generisch ist – eine Vermutung, die durch den oben bereits erwähnten gemeinsamen mikroskopischen Ursprung aller Dispersionskräfte zusätzlich untermauert wird.

Im zweiten Teil der Untersuchungen wird erstmals eine dynamische Theorie der Casimir–Polder-Kraft entwickelt. Ausgangspunkt hierzu ist die operatorwertige Lorentzkraft auf das Atom. Wie gezeigt wird, hängt diese in elektrischer Dipolnäherung in einfacher Weise vom elektrischen Dipolmoment des Atoms und dem quantisierten elektromagnetischen Feld ab, wobei minimale und multipolare Kopplung auf identische Ergebnisse führen. Aus dem gewonnenen allgemeinen Ausdruck für quantenelektrodynamische Strahlungskräfte auf Atome ergibt sich insbesondere auch die Casimir–Polder-Kraft als die vom Vakuumfeld hervorgerufene Kraft. Explizite Ausdrücke für die zeitabhängige Kraft ergeben sich durch Lösen der gekoppelten Atom–Feld-Dynamik; hierbei ist es sinnvoll, die zwei Grenzfälle schwacher und starker Kopplung zu unterscheiden.

Im Fall schwacher Kopplung führt die Markov-Näherung auf allgemeine Ausdrücke für die zeitabhängige Casimir–Polder-Kraft auf ein in einem beliebigen Anfangszustand präpariertes Atom. Wie gezeigt wird, lässt sich die Kraft als Überlagerung von Kraftkomponenten darstellen, die mit den jeweiligen zeitabhängigen atomaren Dichtematrixelementen gewichtet sind. Für ein anfangs in einem Eigenzustand präpariertes Atom klingt die Kraft in Folge spontanen Zerfalls zu energetisch tiefer liegenden Zuständen im Laufe der Zeit ab, so dass sich für hinreichend große Zeiten stets die Grundzustandskraft ergibt. Die Abhängigkeit der einzelnen Kraftkomponenten von Lage und Struktur der Anwesenheit der Körper ist wie schon in der statischen Theorie durch den Greentensor gegeben. Der wesentliche Unterschied besteht in der Tatsache, dass die relevanten atomaren Übergangsfrequenzen aufgrund der Anwesenheit der Körper eine Verschiebung und Verbreiterung erfahren. Insbesondere lässt sich in Folge der hierdurch zusätzlich auftretenden Positionsabhängigkeit die dynamische Casimir–Polder-Kraft nicht in der üblichen Art und Weise als Potentialkraft darstellen.

Außerdem können Linienverschiebung und -verbreiterung zu einer nicht unerheblichen Abschwächung speziell der resonanten Kraftkomponenten führen, die das Verhalten der Kraft auf angeregte Atome dominieren. Die Ergebnisse stellen somit eine Verallgemeinerung der statischen Theorie mit teilweise überraschenden Ergebnissen dar. Darüber hinaus eröffnet sich die Möglichkeit, die Kraft auf Atome zu diskutieren, welche anfangs in kohärenten Überlagerungen von mehreren Eigenzuständen präpariert sind. Die entwickelte Theorie sagt für diesen Fall das Auftreten gedämpfter, schnell oszillierender Kraftkomponenten voraus, welche eine interessante neuartige Vektorstruktur aufweisen.

Starke Atom–Feld-Kopplung tritt als wesentliches Merkmal in vielen neueren Experimenten auf, in denen angeregte Atome in Resonatoren hoher Güte eingebracht werden. Die auftretende resonante Wechselwirkung eines atomaren Übergangs mit einer einzelnen Quasimode des Resonators lässt sich am besten durch Beschränkung auf ein Zwei-Niveau-Atom untersuchen. Durch Abspalten der relevanten Quasimode vom übrigen Feldkontinuum lässt sich die resonante gekoppelte Atom–Feld-Dynamik exakt lösen und so die Casimir–Polder-Kraft für starke Kopplung finden. Es zeigt sich, dass der in Folge der starken Kopplung auftretende reversible Austausch von Energie zwischen Atom und Quasimode zu einem qualitativ neuen Phänomen führt: Die Casimir–Polder-Kraft weist nun gedämpfte Rabi-Oszillationen auf, deren Mittelwert und Amplitude von der anfänglichen Aufteilung der Anregungsenergie auf Atom und Mode abhängen.

Die im Rahmen der vorliegenden Dissertation entwickelte makroskopische Theorie der Casimir–Polder-Kräfte bei Anwesenheit magnetoelektrischer Körper erfüllt alle Anforderungen, die an eine solche im Hinblick auf die Bedürfnisse und Möglichkeiten moderner Experimente und Anwendungen zu stellen sind – wobei sich der Gültigkeitsbereich der Theorie über alle Atom–Körper-Abstände erstreckt, die hinreichend groß gegenüber der internen mikroskopischen Struktur der Körper sind. Insbesondere erlaubt sie eine Untersuchung des Einflusses aller wesentlicher Parameter auf die Kraft, wie z. B. der Form, Anordnung und Materialbeschaffenheit der Körper sowie der Art und des Anfangszustands des betreffenden Atoms. Neben der Beantwortung fundamentaler Fragen bietet die Theorie so die Grundlage für eine zukünftige experimentelle Kontrolle und Manipulation von Casimir–Polder-Kräften. Die im Rahmen der Arbeit entwickelten Ansätze und Methoden erlauben darüber hinaus eine Vielzahl von Verallgemeinerungen. Hierbei sind als spezielle Beispiele unter anderem die Erweiterungen auf thermische oder sogar beliebig angeregte elektromagnetische Felder zu nennen.

Ehrenwörtliche Erklärung

Ich erkläre hiermit ehrenwörtlich, dass ich die vorliegende Aufgabe selbständig, ohne unzulässige Hilfe Dritter und ohne Benutzung anderer als der angegebenen Hilfsmittel und Literatur angefertigt habe. Die aus anderen Quellen direkt oder indirekt übernommenen Daten und Konzepte sind unter Angabe der Quelle gekennzeichnet.

Bei der Auswahl und Auswertung des folgenden Materials haben mir die nachstehend aufgeführten Personen in der jeweils beschriebenen Weise entgeltlich/unentgeltlich geholfen:

1. Lisa Beasly: orthographische Korrekturlesung (unentgeltlich)

Weitere Personen waren an der inhaltlich-materiellen Erstellung der vorliegenden Arbeit nicht beteiligt. Insbesondere habe ich hierfür nicht die entgeltliche Hilfe von Vermittlungsbzw. Beratungsdiensten (Promotionsberater oder andere Personen) in Anspruch genommen. Niemand hat von mir unmittelbar oder mittelbar geldwerte Leistungen für Arbeiten erhalten, die im Zusammenhang mit dem Inhalt der vorgelegten Dissertation stehen.

Die Arbeit wurde bisher weder im In- noch im Ausland in gleicher oder ähnlicher Form einer anderen Prüfungsbehörde vorgelegt.

Die geltende Promotionsordnung der Physikalisch–Astronomischen Fakultät ist mir bekannt.

Ich versichere ehrenwörtlich, dass ich nach bestem Wissen die reine Wahrheit gesagt und nichts verschwiegen habe.

Jena, den 23.01.2007

Lebenslauf

Stefan Yoshi Buhmann, geboren am 25.06.1977 in Münster

Werdegang

1984 – 1988	Rückertschule, Osnabrück
1988 – 1990	Orientierungsstufe „In der Wüste", Osnabrück
1990 – 1997	Gymnasium „In der Wüste", Osnabrück
1997	Abitur
1998 – 2000	Studium Physik (Diplom) und Mathematik (Diplom), Universität zu Köln
2001	Studium Physics (Honours), University of New South Wales, Sydney
12.04.2002	Bachelor of Science with Honours in Physics, University of New South Wales, Sydney

Berufliche Tätigkeiten

01.09.1997 – 30.09.1998	Zivildienstleistender am Heilpädagogischen Bildungszentrum, Osnabrück
16.10.2000 – 28.02.2001	Übungsgruppenleiter für Analysis I, Universität zu Köln
31.08.2001 – 22.11.2001	Tutor für Lineare Algebra, University of New South Wales, Sydney
01.10.2002 – 31.03.2003	Übungsgruppenleiter für Analysis I, Friedrich-Schiller-Universität Jena
seit 15.05.2005	Wissenschaftlicher Mitarbeiter, Friedrich-Schiller-Universität Jena

Stipendien und Auszeichnungen

26.02.2001 – 27.11.2001	Jahresstipendium des Deutschen Akademischen Austauschdienstes,
12.04.2002	The Head of School's Prize in Physics for the best Year 4 Honours Thesis in Physics in the Bachelor of Physics Program, University of New South Wales, Sydney
01.09.2002 – 31.08.2004	Landesgraduiertenstipendium des Landes Thüringen
01.09.2004 – 30.04.2005	Promotionsförderung der E.–W. Kuhlmann-Stiftung

Jena, den 23.01.2007